Imidazole based Polymers as Ion Exchange Membranes

A Thesis Submitted for the degree of

DOCTOR OF PHILOSOPHY

By

Balakondareddy Sana

School of Chemistry
University of Hyderabad
Hyderabad-500 046
INDIA

June 2018

Dedicated to My Family

DECLARATION

I hereby declare that the matter embodied in the thesis entitled "***Imidazole based Polymers as Ion Exchange Membranes***" is the result of investigations carried out by me in the School of Chemistry, University of Hyderabad, Hyderabad, India under the supervision of **Prof. Tushar Jana** and it has not been submitted elsewhere for the award of any degree or diploma or membership, etc.

In keeping with the general practice of reporting scientific investigations, due acknowledgements have been made wherever the work described is based on the findings of other investigators. Any omission or error that might have crept in is regretted. This research work is free from Plagiarism. I hereby agree that my thesis can be deposited in shodganga/INFLIBNET. A report on plagiarism statistics from the University of Hyderabad Librarian is enclosed.

June 2018 **Balakondareddy Sana**

CERTIFICATE

This is to certify that the thesis entitled **"*Imidazole based Polymers as Ion Exchange Membranes*"** submitted by **Balakondareddy Sana** bearing registration number **12CHPH12** in partial fulfillment of the requirements for award of Doctor of Philosophy in the School of Chemistry is a bonafide work carried out by him under my supervision and guidance. This thesis is free from plagiarism and has not been submitted previously in part or in full to this or any other University or Institution for award of any degree or diploma. Further the student has four publications before submission of the thesis for adjudication and has produced evidences for the same in the form of reprints.

Parts of this thesis have been published in the following publications:

1. Sana, B.; Jana, T. *Eur. Polym. J.* **2016**, *84*, 421-434. **(Chapter 3)**
2. Sana, B.; Jana, T. *Polymer* **2018**, *137*, 312-323. **(Chapter 4)**
3. Sana, B.; Jana, T. (Communicated) **(Chapter 5)**

He has also made presentation in the following Conferences:

1. Asian Polymer Association (APA-2015) (Oral)
2. 14th Annual In-house Symposium (CHEMFEST-2017) (Oral)
3. International Conference on Polymer Science and Technology (MACRO-2017)

Further the student has passed the following courses towards fulfillment of course work requirement for Ph.D:

	Course	Title	Credits	Pass/Fail
1.	CY-801	Research Proposal	3	Pass
2.	CY-802	Instrumental Methods A	3	Pass
3.	CY-806	Instrumental Methods B	3	Pass
4.	CY-850	Chemistry of Materials	3	Pass

Prof. Tushar Jana
(Thesis Supervisor)

Dean
School of Chemistry

PREFACE

The present thesis entitled *"Imidazole based Polymers as Ion Exchange Membranes"* has been divided into eight chapters. ***Chapter 1*** provides a brief introduction of fuel cells, working principle of proton exchange membrane fuel cell (PEMFC), properties of proton exchange membrane (PEM) and their types, and applications. The most advanced application of phosphoric acid doped polybenzimidazole (PBI) membrane as a polymer electrolyte membrane in high temperature PEM fuel cell has also discussed. Alkaline anion exchange membrane fuel cell (AAEMFC) principle, properties of anion exchange membrane (AEM) and different types of cationic groups along with the various polymer backbones are also discussed in this chapter. ***Chapter 2*** describes the source of materials, methods and experimental techniques used for working chapters. ***Chapter 3*** describes the development of PBI composite membranes using acidic surfactant like molecule (ASM) by solution blending process. The effects of ASM on the properties of PBI/ASM composite PEM are studied in depth. ***Chapter 4*** deals with the synthesis of different types of functionalized pyridine bridged polybenzimidazoles (PyPBI) from efficient, economically less expensive pyridine bridged tetramine (PyTAB) monomer derivatives. ***Chapter 5*** describes the synthesis of various types of poly (methylated pyridinium benzimidazolium) iodides (PMPBI) from PyPBI polymers for use as AEM. ***Chapter 6*** describes the development of various kinds of poly(alkylated pyridinium benzimidazolim) anion exchange membranes from different polybenzimidazoles (PBIs, PyPBIs and tertiary butyl PyPBIs) by altering the structure of alkyl iodide and also studied AEM properties. ***Chapter 7*** describes the development of five different types of alkali stable cross-linked PBPBIs AEMs from PyPBIs by utilizing alkylation method. ***Chapter 8*** summarizes the findings of the present investigations, presents a concluding remark and the future scope and upcoming challenges.

June, 2018 **Balakondareddy Sana**

Acknowledgements

It is my immense pleasure to express my sincere gratitude to my research supervisor Prof. Tushar Jana, for his constant cooperation, encouragement and kind guidance. He has been quite helpful to me in both academic and personal fronts. It has been great pleasure and fortune to work with him who introduced me to the field of Polymer Chemistry. His discipline working style and honesty for the research has paved a new path in my career. I am also indebted to him for the work freedom he has given me during the last five years.

I would like to thank the former and present Dean, School of Chemistry, for their constant inspiration and for allowing me to avail the available facilities. I am extremely thankful individually to all the faculty members of the school for their kind help and cooperation at various stages of my stay in the campus. I am also grateful to all my former teachers for their help.

I am very grateful to the members of my Ph.D doctoral committee Prof. Anunay Samanta and Prof. T. P. Radhakrishnan for their constant support throughout my research career.

Financial assistance from UGC, New Delhi for providing Research Fellowship as well as various instrumental facilities, is sincerely acknowledged.

I would also like to express my sincere gratitude to Mr. Sunil and Mr. Durgaprasad of School of Chemistry, UoH for their help with FE-SEM experiments. I sincerely acknowledge Mr. Durgaprasad (Centre for Nanotechnology, UOH) for helping me with TEM experiments.

I am deeply predicated to all my teachers starting from my school to the university for their wonderful teaching and education throughout my academics.

I felt very lucky and proud to have labmates like Mousumi, Sudhangshu, Niranjan, Malkappa, Shuvra, Raju, Narasimha, Rambabu, Moumita, Harilal, Nilanjan, Anupam, Jorphin sir, Krishna, Konda Reddy, Ramesh and Venkanna in my ph.d life. My special thanks to project students Radhika, Srinivas, Arindam, Naman, Sahlini, Maduri and Saravanan.

I also thank all non-teaching staff for their timely help, I thank Mr. Durgesh and Thurab for their help in recording NMR spectra. I thank to all non-teaching staff specially Mr. Venkatesh.

I am really lucky for my close association with 'the gang' of HCU like Srinivas, Krishna Reddy, Mohan, Satyanarayana, Narendra, Uday, Ramesh, Venkata ramudu, Harish, Anand, Sivareddy, Kesav and so many others in HCU with whom I have some wonderful memories in Hyderabad throughout my Ph.D. life.

I would also like to express my sincere thanks to all my close friends Venkatadri, Pradeep, Subbu, Chandra, Dharani, Rafi, Sandeep, Chandu, Nagendra. B, Satheesh, Alluraiah, Obulasu, Uday kumar, Raghu and other school friends for their help and encouragement in various stages of my life.

My parents – my beloved Mother Ramasubbamma and Father Chinna Kondareddy, without their sacrifice and mental support I would not have reached to this stage of my life. I am greatly indebted from the bottom of my heart to my Mother and Father for their spiritual guidance and stay as a philosopher of my life. My Mother deserves special mention for her inseparable support and prayers.

Words are not enough to express my appreciation, gratitude earnest feelings to my wife Malleswari for giving me her constant mental support and encouragement in the last period of my Ph.D life and my little princess, Siva Sevita who is a blessing in the guise of daughter.

June 2018 **Balakondareddy Sana**

University of Hyderabad,

Hyderabad-500 046

India

Common Abbreviations

OPBI	Poly(4,4'-diphenylether-5,5'-bibenzimidazole)
FA	Formic acid
DMAc	*N*,*N*′-dimethyl acetamide
DMSO	Dimethyl sulfoxide
DMF	*N*,*N*′-dimethyl formamide
DMA	Dynamic mechanical analyzer
DCA	Dicarboxylic acid
TMC	Total monomer concentration
FTIR	Fourier transforms infrared spectroscopy
NMR	Nuclear magnetic resonance
IPA	Isophthalic acid
IV	Inherent viscosity
MW	Molecular weight
TPA	Terephthalic acid
BDA	Biphenyl 4,4′-dicarboxylic acid
OBA	4,4′-Oxybis(benzoic acid)
BPDA	4,4′-Dicarboxy benzophenone
HFIPA	4,4′-(Hexafluoroisopropylidene)bis(benzoic acid)
NMR	Nuclear magnetic resonance
NMP	N-methyl-2-pyrrolidone
NASA	National Aeronautics and Space Administration
PA	Phosphoric acid
PPA	Polyphosphoric acid
PBI	Polybenzimidazole
PyPBI	Pyridine based polybenzimidazole
PyTAB	2,6-Bis(3′,4′-diaminophenyl)-4-phenylpyridine
MEA	Membrane electrode assembly

PEMFC	Polymer electrolyte membrane fuel cell
PEM	Proton exchange membrane
AEMFC	Anion exchange membrane fuel cell
AEM	Anion exchange membrane
IEC	Ion exchange capasity
T_g	Glass transition temperature
TAB	3,3′,4,4′-Tetraaminobiphenyl
TGA	Thermogravimetric analyzer
T	Temperature
MSA	Methane sulfonic acid
WXRD	Wide angle X-ray diffraction

CONTENTS

Chapter 1

Introduction

1.1. FUEL CELL

Fuel cells are one of the energy conversion technologies yet the origin of this invention is not very clear. Sir William Grove is known as the father of fuel cells and was one of the first to put forward the concept of fuel cell. It was explained further (according to the United States Department of Energy), by Christian Friedrich Schonbein who first published it in the philosophical magazine in January 1839. Another name associated with this concept of fuel cell is Francis Thomas Bacon. He experimented with alkaline electrolytes instead of acid based electrolytes and found that the potassium hydroxide electrolytes worked as along with acid based electrolytes. Fuel cells are electrochemical energy conversion devices that convert chemical energy of hydrogen directly into the electrical energy via a chemical reaction.[1-5]

Fuel cell composed of three main components an anode, cathode and electrolyte. The oxidant is reduced at the cathode and fuel is oxidized at anode. Ions move through the electrolyte and a current is produced at the external circuit that is used to power a device. The basic building block of a fuel cell usually consists of an electrolyte layer sandwiched between porous anode and a cathode.[4, 5] The anode serves as an interface between the fuel (e.g. H_2) and the electrolyte, catalyzes the oxidation reaction and provides a path through which free electrons can conduct to the load via the external circuit. The cathode provides an interface between the oxygen and the electrolyte, catalyzes the oxygen reduction reaction, and provides a path through which free electrons are conducted from the load to the electrode via the external circuit. The electrolyte acts as a physical barrier between hydrogen and oxygen to prevent directly mixing but conducts ionic charge between the electrodes and the complete cell electric circuit. The cell reactions and are shown schematic representation of fuel cell (Figure 1.1).

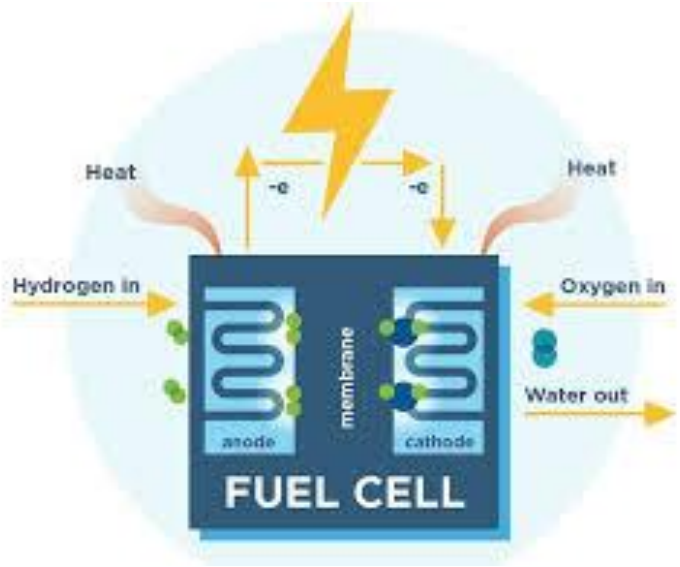

Figure 1.1. *Schematic representation of the general fuel cell diagram. (Image adopted from google)*

Cell reaction:

$$\text{At Anode: } 2H_2 \rightarrow 4H^+ + 4e^-$$

$$\text{At Cathode: } O_2 + 4H^+ + 4e^- \rightarrow 2H_2O$$

$$\text{Overall cell: } 2H_2 + O_2 \rightarrow 2H_2O + \text{electrical energy} + \text{heat}$$

In general, fuel cells are various types according to their operating temperature, electrolyte type, efficiency, applications and costs (Table 1.1). Fuel cells are classified into five types based on the choice of electrolyte. These are: 1) Proton exchange membrane fuel cell (PEMFC) or Polymer electrolyte fuel cell (PEFC), 2) Alkaline fuel cell (AFC) or Alkaline anion exchange membrane fuel cell (AAEMFC), 3) Phosphoric acid fuel cell (PAFC), 4) Molten carbonate fuel cell (MCFC) and 5) Solid oxide fuel cell (SOFC).

Table 1.1. *Various information of different types of fuel cells*

S.No	Type of fuel cell	Electrolyte	Operating temperature	Electric Power	Applications
1	PEMFC	Polymer membrane	60-160 °C	Up to 250 kW	Vehicles, stationary
2	AFC	Potassium hydroxide	100 °C	Up to 20 kW	Spacecrafts
3	PAFC	Phosphoric acid	180-200 °C	> 50 kW	Power stations
4	MCFC	Potassium carbonate	650 °C	> 1 MW	Power stations
5	SOFC	Yittria stabilized Zirconia	1000 °C	> 200 kW	Power stations

Fuel cells are also classified based on the type of fuel used. These are

a) Direct alcohol fuel cell (DAFC)

In this type of fuel cells, alcohol is used as a fuel without reforming. Most commonly, methanol used as a fuel instead of pure hydrogen, so this kind of cell called as direct methanol fuel cell (DMFC). There is no need to use complicated catalytic reforming process. Storage of methanol is much easier compared to the hydrogen because it is not required high pressure or low temperature.

b) Direct carbon fuel cell (DCFC)

In this fuel cells, solid carbon such as coal, pet coke and biomass are used as a fuel

directly at the anode, without an intermediate gasification step. In this fuel cell energy is produced by combining carbon and oxygen and carbon dioxide is released as a by-product. This used of cells are called as coal fuel cells (CFCs) or carbon-air fuel cells (CAFCs).

In this thesis we have synthesized various types of polybenzimidazoles and quaternized polybenzimidazoles for the development of proton exchange membranes (PEMs) and anion exchange membranes (AEMs). Therefore, in the following section, we are discussed in detail about the proton exchange membrane fuel cell (PEMFC) and anion exchange membrane fuel cell (AEFC) among the various types of fuel cells.

1.2. PROTON EXCHANGE MEMBRANE FUEL CELL (PEMFC)

Proton exchange membrane or polymer electrolyte membrane fuel cells (PEMFCs) are considered to be promising candidates and more attractive fuel cell technology among various types of fuel cells due to their simplicity in use in automobile, portable power and stationary applications.[6-9] The PEMFC was first developed for the Gemini space vehicle. The important features of the PEMFCs are: pollution free operation, and all-solid construction and therefore less corrosion. The PEMFC is low cost and more compact than all other types of fuel cells. Depending upon the polymer electrolytes, PEMFCs can operate starting from low temperature to high temperature (30 to 180 $^{\circ}$C) and produces high power density than any other type of fuel cell.[9-12]

1.2.1. Working principle of PEMFC

In PEM fuel cell, hydrogen used as fuel and oxygen used as oxidant, and it is made up of two electrodes (anode and cathode) and a polymer membrane as electrolyte which is present between the two electrodes. The working principle of PEMFC technology involves the hydrogen oxidation at the anode and the oxygen reduction at the cathode.[3-5, 13] Both oxidation and reduction reactions occurred in the presence of platinum catalyst. The hydrogen molecules split into protons and electrons at the anode. The resulting protons are transported through the electrolyte (polymer membrane) from

anode to cathode compartment because the polymer membrane is only permeable for protons. Thus the electrons should move through an external circuit and create the source of a direct electrical current. At the cathode oxygen is reduced and combines with protons which are coming from the proton exchange membrane electrolytes and generates water.

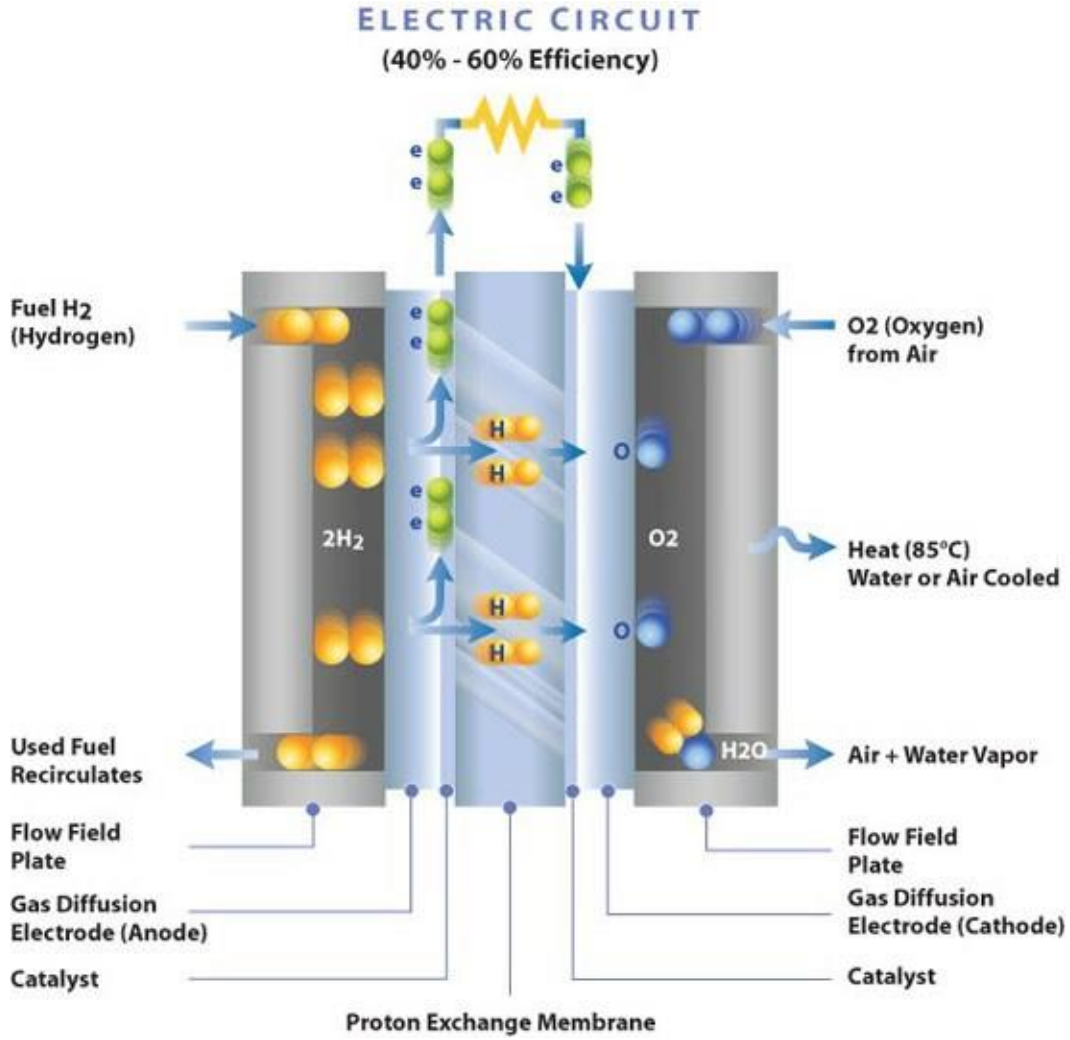

Figure 1.2. *Polymer Electrolyte Membrane Fuel Cell (PEMFC). (Adapted from pine research.com)*

1.2.2. Required properties of proton exchange membrane

A proton exchange membrane (PEM) not only transport protons from anode to cathode and thereby completes the cell electrical circuit but it has also to provide a physical barrier to stop the direct mixing of fuel (H_2) and oxygen. To achieve high performance polymer electrolyte membrane fuel cell (PEMFC), the polymer membrane should have the following properties.[5-8, 12, 14, 15] High proton conductivity, High mechanical stability, High thermal and chemical stability, Low gas permeability, Good film-formation capacity, Low cost, Capable of fabrication into MEAs and Mechanical durability at high temperature (80–140^{o}C).

1.2.3. Proton conducting polymer membranes

The fuel cell efficiency is highly dependent on the proton conducting characteristics polymer electrolyte membrane or proton exchange membranes. PEMFCs have been traditionally developed by using perfluorinated polymer membranes in which polymer backbone structure of these polymers is similar to the polytetrafluoroethylene (Teflon, PTFE) structure.[16, 17] Commercially, these polymers are using a trade name Nafion. These polymers contain pendant PTFE side chains attached to the main chain by the ether linkage and sulfonated functional groups attached at the end of the pendant chains. The teflon-like backbone provides Nafion with excellent long term stability in both oxidative and reductive environment. Among the various types of perfluorosulfonated membranes, the most widely studied ones are based on polymers which were developed by Dupont in 1968. Nafion® (Scheme 1.1) is the most commonly used polymer electrolyte membrane due to its high proton conductivity, excellent chemical stability, good mechanical strength, and it is also commercially available.[5, 13]

The most efficient polymer electrolyte membrane is perfluoro sulfonated membrane and which is showing excellent performance up to 100 °C temperature in hydration conditions. However, Nafion membrane having several drawbacks such as low operating temperature, very high cost, carbon monoxide poisoning, high fuel cross over and difficulty in water management.[11, 12, 18, 19] In hydrated condition, the Nafion

membrane exhibit high proton conductivity ~10^{-2} S.cm^{-1} but gradually conductivity decreases with temperatures beyond 100 °C because of the loss of water from the membrane. To maintain this high conductivity, fuel gases (H_2 and O_2 or air) must be carefully hydrated. Humidity management has been rather important to keep membrane humidification and at the same time avoid flooding of the electrodes.

To overcome these disadvantages, considerable efforts have been made to modify the conventional polymers or to prepare new alternative polymers for operation at high temperatures and in lower hydration condition. A variety of approaches have been attempted to develop thermally stable polymer electrolyte membranes.[4, 5, 7, 9] One of the best approaches has been the introduction of sulfonic acid functionality on to the stable aromatic polymers in order to achieve alternative to Nafion membrane. Till now, most of them are non-fluorinated polymers are sulfonated polymers. Polystyrene sulfonic acids,[20] sulfonated polysulfone,[21] sulfonated poly(ether ether ketone),[22] sulfonated poly(phenylene ethers),[23] sulfonated polymers[24] have been reported as alternative to Nafion sulfonated polymer structures reported in the literature few representative are shown in Scheme 1.2. It has been noticed that the thermal degradation of these aromatic sulfonated polymers is in the range of 200 to 400 °C.

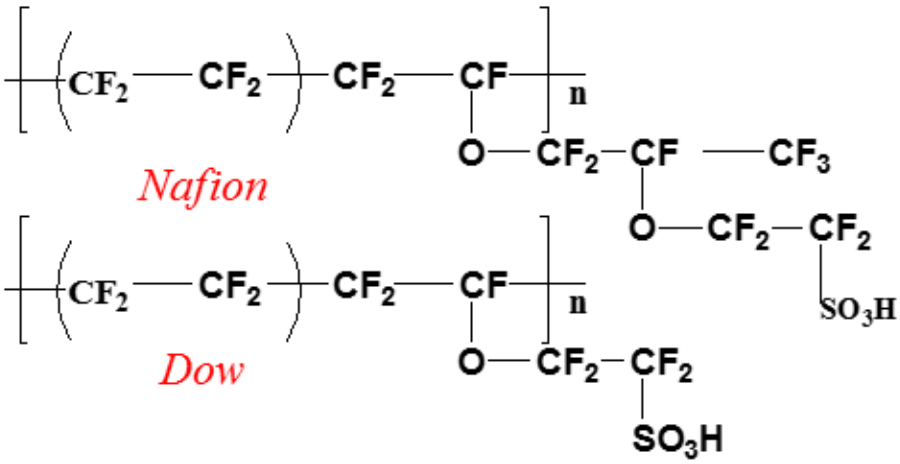

Scheme 1.1. *The chemical structures of Nafion and Dow membranes.*

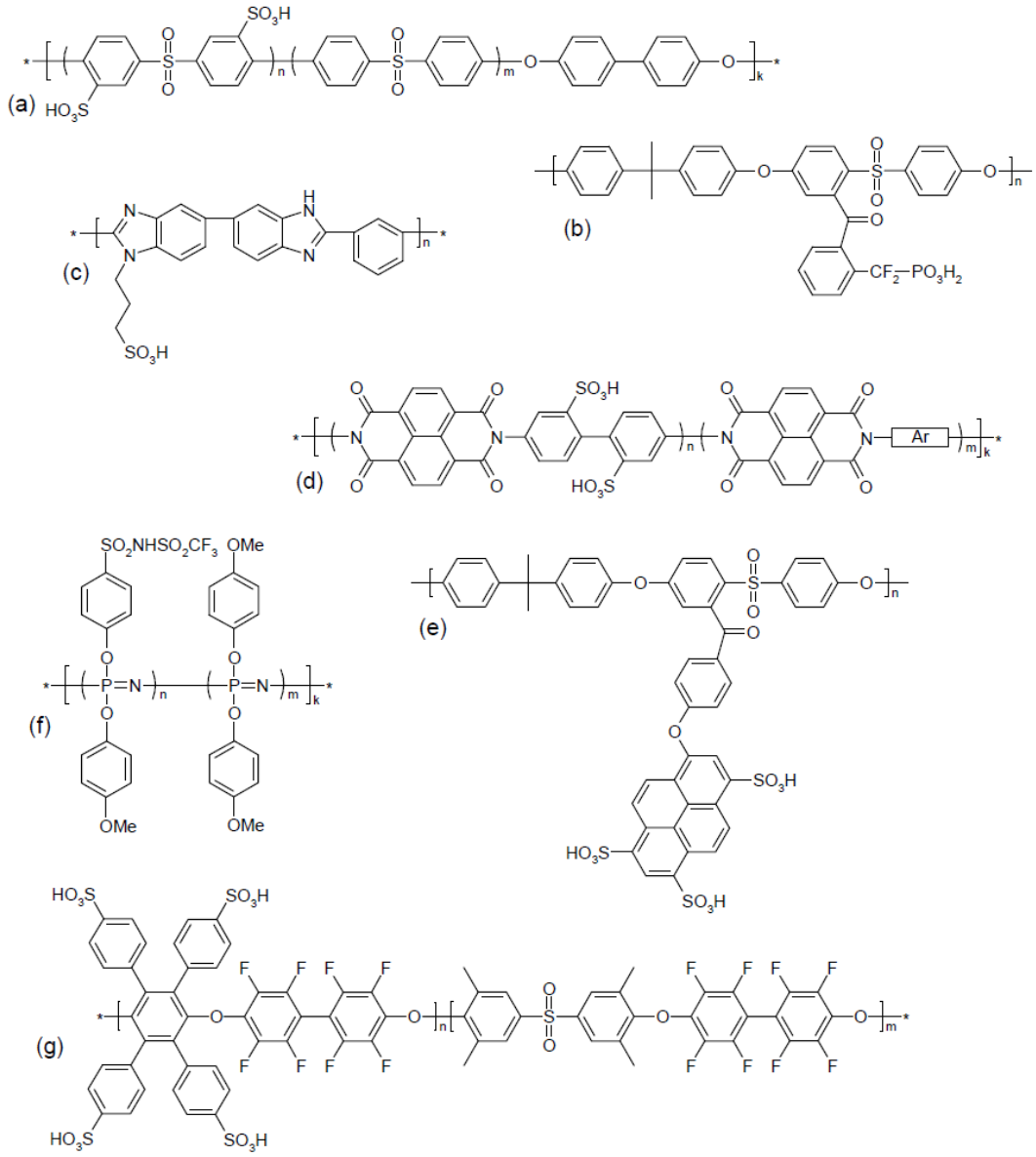

Scheme 1.2. *Examples of proton-conducting polymers designed for PEM materials: as alternative to Nafion (a) sulfonated poly(arylene ethersulfone); (b) polysulfone; (c) sulfopropylated PBI; (d) sulfonated naphthalenic polyimide; (e) polysulfone carrying trisulfonated arylene ether side chains; (f) poly(aryloxyphosphazene); and (g) partially fluorinated and sulfonated poly(arylene ether sulfone) copolymer. (Taken from reference 20-24)*

1.3. ALKALINE FUEL CELL (AFC)

In 1950s, NASA Apollo space program started using AFC systems and this technology is still used for today's shuttle missions. Many research groups started focusing on AFCs for other applications. By 1970s, a car had been built, by Kordesch[25], which ran on (AFC) combined with a lead-acid battery. The AFC is the first fuel cell technology to be developed towards practical application in the 20th century. In AFCs aqueous potassium hydroxide (KOH) used as an electrolyte in which hydroxide ions in an alkaline electrolyte solution travel from cathode to anode. This is exactly a reverse direction when compared with the PEMFCs. An AFC usually operates at relatively low temperature varying from 20 °C to 80 °C, offering a lower possibility of thermal and chemical degradation.[26] The anode and cathode cell reactions and AFC diagram are presented in the Figure 1.3.

At Anode: $2H_2 + 4OH^- \rightarrow 4H_2O + 4e-$

At Cathode: $O_2 + 2H_2O + 4e- \rightarrow 4OH^-$

Overall cell: $2H_2 + O_2 \rightarrow 2H_2O$ + electrical energy + heat

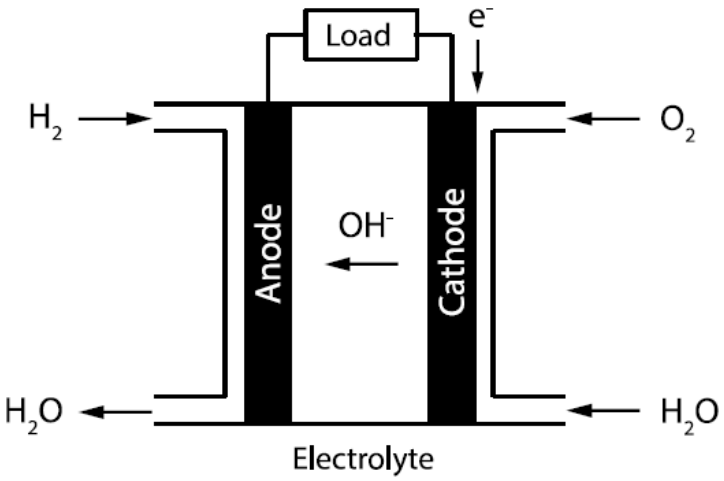

Figure 1.3. *Schematic representation of the alkaline fuel cell diagram. (Adapted from google)*

1.3.1. Drawbacks of AFC

In AFCs, the liquid solution of electrolyte (aqueous KOH) has been the major cause of concerns. Generally in AFCs, highly concentrated alkaline solution (6 M KOH) used as electrolyte, which has more affinity towards CO_2 from the air and hence resulted in the generation of carbonates or bicarbonate ions under the carbonate process as shown below.[27, 28]

$$CO_2 + 2OH^- \rightarrow CO_3^{2-} + H_2O$$

$$CO_2 + OH^- \rightarrow HCO_3^-$$

Hence, the number of hydroxide ions availability decreases and CO_3^{2-} or HCO_3^- ions are increases at the anode. The mobility of CO_3^{2-} or HCO_3^- ions is slower than OH^- ions which results in the decrease in conductivity of OH^- ion thus reducing the fuel cell performance. Furthermore, carbonate deposition can result in a precipitate that blocks micro pores in the electrodes, resulting in a further decrease in AFC performance.[29, 30] Corrosion management is a problem during the operation because the KOH electrolyte can degrade most of the materials. Therefore, all the fuel cell materials that come in contact with the electrolyte need to be highly alkaline stable, which also leads to higher cost. The amount of liquid electrolyte also affects the performance, as the electrode can suffer from drying due to the lack of liquid electrolyte, while excess of liquid electrolyte can lead to the flooding of the electrode.

1.3.2. Anion exchange membrane fuel cell (AEMFC)

To address the above mentioned drawbacks the researchers have started developing the anion exchange membrane fuel cell (AEMFC) by introducing anion-conducting solid polymer electrolytes to replace the KOH solution as liquid electrolyte. In this design, the solid polymer electrolyte membrane acts as separator and conductive support between the anode and cathode. In this structure, the membrane electrode assembly (MEA), sandwiches the membrane between the two electrodes, which include the catalyst layer and the gas diffusion layer. The reaction scheme for the solid

electrolyte fuel cell is similar to the liquid fuel cell. The hydrogen oxidation and oxygen reduction take place at the anode and the cathode, respectively.

1.3.3. Working principle of AEM

In the working principle, functioning of alkaline anion exchange membrane fuel cells (AAEMFCs) using H_2 as fuel and O_2 as oxidant. In an AMFC, hydroxide ions are generated during electrochemical oxygen reduction at the cathode. They are transported from cathode to anode through the anion conducting polymer electrolyte where in the hydroxide ions are combining with hydrogen to form water. The electron generated during hydrogen oxidation pass through the external circuit to the cathode where the electrons participate in the electrochemical reduction of oxygen to form hydroxyl ions.

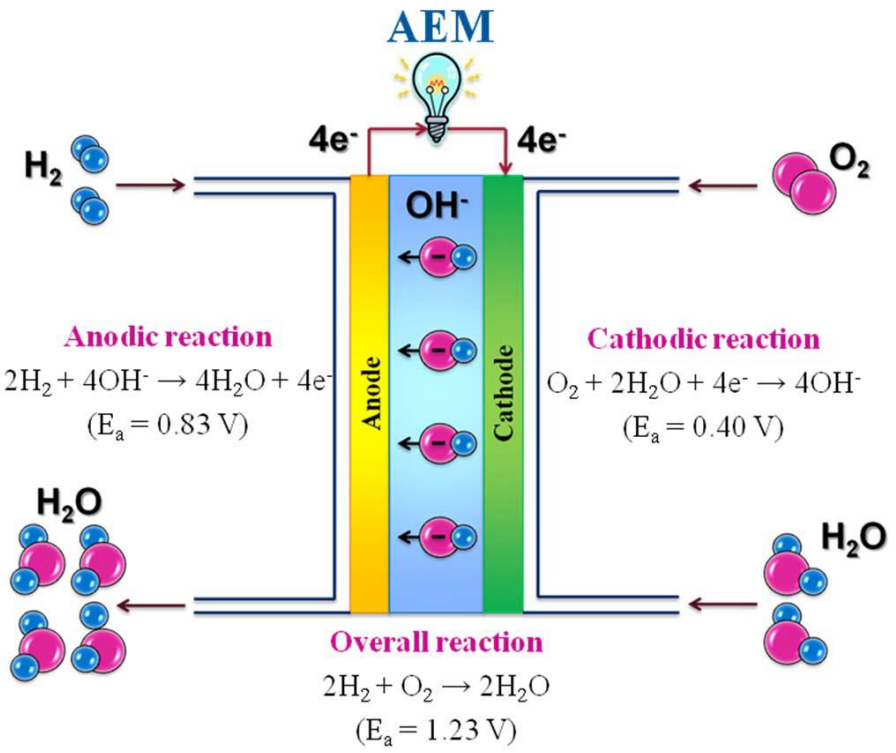

Figure 1.4. *Schematic representation of the anion exchange membrane fuel cell (AEMFC) diagram. (Adapted from Hadis Zarrin thesis from University of Waterloo)*

1.3.4. Advantages of anion exchange membrane over liquid electrolyte

- Anion exchange membrane serves as electrolyte.
- Anion exchange membrane is less sensitivity towards CO_2.
- Potentially reduced the corrosion problems.
- No electrolyte weeping or leaking.
- Reduced alcohols crossover.
- The cationic species or conducting species are tethered with solid polymer.
- Solid crystals of metal carbonate or carbonate precipitation will not be formed.
- Solvent-free conditions and easy handling.
- Increases the efficiency and life time of AEMFC.

1.3.5. Advantages of AEMFC over PEMFC

- Use non precious metal catalyst.
- Easier to handle.
- The operating temperature is relatively low.
- Higher reaction kinetics at the electrodes than in acidic conditions.
- Higher cell voltage.
- Low cost.

1.3.6. Disadvantages of AEMFC compare to PEMFC

- The ion conducted in AEMFC is hydroxide, which is larger size compared to a proton resultingin lower mobility.[31]
- The hydroxide ionic conductivity highly depends on environmental humidity, which also limits its wide application.[32]

- AEM shows low ionic conductivity and instability than PEM.

1.3.7. Desired properties of anion exchange membrane (AEM)

The anion exchange membrane fuel cell efficiency can be affected by several factors, and the AEM is one of the important core components in AEMFCs. To be effective, the solid polymer membrane should have certain desired properties that can influence the AEMFC performance. List of these properties highlighted below:

- The AEM should tethered at least one cationic site or anion exchange site for hydroxide conduction. Various types of cationic sites are reported in the literature. They are

  a) quaternary ammonium groups b) imidazolium or benzimidazolium based systems c) pyridinium groups d) guanidinium systems e) phosphonium groups f) sulfonium types and g) metal-based systems.

- The membrane must be stable thermally and chemically under basic conditions.
- Polymer backbones and cationic sites should be mechanically stable so that membrane durability under AFC operating conditions can be maintained.
- AEM should yield high ionic conductivity.
- The AEM electrolyte ionic conductivity must be high under different temperature and humidified conditions and should not vary.
- The AEM should act as a barrier to prevent electron conduction and fuel cross over in the membrane.
- The preparation and fabrication of the AEM must be low cost.

Diffrent cationic functional groups (anion exchange sites) and polymer backbones have been studied as anion exchange membranes.[26, 29, 30, 33] The structure of these cationic sites are shown in Scheme 1.3.

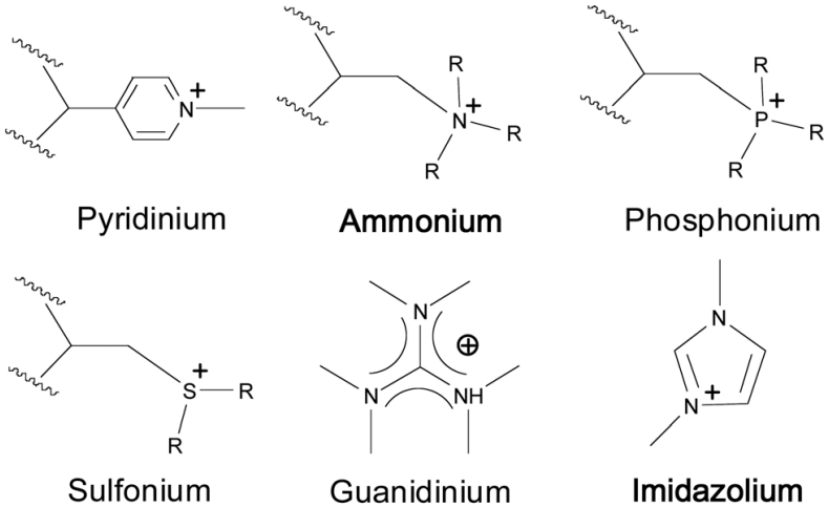

Scheme 1.3. *Structures of cationic groups used as anion exchange sites in AEM.*

1.3.8. AEMs based on quaternary ammonium cation

Functionalization of a polymer backbone with a quaternary ammonium (QA) group is the simplest and most widely studied way to introduce a tethered cationic group to form an anion exchange membrane. Initially, it was considered that the QA groups containing AEMs are chemically more stable than the other cationic groups. Unfortunately, QA groups are degraded by hydroxide ion (OH^-) nucliophilic attack and showed some severe drawbacks.

1) Hofmann degradation

The cleavage of the QA group by hydroxide ion (OH^-) followed by the elimination is called as Hofmann degradation or E2 elimination (Scheme 1.4). In this process the hydroxide ions selectively attack on the β hydrogen from the positively charged nitrogen atom (ammonium). The degradation leads to the formation of amine, alkene and water molecule.[34]

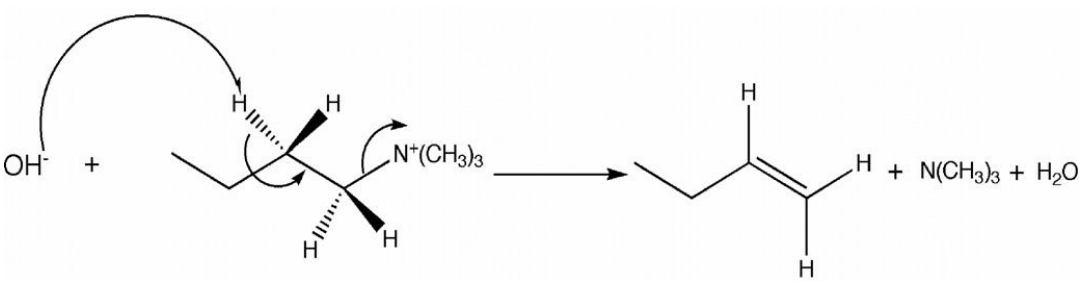

Scheme 1.4. *Degradation of a quaternary ammonium group by the Hofmann elimination (Taken from reference 26)*

2) S_N2 substitution

In the absence of β hydrogen nucliophilic substitution occurs by the hydroxide attack on α hydrogen atom on the ammonium group and produces alcohol and amine.[35]

3) E1 elimination

When there is a steric hindrance at α and β positions of the quaternary ammonium cation, degradation occur through an E1 elimination process.[36] Degradation of the cations results in decrease of ion exchange capacity (IEC) and conductivity of the membrane.

Polysulfones are a class of poly(aryl ether) materials that have been widely studied for use in nanofiltration, gas separation, and PEMFC because of their good properties and their capability for functionalization to introduce cationic groups. A large number of poly(aryl ether) based anion exchange membranes such as poly(ether imide),[37] poly(ether ketone),[38] poly(ether sulfone)[39] and poly(phthalazinone ether sulfone ketone)[40] have been developed for potential application in AEMFCs (Scheme 1.5). Polysulfones are commonly modified by chloromethylation method, followed by quaternization to produce benzyltrimethyl ammonium groups. Disadvantages of this method discussed in the introduction of Chapter 5.

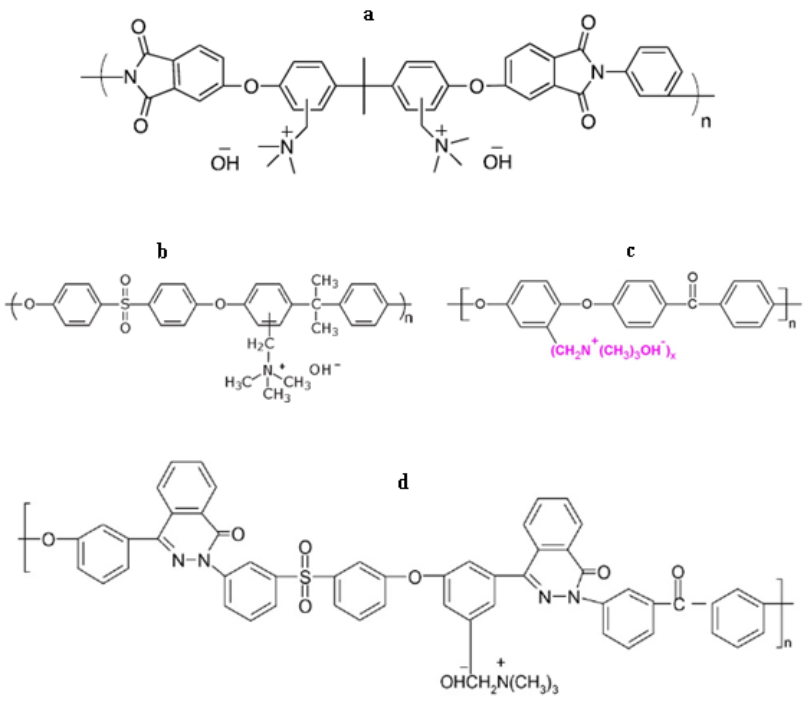

Scheme 1.5. *Examples of QA groups on poly(ether sulfone) backbone by chloromethylaton method. a) poly(ether imide), b) poly(ether sulfone), c) poly(ether ketone) and d) poly(phthalazinone ether sulfone ketone). (Taken from reference 26)*

1.3.9. AEMs based on pyridinium cation

Few reports are available in the literature about pyridinium groups as an anion exchange site for anion exchange membrane. Neagu *et al.* addressed the stability of 4-vinyl pyridinium groups and observed rapid degradation in the presence of base.[41] Sata *et al.* reported poly(vinyl pyridinium) membranes. Even though these AEM perform good electrochemical properties in electrodialysis, the pyridinium groups showed degradation in the presence of alkaline media. At high pH, the pyridinium groups are chemically degraded by the hydroxyl ions. This degradation is shown in Scheme 1.6 leads to the formation of a pyridone.

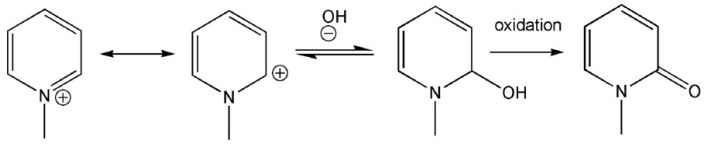

Scheme 1.6. *Degradation of the pyridinium groups in alkali media: reversible addition of the hydroxide ion to the methylated pyridine followed by an irreversible oxidation to the N-methyl-2-pyridone. (Taken from reference 26)*

The hydroxide conductivity of the ionized poly(arylene ether sulfone) membrane containing pyridinium (IPAES-Py) demonstrates very less water uptake, IEC and inonic conductivity. The possible reason is that the thermal properties of the IPAES-Py membrane is inadequate in the presence of oxygen at higher temperature this is because pyridinium groups are converted into neutral pyridone (Scheme 1.7).[43] The more discussion on this is presented in the introduction of the Chapter 5.

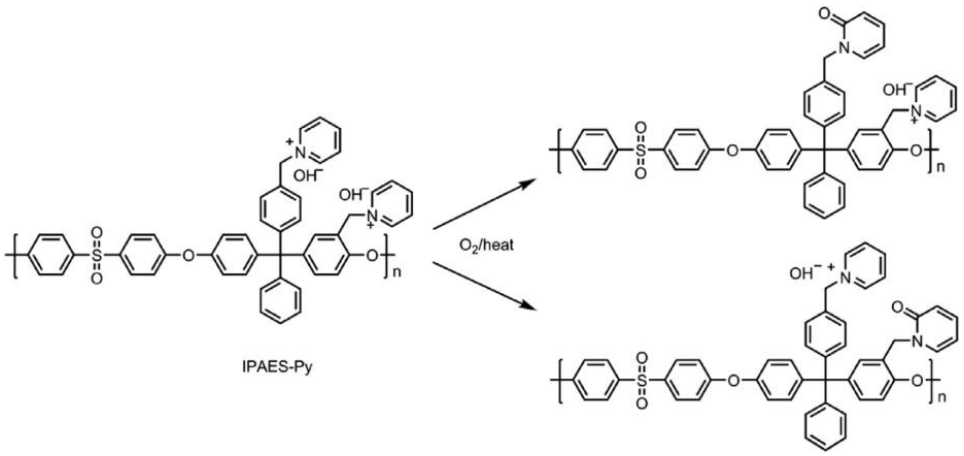

Scheme 1.7. *Thermal oxidation of IPAES-Py. (Taken from reference 43)*

1.3.10. AEMs based on imidazolium and benzimidazolium cationic groups

Despite the above structural innovations, decomposition of quaternary ammonium and pyridinium cationic groups still persists in alkaline conditions and it is a challenge to achieve complete removal of decomposition. There is a need to discover and explore

positively charged polymers that offer the potential of improving the alkaline stability. Recent days in the literature, the researchers are found that the imidazolium cationic groups are alternative to the quaternary ammonium cations. Imidazolium can be either prepared in the polymer backbone as polybenzimidazolium or as pendent cationic group tethered onto the polymer backbone. It is potentially more stable for its resonant structure, where the positive charge is delocalized over the ring and its interaction with hydroxide ion can be weakened. Li and co-workers synthesized a poly(arylene ether sulfone) AAEM containing N-methyl imidazolium (IPAES-MIm) and as well as poly(arylene ether sulfone) tethered with quaternary ammonium group (IPAES-TEA).[44] The two structures are given in Scheme 1.8. Among these two N-methyl imidazolium AEM exhibited greater chemical stability than that functionalized with quaternary ammonium after treatment with 1 M NaOH at 60 °C for 170 h. The excellent stability of IPAES-MIm is attributed to the resonance effect of the conjugated 1,3-alkyl substituted imidazolium cation, which reduces the positive charge density of the cation and weakens the interaction with the hydroxide.

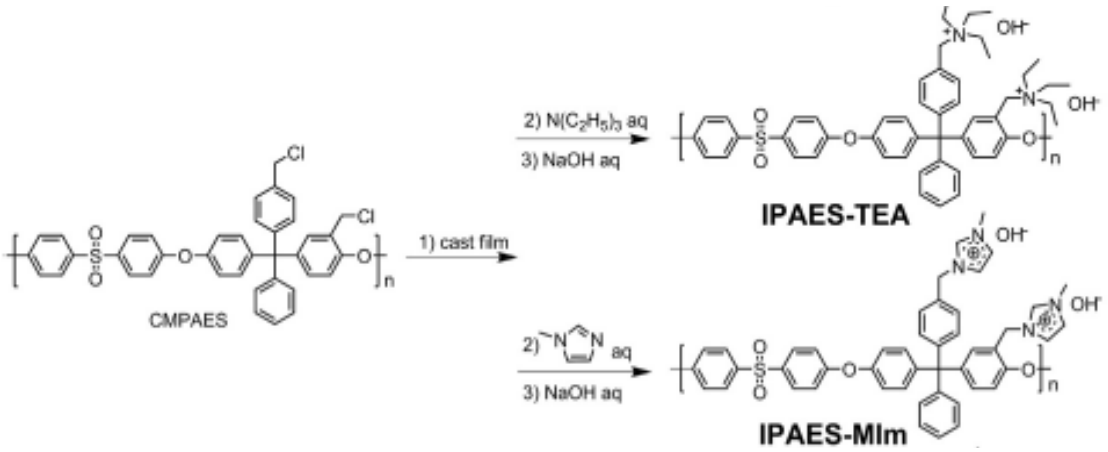

Scheme 1.8. *Chemical structures of IPAES-TEA and IPAES-MIm. (Taken from reference 43)*

Recently, pendent imidazolium functionalized membrane was prepared based on tetramethyl bisphenol A polysulfone block copolymer (Scheme 1.9).[45] The polysulfone

polymer was brominated and then functionalized with imidazolium homogeneously. The membrane with an IEC of 1.45 meq/g exhibited high hydroxide conductivity of 100 mS/cm at 80 °C with a reasonable water uptake. The alkaline stability was also investigated with only a slight decrease in hydroxide conductivity observed after immersing in 2 M NaOH solution at 60 °C for 7 days.

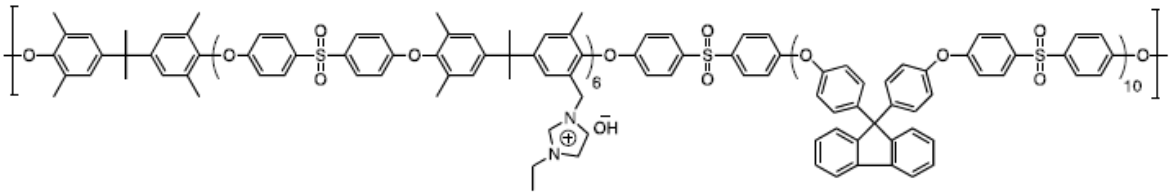

Scheme 1.9. *Imidazolium functionalized poly(arylene ether sulfone) block copolymer as an anion exchange membrane (Taken from reference 44).*

Polybenzimidazole was methylated to generate the cationic poly(benzimidazolium) functional polymer and produce anion exchange membrane. Henkensmeier and co-workers synthesized poly(benzimidazoliums) for anion exchange membrane fuel cells. The membrane flexibility was investigated qualitatively by immersion in alkaline solutions. It was observed that a methylated-PBI membrane gets rapidly brittle when immersed in 0.5 M KOH at room temperature and breaks when touched with tweezers after 3 days. Some structural variants PBI based membranes remained flexible even after 3 days and 5 days. However, brittleness was observed at elevated temperatures. The introduction of heteroatoms in para-position of the phenyl substituent of 2-phenyl-imidazolium systems was found to be stabilizing the imidazolium. Membranes based on hydroxyl exchanged methylated PBI (OPBI) remained flexible for a longer time than PBI (m-PBI) based membranes. They were proposed degradation mechanism of poly (benzimidazoliums) by ring opening reaction to produces amine-amide products in the presence of alkaline solutions.[46, 47] Finally, it was concluded that, further stabilization of the imidazolium ions by additional groups seems to be possible and is the goal of future work.

Kim and co-workers synthesized and studied about various kinds of poly(benzimidazoliums). Those AEMs were immersed in water after doping with alkaline solutions. They observed that some of the membranes got dissolved, some of the membranes got partially dissolved and some of the membranes had brittle nature except ether based AEM. The reason could found that the mesomeric stabilization should be stronger for phenylether linked structures (which has two phenyl rings and an ether oxygen atom in para position to C2) than for benzene linked other systems.[48] Based on these results, they would be expected that new polymer design would increase the durability by the proper delocalization of per methylated benzimidazolium ring.

Holdcroft and co-workers thought that benzimidazolium hydroxide salts can be stabilized by steric crowding around the labile benzimidazolium C2 position and consequently use this strategy to synthesize novel polymers with greatly enhanced stability toward alkaline solutions. The novel polymer reported herein, Mes-PBI is a sterically crowded PBI synthesized from a tetraamine and a mesitylene-containing dicarboxylic acid (DCA). The mesitylene-poly (dimethyl benzimidazolium) hydroxide (Mes-PDMBI-OH^-) polymer synthesized from sterically crowded Mes-PBI (Scheme 1.10). The Mes-PDMBI-OH^- polymer membrane did not show any degradation in 2 M KOH solution at 60 °C, owing to the sterically crowded mesitytene group which protected the C2 position against hydroxide (OH^-) attack. But the problem associated with this was the easy solubility in water due to the bulky nature of the mesitylene group. Some of the alkali doped AEM polymers were shown in Scheme 1.10.

To address these issues, we have introduced poly(alkylated pyridinium benzimidazolium) (Scheme 1.10) iodide polymers for AEMs (Discussion about these polymers can be found in the Chapters 5, 6 and 7). poly(methylated pyridinium benzimidazolium) membranes showed higher ionic conductivity than the benzimidazolium based reports. The reason could be the presence of both pyridinium and benzimidazolium which are acted as cationic sites. poly(butylated/isobutylated pyridinium benzimidazolium) membranes displayed very high chemical stability compared to the other poly(benzimidazolium) reports.

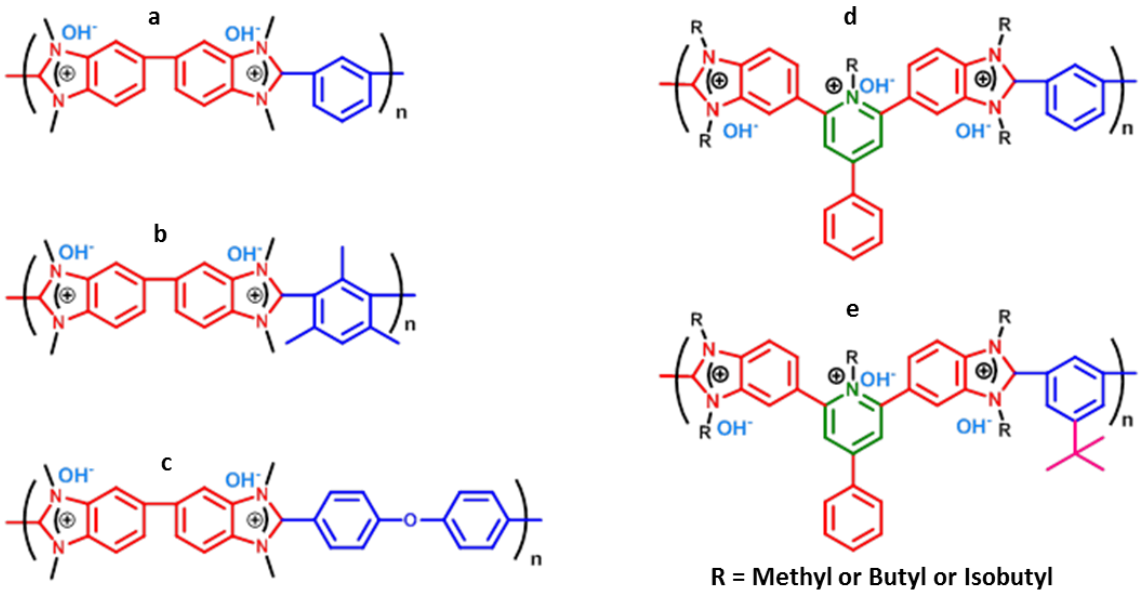

Scheme 1.10. *Examples of polybenzimidazolium polymers designed for AEM materials: a) Poly(methylated benzimidazolium)-IPA, b) Poly(methylated benzimidazolium)-mesitylene, c) Poly(methylated benzimidazolium)-OBA, d) Poly(alkylated pyridinium benzimidazolium)-IPA and e) Poly(alkylated pyridinium benzimidazolium)-5-tertiary butyl-IPA.(Taken from reference 46-48)*

1.4. POLYBENZIMIDAZOLES (PBIs)

Polybenzimidazoles comprises of a class of aromatic heterocyclic rigid structure polymeric materials possessing very high thermal and mechanical stability. Introduction of polybenzimidazoles came from US Patent 2, 895, 948 in 1959 by Brinker and Robinson.[49] Initially, polybenzimidazoles was synthesized by Prof. Marvell and Vogel from Illinois University in 1961 but they apprehended the material without any target[50-53]. Later on, due to the remarkably high thermal and chemical stability of polybenzimidazoles, to meet the demands of the NASA scientific requirements like fire and heat proof material; NASA and Air Force Material Laboratory (AFML) triggered the use of all types of polybenzimidazoles to fulfil their requirements and get the extensive properties to form the flake and the fibre.[54-56] This helped in the exploration

and synthesis of polybenzimidazoles for a wide variety of applications like flame retardation property, radiative stability, excellent mechanical, thermal stabilities and strength retention over wide range of temperatures, toughness, chemically resistance and adhesion characteristics. After the advanced analysis of these various properties exhibited by polybenzimidazoles NASA fostered the Celanese Company to produce large amount of polybenzimidazoles to utilize them as fire resistance jackets, adhesive foams and fibres for their requirements. In 1980s low molecular weight polybenzimidazoles was marketed under the name of "**Celazole**" as moulding resins. Then, in 1983, Celanese company produced polybenzimidazoles with meta phenylene linkage, poly[2,2′-(*m*-phenylene)-5,5′-bibenzimidazole] named as "**PBI**" for use in wide range of textile fibers. This stimulated them to produce PBI in large scale and commercialized it worldwide. PBI, being high performance fibers have been used for several decades for high comfort, non-flammable fabrics such as flight suits, fire-proof clothing, and hand gloves for astronauts and pilots. Several research groups have made extensive efforts in enhancing the properties of PBI and thereby over the years many reviews in the appeared literature.[57-63]

1.4.1. Polybenzimidazoles Synthesis

Various polymerization techniques have been explored for the subsequent synthesis of polybenzimidazoles by Marvell and Vogel in 1961. The prevalent synthetic procedure of PBI is the polycondensation reaction of aromatic tetraamines (bis-o-diamines) and aromatic dicarboxylates (acid, ester or amides).[50, 51, 54, 58] Of all the different types of techniques available in literature, the most widely known technique is the solution medium polycondensation by using polyphosphoric acid (PPA). The different type of monomers has been used are tabulated in the Table 1.2. All these various techniques were performed at higher heating condition and under nitrogen atmosphere. A brief discussion about the solution polymerisation is summarized here.

1.4.2. Solution Polymerization

Several techniques have been investigated for the solution polymerization processes. Different types of high boiling solvents such as *N*,*N*-dimethyl acetamide (DMAc), *N*,*N*-dimethyl formamide (DMF) can be used.[64-66] But one of the main limitations in using these solvents is that the resulting PBI has low inherent viscosity (I.V). Even though, the high molecular weight PBI can be obtained at higher temperatures, these solvents cannot remain in the reaction medium above 200 °C and it is quite difficult to extract the product from the melted and solidified reaction mixture thus obtained.

In 1964, Iwakura et al.[67] took the first attempt of solution polymerization technique in PPA medium, where PPA has been used as a both solvent as well as catalyst for polyheterocyclization reactions.[68-70] The procedure is that, equimolar mixture of tetramine and dicarboxylic acid in polyphosphoric acid medium was kept under continuous flow of nitrogen gas at 180-210 °C for 24h. If the diammines contain acid salts then first tetrammines are kept at 140 °C and after complete removal of hydrochloride (HCl) gas[54] ,equal moles of dicarboxylic acid can be added. The continuous nitrogen flow is an essential requirement for the removal of by-products like water and phenol from the reaction mixture. The main highlight of using PPA medium is that high MW PBI can be synthesized and it can be easily extracted from the hot reaction mixture. The reaction procedure and the conditions are shown in the Scheme 1.11.

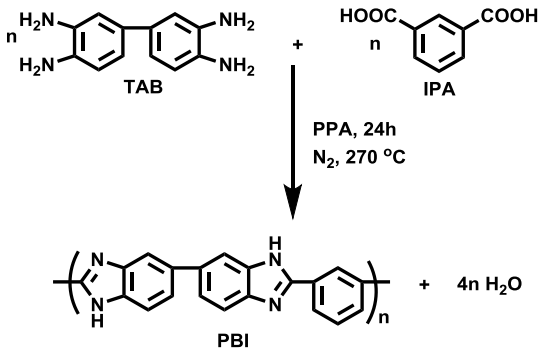

Scheme 1.11. *Solution polymerization process for synthesis of polybenzimidazole (PBI) in polyphosphoric acid (PPA) medium (Adopted from A. Sannigrahi thesis, UOH, 2010).*

Table 1.2. *Different types of aromatic tetraamine and dicarboxylic acid monomers for polybenzimidazole (PBI) synthesis.*

Tetraamine Monomer	MP (°C)	Dicarboxylic Monomer	MP (°C)
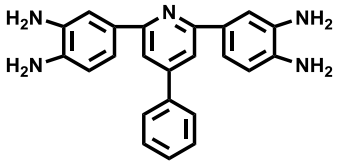 2,6-bis(3,4-diaminophenyl)-4-phenylpyridine	221	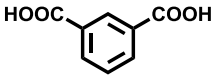 Benzene-1,3-(dicarboxylic acid)	342
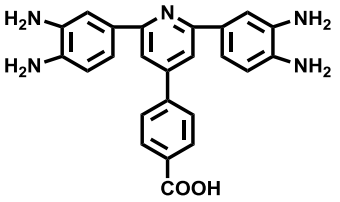 4-(2,6-bis(3,4-diaminophenyl)pyridin-4-yl)benzoic acid		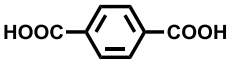 Benzene-1,4-(dicarboxylic acid)	>300
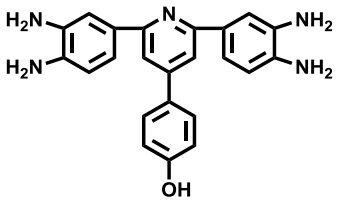 4-(2,6-bis(3,4-diaminophenyl)pyridin-4-yl)phenol		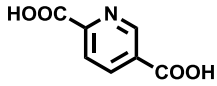 Pyridine-2,5-(dicarboxylic acid)	245
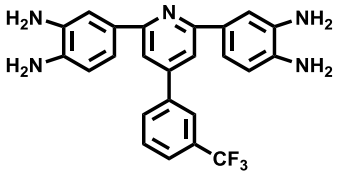 2,6-Bis(3' ,4'- diamino)phenyl-4-(3"-trifluoromethyl) phenyl pyridine		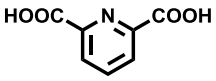 Pyridine-2,6-(dicarboxylic acid)	249
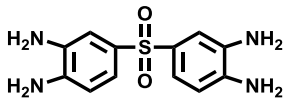 3,3',4,4'-Tetraaminodiphenylsulfone	217	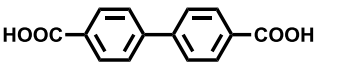 Biphenyl-4,4'-(dicarboxylic acid)	>300
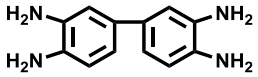 3,3',4,4'-Tetraaminobiphenyl	—	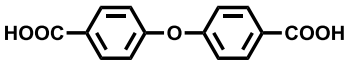 4,4'-Oxybis(benzoic acid)	—
		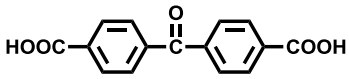 Benzophenone-4,4'-(dicarboxylic acid)	—
		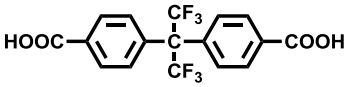 4,4'-(Hexafluoroisopropylidene)bis(benzoic acid)	272

1.4.3 Different types of Polybenzimidazoles

Since 1961, after the synthesis of PBI by Marvell et al. Several research groups have been exploring and modifying the structure of high temperature resistant PBI for employing them in a wide variety of areas and advanced fields. PBI possesses very unique properties as well as some restraints, so in order to improve their properties as per the requirements; researchers have synthesized different varieties of PBI. The varieties of PBI include poly[2,2′-(1,4-phenylene)-5,5′-benzimidazole] (known as *p*-PBI),[71] poly(4,4′-diphenylether-5,5′-bibenzimidazole) (OPBI),[72-74] poly(2,5-benzimidazole) (AB-PBI),[75] pyridine based PBI (Py-PBI),[76-78] sulfonated PBI,[79] cross-linked and hyperbranched PBI,[80-83] naphthalene based PBI,[84] fluorinated PBI,[85] N-substituted PBI (N-PBI),[86-88] meta-para random PBI copolymer,[89] PBI with sulfone or sulfonic acid groups in the backbone[90] and many others. PBI possesses strong inter-molecular and intra-molecular chain hydrogen bonding and also a highly rigid rod-structure that results in poor solubility in common organic solvents. The incorporation of the hetero atoms[91] in the polymer main chain or by N-substitution post polymerization with sulfonic or the aliphatic groups have been found by the researchers to improve the solubility , acid uptake capability and thereby increasing the acid doping level for application in fuel cells. Flexibility was increased by modifying the main chain or side chain with the incorporation of flexor groups like para linkage monomer or aliphatic group or bulky group containing hetero atom. The presence of sulfonated acid groups in PBI increases its water and acid uptake capacity. Likewise many more modification techniques have been explored to improve the membrane quality, thermal and mechanical properties. Recently, our group also has implemented certain modifications with side and the main chain of PBI which increases solubility, flexibility and acid doping capability. Some of these modified structures of PBI have been discussed in Chapter 4 and representative structures are shown in Scheme 1.12.

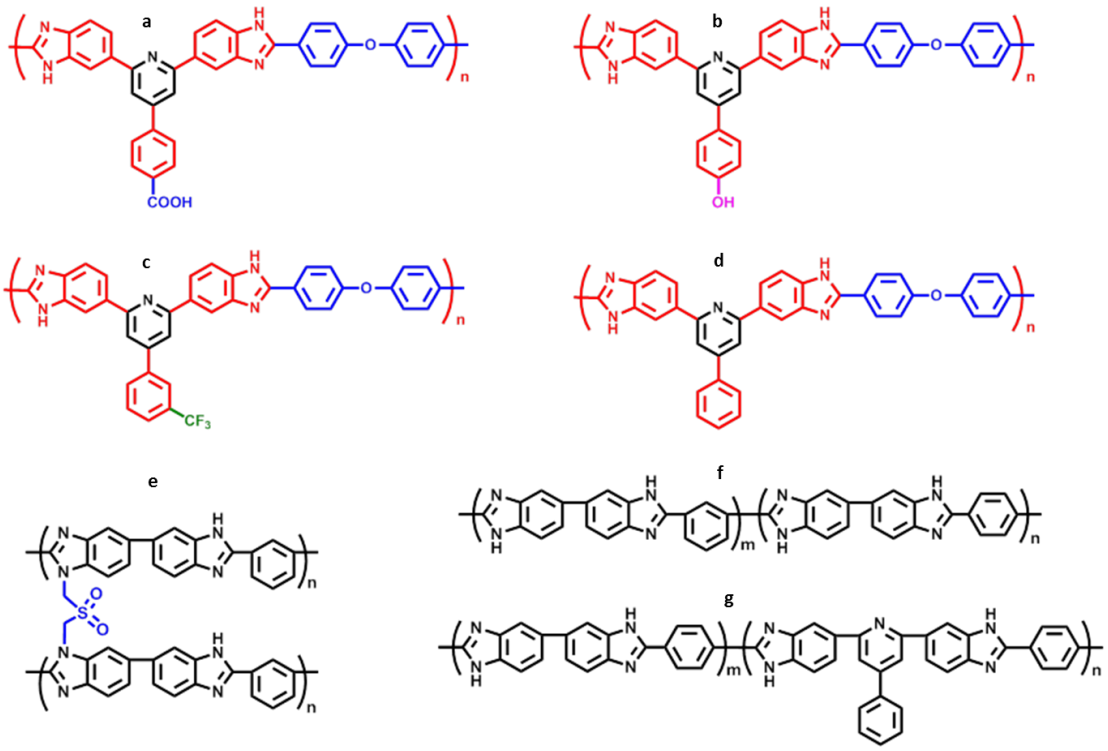

Scheme 1.12. *Functionalised pyridine based polybenzimidazoles (a, b and c), non-functionalised pyridine based polybenzimidazoles (d), cross-linked polybenzimidazoles (e), random copolymer (f), block copolymer (g). (Taken from reference 76, 89, 90)*

1.4.4. Phosphoric acid (PA) doped PBI for PEMFC

Several research groups have examined phosphoric acid doped PBI as a very good proton-conducting membrane for proton-exchange membrane fuel cells and they considered as alternative to Nafion for high temperature fuel cell operation. First Savinell's group achieved 250 mW cm^{-2} at 150 °C for membrane electrode assemblies (MEAs) using phosphoric acid doped PBI.[92] After that Savadogo achieved promising MEAs by preparing phosphoric acid and sulphuric acid doped PBI membranes. In this report, Savadogo reported that sulphuric acid doped PBI shows better performance compared to Nafion at lower temperature.[93] PA doped polybenzimidazoles offers several potential benefits such as high electrode kinetics, high CO tolerance, simplified thermal, water management systems and enhanced efficiency of the waste heat

utilization. The PBI polymer is a basic character with excellent thermal, mechanical and chemical stability. When it is dipped in aqueous phosphoric acid to form an acid-base complex, the PBI/ H_3PO_4 complex shows high proton conductivity at high temperatures even in the anhydrous state, low gas permeability, and nearly zero water drag coefficient.[94-100] PBI polymeric membranes form strong hydrogen bonding sites due to the presence of proton donor (-NH-) and proton acceptor (-N=) hydrogen bonding sites, in which protons can readily transfer by hydrogen bond breaking and forming processes. It has been realized that this system is a promising candidate for high-temperature (from 100 to 200 °C) PEM fuel cell.

In amembrane transfer of proton depends on the nature of the acid used, polymer structure, humidity and temperature. Savadogo examined the protonic conductivity of acid doped PBI membrane in various acids and reported that the conductivity values are varying in the order of H_2SO_4 > H_3PO_4 > $HClO_4$ > HNO_3 > HCl for high doping levels.[101] The conductivity values achieved for each acid are detailed in Table 1.3. The sulphuric acid doped PBI membrane shows higher proton conductivity among all various acid doped membranes. Phosphoric acid is the best solvent for doping at higher temperature and anhydrous condition. In all the cases, the conductivity depends on the amount of acid present in the membrane. Proton conduction of PA doped PBI follows two types of mechanisms. The proton conductivity mechanism of acid-doped PBIs is mainly by a Grotthus mechanism especially at below 100 °C temperatures. In this Grotthus mechanism, proton transfer hopping between two molecules such as acid–acid, acid–water, or acid-imidazole ring (Scheme 1.13).[100] In the other mechanism, the proton moves solvated by water molecules which are called as vehicle mechanism. The proton diffuses through the membrane dragged by a ‘‘vehicle’’ which is H_3O^+ when the membrane is hydrated.[102] When the PBIs doped with phosphoric acid, the composite system will further encounter several drawbacks, including leaching out of phosphoric acid from the membrane, poisoning of cathode Pt electro catalyst by PA, self-dehydration of H_3PO_4 at higher temperatures, low loading level of PA, and it loses the mechanical stability by PA particularly at high PA concentrations and high

temperatures. To address these problems, several authors has been developed inorganic additives,[103-107] polymer blends,[108-112] and doping with different electrolytes[113-117] and the synthesis of PBIs with different structures.[118-127]

Table 1.3. *Conductivity values of PBI films after immersion into various acid solutions of the indicated concentrations. (Taken from reference 101)*

S.No	Acid used for PBI doping (concentration)	Proton conductivity values (S/cm)
1	Sulphuric acid (16 M)	6×10^{-2}
2	Phosphoric acid (14.4 M)	1.9×10^{-3}
3	Nitric acid (15.8 M)	1.8×10^{-3}
4	Per chloric acid (11.6 M)	1.6×10^{-3}
5	Hydrochloric acid (11.8 M)	1.4×10^{-3}

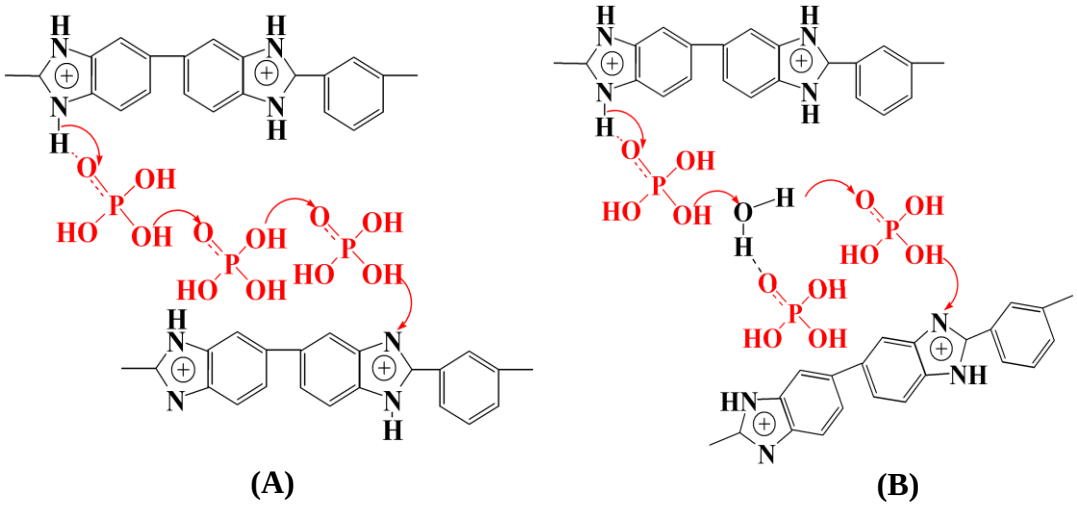

(A) **(B)**

Scheme 1.13. *Proton transfer process (A) acid- PBI- acid (B) acid- water-acid PBI. (Taken from reference 100)*

1.4.5. PA doped PBI membrane fabrication methods

Various attempts have been made for fabrication of PA doped PBI membranes and among those we have discussed mainly three types of fabrication methods here as follows:

1) *The sol-gel process*

In 2005, Benicewicz et al. reported a new method for developing PBI membranes imbibed with phosphoric acid solvent.[69] This process can be called as a sol-gel process or PPA (polyphosphoric acid) process, which utilizes PPA as both the polymerization solvent and as well as the casting solvent for PBI polymers. In this process, dicarboxylic acids (DCA) and tetramines (TAB) are polymerized in PPA at 190-220 °C temperature and produced high molecular weight of PBI polymers. After polymerization, the PPA solution containing PBI is directly cast onto the clean flat glass plate. After casting, the hydrolysis of PPA to phosphoric acid is allowed to take place by absorbing the moisture from the surrounding environment which induces a sol-gel transition, resulting in phosphoric acid-doped PBI membranes. These membranes have high proton conductivities, good PA loading levels, greater mechanical properties and excellent long term stabilities than membranes formed through other fabrication processes.

2) *Imbibing process*

Imbibing process first developed by Savinell et al.[128] in which PBI membrane fabricates from dimethyl acetamide (DMAc) solution with the addition of lithium chloride as a stabilizer at a particular temperature and followed by solvent evaporation. After that the membrane peeled off from the glass plate. Then the membrane was washed with hot water in order to remove the stabilizer (LiCl) and trace amount of DMAc. The organic solvent, such as DMAc, are generally poisonous to the platinum fuel cell catalyst so it is very important to remove. Then the membranes are immersing in PA acids and this whole process can be called as imbibing process. The mechanical property is good enough for the fabrication of membrane electrode assembly (MEA). In

this method the acid loading varies from 5 to 16 moles per repeat unit.[129]

3) *Porogen process*

Another important approach is the development of the porous PBI membrane by the removal of low molecular weight compounds using suitable solvent (methanol, hydrazine and water) for porogen and followed by immersing the membrane into PA bath. This result in obtaining a porous PA doped PBI membrane and this total process can be called as porogen process and it shown in Figure 1.5. In this process, they have use different phthalates (dimethyl, diethyl, dibutyl and diphenyl, as well as triphenyl phosphate) as porogens.[130-132]

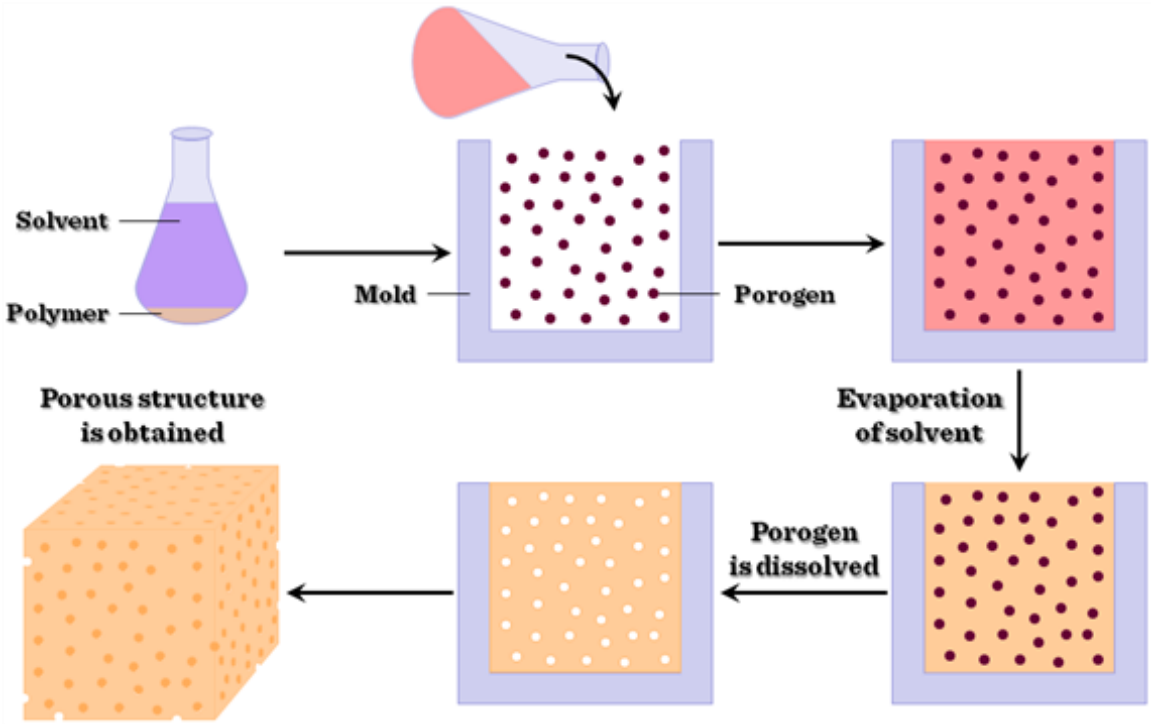

Figure 1.5. *Method development for porous structure in the PBI membrane. (Taken from reference 132)*

1.5. POLYMER NANOCOMPOSITE

As the name suggests, polymer nanocomposite comprises of a mixture of two main components: the nanofiller and the polymer matrix in which the nanofiller is embedded. Emergence of nanocomposites opened a huge area of research as they provide a wide range of applications in industrial as well as daily life applications. [133-142] Up to now, a variety of nanofillers have emerged like carbon nanotube,[137, 138] graphene,[142] chemically modified silica particles,[134, 141] clay,[133, 140] fullerene.[136, 137] etc. Among all, carbon nanotube, graphene and chemically modified silica which provide high performance of the resulting nanocomposites is the major attraction. The addition of even a small amount of nanomaterials brings about a huge change in the polymer properties without disturbing the polymer backbone and processability of the polymer. The change is observed in the polymer properties particularly increased mechanical strength and heat resistance, decreased gas permeability and flammability, increased biodegradability of biodegradable polymers, mechanical properties, increase thermal and oxidative stability and acid loading capacity as well as the proton conductivity. The nanofillers have this much impact on the polymer properties as a result of its unique properties such as, (i) low percolation threshold, (ii) arising a low volume fraction due to particle-particle correlation (orientation and position), (iii) extensive interfacial area (communication between matrix and filler) per volume of particles, (iv) short distances between the particles and (v) comparable size scales among the rigid nanoparticles inclusion. Nanofillers can be mainly classified into three, on the basis of dimensions, that is, (i) one dimension (e.g., clay) (ii) two dimension (e.g., carbon nanotube, graphene) and (iii) three dimension (e.g., silica). In the recent times, various modifications have been developed on PBI using different types of nano fillers. [143-148] The phosphoric acid doping level as well as the proton conductivity and the mechanical stability can be improved using silicotungstic acid[145] and phosphotungstic acid.[144] Carbon nanotube and grapheme are also capable of increasing the several properties of the PBI.[146, 147] Shao et.al. synthesized the multiwall carbon nanotubes (MWNTs) containing 0.1-1 wt% nanofillers in OPBI nanocomposites.[147] In recent times, our

group has synthesized the ammine modified silica particle[149] and the montmorillonite clay (Figure 1.6) to influence the properties of the OPBI.[133]

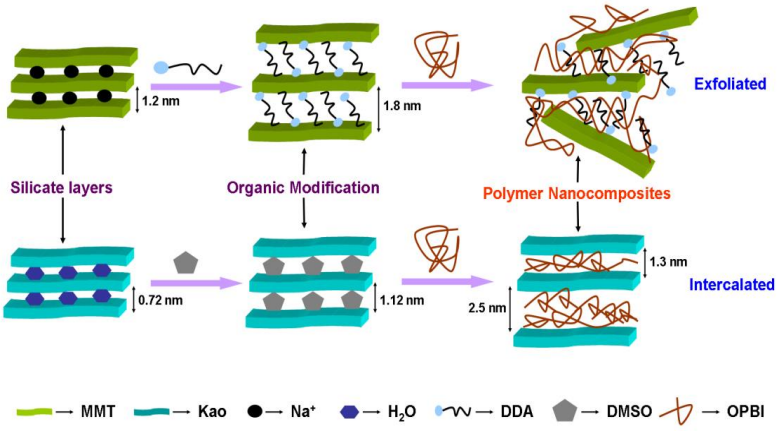

Figure 1.6. *Schematic representation of OPBI nanocomposites with the organoclays (Adapted from reference 133).*

1.6. AIMS of the Thesis

The above discussions in this chapter about the PBI types of polymers offer many opportunities to study the PBI chemistry. Despite the presence of huge literature on the PBI type materials, we found out that there are many issues which were not addressed with and discussed in the literature adequately. Large numbers of efforts have been made to develop variety of PBI-nanocomposite membranes. However no attempts have been made to resolve acid leaching, long-term membrane stability and durability. Hence we have attempted to explore these aspects in Chapter 3 by using simple organic molecules as a composite. We have explored new PyTAB monomer derivatives which contain some functional groups and affect the entire properties of PBI polymers. Chapter 4 deals with the stability of the polymer in phosphoric acid, low swelling and high proton conductivity due to the presence of functionality in the PyPBI polymers. Very limited efforts have been made in literature about the use of PBI as anion exchange membrane (AEM). For the first time, we have developed PyPBI polymers as

alkaline anion exchange membranes (AAEMs). Chapter 5 deals with the quarterization of PyPBI polymers, doping with alkaline solutions, and stability in alkaline condition, ionic conductivity and all other AEM properties. Till today the appropriate stable alkaline anion exchange membrane has not been achieved by using PBI polymer. We have designed and developed a new poly(alkylated pyridinium benzimidazolium) membranes by altering the alkylated structures and cross-linked poly(alkylated pyridinium benzimidazolium) membranes for higher alkaline stability. These topics are discussed in Chapter 6 and 7. Therefore the thesis projects development of new generation polymer electrolyte membranes based on PBI for the use as potential PEM and as well as AEM in fuel cell. The aims and objectives of each chapter of this thesis are elaborated at the end of the introductory part of the individual chapters.

REFERENCES

[1] Yeager, E. *Science* **1961**, *134*, 1178.

[2] *Fuel Cell Handbook, 6th Edition, EG & G Technical Services, Inc. U. S. Department of Energy;* November, **2002**.

[3] Mench, M. M. *Fuel Cell Engines, John Wiley & Sons, Inc.;* **2008**.

[4] Blomen, L. J. M. J. *Fuel Cell Systems; Plenum Press*, New York, **1993**.

[5] Rikukawa, M.; Sanui, K. *Prog. Polym. Sci.* **2000**, *25*, 1463.

[6] Hickner, M. A.; Ghassemi, H.; Kim, S. Y.; Einsla, B. R.; McGrath, J. E. *Chem. Rev.* **2004**, *104*, 4587.

[7] Kerres, J. A. *J. Membr Sci.* **2001**, *185*, 3.

[8] Li, Q.; He, R.; Jensen, J. Q.; Bjerrum, N. J. *Chem. Mater.* **2003**, *15*, 4896.

[9] Roziere, J.; Jones, D. J. Annu. *Rev. Mater. Res.* **2003**, *33*, 503.

[10] Smitha, B.; Sridhar, S.; Khan, A. A. *J. Membr. Sci.* **2005**, *259*, 10.

[11] Maier, G.; Meier-Haack, J. *Adv. Polym. Sci.* **2008**, *216*, 1.

[12] Xiao, L. *Ph.D. Thesis; Rensselaer Polytechnic Institute:* Troy, New York, **2003**.

[13] Winter, M.; Brodd, R. J. *Chem. Rev.* **2004**, *104*, 4245.

[14] Einsla, B. R. *Ph.D.Thesis, Virginia Polytechnic, Blackburg*, Virginia, **2005**.

[15] Sukumar, P. R.; *Ph.D.Thesis*, *Max-Planck-Institute for Polymer Science*, Mainz, **2006**.

[16] Mauritz, K. A.; Moore, R. B. *Chem. Rev.* **2004**, *104*, 4535.

[17] Yoshitake, M.; Watakabe, A. *Adv Polym Sci.* **2008**, *215*, 127.

[18] Mehta, V.; Cooper, J. S. *J. Power Sources* **2003**, *114*, 32.

[19] Shao, Y.; Yin, G.; Wang, Z.; Gao, Y. *J. Power Sources* **2007**,*167*, 235.

[20] Gubler, L.; Scherer, G. G. *Adv. Polym. Sci.* **2008**, *215*, 1.

[21] Gilchrist, T. L. Heterocyclic Chemistry, 3rd Edition, **1997**.

[22] Gasa, J. V.; Weiss,R. A.; Shaw, M. T. *J. Polym. Sci., Part B: Polym. Phys.* **2006**, *44*, 2253.

[23] Iwakura, Y.; Uno, K.; Nume, K. US Patent, 3741938, 1973.

[24] Arnold, F. E. US Patent, 495452, 1974.

[25] Kordesch, K. J. *Electrochem. Soc.* **1971**, *118*, 812.

[26] Merle, G.; Wessling, M.; Nijmeijer, K. *J. Membr. Sci.* **2011**, *377*, 1.

[27] Cifrain, M.; Kordesch, K. V. *J. Power Sources* **2004**, *127*, 234.

[28] Gülzow, E.; Schulze, M. *J. Power Sources* **2004**, *127*, 243.

[29] Couture, G.; Alaaeddine, A.; Boschet, F.; Ameduri, B. *Prog. Polym. Sci.* **2011**, *36*, 1521.

[30] McLean, G. F.; Niet, T.; Prince-Richard, S.; Djilali, N. *Int. J. Hydrogen Energy* **2002**, *27*, 507.

[31] Hibbs, M. R.; Hickner, M. A.; Alam, T. M.; McIntyre, S. K.; Fujimoto, C. H.; Cornelius, C. *J. Chem. Mater.* **2008**, *20*, 2566.

[32] Varcoe, J. R. Phys. Chem. Chem. Phys. **2007**, *9*, 1479.

[33] Varcoe, J. R.; Slade, R. C. T. *Fuel Cells* **2005**, *5*, 187.

[34] Iojoiu, C.; Chabert, F.; Mare´chal, M.; Kissi, N. E.; Guindet, J.; Sanchez, J. Y. *J. Power Sources* **2006**, *153*, 198.

[35] Chempath, S.; Einsla, B. R.; Pratt, L. R.; Macomber, C. S.; Boncella, J. M.; Rau, J. A.; Pivovar, B. S. *J. Phys. Chem. C* **2008**, *112*, 3179.

[36] Cope, A. C.; Mehta, A. S. *J. Am. Chem. Soc.* **1963**, *85*, 1949.

[37] Wang, G.; Weng, Y.; Chu, D.; Xie, D.; Chen, R. *J. Membr. Sci.* **2009**, *326*, 4.

[38] Yan, X.; He, G.; Gu, S.; Wu, X.; Du, L.; Zhang, H. *J. Membr. Sci.* **2011**, *375*, 204.

[39] Pan, J.; Lu, S. F.; Li, Y.; Huang, A. B.; Zhuang, L.; Lu, J. T. *Adv. Funct. Mater.* **2010**, *20*, 312.

[40] Fang, J.; Shen, P. K. *J. Membr. Sci.* **2006**, *285*, 317.

[41] Neagu, V.; Bunia, I.; Plesca, I. *Polym. Degrad. Stab.* **2000**, *70*, 463.

[42] Bauer, B.; Strathmann, H.; Effenberger, F. *Desalination* **1990**, *79*, 125.

[43] Li, X.; Yu, Y.; Liu, Q.; Meng, Y. *Int. J. Hydrogen Energy* **2013**, *38*, 11067.

[44] Rao, A. H. N.; Thankamony, R. L.; Kim, H.-J.; Nam, S.; Kim, T.-H. *Polymer* **2013**, *54*, 111.

[45] Henkensmeier, D.; Cho, H.-R.; Kim, H.-J.; Nunes Kirchner, C.; Leppin, J.; Dyck, A.; Jang, J. H.; Cho, E.; Nam, S.-W.; Lim, T.-H. *Polym. Degrad. Stab.* **2012**, *97*, 264-272.

[46] Henkensmeier, D.; Kim, H.-J.; Lee, H.-J.; Lee, D. H.; Oh, I.-H.; Hong, S.-A.; Nam, S.-W.; Lim, T.-H. *Macromol. Mater. Eng.* **2011**, *296*, 899.

[47] Lee, H. J.; Choi, J.; Han, J. Y.; Kim, H. J.; Sung, Y. E.; Kim, H. *Polym. Bull.* **2013**, *70*, 2619.

[48] Thomas, O.D.; Soo, K. J. W. Y.; Peckham, T. J.; Kulkarni, M. P.; Holdcroft, S. *J. Am. Chem. Soc.*, **2012,** *134*, 10753.

[49] Brinker, K. C.; Robinson, I. M.U. S. Patent 2,895,948, 1959.

[50] Vogel, H. A.; Marvel, C. S. *J. Polym. Sci.***1961**, *50*, 511.

[51] Vogel, H.; Marvel, C. S. *J. Polym. Sci. A* **1963**, *1*, 1531.

[52] Plummer. L.; Marvel, C. S. *J. Polym. Sci. A* **1964**, *2*, 2559.

[53] Marvel, C. S.; Ariz, T.; Vogel, H. A. U. S. Patent 3,174,947,1965.

[54] Choe, E. W.; Choe, D. D. *InPolymeric Materials Encyclopedia*; Salamone, J. C.; CRC Press: New York, **1996,** 5619.

[55] Lee, H.; Stoffey, D.; Neville, K. *New Linear Polymers;* McGraw-Hill, New York, **1967**, Chapter 9.

[56] Frazerr, A. H. High *Temperature Resistant Polymers;* Interscience: New York,

1968, 138.

[57] Critchley, J. P. *Prog. Polym. Sci*. **1970**, *2*, 47.

[58] Neuse, E. W. *Adv. Polym. Sci.* **1982**, *47*, 1.

[59] Power, E. D.; Serad, G. A. *High Performance Polymer: Their origin and Development*, Elesevier, New York, **1986**, 355.

[60] Buckley, A.; Stuetz, D.; Serad, G.A. *Encyclopedia of Polymer Science andEngineering*, Wiley, New York, **1987**, 572.

[61] Critchley, J. P.; Knight, G. J.; Wright, W.W. *Heat-resistant Polymers*, Plenum Press, New York, **1983**,259.

[62] Prince A. E. U. S. Patent 3,509,108, 1970.

[63] Eguchi, T.; Ohfuji, Y. U. S. Patent 3,655,632, 1972.

[64] Neuse, E.W.; Loonat, M. S. *Macromolecules* **1983**, *16*, 128.

[65] Brand, R. A.; Bruma, M.; Kellman, R.; Marvel, C. S. J. *Polym. Sci., Polym. Chem.Ed.* **1978**, *16*, 2275.

[66] Higgins, J.; Marvel, C. S. *J. Polym. Sci.* **1970**, *A-1*, 171.

[67] Iwakura,Y.; Uno, K.; Imai, Y. *J. Polym. Sci.* **1964**, *A2*, 2605.

[68] Li, Q.;He, R.;Jensen, J. Q.; Bjerrum, N. J. *Chem. Mater*. **2003**, *15*, 4896.

[69] Xiao, L.; Zhang, H.; Scanlon, E.; Ramanathan, L. S.; Choe, E. W.; Rogers, D.; Apple, T.; Benicewicz, B. C. *Chem. Mater*. **2005**, *17*, 5328.

[70] Li ,Q.; Jensena, J. O.; Savinell, R. F.; Bjerrum, N. J. *Prog. Polym. Sci.* **2009**, *34*, 449.

[71] Lobato, J.; Caenizares, P.; Rodrigo, M. A.; Linares, J. J.; Manjavacas, G. *J. Membr. Sci.* **2006**, *280*, 351.

[72] Xu, H.; Chen, K.; Guo, X.; Fang, J. *Polymer* **2007**, *48*, 5541.

[73] Chen, C. C.; Wang, L. F.; Wang, J. J.; Hsu, T. C.; Chen, C. F. *J. Mater. Sci*. **2002**, *37*, 4109.

[74] Sannigrahi, A.; Ghosh, S.; Lalnuntluanga, J.; Jana, T. *J. Appl. Polym. Sci*. **2009**, *111*, 2194.

[75] Asensio, J. N.; Borros, S.; Gomez-Romero, P. *J. Electrochem. Soc. A* **2004**, *151*,

304.

[76] Maity, S.; Jana, T. *Macromolecules* **2013**, *46*, 6814.

[77] Xiao, L.; Zhang, H.; Jana, T.; Scanlon, E.; Chen, R.; Choe, E. W.; Ramanathan, L. S.; Yu, S.; Benicewicz, B. C. *Fuel Cells* **2005**, *5*, 287.

[78] Sannigrahi, A.; Ghosh, S.; Maity, S.; Jana, T. *Polymer* **2010**, *51*, 5929.

[79] Jouanneau, J.; Mercier, R.; Gonon, L.; Gebel, G. *Macromolecules* **2007**, *40*, 983.

[80] Sansone,M. J. U. S Patent 4 666 996, 1987.

[81] Jorgensen,B. S.;Young, J. S.; Espinoza,B. F. U. S Patent 6,946,015, 2004.

[82] Wang, K. Y.;Xiao,Y. C. Chung, T. S. *Chem. Eng. Sci*. **2006**, *61*, 5807.

[83] Xu, H.;Chen, K.; Guo, X.; Fang,J.; Yin, J. *J. Membr. Sci*. **2007**, *288*, 255.

[84] Carollo, A.; Quartarone, E.; Tomasi, C.; Mustarelli, P.; Belotti, F.; Magistris, A.; Maestroni, F.; Parachini, M.; Garlaschelli, L.; Righetti, P. P. *J. Power Sources* **2006**, *160*, 175.

[85] Chuang, S. W.; Hsu, S. L. C. *J. Polym. Sci., Part A: Polym. Chem*. **2006**, *44*, 4508.

[86] Maity, S.; Sannigrahi, A.; Ghosh, S.; Jana, T. *Euro. Polym. J.* **2013**, *49*, 2280.

[87] Klahen, J. R.; Luther, T. A.; Orme, C. J.; Jones, M. G.; Wertsching, A. K.; Peterson, E. S. *Macromolecules* **2007**, *40*, 7487.

[88] Gieselman, M. B.; Reynolds, J. R. *Macromolecules* **1992**, *25*, 4832.

[89] Sannigrahi, A.; Arunbabu, D.; Sankar, R. M.; Jana, T. *J. Phys. Chem. B* **2007**, *111*, 12124.

[90] Qing, S.; Huang, W.; Yan, D. *Euro. Poly. J.* **2005**, *41*, 1589.

[91] Pu, H. T.; Liu, Q. Z. ; Liu, G. H. *J. Membr. Sci.* **2004**, *241*, 169.

[92] J. T. Wang, J. Wainright, H. Yu, M. Litt and R. F. Savinell, Proc.-Electrochem. Soc. 95–23 (Proton Conducting Membrane Fuel Cells I), 1995, 202–213.

[93] Xing, B.; Savadogo, O. *J. New Mater. Electrochem. Systems* **2000**, *3*, 345.

[94] Li, Q.; Jensena, J. O.; Savinell, R. F.; Bjerrum, N. J. *Prog. Polym. Sci.* **2009**, *34*, 449.

[95] Savinell, R.; Yeager, E.; Tryk, D.; Landau, U.; Wainright, J.; Weng, D.; Lux, K.; Litt, M.; Rogers, C. *J. Electrochem. Soc.* **1994**, *141*, L46.

[96] Samms, S. R.; Wsmus, S.; Savinell, R. F. J. *Electrochem. Soc.* **1996**, *143*, 1225.

[97] Mader, J.; Xiao, L.; Schmidt, T, J.; Benicewicz, B, C. *Adv Polym Sci.* **2008**, *216*, 63.

[98] Zhang, J.; Xie, Z.; Zhang, J.; Tang, Y.; Song, C.; Navessin, T.; Shi, Z.; Song, D.; Wang, H.; Wilkinson, D. P.; Liu, Z.-S.; Holdcroft, S. *J. Power Sources* **2006**, *160*, 872.

[99] Wainright, J. S.; Wang, J-T.; Weng, D.; Savinell, R. F., Litt, M. *J. Electrochem. Soc.* **1995**, *142*, L121.

[100] Bouchet, R.; Siebert, E. *Solid State Ionics.* **1999**, *118*, 287.

[101] Xing, B.; Savadogo, O. *J. New. Mater. Electrochem. Syst.* **1999**, *2*, 95.

[102] Pu, H.; Meyer, W.; Wegner, G. *J. Polym. Sci., Part B: Polym. Phys.* **2002**, *40*, 663.

[103] Li, M. Q.; Shao, Z. G.; Scott, K. *J. Power Sources* **2008**, *183*, 69.

[104] Quartarone, E.; Mustarelli, P.; Carollo, A.; Grandi, S.; Magistris, A.; Gerbaldi, C. *Fuel Cells* **2009**, *9*, 231.

[105] Mustarelli, P.; Quartarone, E.; Grandi, S.; Carollo, A.; Magistris, A. *Adv. Mater.* **2008**, *20*, 1339.

[106] Suryani; Liu, Y. L. *J. Membr. Sci.* **2009**, *332*, 121.

[107] Li, Q. F.; Hjuler, H. A.; Bjerrum, N. J. *J. Appl. Electrochem.* **2001**, *31*, 773.

[108] Lin, H. L.; Chen, Y. C.; Li, C. C.; Cheng, C. P.; Yu, T. L. *J. Power Sources* **2008**, *181*, 228.

[109] Lin, H. L.; Hsieh, Y. S.; Chiu, C. W.; Yu, T. L.; Chen, L. C. *J. Power Sources* **2009**, *193*, 170.

[110] Kerres, J.; Schonberger, F.; Chromik, A.; Haring, T.; Li, Q.; Jensen, J. O.; Pan, C.; Noye, P.; Bjerrum, N. J. *Fuel Cells* **2008**, *8*, 175.

[111] Li, Q.; Jensen, J. O.; Pan, C.; Bandur, V.; Nilsson, M. S.; Schonberger, F.; Chromik, A.; Hein, M.; Haring, T.; Kerres, J.; Bjerrum, N. J. *Fuel Cells* **2008**, *8*,

188.

[112] Li, M. Q.; Scott, K. *Electrochim. Acta* **2010**, *55*, 2123.

[113] Larson, J. M.; Hamrock, S. J.; Haugen, G. M.; Pham, P.; Lamanna, W. M.; Moss, A. B. *J. Power Sources* **2007**, *172*, 108.

[114] Noy, P.; Li, Q. F.; Pan, C.; Bjerrurn, N. *J. Polym. Adv. Technol.* **2008**, *19*, 1270.

[115] Jiang, F. J.; Pu, H. T.; Meyer, W. H.; Guan, Y. S.; Wan, D. C. *Electrochim. Acta* **2008**, *53*, 4495.

[116] Ye, H.; Huang, J.; Xu, J. J.; Kodiweera, N. K. A. C.; Jayakody, J. R. P.; Greenbaum, S. G. *J. Power Sources* **2008**, *178*, 651.

[117] Hong, S. G.; Kwon, K.; Lee, M. J.; Yoo, D. Y. *Electrochem. Commun.* **2009**, *11*, 1124.

[118] Kim, T. H.; Lim, T. W.; Lee, J. C. *J. Power Sources* **2007**, *172*, 172.

[119] Yu, S.; Xiao, L.; Benicewicz, B. C. *Fuel Cells* **2008**, *8*, 165.

[120] Yu, S.; Zhang, H.; Xiao, L.; Choe, E. W.; Benicewicz, B. C. *Fuel Cells* **2009**, *9*, 318.

[121] Diaz, L. A.; Abuin, G. C.; Corti, H. R. *J. Power Sources* **2009**, *188*, 45.

[122] Wannek, C.; Kohnen, B.; Oetien, H. F.; Lippert, H.; Mergel, J. *Fuel Cells* **2008**, *8*, 87.

[123] Wannek, C.; Lehnert, W.; Mergel, J. *J. Power Sources* **2009**, *192*, 258.

[124] Kim, T. H.; Lim, T. W.; Park, Y. S.; Shin, K.; Lee, J. C. *Macromol. Chem. Phys.* **2007**, *208*, 2293.

[125] Kim, S. K.; Kim, T. H.; Jung, J. W.; Lee, J. C. *Macromol. Mater. Eng.* **2008**, *293*, 914.

[126] Qian, G. Q.; Benicewicz, B. C. *J. Polym. Sci., Part A: Polym. Chem.* **2009**, *47*, 4064.

[127] Chuang, S. W.; Hsu, S. L. C.; Hsu, C. L. *J. Power Sources* **2007**, *168*, 172.

[128] Schechter, A.; Savinell, R. F. *Solid State Ionics* **2002**, *147*, 181.

[129] Mader, J.; Xiao, L.; Schmidt, T, J.; Benicewicz, B, C. *Adv. Polym. Sci.* **2008**, *216*, 63.

[130] Yu, S.; Benicewicz, B. C. *Macromolecules* **2009**, *42*, 8640.

[131] Mecerreyes, D.; Grande, H.; Miguel, O.; Ochoteco, E.; Marcilla, R.; Cantero, I. *Chem. Mater.* **2004**, *16*, 604.

[132] Sampath, U. G.; Ching, Y. C.; Chuah, C. H.; Sabariah, J. J.; Lin, P. C. *Materials* **2016,** *9*, 991.

[133] Ghosh, S.; Sannigrahi, A.; Maity, S.; Jana, T. *J. Phys. Chem. C* **2011**, *115*, 11474.

[134] Ghosh, S.; Maity, S.; Jana, T. *J. Mater. Chem.* **2011**, *21*, 14897.

[135] Wang, S.; Zhao, C.; Ma, W.; Zhang, N.; Zhang, Y.; Zhang, G.; Liu, Z.; Na,H.*J. Mater. Chem. A* **2013**, *1*, 621.

[136] Cao, T.; Webber, S. E. *Macromolecules* **1995**, *28*, 3826.

[137] Loy, D. A.; Assink, R. A. *J. Am. Chem. Soc*. **1992**, *114*, 3977.

[138] Ajayan, P. M.; Stephen, O.; Colliex, C.; Trauth, D. *Science* **1994**, *265*, 1212.

[139] Ajayan, P. M.; Schadler, L. S.; Giannaris, C.; Rubio, A. *Adv. Mater.* **2000**, *12*, 750.

[140] Vaia, R. A.; Krishnamoorti, R. *In Polymer Nanocomposites: Synthesis Characterization and Modeling; American Chemical Society:* Washington, DC, **2001**, *1*.

[141] (a) Althues, H.; Henle, J.; Kaskel, S. *Chem. Soc. Rev.* **2007**, *36*, 1454, (b) Kickelbick, G. *Prog. Polym. Sci.* **2003**, *28*, 83. (c) Antonucci, P. L.; Arico, A. S.; Creti, P.; Ramunni, E.; Antonucci, V. *Solid State Ionics* **1999**, *125*, 431, (d) Akcora, P.; Liu, H.; Kumar, S. K.; Moll, J.; Li, Y.; Benicewicz, B. C.; Schadler, L. S.; Acehan, D.; Panagiotopoulos, A. Z.; Pryamitsyn, V.; Ganesan, V.; Ilavsky, J.; Thiyagarajan, P.; Colby, R. H.; Douglas, J. F. *Nat. Mater.* **2009**, *8*, 354.

[142] Verdejo, R.; Bernal, M. M.; Romasanta, L. J.; Lopez-Manchado, M. A. *J. Mater. Chem*. **2011**, *21*, 3301

[143] He, R.; Li, Q.; Xiao, G.; Bjerrum, N. J. *J. Membr. Sci*. **2003**, *226*, 169.

[144] Staiti, P.; Minutoli, M.; Hocevar, S.*J. Power Sources* **2000**, *90*, 231.

[145] Staiti, P. *Mater. Lett.* **2001**, *47*, 241.

[146] Javaid Zaidi, S.M. *Electrochem. Acta*. **2005**, *50*, 4771.

[147] Shao, H.; Shi, Z.; Fang, J.; Yin, J. *Polymer* **2009**, *50*, 5987.

[148] Kang, J. Y.; Eo, S. M.; Jeon, I. Y.; Choi, Y. S.; Tan, L. S.; Baek, J. B. *J . Polym. Sci.: Part A: Polym. Chem.* **2010**, *48*, 1067.

[149] Singha, S.; Jana, T. *ACS Appl. Mater. Interface*, **2014**, *6*, 21286.

Chapter 2

Materials and Experimental methods

This chapter describes the source of materials, detailed experimental procedures, all the characterization techniques and the corresponding instruments used in Chapters 3 to 7.

2.1. MATERIALS

Formic acid (99%) and ortho phosphoric acid (85%) were purchased from Merck, India. D (+)-10-Camphorsulfoinc acid (CSA) was obtained from Acros Organics. P-toluenesulfonic acid (PTSA), potassium hydroxide (KOH) and potassium carbonate (K_2CO_3) was obtained from Thomas Chemicals Limited. Mono-n-dodecyl phosphate, (MDP) was purchased from Alfa Aesar Chemicals, India. Acetic acid (99.5%), dimethylacetamide (DMAc), dimethyl sulphoxide (DMSO), dimethyl formamide (DMF), *N*-methyl-2-pyrrolidone (NMP), sulphuric acid (99.8%), sodium hydride (NaH) and methyl iodide (CH_3I) were procured from Finar Chemicals Ltd, India. Ammonium acetate (96%), acetic anhydride (97%), hydrogen peroxide and hydrazine monohydrate were obtained from Fisher Scientific, India. Fuming nitric acid was purchased from Faiz chemicals, India. Isophthalic acid (IPA), terephthalic acid (TPA), p-hydroxy benzaldehyde, benzaldehyde and 4-amino acetophenone were procured from SRL, India. The NMR solvent dimethyl sulfoxide (DMSO-d_6), 5-*tert*-butyl isophthalic acid, (3, 3', 4, 4'-tetraaminobiphenyl (TAB), butyl iodide, isobutyl iodide, 4, 4′-oxybis (benzoic acid) (OBA), 4,4′-dicarboxy benzophenone (BPDA), 4, 4′-(hexafluoroisopropylidene) bis (benzoic acid) (HFIPA), polyphospharic acid (PPA, 115%), 3-(trifluoro methyl) benzaldehyde and 4-formyl benzoic acid were procured from Sigma-Aldrich, India. All chemicals were used without further purification.

Synthesis of monomers, polymers, composites, fabrication of both proton and alkaline anion exchange membranes and all other sample preparation details are discussed in the individual chapters for better clarity.

2.2. CHRACTERIZATION MEHODS

2.2.1. Viscosity measurement

The viscosity measurements of the polymer solutions in H_2SO_4 were carried out at 30 °C in water bath with the help of Cannon (model F725) Ubbelohde capillary dilution viscometer and the inherent viscosity (I.V.) values are calculated from the flow time

data. For all the flow time measurements, 0.2 g/dL polymer solution in H_2SO_4 (98 %) were used. The molecular weight of PBI in the literature has been expressed in terms of I.V. measured from sulfuric acid solution.

2.2.2. Spectroscopy studies

2.2.2.1. FT-IR study

The infrared spectra of all the various type of proton exchange membranes (PEMs) (3 and 4 chapters) and anion exchange membranes (AAEMs) (5, 6 and 7 chapters) were taken on a Nicolet 5700 FTIR spectrometer at a resolution of 0.5cm^{-1} with an average of 32 scans.

2.2.2.2. ^{13}C CPMAS solid state NMR study

Solid-state ^{13}C CPMAS NMR spectra (in the Chapters 3) of ASM composite samples were obtained at ambient temperature with Bruker AV 400 MHz NMR spectrometer operating at 500 MHz at a spinning rate of 5 kHz and a contact time of 2 ms.

2.2.2.3. ^{1}H NMR study

The proton NMR spectra of various pyridine bridged polybenzimidazoles (PyPBI) polymers and different type of AAEMs (carried out for Chapters 5, 6 and 7) were recorded by using Bruker AV 400 MHz NMR spectrometer at room temperature using DMSO-d_6 as NMR solvent. The degree methylation, degree of alkylation and degree of degradation was estimated from ^{1}H NMR spectra.

2.2.3. Solubility test

The solubility of different type of derivatives of pyridine based polybenzimidazoles (PyPBI) polymers were checked in common organic solvents such as DMAc, DMSO, DMF, NMP, FA, MSA and H_2SO_4. The solubility was checked up to 2 wt%. The solubility was first carried out at room temperature and as well as at heating condition.[1]

2.2.4. Thermal analysis

The thermal stability studies of all the PEMs (used in Chapters 3 and 4) were investigated using a model (Netzsch STA 409 PC) TG-DTA instrument and AEMs (used in Chapters 5-7) was conducted on a model (TGA Q 500) TG-DTA instrument operated at a scanning rate of 10 °C / min starting from 30 °C to 800 °C under nitrogen gas purging.

2.2.5. Mechanical stability study

2.2.5.1 Dynamic mechanical analysis (DMA)

The temperature dependent dynamic mechanical stability studies of all samples were carried out using dynamic mechanical analyzer (DMA model Q-800 TA) Instruments. The membranes were cut in 25 mm × 5 mm × 0.03 mm (L × W × T) dimension and clamped on to the fixed tension clamp of the instrument. The samples were first annealed at 400 °C for 20 minutes followed by equilibration at 100 ºC for 20 minutes and then scanned from 100 °C to 450 °C at a scanning rate of 4 °C/min. The storage modulus (E'), loss modulus (E'') and tan δ values were measured at a linear frequency of 1 Hz or 10Hz with a preload force of 0.01 N.

2.2.5.2 Universal testing measurement (UTM)

The tensile properties (stress-strain relationship) of the membranes (used in Chapter 5, 6 and 7) were performed using Universal Testing Machine, UTM (Instron instrument, model No.5965). Dumbbell shaped specimens were prepared from membranes following ASTM standard D638 (Type IV specimen) and fixed between the holders and pulled at a cross-head speed of 10 mm/min. The measurements were done at room temperature. All measurements were repeated three times to check for the reproducibility.

2.2.6. Wide angle x-ray diffraction

The wide angle X-ray diffraction patterns (WAXD) of all membrane samples (in

the Chapters 3) were obtained from Philips powder diffraction instrument (model PW 1830). The samples were placed on a glass slide, and the diffractograms were recorded with Cu Kα radiation (λ = 1.5406 Å) operated at 40 kV and 30 mA current in the angular range (2θ) of 5-60° at a scanning rate of 1°/1.3 minutes.

2.2.7. Phosphoric acid loading

For polyphosphoric acid (PA) doping level measurement of all the membranes was doped in PA for 5 days (in Chapter 3) and 3 days (in Chapter 4). Then the membranes were taken out, excess acid wiped off and titrated against pre-standardized 0.1 N sodium hydroxide using Metrohm autotitrator (model 702). The PA doping level was calculated as the number of moles of PA present per PBI repeat unit. The measurement was performed in triplicate with three similar-size samples to ensure the reproducibility of the results. The PA loading levels reported in the 3 and 4 chapters are the average values of the three measurements.

2.2.8. Water uptake, swelling ratio and swelling volume in water and PA

For water uptake, swelling ratio and swelling volume measurements in both water and acid, initially the membranes were dried thoroughly in vacuum oven at 100 ºC for 24 hours. The similar sized membranes were taken in triplicate and their weights and dimensions are noted. They were then immersed in de-ionized water for 5 days for composites and 3 days for PyPBI derivatives (for measurements in water and PA). The AAEMs which is used in 5, 6 and 7 chapters, those samples immersed in de-ionized water for 24 hours. After the specified time period the wet membranes were wiped with filter paper and their dimensions and weights noted again. Water uptake, swelling ratio and swelling volume were calculated as the following equations.

$$\text{Water Uptake} = \frac{W_w - W_d}{W_d} \times 100\ \% \qquad (2.1)$$

$$\text{Swelling ratio in PA and water} = \frac{L_w - L_d}{L_d} \times 100\ \% \qquad (2.2)$$

$$\text{Swelling Volume in PA and water} = \frac{V_w - V_d}{V_d} \times 100\,\% \qquad (2.3)$$

Where, W_w, L_w and V_w are the weight, length and volume of the wet membranes, respectively and W_d, L_d and V_d are the weight, length and volume of the dry membranes, respectively. These measurements were carried out in triplicate independently with three similar sized pieces of the membranes to check for reproducibility and the average values were reported in all the chapters.

2.2.9. Oxidative stability

The oxidative stability of the derivatives of PyPBI polymer membranes (used in Chapter 4) were investigated by immersing the membranes into Fenton's reagent (3% H_2O_2 aqueous solution containing 4 ppm ammonium iron (II) sulfate, or Mohr's Salt) at 70 °C. Five similar sized pieces of the membranes were taken for Fenton's test. The oxidative stability was measured for time variation up to 100 hours. The membranes were taken out at certain time intervals, dried in vacuum oven at 100 °C for 24 hours, and again weights were recorded. The oxidative stabilities of all the membranes were calculated as a weight remained after taking out the membranes from the Fenton's reagent.

2.2.10. Proton conductivity study

Proton conductivity of all the PA doped membranes was measured with Zahner Impedance spectrometer (ZENNIUM PP211) over the frequency range 1 Hz to 100 kHz. The membranes were fixed to a homemade Teflon conductivity cell (Figure 2.1) with four platinum electrodes; two outer electrodes 1.5 cm apart supply current to the cell, while the two inner electrodes 0.5 cm apart on opposite sides of the membrane measure the potential drop across the electrodes. The conductivity cell setup along with the membrane was heated at 100 ºC for 2 hours inside the oven, to remove absorbed moisture from the membrane completely. After which cell setup was shifted into the desiccator for allowing cooling to room temperature. The conductivity was measured from room temperature to 180 °C at 20 °C intervals. The samples were held for 30

minutes at each temperature to reach equilibrium and after which impedance was measured. The proton conductivity was calculated using by the given following equation.

$$\sigma = \frac{D}{LBR} \qquad (2.4)$$

Where, σ is the proton conductivity ($S.cm^{-1}$), D is the distance between the two platinum electrodes, B and L are the thickness and width of the membranes, respectively and R is the resistance obtained from Nyquist plots. Figure 2.2 shows a schematic diagram of Nyquist plot.

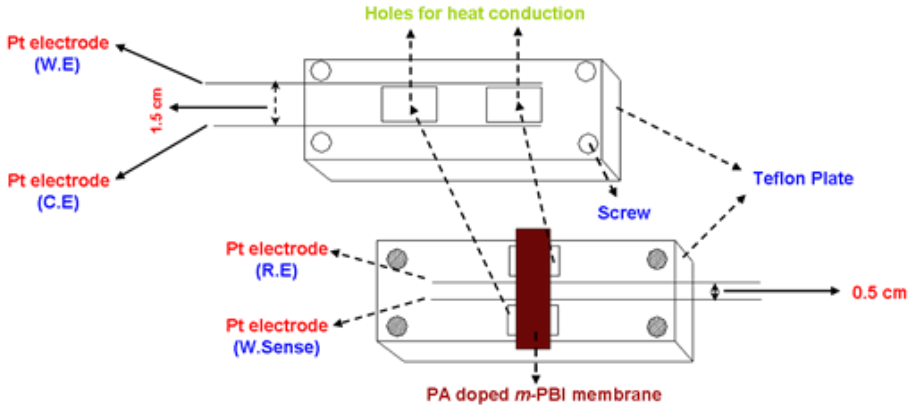

Figure 2.1 *Home-made Teflon conductivity cell used to measure proton conductivity of PA-doped membranes. The two parts as shown in the figure are clamped together by screws and the cell was kept inside a programmable oven to control temperature (Taken from reference 2).*

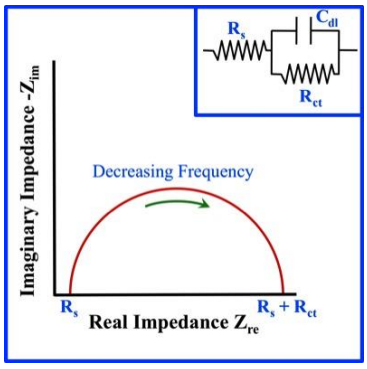

Figure 2.2 *Schematic representation of Nyquist plot. (Adopted from google image)*

2.2.11. Acid retention test

The acid leaching test was performed for the membrane of OPBI and its composite membranes (in Chapter 3) according to the previous reports.[3, 4] The doped membranes were taken out from the phosphoric acid bath medium and excess phosphoric acid was removed by mopped with a tissue paper and their initial weights noted down. The membranes were then placed under the vapour condition at 100 °C for a period of three hours and the weight of the membrane (W_i) after every half an hour was recorded after removing the leached acid from the membrane. The weight loss ratio of acid in the membranes was calculated by using the following formula:

$$R = \frac{W_o - W_i}{W_a} \times 100\ \% \qquad (2.5)$$

Where, W_o is the initial weight of the PA doped membrane, W_i is the weight of the dried PA membrane after leaching at different times and W_a is the original weight of PA present in the membranes calculated from the PA doping level of the membranes.

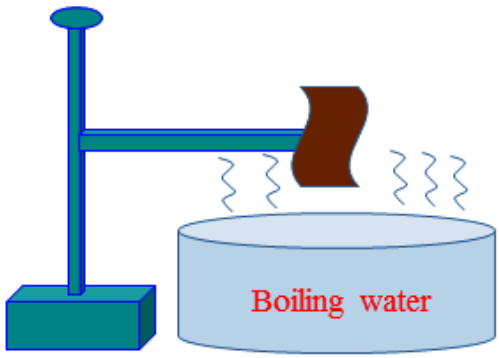

Figure 2.3 *Schematic representation of acid retention test performed in the wet laboratory. (Adopted from S. Singha thesis, UOH, 2015)*

2.2.12. Ion exchange capacity

Ion exchange capacity measurement was performed for alkylated and cross-linked pyridinium benzimidazolium membranes in Chapter 5, 6 and 7, respectively. Ion

exchange capacity (IEC) of the aqueous KOH doped or K_2CO_3 doped membranes was determined by back titration method using an autotitrator (Metrohm model 702 SM titrino). The membrane was soaked in 35 mL of 0.01 M aqueous HCl solution for 48 h, followed by back titration with 0.01 M aqueous KOH solution and used phenolphthalein as an indicator. The IEC was calculated by the given following equation.

$$IEC\ (meq/g) = (V_{x\ KOH} \times C_{KOH} - V_{o\ KOH} \times C_{KOH})/W_{dry} \quad (2.6)$$

Where $V_{o\ KOH}$ and $V_{x\ KOH}$ are the volume of the KOH used in the titration without and with membrane, respectively, C_{KOH} is the mole concentration of the KOH which is titrated by the standard oxalic acid solution, and W_{dry} is the weight of the dried membrane.

2.2.13. Alkaline stability study

The anion exchange membranes (used in Chapters 5, 6 and 7) were immersed in various concentrated alkaline solutions aqueous (KOH or K_2CO_3) at room temperature and on heating at different temperatures. The alkaline stability of all the anion exchange membranes in basic condition was studied with the time. After completion of alkaline stability studies which was observed at higher temperature, those samples were used to record FT-IR and ^1H NMR spectroscopy to quantify the degree of degradation and propose the degradation mechanism

2.2.14. Microscopy analysis

Cross-section morphology of the PEM and AAEMs studied by using field emission scanning electron microscope (model-Carl Zeiss Ultra-55). It has EHT detector with an accelerating voltage of 5 kV. The cross section of membranes was prepared by breaking the samples in liquid nitrogen medium for FE-SEM analysis.

2.2.15. Ionic conductivity study

Ionic (hydroxide or carbonate) conductivities of the alkali doped (KOH or K_2CO_3) membranes (in Chapters 5, 6 and 7) were measured by AC impedance spectroscopy

using Zahner Impedance spectrometer (ZENNIUM PP211) employing four-probe electrode system. Prior to the measurement, alkali doped membranes were immersed in de-ionized water for 24 hours to avoid the bicarbonate formation from the atmospheric carbon dioxide. After which, this whole conductivity cell set up was placed in deionized water to maintain 100% relative humidity. The ionic conductivities of the membranes were measured at an interval of 10 °C raise from room temperature to 80 °C. At each temperature of the ionic conductivity (resistance) measurement the sample was kept for 30 minutes to attain isothermal equilibrium. The conductivities of the membranes were calculated using equation 2.4. For control experiment, a blank cell (without membrane) was subjected to measurement using the similar protocol as discussed above.

REFERENCES

[1] Sannigrahi, A.; Ghosh, S.; Maity, S.; Jana, T. *Polymer* **2010**, *51*, 5929.

[2] Sannigrahi, A. *Ph.D Thesis*; University of Hyderabad: Hyderabad, India, **2010**.

[3] Pu, H.; Liu, L.; Chang, Z.; Yuan, J. *Electrochim. Acta* **2009**, *54*, 7536.

[4] Pu, H.; Qin, Y.; Tang, L.; Teng, X.; Chang, Z. *Electrochim. Acta* **2009**, *54*, 2603.

Chapter 3

Polybenzimidazole composite with acidic surfactant like molecules: A unique approach to develop PEM for fuel cell

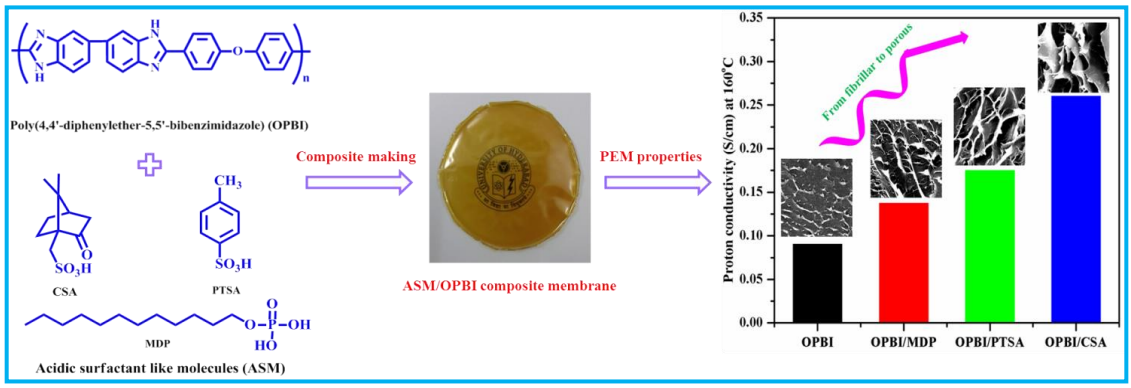

In this work, proton exchange membrane (PEM) based on series of polybenzimidazoles (PBI) composites are prepared with acidic surfactant like molecules (ASMs) with an objective to improve properties of PEM especially proton conductivity. The influences of ASM composite on the properties of PEM were investigated.

Sana, B.; Jana, T. *Eur. Polym. J.* **2016**, *84*, 421-34.

3.1. INTRODUCTION

Fuel cell is an electrochemical energy conversion device which transforms chemical energy directly into electrical energy.[1-3] Over the past few decades, polymer electrolyte membrane fuel cell (PEMFC) has attracted attention of researchers across the world because of the exceptional tunable nature of proton conducting polymeric membrane.[4-7] Until now, many research groups have worked on perfluorosulphonated type (Nafion) membranes because of their chemical and mechanical stabilities along with the long term durability. However, Nafion membrane has number of limitations owing to its high cost and low operation temperature because of dehydration of membrane above 80 °C.[8-11] Inevitably, some researchers have developed sulphonated aromatic polymers as an alternative for Nafion which can operate and be used at high temperature PEMFC (HT-PEMFC).

Blends and composites of several polymers like polyimides[12, 13], polysulphons[14], polybenzoxazoles[15], poly (ether ether ketones)[16-19], poly arylene ethers[20, 21] have been widely investigated for the purpose of use as PEM. Polybenzimidazole (PBI), which has high heat resistance, is also thermally, chemically and mechanically stable due to their rigid structure and therefore has a great potential for use in PEMFCs.[22-24] Savadogo and Xing[25] observed proton conductivity of the PBI membrane with different acids such as H_2SO4, H_3PO4, $HClO_4$ and HCl. The H_3PO_4 doped membrane exhibited more desired properties for fuel cell operation than the PBI membrane doped with other acids.[22] Since then, several authors highlighted the use of phosphoric acid (PA) doped PBI membrane in HT-PEMFC applications.[26-35] The proton conductivity of PA doped PBI membrane is highly dependent on the doping level of phosphoric acid. Several research groups reported that conventional membrane fabrication methods often fail to achieve high acid loading without losing their targeted mechanical properties. Previously our research group has investigated PA doped membrane of the PBI composite with silica and nano clay[36-38] and have reported some limitations. Our groups also reported that the PBI membrane obtained from thermo reversible gel of PBI in PA can entrapped more number of phosphoric acid molecules because of the presence of polymer network.[39]

But, we observed few disadvantages like leaching out of PA from the membrane. In addition, the gel formation is very specific to PBI backbone structure and hence cannot be implemented because all PBI structures may not form gel in PA. Several research groups reported high proton conductivity of PBI membrane by using direct casting method, but such membranes with high PA content give poor mechanical characteristics. Therefore, it remains a challenge to improvise the available methodology for the fabrication of PA doped PBI membrane possessing high proton conductivity, elevated acid loading, low acid leaching, and without disturbing thermo-mechanical properties.

It is worth mention at this point that, in a significant number of reports charged surface modifying macromolecules (CSMM) were used as additives to develop polymeric nanocomposite membranes for the use in fuel cell.[40-45] Here, we used three different kinds of acidic surfactant like molecule (ASM) namely camphor sulfonic acid (CSA), p-toluenesulfonic acid (PTSA) and mono-n-dodecyl phosphate (MDP) for the preparation of composite membranes with poly (4, 4'-diphenylether-5, 5'-bibenzimidazole) (OPBI) polymer. In this way, we wish to achieve high proton conductivity, higher PA doping level and try to decrease the acid leaching by the inclusion of sulphonic and phosphonic functional groups in the composites. Another feature which we may observe here is that the thermal stability of the PA doped composite membrane. To study these composites, several characterizations like isothermal conductivity, swelling properties, isothermal TGA, UV-Visible, WAXD, FT-IR and ^{13}CCPMAS SS-NMR are carried out and compared with pristine OPBI.

3.2 EXPERIMENTAL SECTION

The source of all materials is described in Chapter 2. Synthesis of poly (4, 4'-diphenylether-5, 5'-bibenzimidazole) (OPBI), inherent viscosity or molecular weight of OPBI, Preparation of OPBI/ASM composite membrane and Doping OPBI/ASM composite membranes with phosphoric acid are described as follows.

3.2.1. Polymer synthesis

The poly (4, 4'-diphenylether-5, 5'-bibenzimidazole) (OPBI, Figure 3.1) was synthesized according to the process from our previous reports. Briefly the process is as follows: equal mol ratio of TAB, OBA and polyphosphoric acid (PPA) was placed in a 250 ml 3 neck round bottom flask equipped with mercury sealed overhead mechanical stirrer. The reaction mixture was carried out under inert atmosphere for approximately 26 hrs at 190-220^{o}C temperature. After completion of polymerization reaction, the obtained viscous solution was slowly poured into the cold deionized water and the polymer was obtained in the form of fibre. The polymer was neutralized with sodium bicarbonate solution, filtered and washed thoroughly with deionized water for removing excess base from polymer. Finally the polymer was dried in vacuum oven for 24 h at 100°C temperature and the obtained brown coloured powder stored in desiccator for further characterizations.

3.2.2. Molecular weight of OPBI

The molecular weights of PBI polymers are often judged by measuring inherent viscosity (I.V.) of the polymer, higher I.V. value indicate higher molecular weight. The Inherent viscosity (I.V.) of the poly (4,4'-diphenyl-5,5'-bibenzimidazole) (OPBI) polymer was measured at 30 °C in water bath with the help of Cannon (model F725) Ubbelohde capillary dilution viscometer and the I.V. values are calculated from the flow time data. A solution of OPBI in H_2SO_4 was used for the viscosity measurement. The concentration of the OPBI solution in H_2SO_4 is 0.2 g/dL. The obtained I.V. value of the synthesised OPBI is 2.35 dL/g.

3.2.3. Preparation of OPBI/ASM composite membrane

The entire process for the preparation of OPBI/ASM composite membranes is schematically represented in Figure 3.1. Three types of ASM: CSA, PTSA and MDP were used to make three types of OPBI/ASM composites which are abbreviated as OPBI/CSA, OPBI/PTSA and OPBI/MDP composites, respectively. 2% (w/v) of OPBI

solution were prepared in formic acid by vigorously stirring the polymer in formic acid at room temperature. Required weight% (w/v) of ASM were added to this OPBI solution and vigorously stirred for 24 h at room temperature. The weight% of ASM's was altered in the preparation as follows: 5%, 10%, 15% and 20% with respect to OPBI weight. The composites are abbreviated as OPBI/ASM-X% where ASM are CSA, PTSA and MDP and X are 5, 10, 15, 20. The homogeneous solution so obtained after 24 h was poured on to a clean glass petridish. Solvent was removed from the solution by keeping at 60 °C in an oven for 2-3 h. The composite membrane so formed was peeled off from the petridish. The OPBI/CSA and OPBI/PTSA composite membranes were both transparent and homogeneous. But in the case of OPBI/MDP composite membrane, seemed to possess not much transparency though homogeneous. The membranes were dried in vacuum oven at 100 °C for 24 h to remove any trace amounts of solvent and moisture absorbed by the membrane and then used for further characterization.

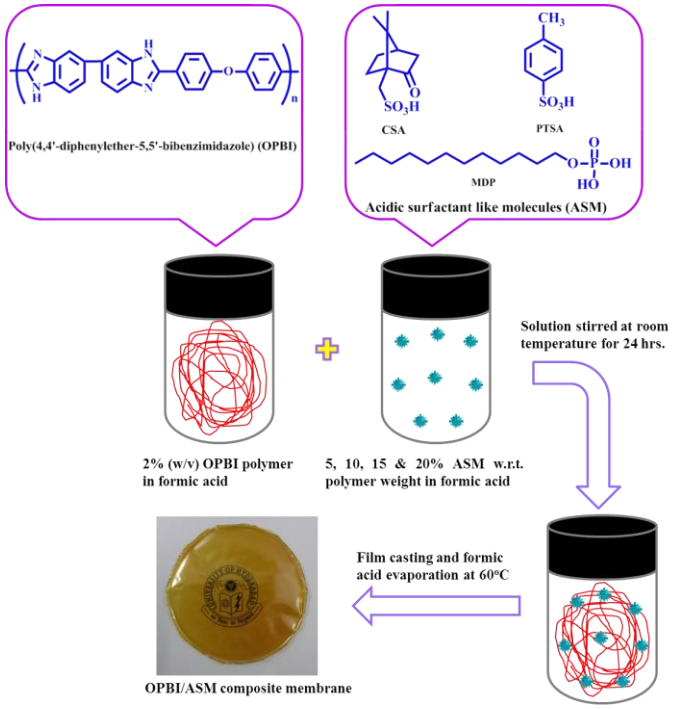

Figure 3.1. *Schematic representation for the preparation of OPBI composite membrane with acidic surfactant like molecule (ASM).*

3.2.4. Doping OPBI/ASM composite membranes with phosphoric acid

The dried composite membranes were dipped in 85% phosphoric acid (PA) for 5 days. Three pieces of membranes of identical size were used for doping study. After 5 days, free standing PA doped membranes were removed from PA bath and excess PA was removed from the surface by using filter paper, and the doped membranes were stored in tightly packed zip-lock covers for further characterizations.

The characterizations which are included are: spectroscopic (FT-IR, SS-NMR), wide angle X-ray, thermal, temperature dependent dynamical mechanical analysis, morphological, doping level, swelling behavior in PA and H_2O, proton conductivity and leaching (acid retention) studies are described in Chapter 2.

3.3 RESULTS AND DISCUSSION

3.3.1. FT-IR Spectroscopy

The IR spectra of OPBI, OPBI/CSA, OPBI/PTSA and OPBI/MDP composite membranes are presented in Figure 3.2A. Only dried samples which were kept at 100 °C in vacuum oven for 24 h were used to record the spectra. In the case of OPBI/CSA membranes, a peak is observed at 1738 cm^{-1} owing to the C=O bond stretching frequency due to the presence of camphor sulphonic acid in the composite.[46] The C=O peak intensity increases with increasing composite loading percentage. In pure CSA, a peak is observed at 1275 cm^{-1} for the stretching frequency of sulphonic group (-S=O). In the case of OPBI/CSA composites, this S=O bond frequency gradually shifts to 1245 cm^{-1} which indicates the interaction between the S=O of CSA and N-H of imidazole group of the OPBI polymer. In the case of pure PTSA, the S=O bond peak is observed at 1165 cm^{-1}, but this peak gradually shifts to 1133 cm^{-1} in OPBI/PTSA composites because of the interaction between PTSA and –N-H group of the OPBI polymer. In pure MDP, the P=O and P-OH bond peaks are observed at 1209 cm^{-1} and 1016 cm^{-1}, respectively[47] due to the presence of phosphate group. But in the case of OPBI/MDP composites, this peak gradually moves to 1160 cm^{-1} and 979 cm^{-1}, respectively because

of the interaction between the MDP and –N-H group of the OPBI polymer. In all the three composite membranes, the peak at 3415 cm^{-1} due to N-H of imidazole group disappears (Figure 3.2B) indicating the strong interaction in composites between –N-H group of the OPBI polymer and functional groups of ASMs.

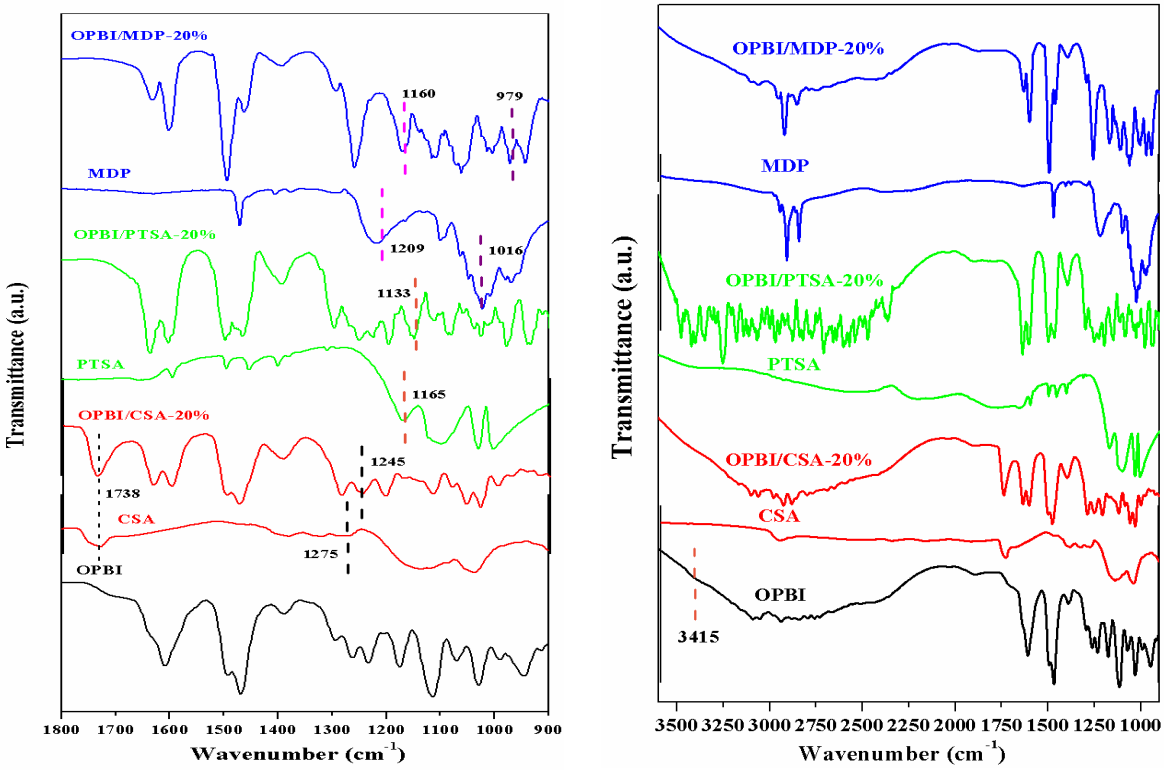

Figure 3.2. *Representative FT-IR spectra of OPBI/ASM-20% composites in the range of interests. Also, pristine OPBI and ASM's (CSA, PTSA and MDP) spectra are incorporated for comparison. Important peaks which are discussed in the text are marked with dotted lines (A). FT-IR spectra of the representative composites along with pristine OPBI and ASMs (B).*

3.3.2. Solid-state NMR (SS-NMR) study

The ^{13}C CPMAS NMR spectra of the OPBI, OPBI/CSA, OPBI/PTSA and OPBI/MDP composites are shown in Figure 3.3 The lines in OPBI spectrum can be recognized as lines arising from the carbons of imidazole rings attached to phenylene rings (151 ppm), the carbons connecting benzimidazole rings in the bibenzimidazole

system (142 ppm), and the aromatic carbons bound to the nitrogen atoms (134 ppm). The remaining ones are 129, 120, 111 ppm also assigned to the other groups as reported by us earlier in the literature.[48] The SS-NMR spectra of OPBI/ASM composite almost similar to that of pristine OPBI except the existence of carbon signals coming from ASM structures. In the case of OPBI/CSA composite membrane, four peaks in higher field region are observed at 18, 40, 45 and 58 ppm corresponding to $-CH_3$, $-CH_2$, -CH and -C groups, respectively and these are due to the presence of CSA in the composite. In the case of OPBI/PTSA composite membrane, the peak at 18 ppm indicates the presence $-CH_3$ group of the PTSA in the composite and for OPBI/MDP composite membrane, three ^{13}C resonances peaks at 13, 30 and 56 ppm are observed corresponding to $-CH_3$, $-CH_2$ and $-CH_2O$ groups of the MDP in the composite. Although SS-NMR spectra did not display any shifting of peaks which may be responsible for interaction between OPBI and ASM, however spectra clearly indicate the presence of both OPBI and ASM peaks in the composites.

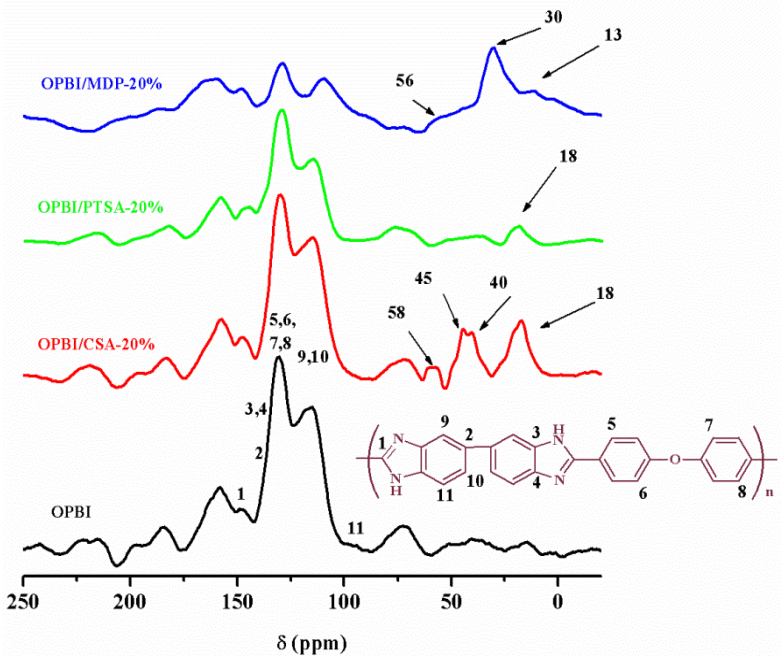

Figure 3.3. *Solid-state ^{13}C CPMAS NMR spectra of OPBI, OPBI/CSA, OPBI/PTSA and OPBI/MDP composite.*

3.3.3. X-ray study

The wide angle X-ray diffraction patterns (WAXD) of OPBI, OPBI/ASM composite membranes are shown in Figure 3.4(A). The OPBI usually exhibit broad peaks which are attributed to the amorphous nature of the polymer as is already reported in the literature. The analysis of the XRD pattern of the three composites reveals the crystalline nature of composite because of the presence of sharp peaks which are coming from the self-organization of ASMs in the polymer matrix. Peaks are more intense (in case of CSA and PTSA composite membranes) than MDP composite[49] and the intensity of the crystalline peaks increases with increasing ASM loading in the composite (Figure 3.5). We believe that the sulphonic acid groups in CSA and PTSA composites strongly interact with the OPBI chains through hydrogen bonding between –S=O and –N-H of imidazole. When ASM loading percentage increases in the composite, then the crystalline peak intensities also increases due to the involvement of more number of sulphonic groups with more number of the OPBI chains. Similarly in the case of MDP composite membranes, the sharp crystalline peaks are attributed to the presence of the hydrogen bonding between the phosphate group and OPBI chains. However the MDP composite membranes diffraction patterns are found to be of less intensity, the reason for which is that the hydrogen bonding interaction of phosphate group is comparatively less with the imidazole group of the OPBI when compared with the sulphonic group of the CSA and PTSA composites.

It has been reported earlier that up to a certain limit of crystallinity of the matrix polymer (in this case OPBI) helps in improving conductivity of acid doped PBI in which acid molecules (means PA) are forced to go to the amorphous region of PBI chain and creates a more proton accessible conduction path.[38] Given this information, we can presume that our OPBI/ASM composites might give better proton conductivity than pristine OPBI since composites have crystallinity (as seen in Figure 3.4) and it should increase with increasing ASM loading as crystallinity increases with increase ASM loading (Figure 3.5). However, one should ensure that this crystallinity of composite membrane remains even after doping/soaking with PA. That is why we

collected PXRD pattern of PA loaded composite membranes and representative pattern are shown in Figure 3.4(B) and Figure 3.6. The XRD pattern of the PA loaded composite membranes show intense sharp peaks and the decrease in sharpness is very little when compared with their dried composite membranes in all the three cases. This attributes that the phosphoric acid molecules could not influence the crystalline nature of composite membranes significantly. Hence, we can expect increase in proton conduction of composite samples from pristine OPBI which is indeed found to be true as will be discussed in later section of this article.

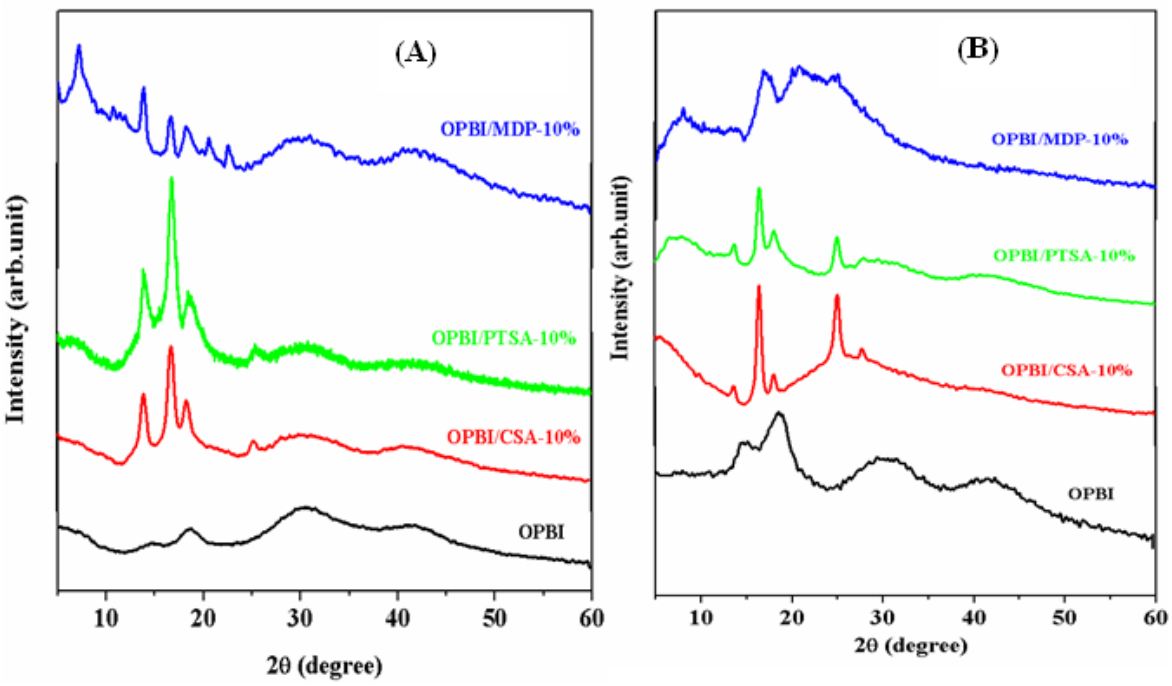

Figure 3.4. *Comparison of PXRD patterns of parent OPBI and OPBI/ASM composites: (A) before PA loading and (B) PA loaded. All 10% weight ASM loading samples patterns are shown in this figure.*

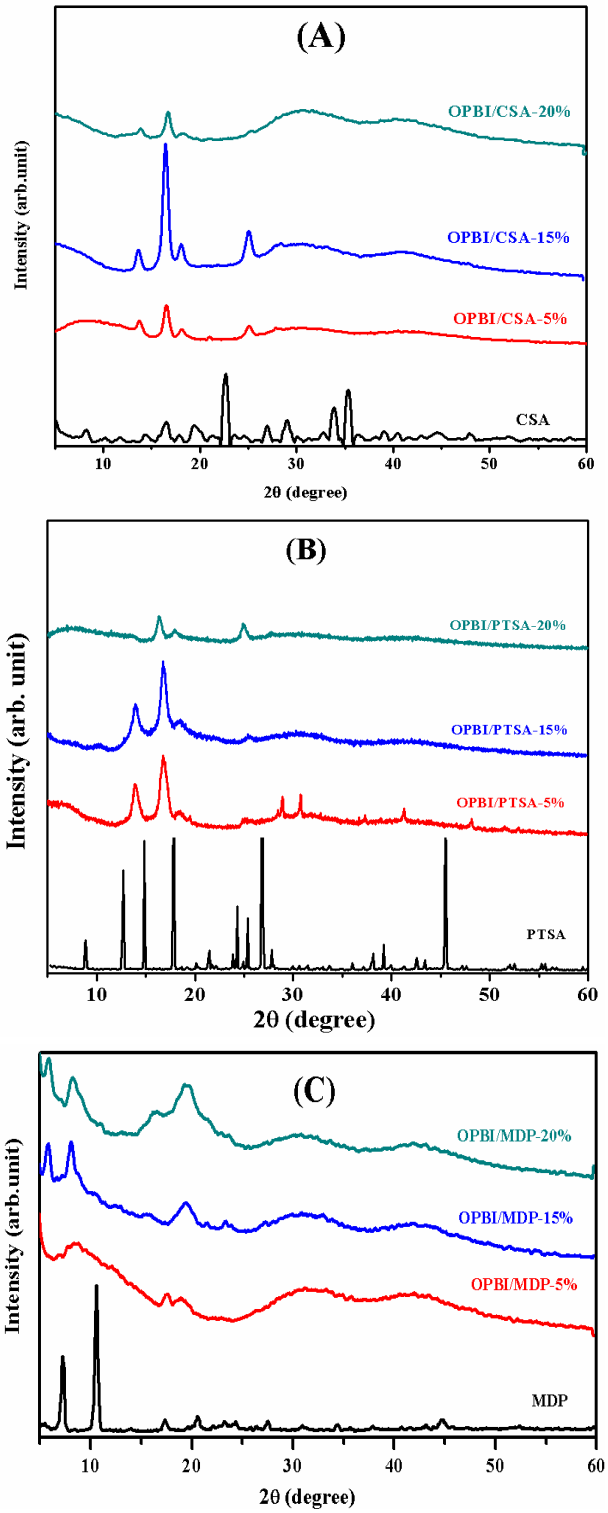

Figure 3.5. *WAXD patterns of OPBI and its composites with ASMs: (A) OPBI/CSA, (B) OPBI/PTSA and (C) OPBI/MDP. Loading in the composites are indicated in the figure.*

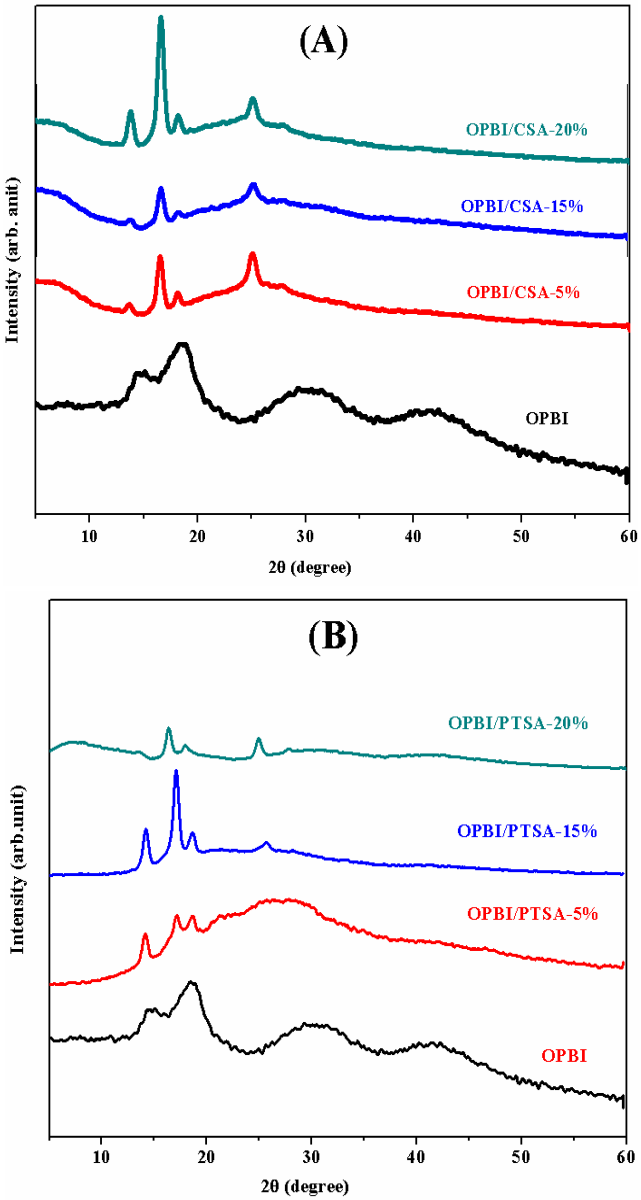

Figure 3.6. *WAXD pattern of the PA loaded OPBI and its composite membranes with different percentage loading of (A) CSA and (B) PTSA.*

3.3.4. Thermal stability

The data obtained from the thermo gravimetric analysis of the OPBI and OPBI/ASM composite membranes are presented in Figure 3.7. The first weight loss is observed in all the cases including pristine OPBI at around 100-110 °C which is due to the loosely bound absorbed water molecules. In case of pure OPBI, sharp weight loss is

spotted at 550 °C due to the degradation of the polymer backbone. In OPBI/CSA and OPBI/PTSA composite membranes, another weight loss is observed at around 150 °C due to the degradation of the -SO_3H groups in CSA and PTSA which may not have formed hydrogen bonds with imidazole group of the OPBI polymer. Another weight loss in these two cases is detected at around 345 °C and 350 °C due to the cleavage of the bicyclic CSA and degradation of the methyl benzene in PTSA, respectively. It is clear from (Figure 3.7 and Figure 3.8) that the thermal stability of OPBI/CSA and OPBI/PTSA composite membranes decreases with increasing loading of ASMs (CSA & PTSA) when compared with the pure OPBI because the CSA and PTSA composites undergo degradation easily. In the case of OPBI/MDP composite membranes (Figure 3.7 and Figure 3.8), the weight loss is observed at 145 °C due to the condensation of the MDP molecules and at around 240 °C which represents the decomposition of the aliphatic hydrocarbon chain in MDP composite. Therefore, overall thermal stability of OPBI/MDP composite membranes also decreases with increasing composite percentage loading (Figure 3.8).

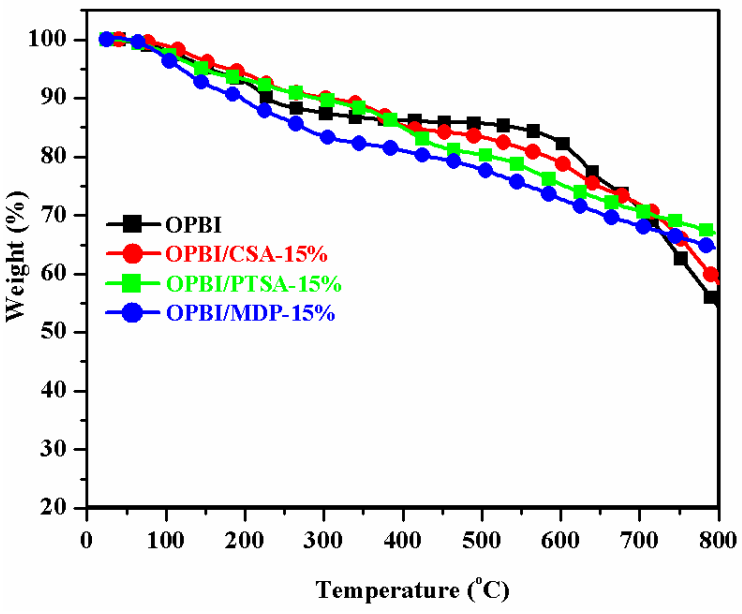

Figure 3.7. *TGA plots of OPBI and its composites with ASM when loading is 15 wt% are shown in this figure.*

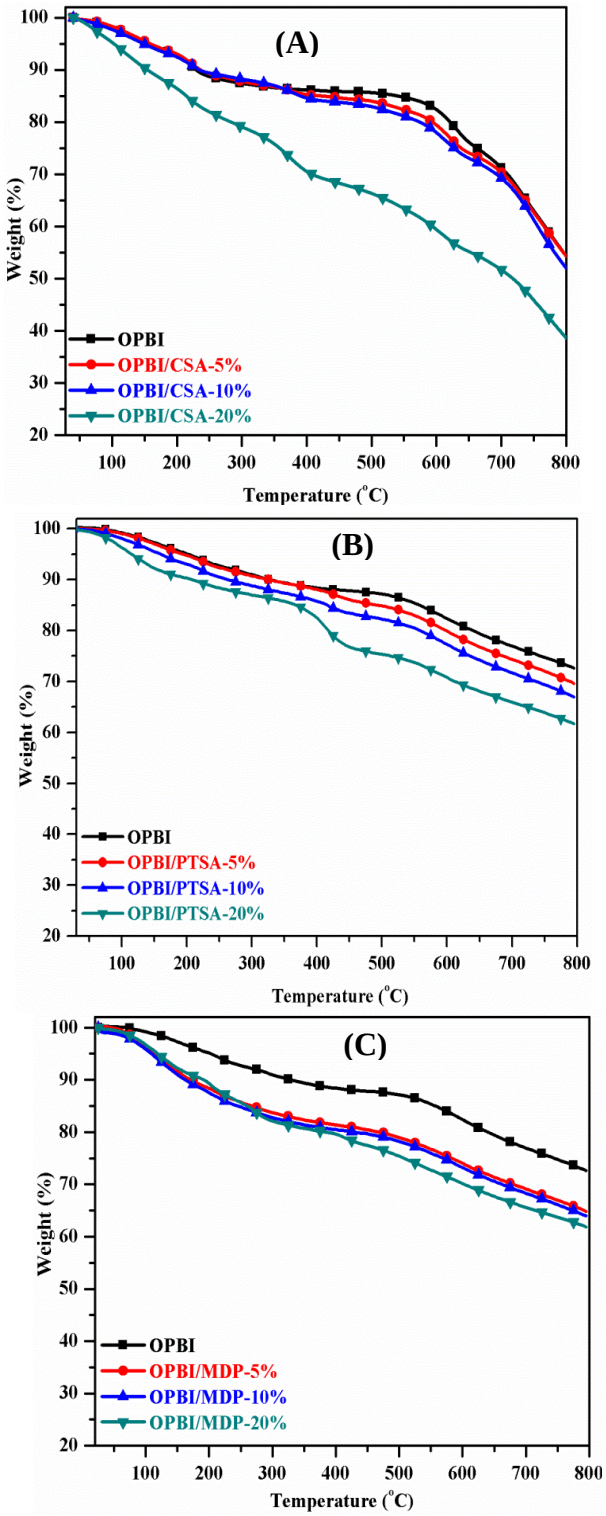

Figure 3.8. *TGA plots of the OPBI and its composite membranes with different percentage loading of (A) CSA (B) PTSA and (C) MDP.*

Since, the PA doped PBI membrane meant to be used as PEM in high temperature PEMFC (HT-PEMFC), hence it is important to study the thermal stability of PA doped membrane. Thermo gravimetric analysis of the PA doped OPBI membrane and PA doped OPBI/ASM composite membranes are presented in Figure 3.9 and in Figure 3.10. In all the cases, a sharp first weight loss occurs between 80 and 150 °C which correspond to evaporation of water molecules from the doped phosphoric acid. After this, continuous weight loss is observed up to 550 °C either because of the degradation of corresponding composite or owing to the self-condensation[49] of phosphoric acid molecules. Beyond 550 °C, all the three composites show sharp degradation of the polymer backbone. Important observations which need to be noticed from Figure 3.9 and Figure 3.10 are: (1) thermal stability of PA loaded composite membranes are higher than the PA loaded pristine OPBI, (2) it increases with increasing loading of ASMs and (3) stability largely depends upon the type of ASM which is used to make the composites. This is because the composites formed strong hydrogen bonding interaction with the phosphoric acid molecules and –N-H of imidazole group of the OPBI polymer. Although the undoped composites have lower stability compared to pristine OPBI (as seen from Figure 3.7 and Figure 3.8) but PA doped composites show higher stability than pristine PA doped OPBI. Therefore these composites are more useful than pristine OPBI for use in HT-PEMFC.

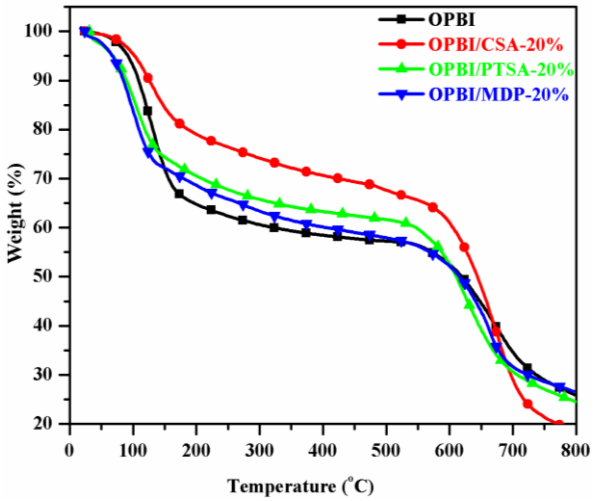

Figure 3.9. *TGA plots of PA loaded OPBI and its composites with ASMs when ASM loading is 20 wt% are shown in this figure.*

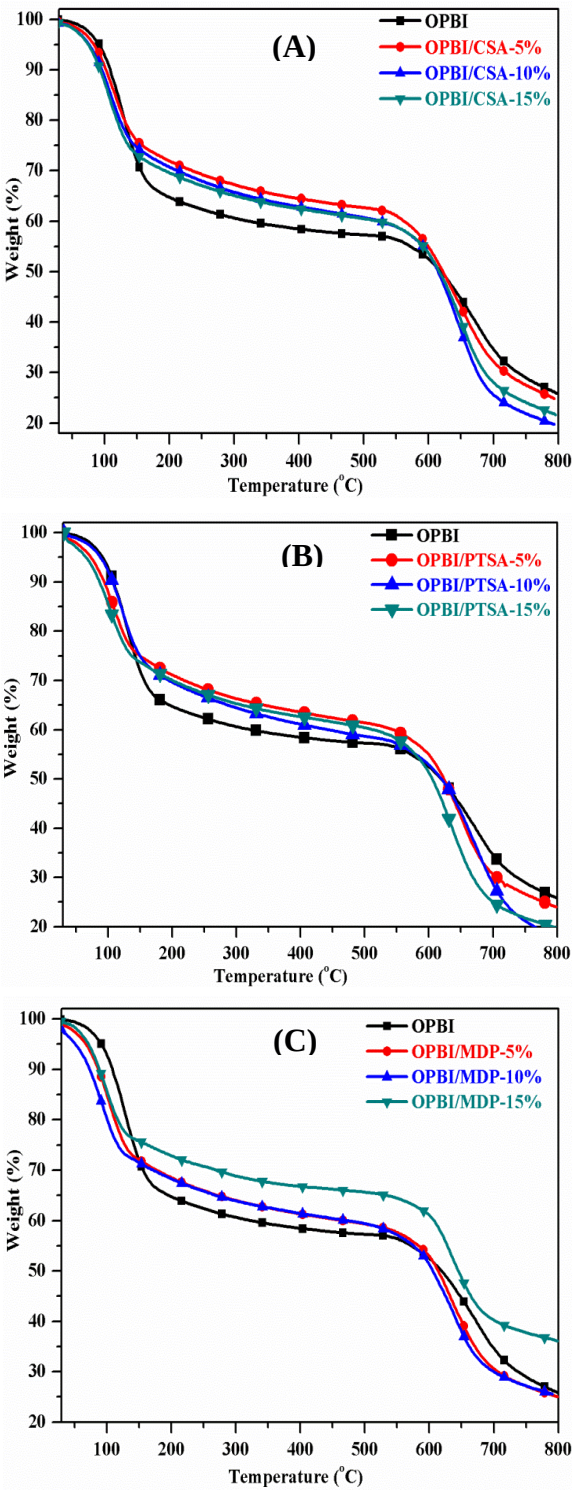

Figure 3.10. *TGA plots of the PA doped OPBI and its composite membranes with different percentage loading of (A) CSA, (B) PTSA and (C) MDP.*

Isothermal heating scan was performed for 24 h at 160 °C under nitrogen environment for phosphoric acid doped OPBI and all the 20% composite membranes, and isothermal curves are displayed in Figure 3.11. From this data, we did not observe any weight loss after 24 h except the initial weight loss which is observed due to the loosely bonded water molecules and phosphoric acid. In fact the composite membranes show higher stability than the pristine OPBI. These isothermal TGA data (Figure 3.11) and PA doped TGA data (Figure 3.9 and 3.10) prove that our composite membranes have very good durability as well as thermal stability and hence can be considered as suitable material for the use as PEM in high temperature fuel cell.[50]

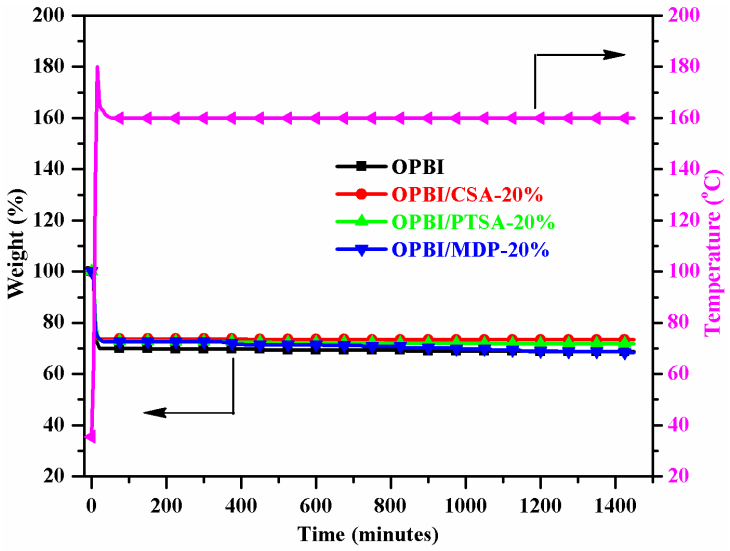

Figure 3.11. *Isothermal TGA curves of OPBI and 20% composite membranes.*

3.3.5. Mechanical study

The dynamic mechanical properties of the OPBI/ASM composite membranes were measured using a dynamical mechanical analyzer (DMA). Figure 3.12 shows the temperature dependent storage modulus (*E'*) plots of the composite membranes along with pristine OPBI. The storage moduli of the composite membranes at 150 °C are tabulated in Table 3.1. Figure 3.12 and Table 3.1 data clearly show that the storage modulus of the composite membranes increases with increasing composite percentage

loading till 15 wt% after which (i.e. for 20 wt% loading) *E'* decreases slightly. However, it must be noted that the storage modulus of all the composite membranes is always more than that of the pristine OPBI for the entire temperature range studied. The reason for increase in modulus in case of composite is attributed to the morphological structure of composite membranes where cross-linking consisting of fibrillar network is observed (will be discussed in the next section). Therefore, the crossed fibre like network morphology leads to the greater mechanical strength of the composite membranes. The loss modulus and tan δ plots against temperature (Figure 3.13) show only one peak for all the samples and the temperature corresponding to the peak marks as the glass transition temperature (T_g) of the OPBI and its composite membranes. The T_g values obtained from tan δ vs. temperature plots of all the composite membranes are summarized in Table 3.1. There is no definite order in change in T_g values, however, the glass transition temperatures of OPBI/PTSA composite membranes are higher than that of the OPBI/CSA composite membranes. We do not know the exact reason for such erratic changes in T_g, could be due to nature of interaction and complex structure formation which may differ from CSA to PTSA.

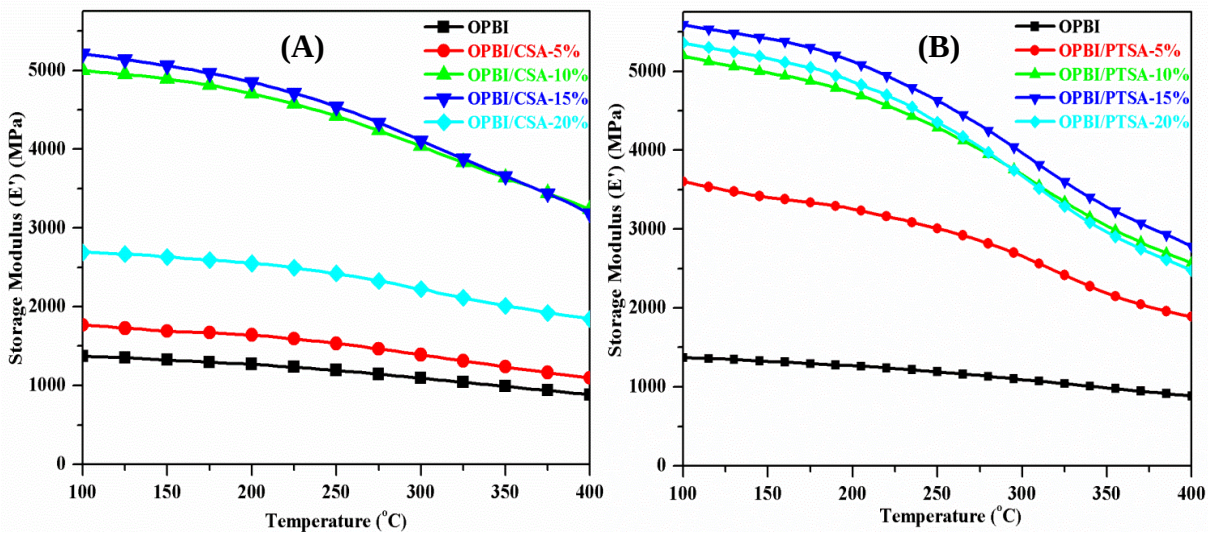

Figure 3.12. *Temperature dependent dynamical mechanical properties of OPBI/ASM composite membranes of different percentage loading of (A) CSA and (B) PTSA.*

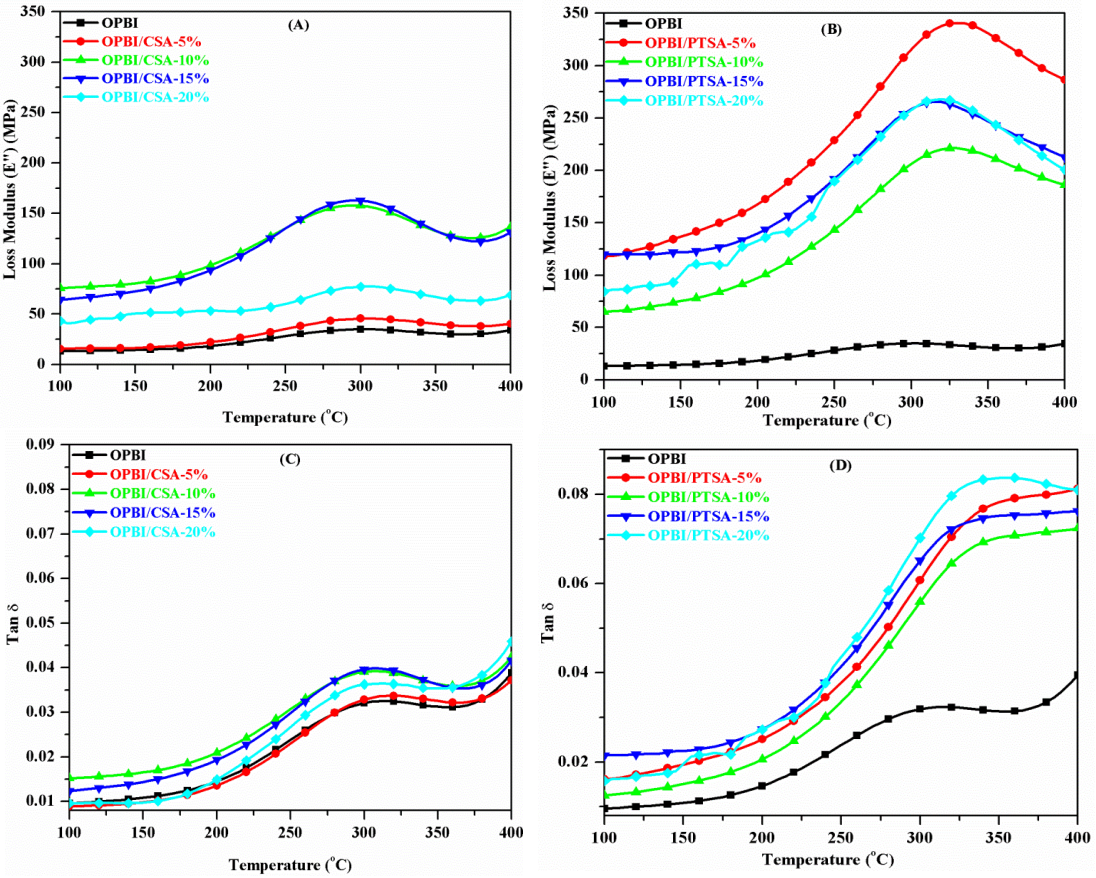

Figure 3.13. *Loss modulus (E'') and tan delta of CSA (A, C) and PTSA (B, D) composites, respectively.*

Table 3.1. *Thermo mechanical data of OPBI/ASM's composite membranes obtained from the DMA study.*

Sample Identification	E' (MPa) at 150°C	T_g (°C) from tan δ
OPBI	1324	311
OPBI/CSA-5%	1690	321
OPBI/CSA-10%	4892	309
OPBI/CSA-15%	5061	309
OPBI/CSA-20%	2633	313
OPBI/PTSA-5%	3405	370
OPBI/PTSA-10%	4983	359
OPBI/PTSA-15%	5416	353
OPBI/PTSA-20%	5166	351

3.3.6. Morphology study

The OPBI, OPBI/CSA, and OPBI/PTSA composite membranes appear very homogeneous and very transparent, but OPBI/MDP composite membranes are homogeneous but not that transparent as can be seen from the photographs of representative films which are given in Figure 3.14. This observation is attributed to complete miscibility. All the composite membranes were characterised by FE-SEM and the morphological features of cross-sectional area are displayed in the Figure 3.15 and Figure 3.16. The cross-section morphologies of various percentages of all the three composite membranes are found to be entirely different from the pristine OPBI. The morphologies features are highly depended on the functional groups (-SO_3H, H_2PO_4) and loading percentage (5%, 10%, 15% and 20%) of ASM in the composite membranes. In the case of OPBI/CSA and OPBI/PTSA composite membranes, a thick fibre like network morphology is observed which is absent in pristine OPBI. In both the cases, if the percentage of composite loading is increased then the number of fibrils increases and thickness of fibrils also increases, and hence morphology appears to be porous. This fibre like network structure and porous structure is more clearly visible in case of 20% CSA and PTSA composite membranes (Figure 3.16). But in the case of OPBI/MDP composite membranes, the morphology is not much of a fibre like network structure even if fibre present they are not that thick like other two ASMs. Also, at very high loading (20% MDP), we do not see much of porous structure as we have observed in case of other two ASMs. Therefore, clearly it is evident that the type and amount of ASM loading influence the morphological structure of the OPBI composite. In the following section, we will notice that the manifestation of this morphological differences in the properties especially the ability of composite membranes to load PA, proton conductivity and holding (less leaching) of PA with time and in presence of humidified condition.

Figure 3.14. *Photographs of OPBI and composite membranes.*

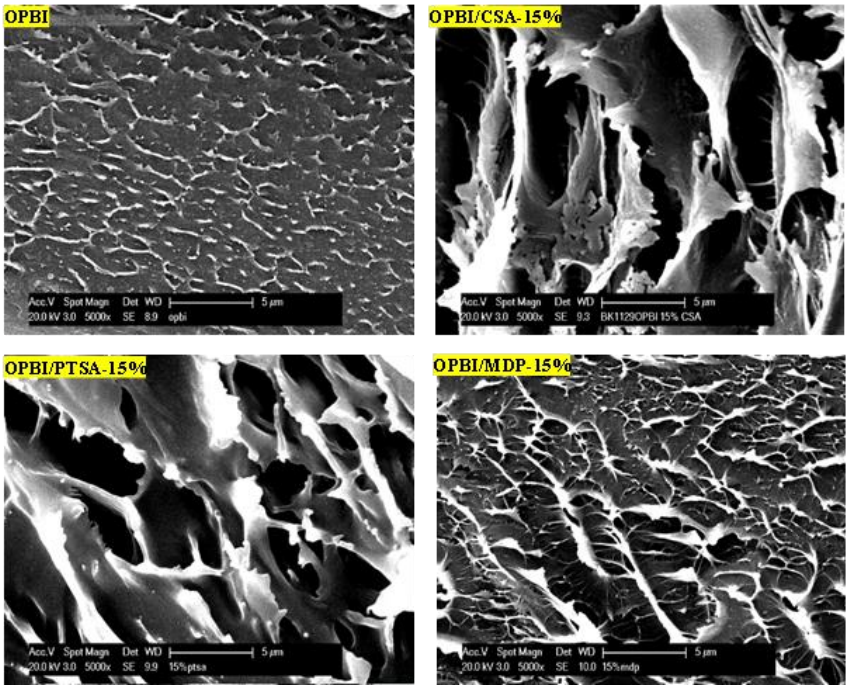

Figure 3.15. *Cross-sectional morphology of OPBI and the composites obtained using FE-SEM. Only 15 wt% ASM loading samples are presented here along with OPBI. In all the images scale bare is exactly identical.*

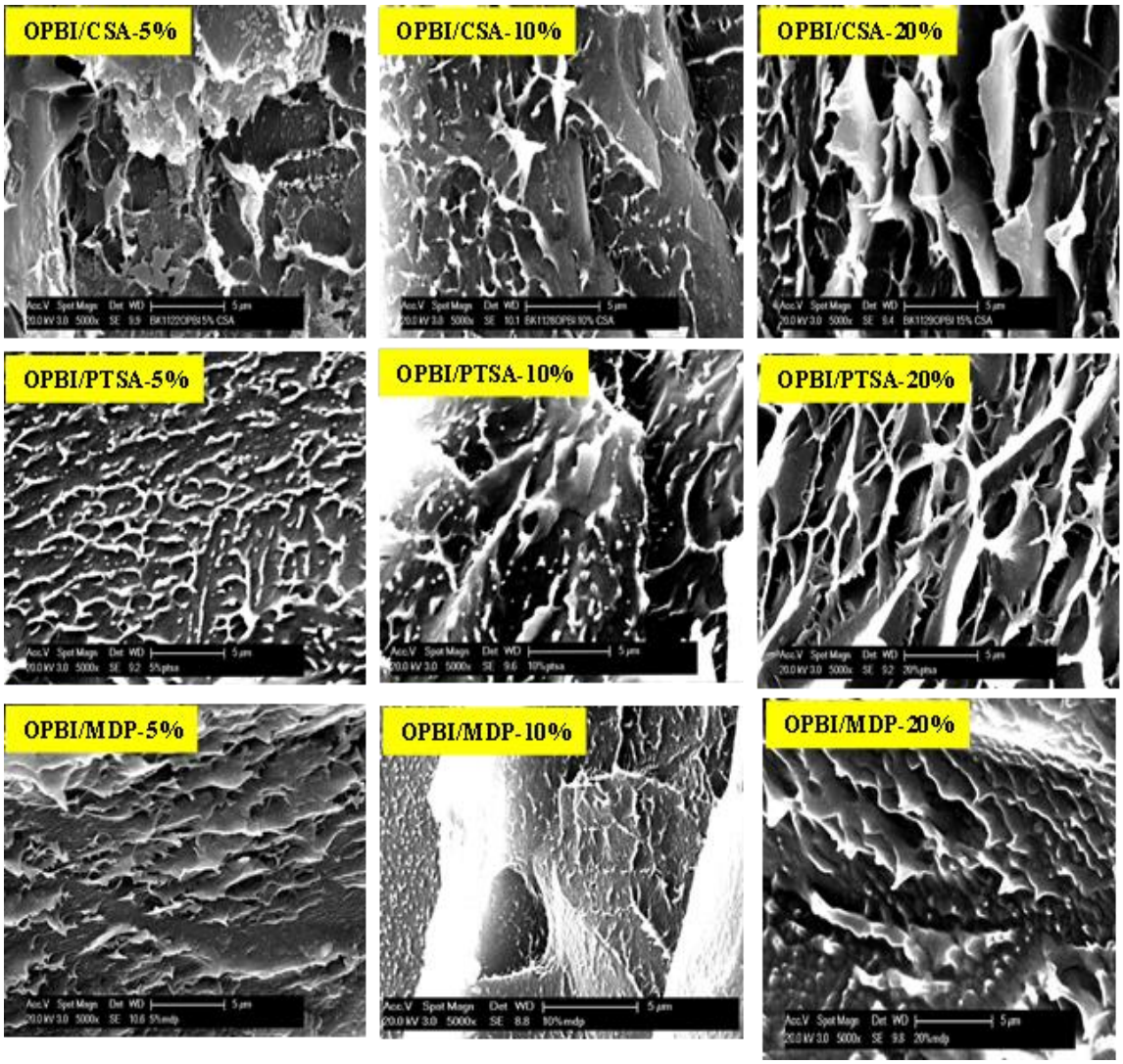

Figure 3.16. *Cross-sectional morphology of various OPBI/ASM composites. Sample identification is indicated in the Figure.*

3.3.7. PA doping, water uptake and swelling ratio studies

The OPBI and OPBI/ASM composite membranes were doped with phosphoric acid for 5 days and then the doping levels of the composite membranes were studied. The proton exchange membrane fuel cell (PEMFC) efficiency is highly dependent on the PA loading capacity of the polymer membranes. Higher acid loading capacity of the membrane enhances the performance of the fuel cell by facilitating the more transfer of

the protons. The PA doping capacity, water uptake and swelling ratio of all the OPBI composite membranes are summarized in Table 3.2. The doping level of the OPBI/CSA, OPBI/PTSA and OPBI/MDP composite membranes are substantially higher when compared with the pure OPBI membrane and PA doping level of the composite membranes increases with increasing ASM percentage loading. The reason is attributed to the presence of sulphonic functional group in CSA and PTSA composites, and phosphate functional group in MDP composites. These functional groups hold more number of PA molecules by hydrogen bonding interaction with PA and also with benzimidazole groups OPBI chain. Also, the composite membranes morphology helps in accommodating more and more number of PA molecules. For example, in case of CSA, morphology is highly porous and hence it loads significantly high PA than PTSA and MDP (Table 3.2). The morphology of PTSA and MDP composites also help in accommodating high PA loading.

Table 3.2 data shows that the water uptake and swelling ratio of the all the three OPBI composite membranes are lower than that of the pure OPBI membrane which gradually decreases with increasing composite percentage loading except one or two cases when loading is high. The reason could be due to the presence of nanoparticles which is evident from surface morphology (Figure 3.17) of the composite membrane which prevents the absorption of water molecules. The swelling ratio decreases in both water and phosphoric acid because of the strong interaction between the chains of OPBI and the ASM, and also due to fibrillar network type morphology as presented in Figure 3.17.

Table 3.2. *Water uptake, swelling ratio and PA doping levels of the OPBI/CSA, OPBI/PTSA and OPBI/MDP composite membranes. Numbers in the bracket are the standard deviation in the measurements.*

Sample identification	Water uptake (Weight %)	Swelling ratio in water (%)	Swelling ratio in PA (%)	PA mols/OPBI repeat unit
OPBI	13.5(1.94)	3.42(0.86)	4.81(1.56)	17.60(0.34)
OPBI/CSA-5%	7.89(0.64)	1.97(0.53)	1.17(0.90)	38.61(7.6)
OPBI/CSA-10%	3.76(0.51)	1.07(0.45)	1.15(0.85)	45.00(5.7)
OPBI/CSA-15%	3.67(1.33)	1.09(0.11)	1.38(0.240	49.11(6.27)
OPBI/CSA-20%	5.24(1.03)	1.89(0.61)	0.87(0.04)	54.35(3.37)
OPBI/PTSA-5%	5.87(0.87)	1.73(0.13)	0.46(0.07)	31.02(2.82)
OPBI/PTSA-10%	2.91(0.80)	1.52(0.69)	0.34(0.02)	33.36(3.69)
OPBI/PTSA-15%	2.09(0.9)	1.53(0.97)	0.92(0.02)	34.96(5.35)
OPBI/PTSA-20%	1.47(0.37)	1.04(0.61)	0.54(0.03)	36.36(2.49)
OPBI/MDP-5%	4.97(1.09)	1.84(0.50)	2.24(0.32)	29.33(3.09)
OPBI/MDP-10%	3.84(1.03)	2.15(0.33)	3.58(0.64)	30.22(6.64)
OPBI/MDP-15%	2.14(0.91)	1.28(0.03)	2.25(0.14)	34.33(3.60)
OPBI/MDP-20%	1.09(0.09)	1.68(0.31)	5.64(1.79)	34.39(6.46)

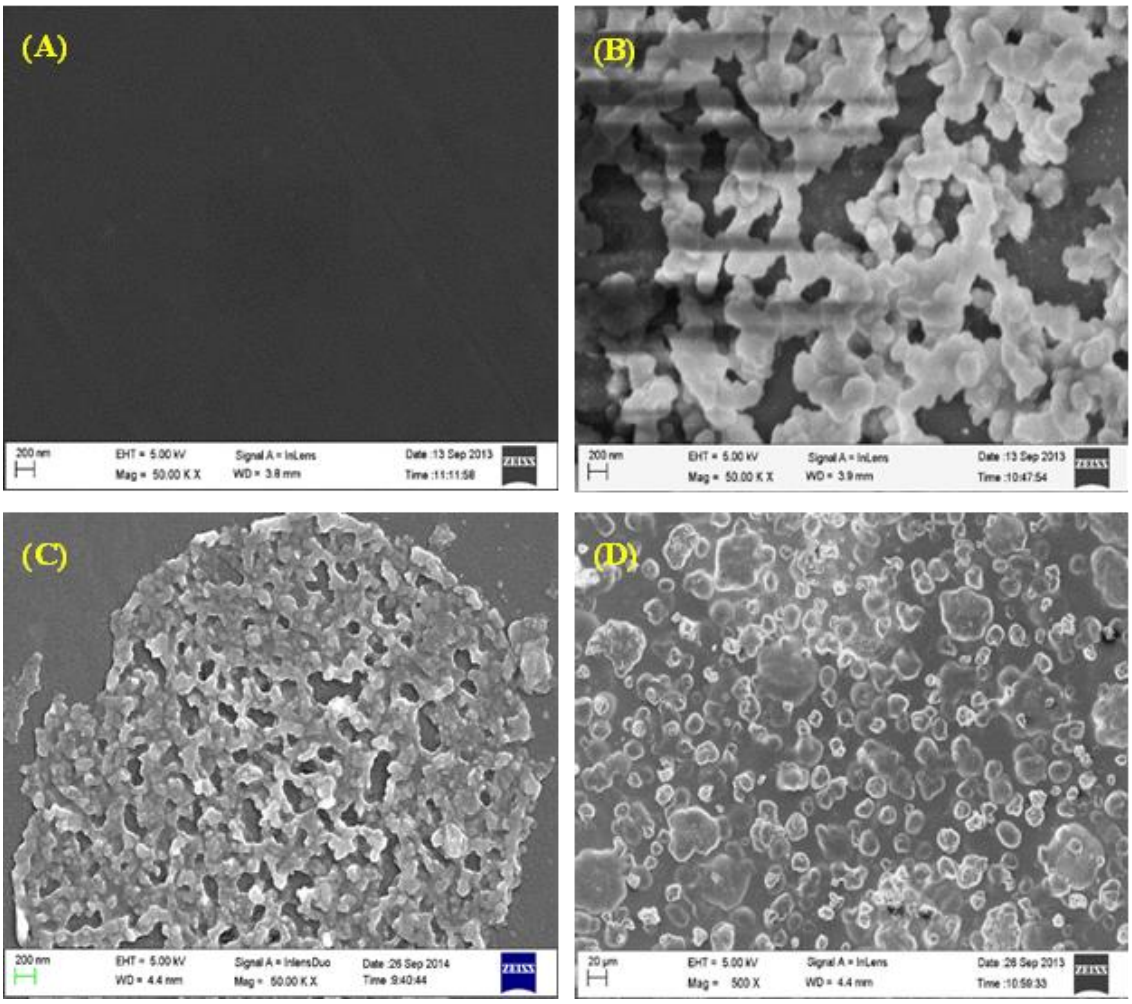

Figure 3.17. *FE-SEM surface images of (A) OPBI, (B) OPBI/CSA-20%, (C) OPBI/PTSA-20% and (D) OPBI/MDP-20% composite membranes.*

3.3.8. Proton conductivity

The proton conductivity studies were performed on OPBI, OPBI/CSA, OPBI/PTSA, and OPBI/MDP composite membranes by measuring the impedance. All the composite membranes were doped with PA for 5 days before the measurement. The membranes were placed between two Teflon plates of the conductivity cell. Before the conductivity measurement, conductivity cell was placed in oven at 100 °C for 2 h to avoid the conduction by the moisture from the membrane. The proton conductivity of

all the composite membranes was measured in the range of 30-180 °C by using an in-house built conductivity cell. The proton conductivities of the OPBI and that of the OPBI composite membranes obtained from the Nyquist plots are plotted against temperature and shown in Figure 3.18. In all the three composites, the proton conductivities of the membrane increases with increasing temperature which is quite well known in case of PA doped PBI. Although in few cases, we observed drop in proton conductivity beyond 160 °C and this may be the stability related issue of PEM. All the three cases of composites proton conductivity increases with increasing ASM loading and significantly higher than that of the pristine OPBI. Once again this result is in accordance with PA doping level (Table 3.2) of composite. In fact the proton conductivities of OPBI/CSA composites are much higher than the other two composites which is also the manifestation of higher loading of former than the later. In addition the presence of $-SO_3H$ and H_2PO_4 groups facilitate the proton conduction by inducing additional hydrogen bonding and hence proton conduction path. It is to be remembered that the morphology (Figure 3.15) and crystalline character (Figure 3.4) of composites also help in enhancing the proton conductivity. The proton conductivity of OPBI is found to be 8.6×10^{-2} S/cm at 180 °C. This value is in agreement with the already reported data. The 20% ASM loaded OPBI/CSA, OPBI/PTSA and OPBI/MDP composite membranes proton conductivities are 2.8×10^{-1} S/cm, 1.7×10^{-1} S/cm, 1.4×10^{-1} S/cm, respectively at 180 °C. Among these three composites, OPBI/CSA composite membranes show higher proton conductivity due to the relatively higher acidic nature of CSA, higher crystallinity, better porous morphology and higher PA loading.

Since durability of PEM is an important property to be studied for the use of PEM, hence one has to determine the stability of proton conductivity at higher temperature over a period of time. Figure 3.19 represents the isothermal proton conductivities, plotted against time, of the OPBI and its 20% composite membranes. The membranes were isothermally kept at 160 °C for 24 h and under this condition, the conductivity of OPBI and composite membranes were measured for every 2 h up to 24 h (excluding night time). From the Figure 3.19, it is clear that at the initial range (2-4 h)

there is decrease in proton conductivity values in all the cases after which the values do not change at all up to 24 h. The PA doped composite membranes shows less decrement in conductivity compared to the PA doped pristine OPBI. This is due to the presence of ASM in the composite membranes. Therefore, we can conclude that our composite membranes have got long term durability in terms of proton conductivity.

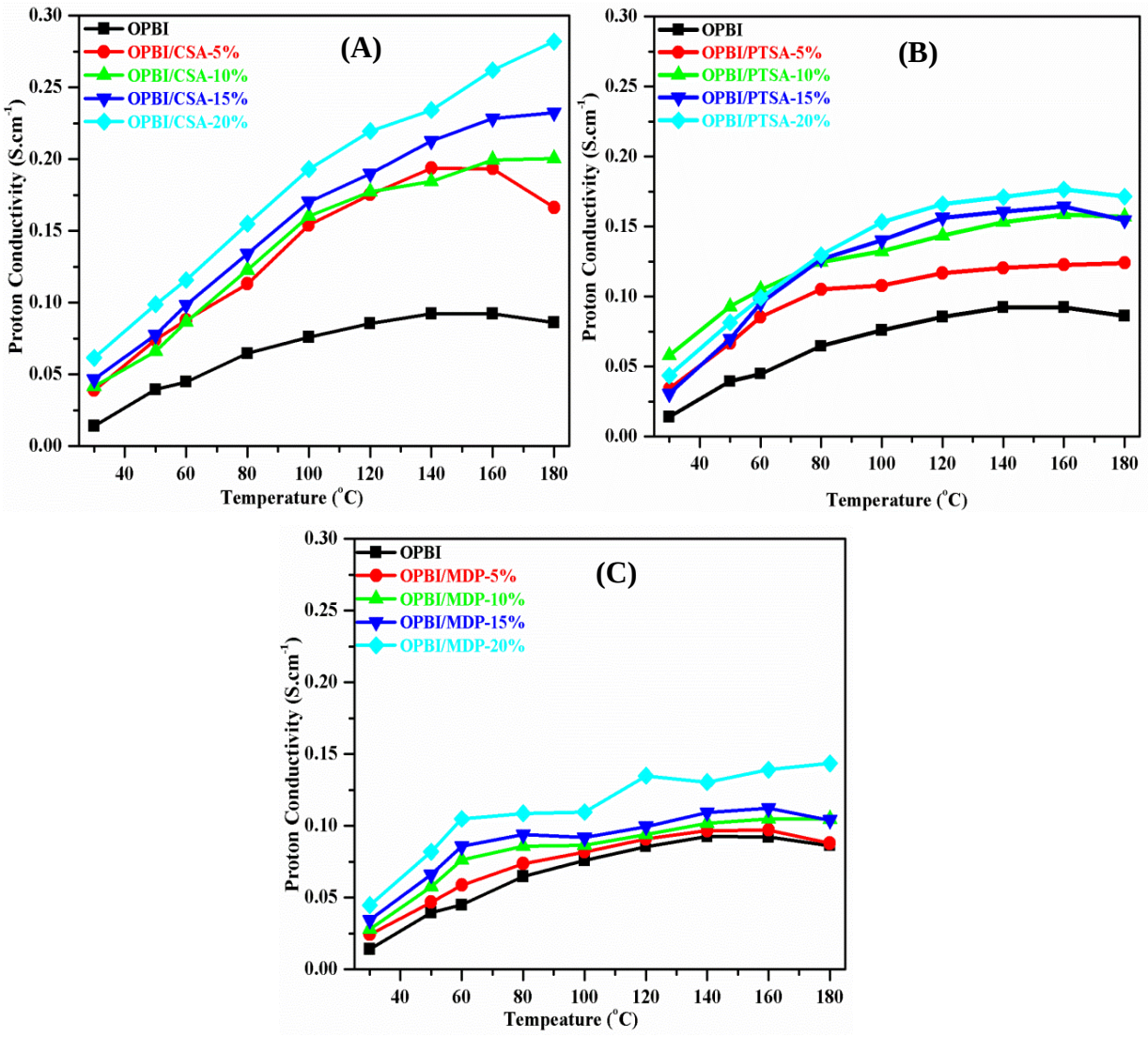

Figure 3.18. *Proton conductivity of (A) OPBI/CSA, (B) OPBI/PTSA and (C) OPBI/MDP composite membranes. All the membranes are doped in 85% PA for five days.*

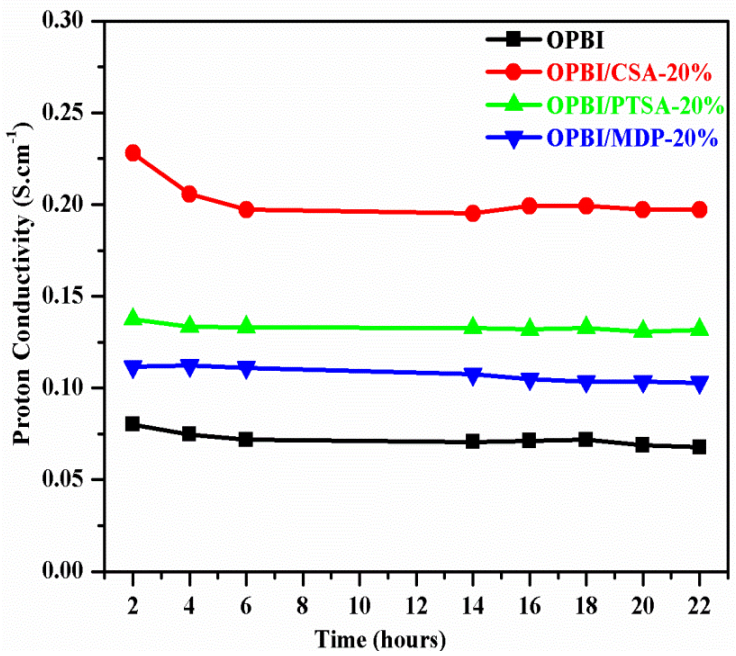

Figure 3.19. *Isothermal conductivity of OPBI and 20% loaded ASM composite membranes at 160 °C for 24 hrs.*

3.3.9. Leaching study

While performing the fuel cell operations at higher temperatures, the PEM suffers acid leaching from the PA doped membrane. This problem has to be minimised by different ways so that the membrane retains sufficient amount of acid in the membrane.[51-53] To test the acid retention ability of the composite membrane, acid leaching test was performed with PA doped OPBI composite membranes. The PA doped membranes were dried, weighed, and kept under water vapour condition at 100 °C for a period of 3 h. After every half an hour, the weight of the acid leached membrane was measured carefully. From this, the weight loss ratio of PA present in the membrane is calculated and the results are shown in Figure 3.20. In the case of OPBI, the weight loss decreases to 64% after first half an hour of leaching of PA. In the case of OPBI/CSA-20%, OPBI/PTSA-20% and OPBI/MDP-20% membranes, after first half an hour of leaching, the corresponding PA weight loss decreases to 27%, 33% and 54%, respectively. From the plot (Figure 3.20), we observed that the acid leaching of

composite membranes is much less compared to the normal OPBI which can be explained by the presence of sulphonic groups in CSA, PTSA and phosphate groups in MDP fostering strong hydrogen bonding interaction between the PA molecules and polymer chains. Also the porous morphology and crystallinity of composite help in retaining the PA inside the matrix. So it is proved that the addition of CSA, PTSA and MDP to the OPBI membranes could enhance the ability to trap (or) hold more PA. Among these three, CSA composite membrane absorbed more PA (Table 3.2) and less PA leaches out from the membrane and this may be due to strong interaction between CSA and OPBI in presence of PA.

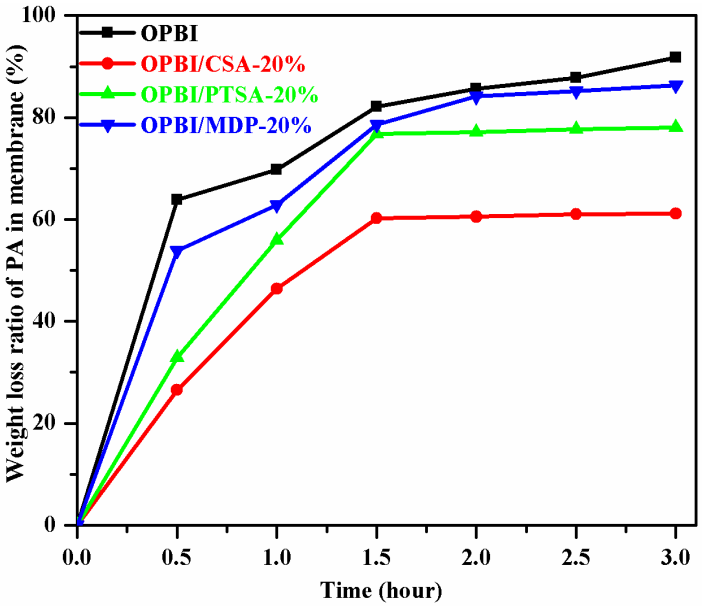

Figure 3.20. *Acid leaching study of OPBI and 20% composite membranes. Weight loss ratios of PA from membranes are plotted against time.*

The acid leaching ability was further confirmed by measuring the proton conductivity of the composite membranes which are leached for 3 h. After the completion of 3 h of acid leaching test, the moisture and acid was wiped from the membrane, the conductivity cell was prepared and the conductivity was measured from 80 °C to 160 °C (fuel cell operating temperature) immediately. Figure 3.21 shows the plots of proton conductivity of acid doped and acid leached OPBI and all the three 20%

composite membranes. The leached OPBI/CSA-20%, OPBI/PTSA-20% and OPBI/MDP-20% composite membranes show proton conductivity of 0.13, 0.11 and 0.04 S/cm, respectively at 160 °C compared to the pure OPBI, which is 0.02 S/cm at this temperature. It must be noted that the decrease in conductivity after leaching is more prominent in case of OPBI, whereas it is relatively less in case of composites. Overall, after leaching test conductivities of composite membrane remain much higher than the pristine OPBI. This would be very useful in terms of durability of PA loaded PBI membrane. From this plot, the role of sulphonic and phosphonic group molecules in retaining acid and in elevating conductivity of the composite membranes are clearly understood. Also, it indicates that these are highly promising candidates for use in high temperature fuel cell.

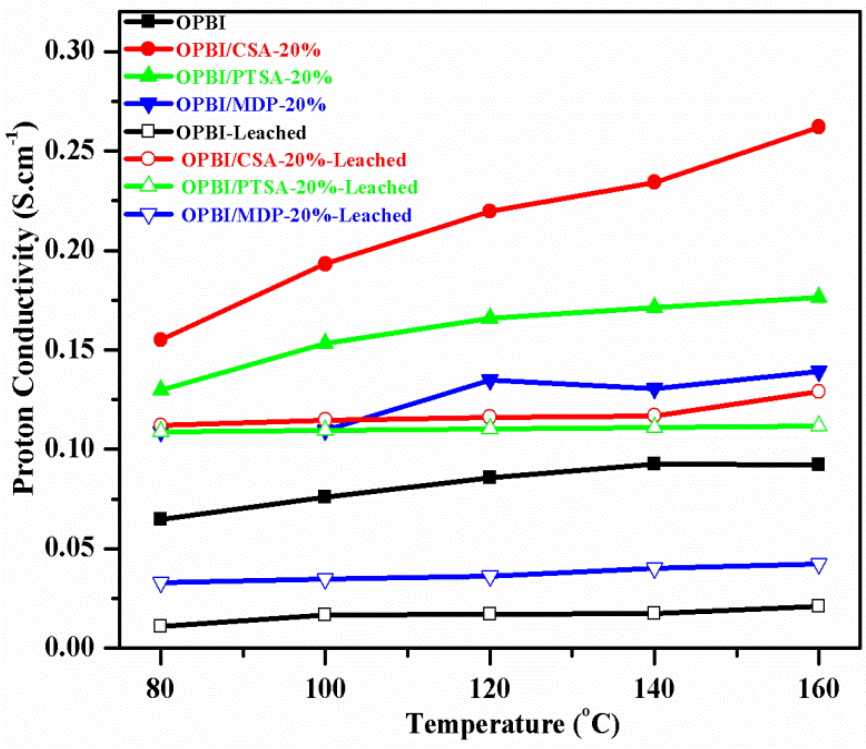

Figure 3.21. *Proton conductivity of PA-doped and PA leached (for 3 hours) OPBI, 20% loaded ASM composite membranes from 80 to 160°C.*

3.4. CONCLUSION

Three sets of different composite membranes OPBI with acid like surfactant molecules (ASM) namely CSA, PTSA and MDP as filler have been prepared and studied thoroughly with an objective to develop PEM with enhanced or better properties for use in fuel cell. The structural, thermal, mechanical, morphological and proton conducting properties of the composite membranes have been investigated and compared with pristine OPBI. The IR and SS-NMR spectra confirmed the interactions between the OPBI and ASM by means of hydrogen bonding. The XRD data confirmed the presence of crystallinity in all three composites. The TGA results inferred that the PA doped composite membranes have high thermal stability than PA doped pristine OPBI. Isothermal conductivity data and Isothermal TGA data proved that the composite membranes have long-term durability which will be beneficial for high temperature fuel cell operation. SEM cross sectional analysis of composite membranes revealed the fibre like network structure which helped in holding large amount of PA molecules and eventually led to higher proton conductivities and reduced acid leaching. Thus, the interaction between OPBI, ASM and PA dictates the morphology, crystallinity of the membrane which finally governs the proton conductivity and PA retention ability of the membrane. These results concluded that the composite membranes are highly promising candidates for high temperature proton exchange membrane fuel cell.

REFERENCES

[1] Heo, P.; Kajiyama, N.; Kobayashi, K.; Nagao, M.; Sano, M.; Hibino, T. *Electrochem. Solid state Lett*. **2008**, *11*, B91.

[2] Peighambardoust, S. J.; Rowshanzamir, S.; Amjadi, M. *Int. J. Hydrogen Energy* **2010**, *35*, 9349.

[3] Trogadas, P.; Ramani, V. In Encyclopedia of Electrochemical Power Sources; Academic Press: Amsterdam, 2009; pp 716.

[4] Kerres, J. *J. Membr. Sci.* **2001**, *185*, 3-27.

[5] Kreuer, K. D. *J. Membr. Sci*. **2001**, *185*, 29.

[6] Carrette, L.; Friedrich, K. A.; Stimming, U. *Chem Phys Chem* **2000**, *1*, 162.

[7] Hickner, M. A.; Ghassemi, H.; Kim, Y. S.; Einsla, B. R.; McGrath, J. *E. Chem. ReV*. **2004**, *104*, 4587.

[8] Li, Q.; He, R.; Jensen, J. O.; Bjerrum, N. *J. Chem. Mater*. **2003**, *15*, 4896.

[9] Mahrenia, A.; Mohamada, A. B.; Kadhum, A. A. H.; Daud, W. R. W.; Iyuke, S. E. *J. Membr. Sci.* **2009**, *327*, 32.

[10] 10. Markova, D.; Avneesh, K.; Klapper, M.; Muellen, K. *Polymer* **2009**, *50*, 3411.

[11] Thompson, E. L.; Capehart, T. W.; Fuller, T. J.; Jorne, J. *J. Electrochem. Soc*. **2006**, *153*, A2351.

[12] Mathews, A. S.; Kim, I.; Ha, C. S. *Macromol. Res*. **2007**, *15*, 114.

[13] Watari, T.; Fang, J.; Tanaka, K.; Kita, H.; Okamoto, K.-I.; Hirano, T. *J. Membr. Sci*. **2004**, *230*, 111.

[14] Lufrano, F.; Gatto, I.; Staiti, P.; Antonucci, V.; Passalacqua, E. *Solid State Ionics* **2001**, *145*, 47.

[15] Einsla, B. R.; Harrison, W. L.; Tchatchoua, C.; McGrath, J. E. *Polym. Prepr*. **2004**, *44*, 645.

[16] Gao, Y.; Robertson, G. P.; Guiver, M. D.; Mikhailenko, S. D.; Kaliaguine, S. *Macromolecules* **2004**, *37*, 6748.

[17] Gil, M.; Ji, X.; Li, X.; Na, H.; Hampsey, J. E.; Lu, Y. *J. Membr. Sci*. **2004**, *234*, 75.

[18] Jin, X.; Bishop, M. T.; Ellis, T. S.; Karasz, F. E. Br. *Polym. J*. **1985**, *17*, 4.

[19] Xing, P.; Robertson, G. P.; Guiver, M. D.; Mikhailenko, S. D.;Kaliaguine, S. *Macromolecules* **2004**, *37*, 7960.

[20] Wang, F.; Hickner, M; Kima, Y. S.; Zawodzinkski, T. A.; McGrath, J.E., J *J. Mebr. Sci*. **2002**, *197*, 231.

[21] Xiao, G. Y.; Sun, G. M.; Yan, D. Y.; Zhu, P. F.; Tao, P. *Polym. Prepr*. **2002**, *43*, 5335.

[22] Zhang, H.; Shen, P. K. *Chem. Rev*. **2012**, *112*, 2780.

[23] Kim, S.-K.; Choi, S.-W.; Jeon, W. S.; Park, J. O.; Ko, T.; Chang, H.; Lee, J.-C. *Macromolecules* **2012**, *45*, 1438.

[24] Mader, J. A.; Benicewicz, B. C. *Macromolecules* **2010**, *43*, 6706.

[25] Xing, B.; Savadogo, O. *J. New. Mater. Electrochem. Syst.* **1999**, *2*, 95.

[26] Kawahara, M.; Rikukawa, M.; Sanui, K.; Ogata, N. *Solid State Ionics* **2000**, *136-137*, 1193.

[27] He, R. H.; Li, Q. F.; Jensen, J. O.; Bjerrum, N. J. *J. Polym. Sci., Part A: Polym. Chem.* **2007**, *45*, 2989.

[28] Lebaek, J.; Ali, S. T.; Moller, P.; Mathiasen, C.; Nielsen, L. P.; Kaer, S. K. *Int. J. Hydrogen Energy* **2010**, *35*, 9943.

[29] Ma, Y. L.; Wainright, J. S.; Litt, M. H.; Savinell, R. F. *J. Electrochem. Soc.* **2004**, *151*, A8.

[30] Singha, S.; Jana, T. *ACS Appl. Mater. Interfaces* **2014**, *6*, 21286.

[31] Weber, J.; Kreuer, K.-D.; Maier, J.; Thomas, A. *Adv. Mater.* **2008**, *20*, 2595.

[32] Wang, S.; Zhao, C.; Ma, W.; Zhang, N.; Zhang, Y.; Zhang, G.; Liu, Z.; Na, H. *J. Mater. Chem. A* **2013**, *1*, 621.

[33] Maity, S.; Jana, T. *Eur. Polym. J.* **2013**, *49*, 2280.

[34] Klaehn, J. R.; Luther, T. A.; Orme, C. J.; Jones, M. G.; Wertsching, A. K.; Peterson, E. S. *Macromolecules* **2007**, *40*, 7487.

[35] Maity, S.; Jana, T. *ACS Appl. Mater. Interfaces* **2014**, *6*, 6851.

[36] Ghosh, S.; Sannigrahi, A.; Maity, S.; Jana, T. *J. Phys. Chem. C* **2011**, *115*, 11474.

[37] Ghosh, S.; Sannigrahi, A.; Maity, S.; Jana, T. *J. Mater. Chem.* **2011**, *21*, 14897.

[38] Singha, S.; Jana, T. *Polymer* **2014**, *55*, 594.

[39] Sannigrahi, A.; Arunbabu, D.; Jana, T. *Macromol. Rapid Commun.* **2006**, *27*, 1962.

[40] Neelakandan, S.; Kanagaraj, P.; Nagendran, A.; Rana, D.; Matsuura, T.; Muthumeenal, A. *Renewable Energy* **2015**, *78*, 306.

[41] Muthumeenal, A.; Neelakandan, S.; Rana, D.; Matsuura, T.; Kanagaraj, P.; Nagendran, A. *Fuel Cells* **2014**, *14*, 853.

[42] Neelakandan, S.; Rana, D.; Matsuura, T.; Muthumeenal, A.; Kanagaraj, P.; Nagendran, A. *Solid State Ionics* **2014**, *268*, 35.

[43] Mohd Norddin, M. N. A.; Rana, D.; Ismail, A. F.; Matsuura, T.; Sudirman, R.;

Jaafar, J.; *J. Ind. Eng. Chem.* **2012,** *18*, 2016.

[44] Mohd Norddin, M. N. A.; Ismail, A. F.; Rana, D.; Matsuura, T.; Tabe, S. *J. Membr. Sci.* **2009**, *328*, 148.

[45] Mohd Norddin, M. N. A.; Ismail, A. F.; Rana, D.; Matsuura, T.; Mustafa, A.; Tabe-Mohammadi, A. *J. Membr. Sci.* **2008**, *323*, 404.

[46] Patil, S. L.; Chougule, M. A.; Pawar, S. G.; Sen, S.; Patil, V. B.; *Soft Nanoscience Lett*. **2012**, *2*, 46.

[47] Yamada, M.; Honma, I. *Electrochim. Acta* **2003**, *48*, 2411.

[48] Hazarika, M.; Jana, T. *ACS Appl. Mater. Interfaces* **2012**, *4*, 5256.

[49] Jiang, F.; Pu, H.; Meyer., W. H.; Guan, Y.; Wan, D. *Electrochim.Acta* **2008**, *53*, 4495.

[50] Sannigrahi, A.; Ghosh, S.; Maity, S.; Jana, T. *Polymer* **2011**, *52*, 4319.

[51] Pu, H. T.; Liu, L.; Chang, Z. H.; Yuan, J. J. *Electrochim. Acta* **2009**, *54*, 7536.

[52] Maity, S.; Singha, S.; Jana, T. *Polymer* **2015**, *66*, 76.

[53] Pu, H.; Wang, L.; Pan, H.; Wan, D. J. *Polym. Sci., Part A: Polym.Chem.* **2010**, *48*, 2115.

Chapter 4

Polymer Electrolyte Membrane from Polybenzimidazoles: Influence of Tetraamine Monomer Structure

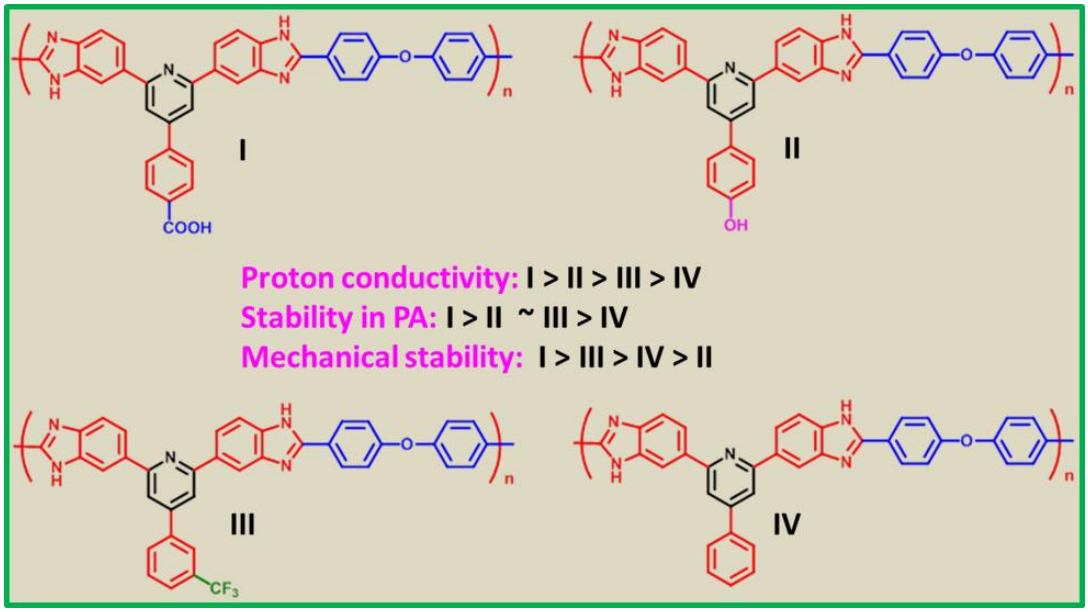

In this chapter, three series of functionalised pyridine bridged polybenzimidazoles (PyPBIs) derivatives have been synthesized. Among these, carboxylic functionalised PyPBIs exhibited excellent PEM properties when compare to the conventional PBI and non-functionalised PyPBI.

Sana, B.; Jana, T. *Polymer* **2018**, *137*, 312-323.

4.1. INTRODUCTION

In recent years, polybenzimidazoles (PBIs) have been found as an alternative polymer electrolyte membrane or proton exchange membrane (PEM) to Nafion because of the several advantages with the former compared to the later[1, 2]. PBIs are widely investigated because of their good mechanical stability, high thermal stability, chemical stability and excellent film forming capacity[3, 4]. PBI exhibits specific interactions with various solvents due to the presence of hydrogen donor (-NH) and acceptor (-N=) sites in its backbone[5]. Phosphoric acid (PA) doped PBI is the most promising PEMs material because it display very high proton conduction at elevated temperatures without any humidification. In addition to this recent use of PBI in PEMs, PBI has been used as a base material in various high temperature and high strength applications. Nevertheless, PBIs also have some caveats mainly owing to its infusibility and poor solubility because of the aromatic heterocyclic rigid structure and high T_g[6, 7].

Various approaches have been explored widely in the literature for addressing the processability issue of PBI and enhancing solubility of PBI[8]. Some of the major chemical methods which were adapted to address these limitations are: sulfonation of PBI with an expectation that this may enhance the solubility, synthesis of polybenzimidazoles with various structural differences in the backbone by using various monomeric structures (mostly varying dicarboxylic acid structures) and here also assumption was that the solubility might improve[9, 10]. Few example of this later method of synthesis of PBIs are: poly(2,5-benzimidazole) (AB-PBI),[11] sulfonated polybenzimidazole,[12, 13] pyridine dicarboxylic acids based PBI, [14] naphthalene dicarboxylic acids based PBI,[15] and hyper branched polybenzimidazoles (HPBI) etc [16]. A few other synthetic approaches have been carried out to increase solubility and processability, such as functionalized alkyl groups or different long chain alkyl groups were introduced on the PBI backbone[17, 18] by substitution in place of imidazole hydrogen. Potrekar *et al.*, have synthesized N-phenyl 1,2,4-triazole containing polybenzimidazole polymers using a newly synthesized 3'-(4-phenyl- 4H-1,2,4-triazole-3,5-diyl) dibenzoic acid (PTDBA) monomer and reported improved dissolution of the synthesized polymer in acidic environ-

ments[19].

Earlier our research group introduced a new tetraamine called 2,6-bis(3′,4′-diaminophenyl)-4-phenyl pyridine (PyTAB) monomer for the synthesis of a new kind of pyridine bridged polybenzimidazoles (PyPBIs)[20]. By using this monomer, we were able to synthesized several PyPBI homopolymers and copolymers[20, 21] using various di-carboxylic acids (DCA) and all these PyPBI exhibited excellent solubility in low boiling solvents such as formic acid (FA) and remarkable improvement PEMs properties after loading with PA in comparison to conventionally synthesized PBI which were made from conventional tetraamine monomer namely 3, 3′, 4, 4′-tetraaminobiphenyl (TAB). However, we have observed one major drawback with our PyPBIs in regard to the stability of PyPBI membrane in PA medium. The PyPBI membranes are stable up to 60% H_3PO_4 solvent during the PA doping process but above this concentration the membranes were completely dissolved. If highly concentrated PA (85% H_3PO_4) used for doping, the membrane often yields higher proton conductivity which ultimately enhances the performance of the fuel cell efficiency. However, our Py-PBI membrane could not sustain 85 % concentrated PA and hence we hypothesized that the modification of the PyTAB monomer structure may help us in synthesizing and developing PyPBIs based PEMs with higher PA stability which eventually will yield higher proton conductivity and hence better cell efficiency can be expected.

In this Chapter, we focussed on synthesizing three new PyTAB monomers with the addition of different functional groups namely *p*-COOH, *p*-OH and *m*-CF_3 on either *para* (or) *meta* position of the PyTAB phenyl ring and finally we obtained PyTAB-COOH, PyTAB-OH and PyTAB-CF_3 monomers, respectively. Then, we polymerized these new monomers to obtain new type of functionalised pyridine bridged polybenzimidazoles and will be called as PyPBI polymer derivatives. Synthesized monomers and polymers are characterized in depth and PEMs obtained from these were studied and compared with conventional PBI and PyPBI results reported in literature.

4.2. EXPERIMENTAL SECTION

The sources of all the materials used in this work are described in the Chapter 2.

Monomers synthesis, polymers synthesis and membrane fabrication are described as follows.

4.2.1. Monomers synthesis

4-[2,6-bis(3′,4′-diaminophenyl) pyridin-4-yl]benzoic acid (PyTAB-COOH) and 2,6-bis(3′ ,4′-diamino)phenyl-4-(3”-trifluoromethyl) phenyl pyridine (PyTAB-CF_3) monomers (Scheme 4.1) were synthesized in our laboratory according to our previous literature reports and by applying some more modification and the ^{1}H NMR spectrums are given below.[16, 20, 22] 4-[2,6-bis(3,4-diaminophenyl)pyridin-4-yl]phenol (PyTAB-OH) monomer (Scheme 4.2) was synthesized for the first time in our laboratory. Synthetic procedure and scheme of PyTAB-OH monomer was given below.

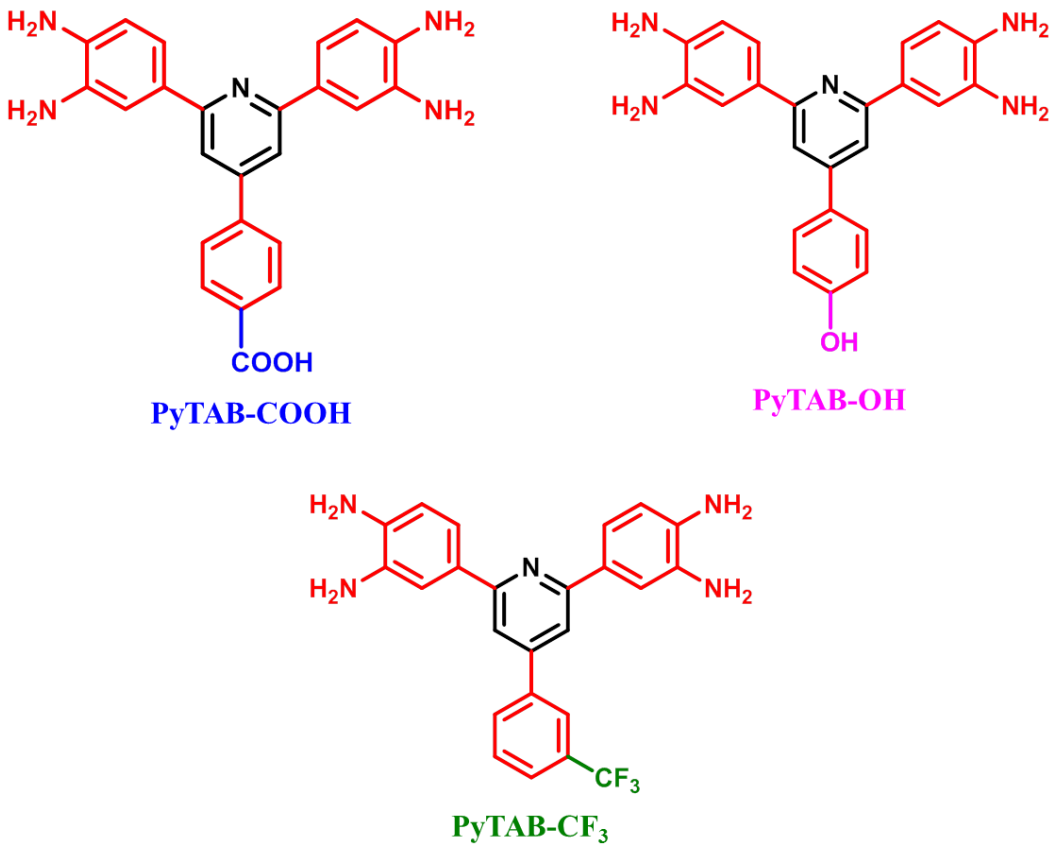

Scheme 4.1. *Chemical structures of PyTAB monomer derivatives.*

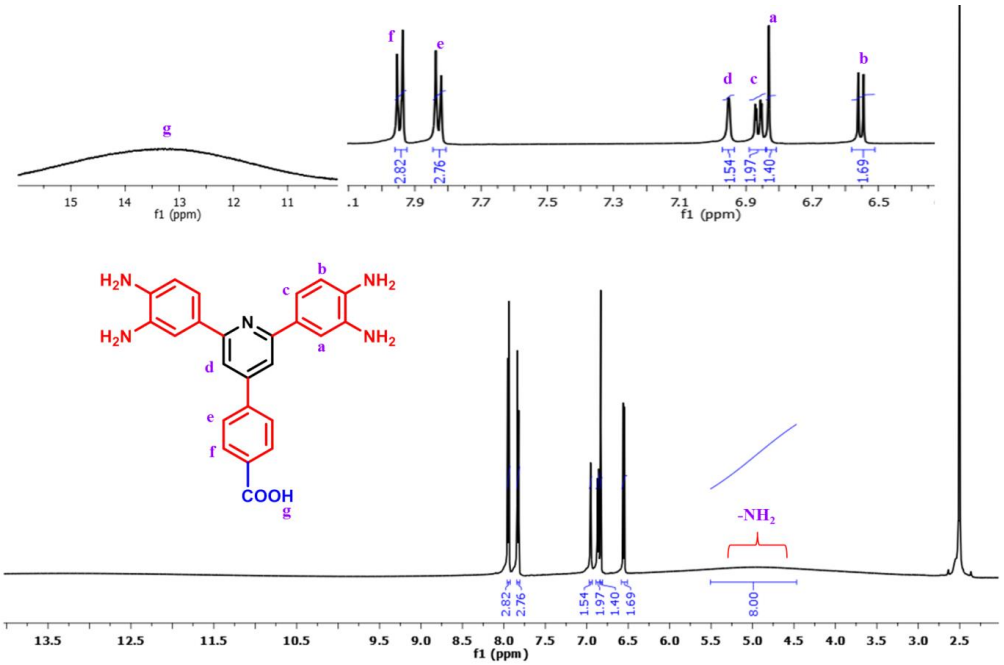

Figure 4.1. *^{1}H NMR spectrum of PyTAB-COOH monomer.*

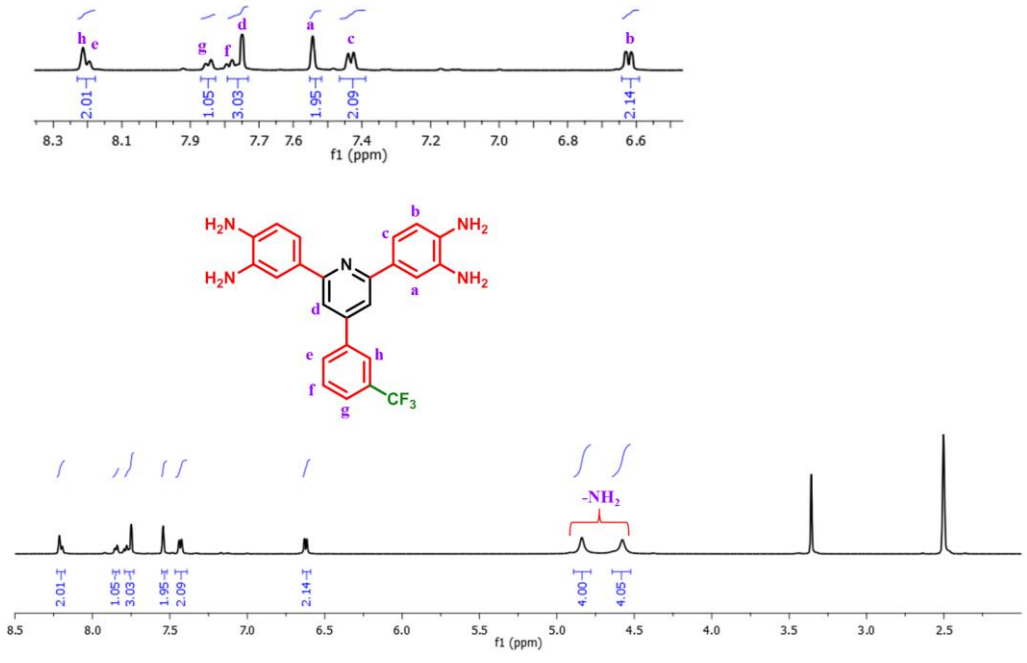

Figure 4.2. *^{1}H NMR spectrum of PyTAB-CF_3 monomer.*

Synthesis of PyTAB-OH monomer:

4-[2,6-bis(3,4-diaminophenyl)pyridin-4-yl]phenol (PyTAB-OH) monomer synthesis was carried out in five steps as shown in Scheme 4.2 and described below.

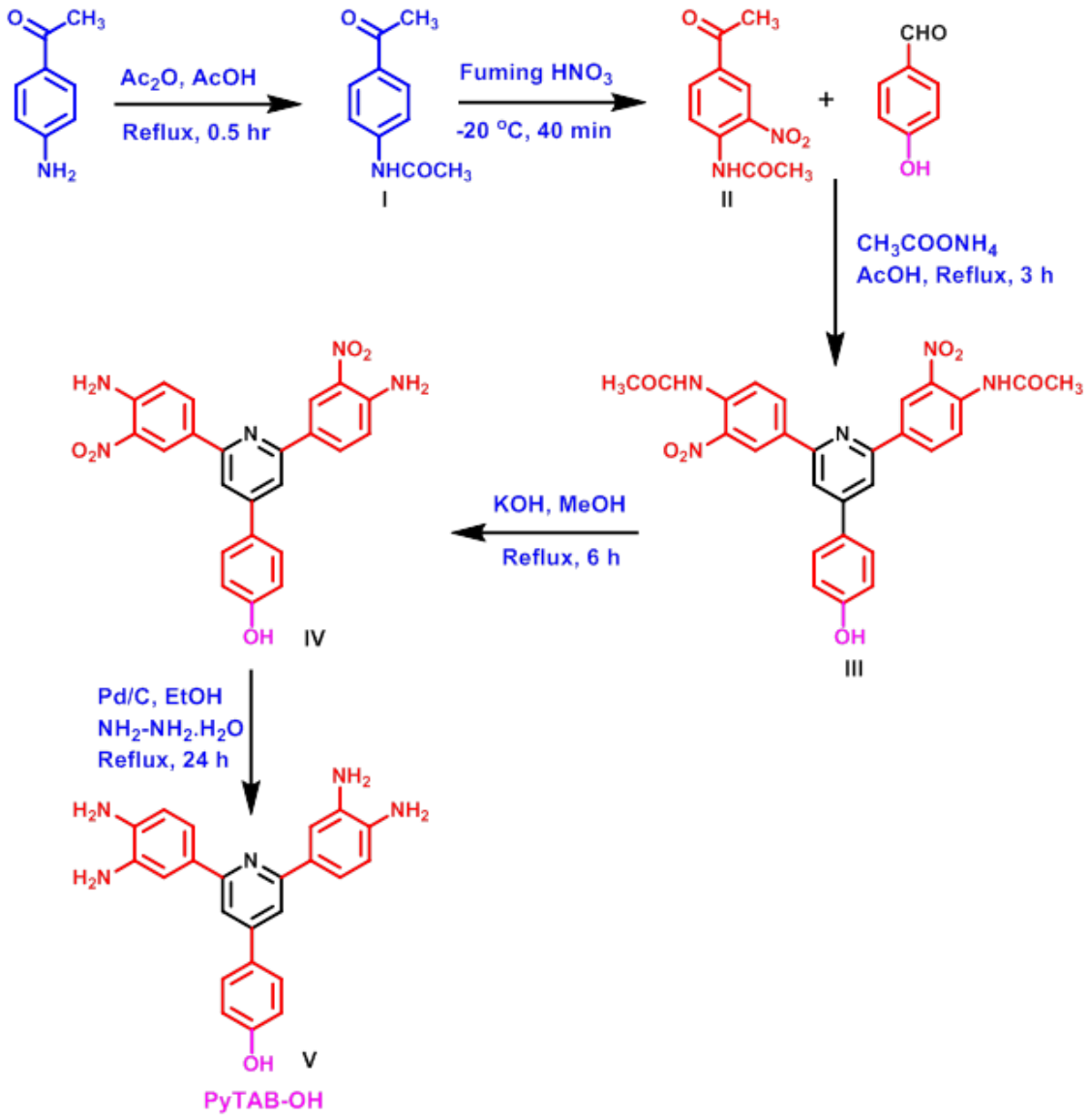

Scheme 4.2. *Synthetic pathway for the synthesis of hydroxyl functionalized tetraamine monomer (PyTAB-OH).*

1. Preparation of acetamidoacetophenone (I): 50 g (0.369 mol) of *p*-amino acet phe-

none was added in to the 500 mL of acetic acid solvent. To this solution 40 mL (0.421 mol) of acetylating agent (acetic anhydride) was added and the total reaction mixture was stirred with refluxing for half an hour. Then the reaction mixture was cooled to room temperature and transferred into the ice to give light yellow precipitate which was collected and washed thoroughly with Millipore water. The dried compound was used to the next step. M.P.: 173-175 °C.

2. Preparation of 3-Nitro-4-acetamidoacetophenone (II): 462 mL (9.56 mol) of fuming nitric acid was cooled in the methanol bath by using a cooling instrument. The small portion of 40 g (0.225 mol) of **I** (acetamidoacetophenone) compound was added slowly into the fuming nitric acid for 25 minutes. Then the reaction was stirred for 15 minutes and temperature was maintained at -20 °C throughout the reaction. The total time consumed for completion of this reaction was 40 minutes. After completion of the reaction, the solution mixture was transferred into the ice to obtained yellow solid. The solid was filtered, washed and dried in vacuum oven at 50 °C for 12 hours. M.P.: 135-137 °C. Compounds **I** and **II** are known in the literature and there melting points are exactly match with the literature reported values.

3. Preparation of N,N'-((4-(4-hydroxyphenyl)pyridine-2,6-diyl)bis(2-nitro-4,1-phenylene))diacetamide (III): 20 g (0.09 mol) of compound **II**, (3-Nitro-4-acetamidoacetophenone) 5.49 g (0.045 mol) of 4-hydroxy benzaldehyde, 45 g (0.585mol) of ammonium acetate and 120 mL of glacial acetic acid were placed into 250 mL single necked round bottom flask equipped with a magnetic stirrer and a reflux condenser. The reaction mixture was refluxed with stirring for 3 h. Then the obtained yellow solid was filtered off and washed thoroughly with 50% of acetic acid 50% of water and finally washed with Millipore water and then dried by using vacuum oven at 70 °C for overnight to obtain product of III.

FT-IR (KBr, cm^{-1}): 3380, 3186, 1594, 1536, 1516; 1370, 1171, 1080, 831.

^{1}H NMR (500 MHz, DMSO-d_6, ppm): 10.4 (s, 2H), 8.84 (s, 2H), 8.63-8.67 (d, 2H), 8.39 (s, 2H), 8.11-8.15 (d, 2H), 7.92-7.95 (d, 2H), 6.97-6.98 (d, 2H), 2.11 (s, 6H)

ESI: 527.

4. 4-(2,6-bis(4-amino-3-nitrophenyl)pyridin-4-yl)phenol (IV): 16 g (0.0303 mol) of compound **III** (N,N'-((4-(4-hydroxyphenyl)pyridine-2,6-diyl)bis(2-nitro-4,1-phenylene))diacetamide) was dissolved in 96 mL of methanol solvent and then the solution was transferred into the 250 mL of round bottom flask. To this solution the methanolic KOH [34 mL methanol and 5.84 g (0.104 mol) of KOH] solution was added drop wise with vigorous stirring for 30 minutes and then 2.92 g of excess KOH solid added to this reaction mixture. The reaction was continued for 6 hours and after that the reaction mixture cooled to the room temperature. Then, the solution mixture was transferred into the deionised water to obtained orange solid. The compound **IV** was collected, washed with water and dried in vacuum oven at 70 °C for overnight.

FT-IR (KBr, cm^{-1}): 3530, 3295, 3180, 1602, 1592, 1537, 1471, 1374, 1320, 1246, 1208, 1081, 878, 827, 783.

^{1}H NMR (500 MHz, DMSO-d_6, ppm): 8.83 (s, 2H), 8.34-8.38 (d, 2H), 8.1 (s, 2H), 7.92-7.95 (d, 2H), 7.85-7.90 (d, 2H), 7.72 (s, 4H), 7.1-7.16 (d, 2H).

ESI: (M+H) 444.

5. 4-(2,6-bis(3,4-diaminophenyl)pyridin-4-yl)phenol (V) or (PyTAB-OH): 10 g (0.0235 mol) of compound **IV** (4-(2,6-bis(4-amino-3-nitrophenyl)pyridin-4-yl)phenol) and 0.54 g of a catalytic amount of 5% Pd/C was dissolved in 340 mL of ethanol solvent and the total solution was placed into the 500 mL of round bottom flask. After that 40 mL of hydrazine monohydrate was added to the reaction mixture at 80 °C for 1.5 hour. The reaction mixture was refluxed for 24 hour. After completion of reaction, the mixture was filtered in hot condition to remove Pd/C. The yellow coloured crystals, was obtained from the filtrate, then the crystals were collected, washed with deionized water, and then dried in vacuum oven at 60 °C for overnight to obtain PyTAB-OH monomer. The Py-TAB-OH monomer was characterized by using LCMS, FT-IR and ^{1}H-NMR spectroscopy Figure 4.3, Figure 4.4 and Figure 4.5, respectively. The monomer structure was confirmed as expected.

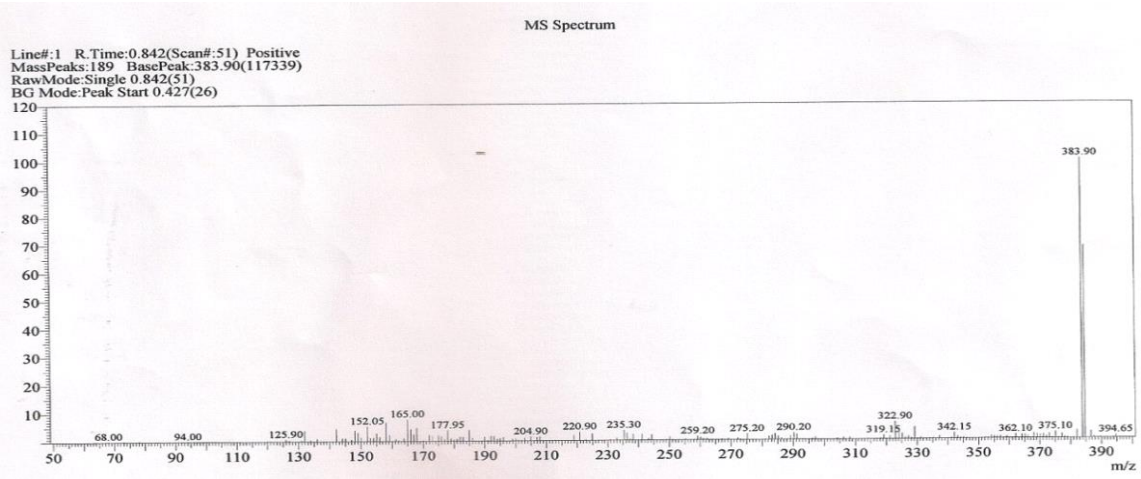

Figure 4.3. Mass spectrum of PyTAB-OH monomer.

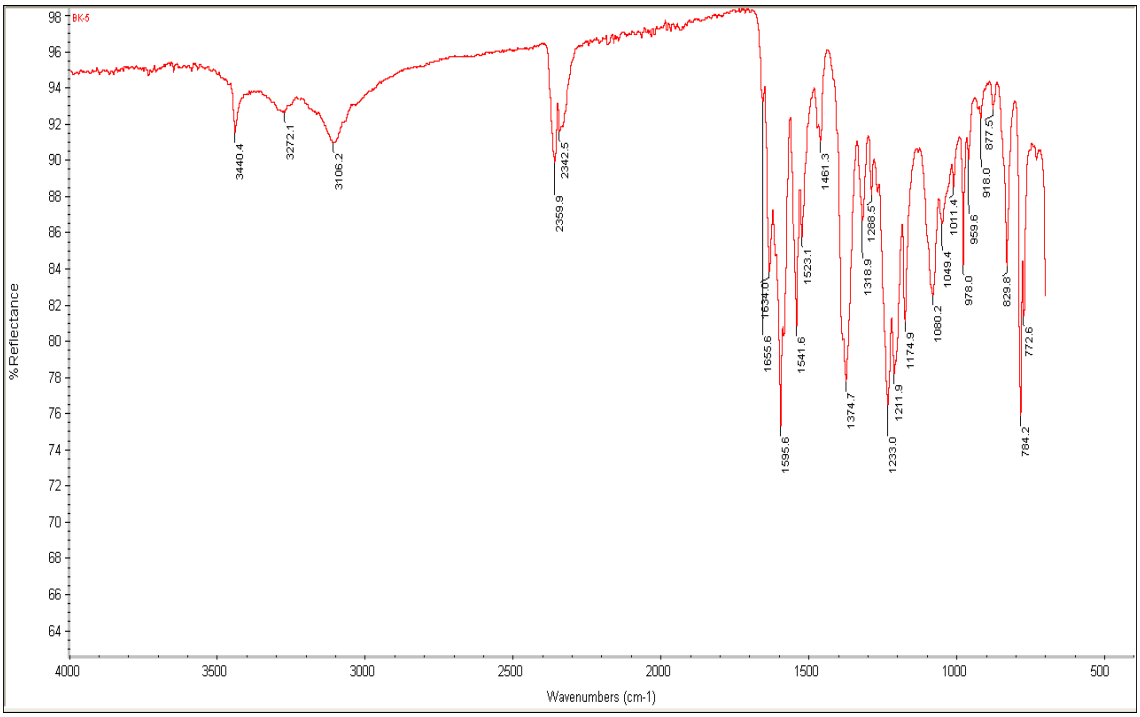

Figure 4.4. *FT-IR spectrum of PyTAB-OH monomer.*

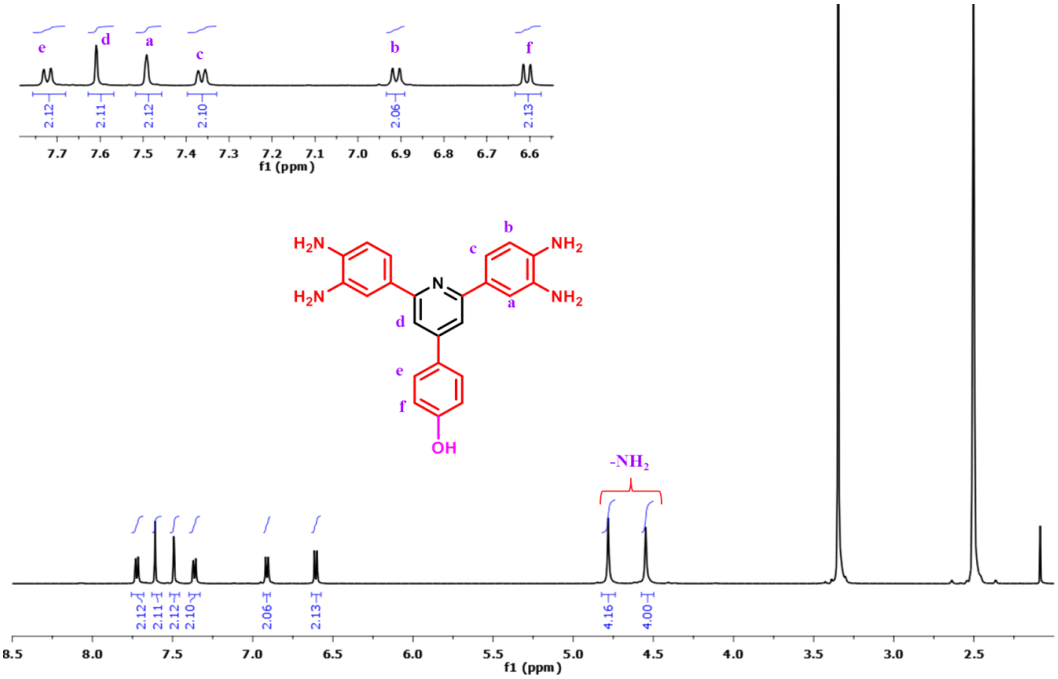

Figure 4.5. *^{1}H NMR spectrum of PyTAB-OH monomer.*

4.2.2. Polymers synthesis

Equal moles of different dicarboxylic acids and PyTAB derivative were taken into a three neck flask with polyphosphoric acid (PPA) for the synthesis of pyridine bridge PBI (PyPBI) homo polymers. Four different dicarboxylic acids were used in this study and these are isophthalic acid (IPA), terephthalic acid (TPA), 4, 4′-oxybis (benzoic acid) (OBA), and 4, 4′-(hexafluoroisopropylidene) bis(benzoic acid) (HFIPA). Monomers were taken along with polyphosphoric acid (PPA) in a 100 mL three neck mercury sealed flask equipped with mechanical stirrer and stirred for 24 hours at 210 °C in continuous nitrogen atmosphere. The total monomer concentrations were varied from 1 – 5% (wt %) to optimize the reaction condition and to obtain high molecular weight PyPBI.[20, 21] For each reaction, the reaction time and temperature (which was usually varied from 50 °C to 210 °C with appropriate ramp and soak time) were optimized. After the complete polymerization, the viscous polymer solutions were slowly poured into de-ionized water and neutralized with sodium bicarbonate. The polymers were filtered

and washed with de-ionized water several times and dried in vacuum oven for 24 h at 100 °C to remove moisture completely. A general polymerization scheme for the synthesis of PyPBIs derivatives is shown in the Scheme 4.3.

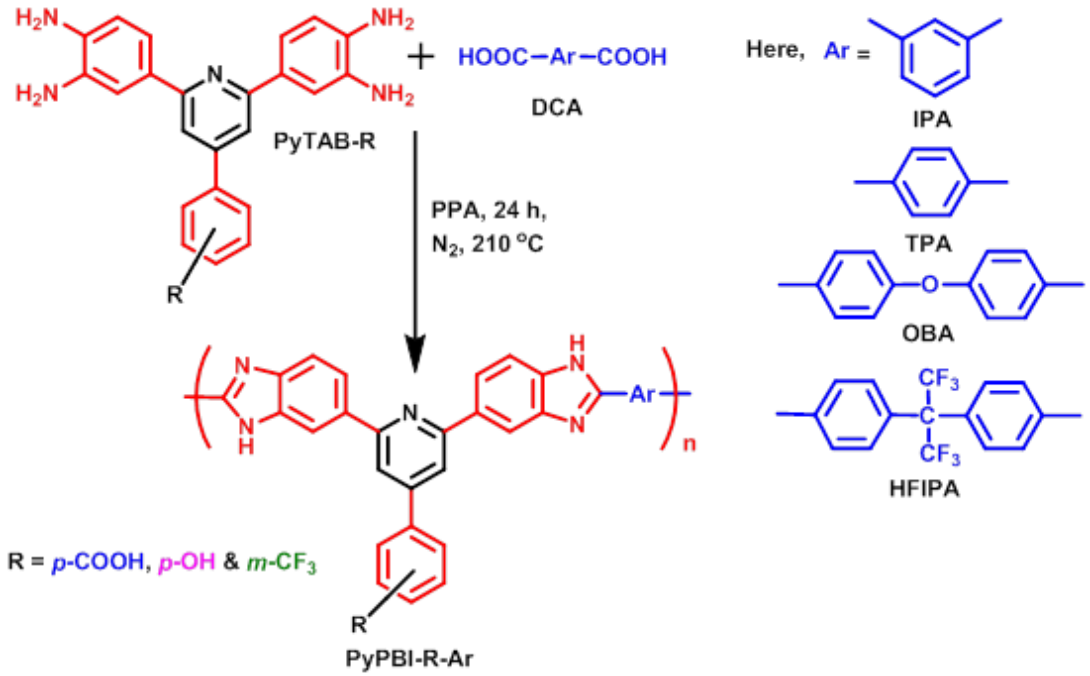

Scheme 4.3. *Derivatives of PyPBI polymers were synthesized from the derivatives of PyTAB monomer with various dicarboxylic acids. The polymers are abbreviated as PyPBI-R-Ar, where R indicates the type of PyTAB derivative and Ar indicates the type of DCA used in the polymerization. A total twelve polymers were made by the combination of various PyTAB and DCAs.*

4.2.3. Membrane fabrication

The highest molecular weight (M.W) of pyridine bridged PBI polymer derivatives were dissolved in suitable solvent for membrane preparation and the polymer solution concentration was kept at 2% (w/v). PyPBI-COOH-OBA and PyPBI-COOH-HFIPA were dissolved in DMSO as well as FA and other derivatives like PyPBI-OH-OBA and PyPBI-CF_3-OBA were dissolved only in DMSO solvent. The solutions were continu-

ously stirred for 24 h at 60 °C temperature then the clear solution were poured into flat glass petridish to fabricate the membranes and then petridish was kept inside the hot air oven for solvent evaporation. For DMSO and FA solvents evaporation temperature were maintained 85 °C for 10-12 h and 70 °C for 4-5 h, respectively. After that the homogeneous membranes was peeled off from the glass Petridis and the membrane was soaked in boiled deionized water to remove trace amount of residual solvent. Finally, these membranes (PyPBI-COOH-OBA, PyPBI-COOH-HFIPA, PyPBI-OH-OBA and PyPBI-CF_3-OBA) dried in vacuum oven for 24 h at 100 °C temperature. The membrane thickness was maintained between 30-40 μm and the membranes were stored in desiccator for further study. The all other polymers did not yield to a membrane. After dissolution in solvent where they get dissolved, these polymer resulted brittle membranes and hence could not considered for further studies.

All the characterization techniques which include viscosity measurement, spectroscopic characterization by Fourier transform infrared spectroscopy (FT-IR) and proton NMR, photophysical studies by UV-visible, thermogravimetric analysis (TGA), dynamic mechanical analysis (DMA) and FE-SEM analysis for all the Py-PBI polymer derivatives are discussed in the Chapter 2. The Py-PBI polymer derivative membranes oxidative stability, H_3PO_4 doping level, water uptake, swelling ratio and the proton conductivity measurements are also discussed in the Chapter 2.

4.3. RESULTS AND DISCUSSIONS

4.3.1. Synthesis of PyPBI derivatives

Three series of PyPBI polymer derivatives have been synthesized by polymerising PyTAB monomer derivatives (PyTAB-COOH, PyTAB-OH and PyTAB-CF_3) with four dicarboxylic acid (DCA) monomers as displayed in the Scheme 4.3. Total 12 polymers are synthesized and abbreviated as PyPBI-R-Ar where R indicates the type of PyTAB used and Ar attributes the DCA type. PyTAB monomers are attractive alternatives because they are economically less expensive and can improve the several properties of PBI polymer very effectively than the conventional TAB. To elucidate the influence of

functional groups of PyTAB on the pyridine based PyPBI polymer derivatives, we prepared polymers with well known, commonly used DCA structures by polymerizing these DCAs with various PyTAB derivatives.

All the PyPBI polymer derivatives produced good amount of yields and the measured inherent viscosity (I.V.) values proves that the PyTAB monomer derivatives can be used for synthesizing PBI type of polymers very readily by replacing conventional TAB. In several literatures, it has been reported that the molecular weight (M.W.) of PBI type polymers can be expressed in terms of inherent viscosity (I.V.) and higher IV value indicates higher MW.[20, 23-28] In all the polymerization reactions carried out for this work, stoichiometric balance was maintained as equal mole ratio between PyTAB monomer derivatives and DCA monomer structures. In all the polymer derivatives, we have maintained similar reaction conditions during the course of polymerisation while changing the initial total monomer concentration (TMC) in the reaction mixture. It is very well established in the PBI literature that the TMC, which is comprising of concentration of the tetraamine monomer and DCA monomer, plays a key role in deciding the course of polymerisation reaction, yield of the reaction and molecular weight (i.e. IV) of the resulting PBI.[9, 20, 21, 23, 24, 28, 29] Therefore, we had to carry out polymerization reaction by varying the TMC in each sets of three PyTAB derivatives and four sets of DCAs. The obtained PyPBI polymers I.V. values were measured and plotted against TMC as shown in Figure 4.6. The data clearly prove that TMC has significant influence in the I.V. values (MW of PBI) of the synthesized polymers. But it is to be noted that the dependence of I.V. (MW) and TMC are also significantly influenced by both the PyTAB derivative and DCA monomers structure. The influence of DCA structure on I.V. values of synthesized PBI are well studied in the literature[9, 14, 20, 28, 29] however, no reports are available on the influence of tetraamine structure. In this study, we have observed that molecular weight of the polymer not only depends on DCA structure but also on the tetraamine monomer and this observation was clearly supported from the results of Figure 4.6. I.V. values of the carboxylic acid based PyPBI polymers (PyPBI-COOH-OBA, PyPBI-COOH-TPA and PyPBI-COOH-IPA) are increasing with the total

monomer concentrations except in case of PyPBI-COOH-HFIPA polymer where it remains unchanged with TMC. I.V. values reaches its maximum at a certain monomer concentration and after that it gradually decreases with the increasing TMC in all the carboxylic acid based PyPBI polymer derivatives. In fact all the polymers display highest molecular weight (I.V.) at 3 wt% TMC (Figure 4.6A).

Among the hydroxyl group containing PyPBI derivatives, PyPBI-OH-OBA and PyPBI-OH-TPA polymers show highest molecular weight (I.V.) at 3 wt% and 2 wt % of the TMC, respectively (Figure 4.6B). The I.V. values of the remaining PyPBI derivatives (PyPBI-OH-IPA and PyPBI-OH-HFIPA) polymers are obtained below 1 dL/g for all the total monomer concentrations (Figure 4.6B) carried out in this study. Another type of derivative that is trifluoro methyl group containing PyPBI, where PyPBI-CF_3-OBA and PyPBI-CF_3-HFIPA polymers have inherent viscosity values 1.2 dL/g and 2.09 dL/g, respectively at 3 wt% total monomer concentration. We could not get any yield of other two polymers (PyPBI-CF_3-IPA and PyPBI-CF_3-TPA) when reactions were carried out between PyTAB-CF_3 with IPA and TPA.

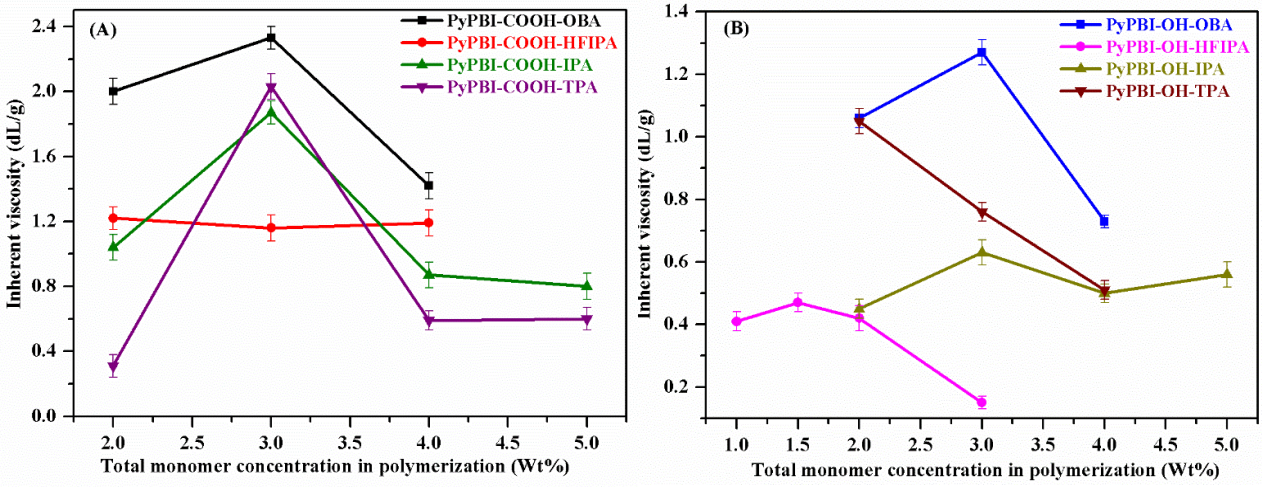

Figure 4.6. *Effect of total monomer concentration on inherent viscosity (a measure of MW of PBI polymer) of PyPBI polymer derivatives.*

A comparison of the all the data as discussed in the above clearly confirms the in-

fluence of structure of both PyTAB derivatives and DCA. A clear picture about this emerges about this when we pick any one system. In the three different polymerization reactions, we have used the same DCA structure (OBA) by varying the PyTAB monomer derivatives to get three types of PyPBI derivatives: PyPBI-COOH-OBA, PyPBI-OH-OBA and PyPBI-CF_3-OBA. A comparison of their I.V. values clearly display that the I.V. is varying by changing the PyTAB monomer derivative. In all the three cases the maximum TMC is 3 wt% but their I.V. values varies and they are 2.33, 1.27 and 1.2 dL/g for PyPBI-COOH-OBA, PyPBI-OH-OBA and PyPBI-CF_3-OBA, respectively. Therefore in this study, we are concluding that the obtained molecular weight (I.V.) of the polymer is not only determined by the DCA structure but also by the type of functional group present in the tetraamine monomer.

4.3.2. Solubility and the preparation of free standing membrane

The solubility of PyPBI derivatives were tested up to 2% (w/v) polymer concentration in various high polar solvents such as methane sulfonic acid (MSA), N-methyl-2-pyrrolidone (NMP), N, N-Dimethylacetamide (DMAc), formic acid (FA) and dimethyl sulphoxide (DMSO). Among the synthesized PyPBI derivatives, the highest I.V. polymers of each type of derivatives were taken for solubility testing and further studies. Also, we made effort to prepare membrane from the solution in which PyPBI derivatives were dissolved. The results of solubility and free-standing membrane formation are summarized in the Table 4.1. The data clearly proves that the solubility of synthesized PyPBI derivatives depends upon the three factors: (1) solvent type, (2) structure of the DCAs used to synthesize PyPBI derivatives and (3) the functionality (-COOH, -OH and $–CF_3$) attached to the PyTAB derivative monomers. Table 4.1 clearly shows that all the polymers are completely soluble on heating both in MSA and NMP. In some cases such as PyPBI-COOH-HFIPA and PyPBI-OH-HFIPA polymers are even completely soluble in room temperature itself in MSA which is attributed to the presence of bulky hexafluoro isopropyledene group.[30, 31] However, all the polymers solutions in both of these solvents (MSA, NMP) did not produce stable free standing films. The resulting

films from these solutions even up to 2 wt% concentration are very brittle in nature and hence these two solvents are not useful for our further studies. Therefore, we moved our focus to the polar solvents like DMSO, DMAC, and FA etc. Solubility testing in DMAc showed that the synthesized polymers are partially soluble on heating except few cases such as PyPBI-COOH-HFIPA and PyPBI-OH-HFIPA, and hence film preparation was not possible from DMAc and the HFIPA based soluble polymer did not produce stable films. The next solvent we tested was DMSO and the results suggest that polymers (highlighted with dotted box) are completely soluble and produce free standing films readily. But there are many, which are not soluble at all or if soluble did not yield free standing films. Similarly we tested the solubility and film formation ability in FA and found except two polymers (PyPBI-COOH-OBA and PyPBI-COOH-HFIPA), other polymers are either not soluble or produce very brittle membrane. Therefore, our remaining study restricted to only with four polymers (PyPBI-COOH-OBA, PyPBI-COOH-HFIPA, PyPBI-OH-OBA and PyPBI-CF_3-OBA) which are soluble and produced stable films in DMSO. It must be noted that if the polymers contain fluorinated functionality or ether functionality (when OBA is used as DCA), then solubility is enhanced and this may be attributed to the electronegativity of fluorine and flexibility due to OBA group.[9, 30-32] In two cases (shown with red dotted line in the Table 4.1) of FA, we are able to obtain membranes and have studied these membranes characteristics to compare the effect solvents.

Table 4.1. Solubility and free-standing membrane formation ability of all the synthesized PyPBI derivatives studies in this work.

			MSA		NMP		DMAc		DMSO		FA	
Entry	Polymer Identity	Maximum IV (dL/g) obtained	Solubility	Stable free standing membrane formation	Solubility	Stable free standing membrane formation	Solubility	Stable free standing membrane formation	Solubility	Stable free standing membrane formation	Solubility	Stable free standing membrane formation
1	PyPBI-COOH-OBA	2.33	+	No	+	No	±	No	+	Yes	+	Yes
2	PyPBI-COOH-HFIPA	1.22	++	No	+	No	+	No	+	Yes	+	Yes
3	PyPBI-COOH-IPA	1.87	+	No	+	No	±	No	±	No	±	No
4	PyPBI-COOH-TPA	2.03	+	No	+	No	±	No	±	No	±	No
5	PyPBI-OH-OBA	1.27	+	No	+	No	±	No	+	Yes	+	No
6	PyPBI-OH-HFIPA	0.47	++	No	+	No	+	No	+	No	+	No
7	PyPBI-OH-IPA	0.63	+	No	+	No	±	No	±	No	±	No
8	PyPBI-OH-TPA	1.05	+	No	+	No	-	No	±	No	±	No
9	PyPBI-CF_2-OBA	1.2	+	No	+	No	±	No	+	Yes	+	No
10	PyPBI-CF_2-HFIPA	2.09	+	No	+	No	+	No	+	No	+	No
11	PyPBI-CF_2-IPA	Did not yield	--	--	--	--	--	--	--	--	--	--
12	PyPBI-CF_2-TPA	Did not yield	--	--	--	--	--	--	--	--	--	--

++ : completely soluble at room temperature, + : soluble on heating, ± : partially soluble on heating, - : Insoluble on heating.
Note: Solubility reported here based on the result obtained upto 2 wt% (w/v). Film formation also tested on 2 wt% (w/v) solution of the polymer

4.3.3. Spectroscopic characterization of synthesized PyPBI derivatives

The IR spectra obtained from the films of PyPBI derivatives are shown in Figure 4.7. All the important stretching frequencies are highlighted with the dotted lines in the IR spectra. The spectral nature and frequencies are matching very well with reported results in the literature.[34-37] Stretching vibrations observed at 3628, 3445, 3212 and 3080 cm^{-1} are due to the O-H of absorbed moisture, non-hydrogen bonded free N-H of imidazole groups, self-associated hydrogen-bonded N-H of imidazole groups and C-H of aromatic ring, respectively. The other vibrational stretching frequencies observed at 1607, 1445 and 840 cm^{-1} are due to the C=C/C=N stretching bands, in plane benzimidazole ring deformation and C-H stretching frequency of pyridine ring, respectively. In the case of carboxylic acid functionality containing PyPBI polymers (PyPBI-COOH-OBA and PyPBI-COOH-HFIPA) a peak at 2860 cm^{-1} is ascribed to the O-H stretching frequency and a peak at 1247 cm^{-1} represents carboxylic acid C-O stretching frequency. Similarly for these two polymers, the absence of C=O peak at around 1780-1710 cm^{-1} may be due to the fact that –COOH functionality might be involved in hydrogen bonding with another chain of carboxylic acid group or imidazole group. In case of PyPBI-CF_3-OBA polymer, the peak at 1370 cm^{-1} is ascribed to the C-F stretching vibration.

The structure of PyPBI polymers were confirmed by the proton NMR spectra which are represented in the Figure 4.8, Figure 4.9 and Figure 4.10. Polymer structures and peaks assignment are included in the spectra. Earlier we reported that, the PyPBI polymers peak positions and chemical shift values varied from one polymer to the other due to the changing DCA in the polymer structure. In this present work, we observed that shifting of chemical shift position not only depends on the DCAs structure but also on the tetraamine structure. The chemical shift values of the imidazole N-H proton of the PyPBI polymers varies between δ 13.15 to 13.36 ppm and aromatic proton resonances also alters between δ 7.0-8.7 due to their varying PyTAB monomer derivative structure and DCA monomer structure.[27, 28, 37, 38] The imidazole N-H peak chemical shift appears at δ 13.15, 13.2 and 13.3 for PyPBI-COOH-OBA, PyPBI-OH-OBA and PyPBI-

CF_3-OBA, respectively. In all these three polymers, DCA is same OBA, but PyTAB derivative was altered and we observed the shift in N-H chemical shift. Similarly a comparison of PyPBI-COOH-OBA, PyPBI-COOH-HFIPA, PyPBI-COOH-TPA and PyPBI-COOH-IPA show their imidazole peak proton resonances at 13.15, 13.28, 13.39 and 13.45, respectively (Figure 4.8). Here, the monomeric structure of PyTAB is same but -N-H peak shifts due to different DCA structures.

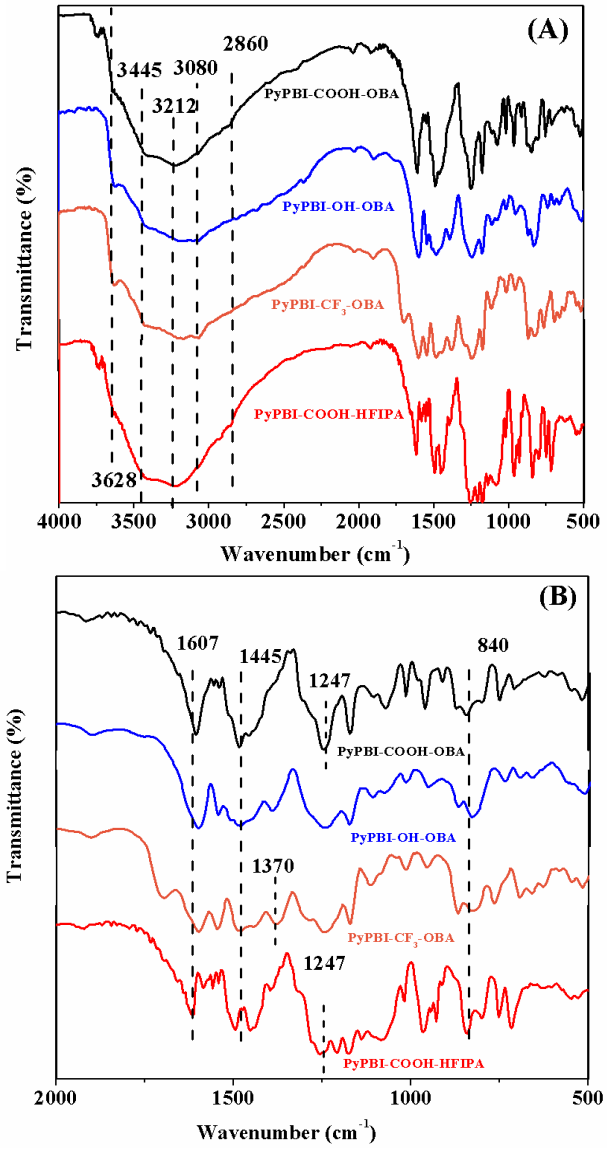

Figure 4.7 (A) FT-IR spectra of PyPBI derivatives polymers, (B) magnified portion of FT-IR spectra of PyPBI derivatives in the region 2000 to 500 cm^{-1}.

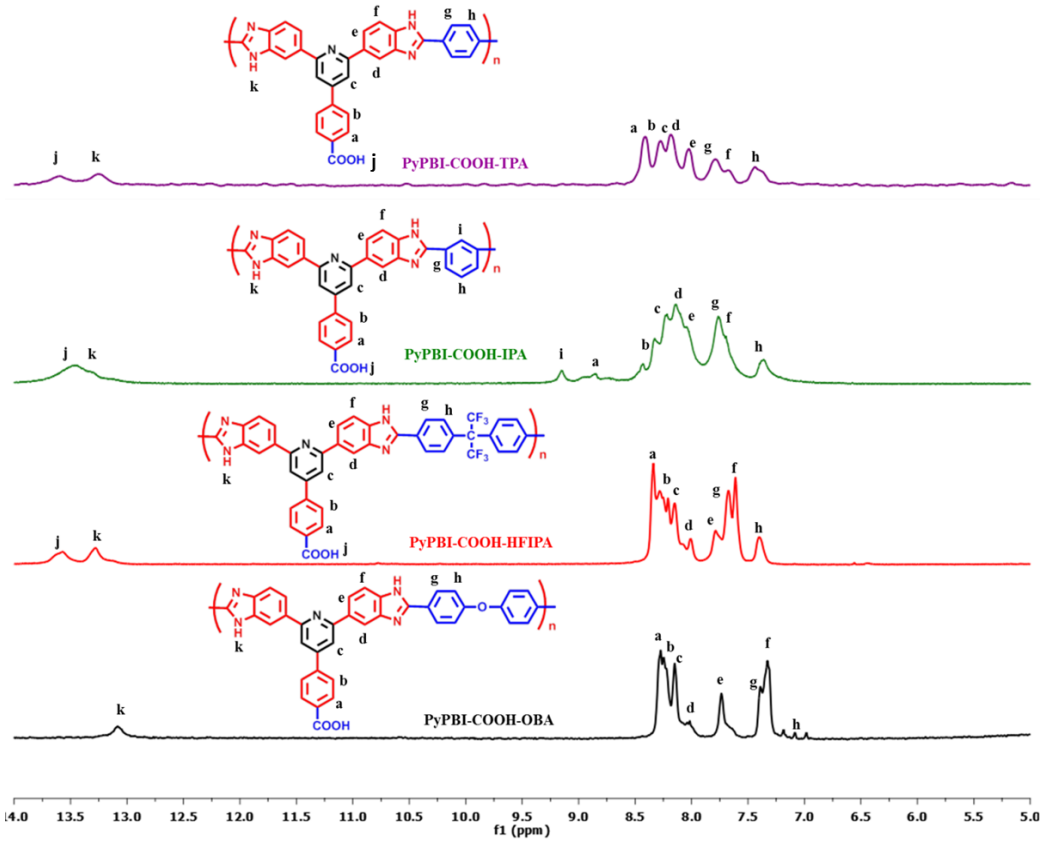

Figure 4.8. *^{1}H-NMR spectra of all PyPBI-COOH derivatives structures of polymers and peak assignments are shown in the Figure.*

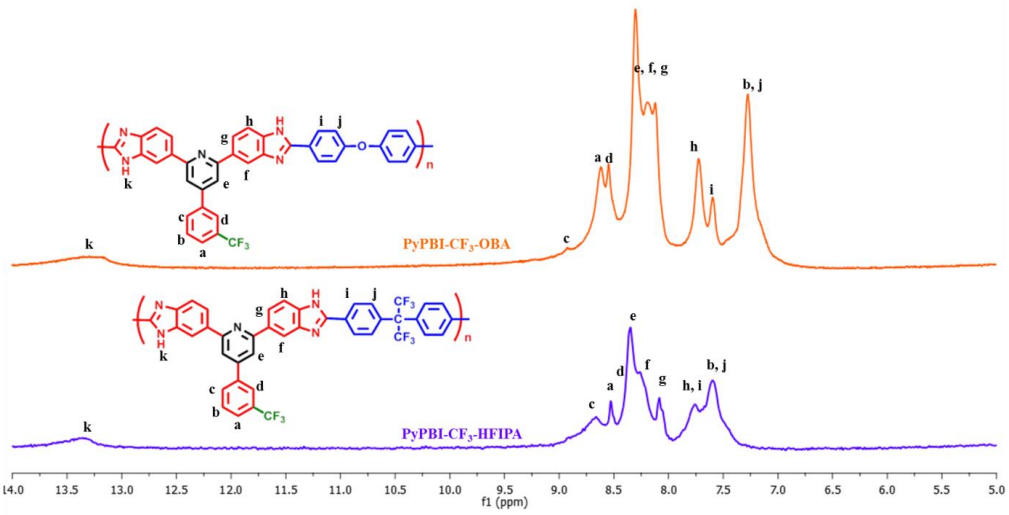

Figure 4.9. *^{1}H-NMR spectra of PyPBI-CF_3 derivatives structures of polymers and peak assignments are shown in the Figure.*

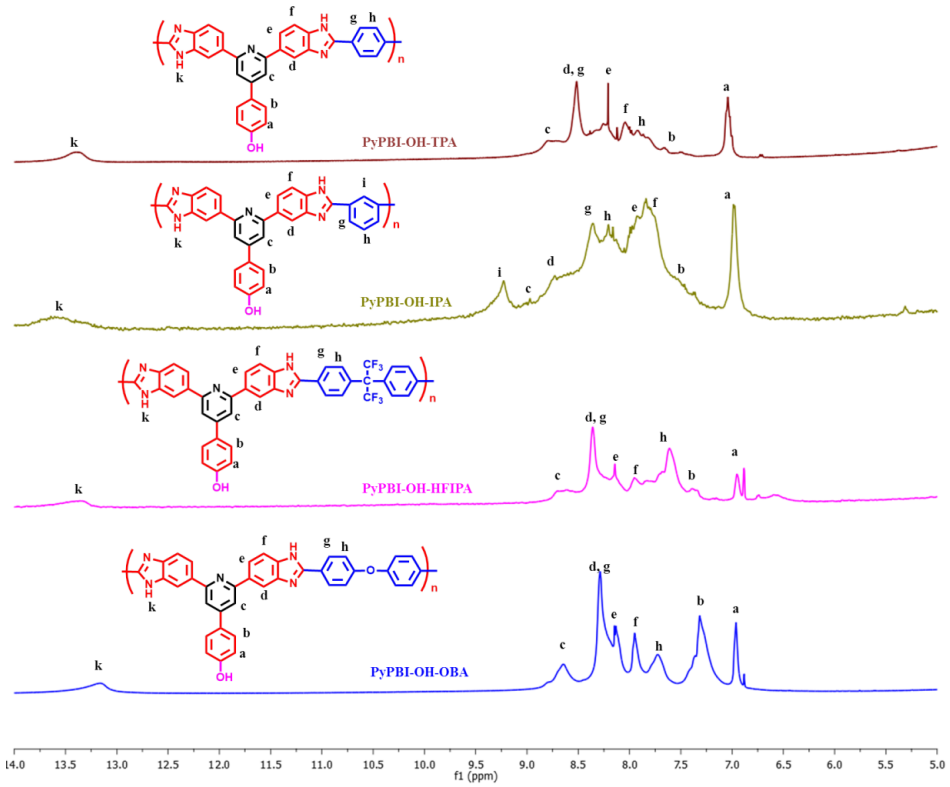

Figure 4.10. *^{1}H-NMR spectra of PyPBI-OH derivatives structures of polymers and peak assignments are shown in the Figure.*

It is known in the literature through our earlier work that dilute solution of PBI in aprotic polar solvent display absorption peaks at around 280 nm and 345 nm owing to the σ-σ* and π-π* transitions. We have also demonstrated earlier that the absorption maxima (λ_{max}) of longer wavelength π-π* transition is highly sensitive to the net electronic conjugation in the PBI backbone and can be readily altered by varying the DCA structure in the PBI backbone.[9, 28, 39] In addition to alternative DCA structure, in the current study we have observed that this shorter energy transition maxima (π-π* transition) can be altered by changing the electron donating/ withdrawing (resonance effect: +R or -R) functionality in the TAB monomer which eventually changes the net electronic conjugation in the polymer backbone by pulling or pushing the electron from the PBI backbone. Figure 4.11 compares the absorption spectra of PyPBI derivatives (with different functionality in TAB) obtained from dilute solution in NMP. In all the cases peak around 280 nm due to σ-σ* transition does not display any variation of wavelength

(though show some changes in peak intensity and broadness) but in all the cases π-π* transition λ_{max} varies as the functional groups changes from an electron withdrawing a +R group (-COOH) to highly electron withdrawing group (-CF_3); for example λ_{max} (π-π*) peak shifts from 342 nm to 332 nm when functional group changes from COOH to CF_3 in case of HFIPA band PyPBI derivatives (Figure 4.11B). Similarly a hypso-chromic shift from 343 nm to 330 nm is observed in case of IPA polymer with change in functional group from COOH to OH (Figure 4.11B). These shifts towards lower wavelength in case of CF_3 or OH derivatives is due to decreasing conjugation because of highly electron withdrawing effect of CF_3 and OH on the PBI backbone.

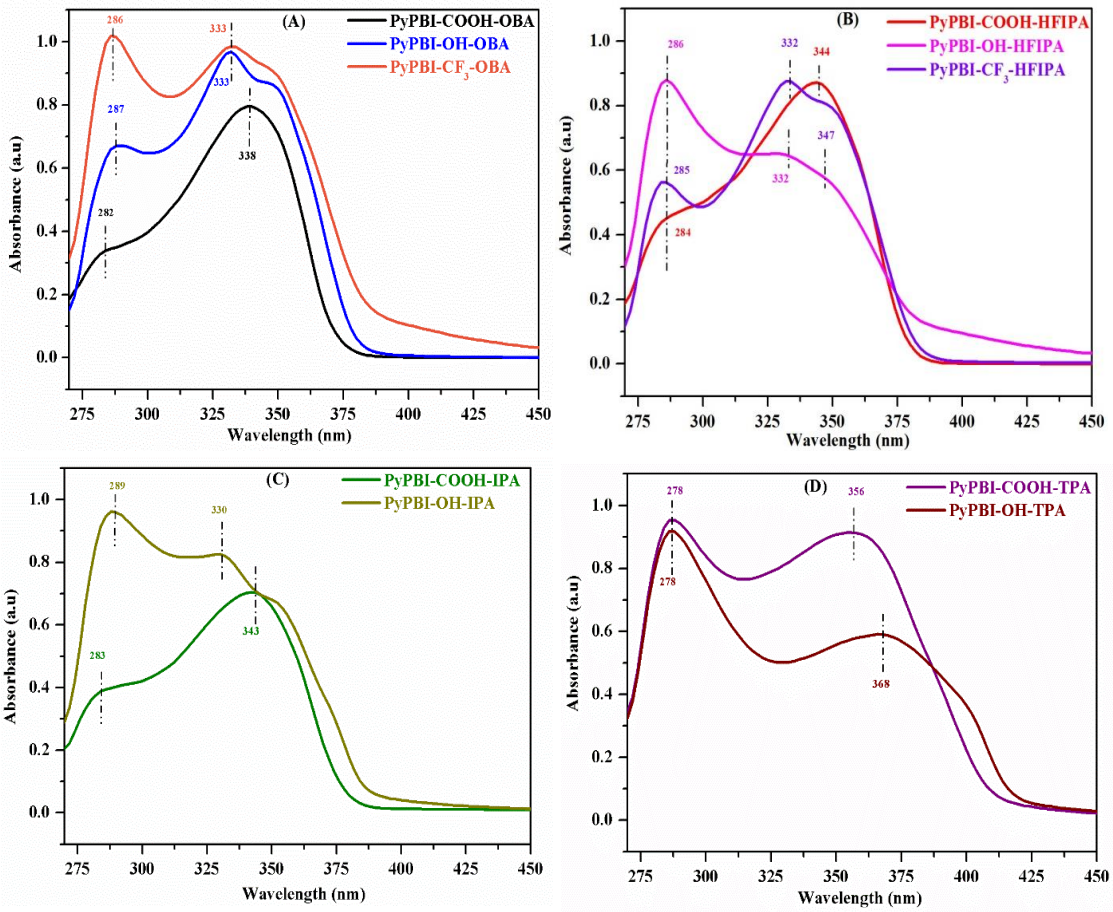

Figure 4.11. *Comparison of absorption spectra of PyPBI derivative polymers in order to see the effect of PyTAB monomer structure. All the spectra were recorder from polymer solution in NMP (1 mg/ mL) using 1 cm path length quartz cuvette.*

4.3.4. Thermal stability

TGA analysis of all the PyPBI derivatives (-COOH, -OH and $–CF_3$) were carried out in nitrogen atmosphere in the temperature ranges between 30-800 °C at a heating rate of 10 °C/min. All the three types of PyPBI derivatives show two evident weight losses (Figure 4.12): the first weight loss was observed at around 100-150 °C temperature which is due to the evaporation of absorbed moisture and another weight loss was observed at around 450-500 °C which is attributed to the decomposition of pyridine ring and benzimidazole groups. In all three cases HFIPA based polymer derivative shows higher thermal stability below 150 °C temperature (Figure 4.12B) which is ascribed to the evaporation of water molecule. This is in resonance with the low water absorption nature of this derivative because of the hydrophobic character of bulky hexafluoroisopropylidene group. However, temperatures beyond 500 °C, HFIPA polymer derivative displayed lower thermal stability in all three derivatives due to the rapid decomposition of hexafluoroisopropylidene group.[20] It should be noted from the Figure 4.12 that the thermal degradation of these PyPBI polymers are quite significantly dependent on backbone structure especially on the type of functional groups in TAB monomer. For example a closer look of the TGA plots of Figure 4.12 (C) and (D) clearly demonstrates that –COOH functionalized PyPBI derivative has displayed higher stability below 450 °C (2^{nd} degradation) whereas shows lower stability after 450 °C in comparison to –OH functionalized PyPBI. Similar trends can be identified in other cases as well. Overall, it is quite clear that the functionality in the TAB monomer plays a crucial role in altering thermal stability.[40]

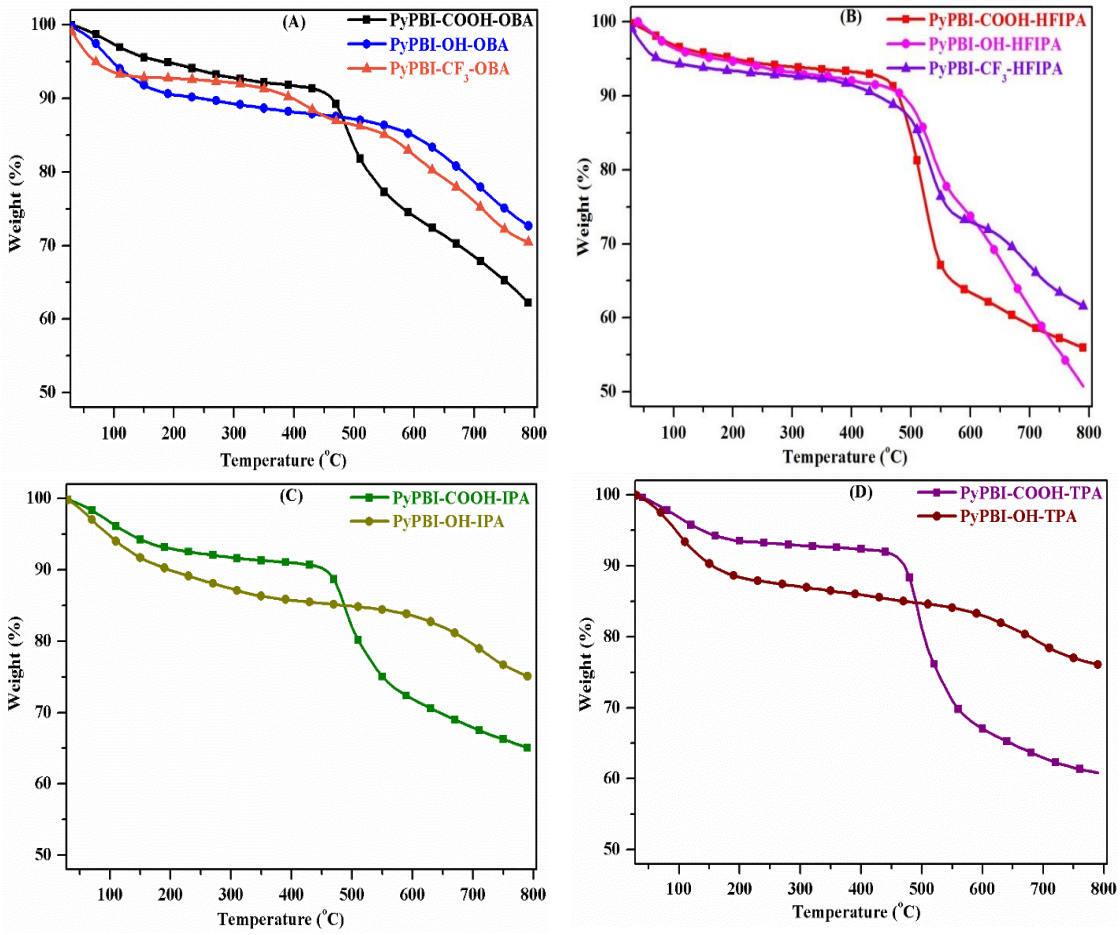

Figure 4.12. *TGA plots of all the synthesized PyPBI derivatives. Experiments were carried out under N_2 atmosphere.*

4.3.5. Thermal transitions and mechanical stability

Temperature dependent storage modulus (E') and loss modulus (E'') and tan δ vs temperature plots of all the PyPBI derivatives are represented in Figure 4.13 Storage modulus ($E^{'}$) and glass transition temperature (T_g) of the PyPBI derivatives at different temperatures are extracted from Figure 4.13A and B are summarized in Table 4.2 for easy comparison of the results. Storage modulus of these polymers decreases with the increasing temperature thus it seems that mechanical strength becomes poorer at higher temperatures. It is known that the DCA structure influence the E' of PBI which is in agreement here as Figure 4.13A clearly displays that OBA polymer shows higher storage modulus than the HFIPA in case of COOH derivatives. However not only DCA

structure, tetraamine monomers also influences the mechanical stability and the stability order as PyPBI-OH-OBA < PyPBI-CF_3-OBA < PyPBI-COOH-OBA and this order is maintained both in rubbery (> 350 °C) and glassy (< 100 °C) region as seen from Table 4.2. Hence, from this study we are concluding that the storage modulus is affected by changing the a) DCA structure and b) tetraamine monomer structure especially the type of functional groups it consists.

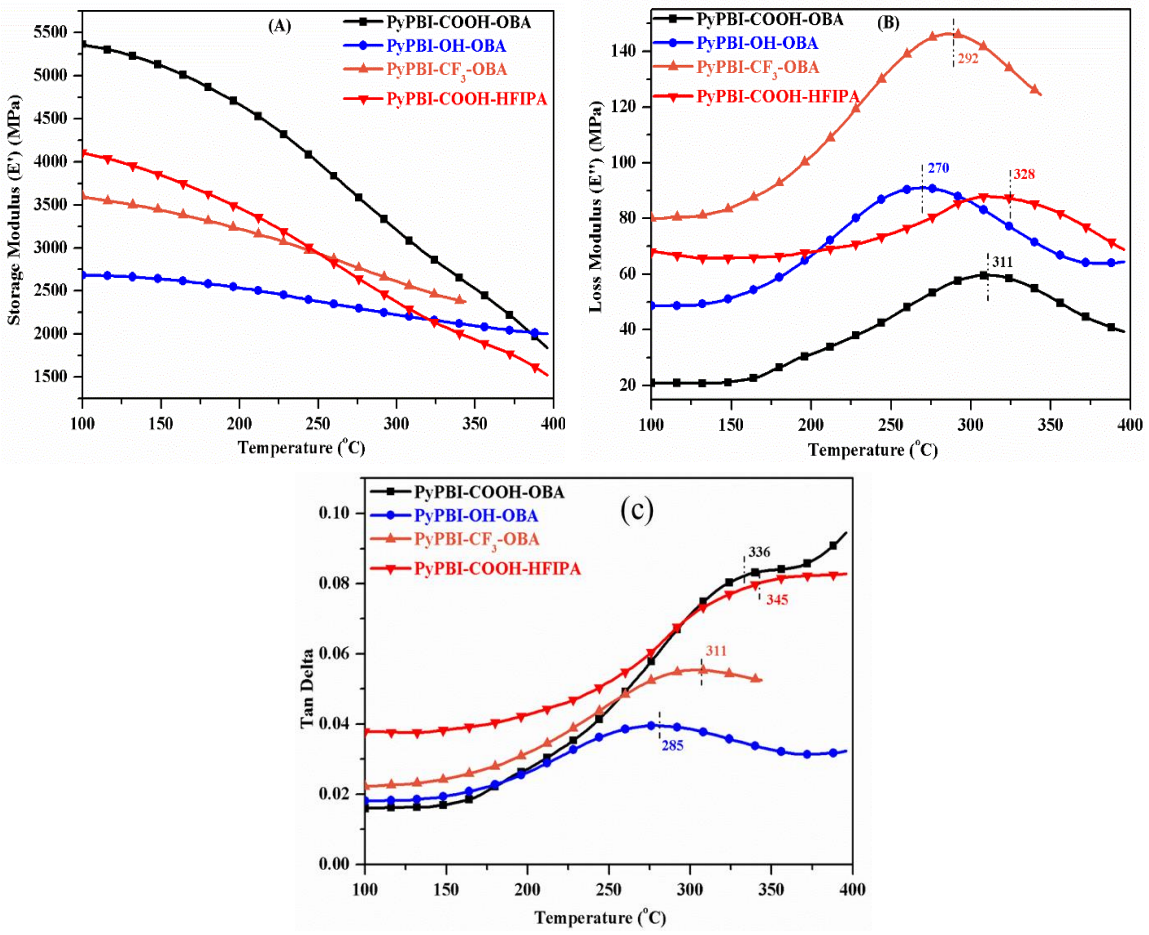

Figure 4.13. Various thermo-mechanical properties of PyPBI polymers obtained from DMA measurement. Temperature dependent plots of storage modulus *(E')* (A), loss modulus *(E'')* (B) and tan delta (C).

The glass transition temperatures (T_g) were measured from Loss modulus (*E''*) (Figure 4.13B) and Tan Delta plots (Figure 4.13C) and the values are tabulated in Table 4.2. Both *E''* and tan δ plots are shown to possess only one relaxation peak. PyPBI-

COOH-HFIPA polymer membranes display higher T_g values than the other PyPBI derivatives and this might be due to the presence of bulky hexafluoroisopropylidene group. Again, it is distinctly clear that T_g values also depends on the type of functionality. T_g values decreases as we change the functional group from COOH (311 °C) to CF_3 (292 °C) to OH (270 °C) as seen in Table for E' data. Similar trend can also be seen from tan δ data. Hence the effect of functional group on TAB monomer is established. It may be pertinent to mention here that most of the PBI literature have discussed about only one T_g which is usually observed at higher temperature (> 200°C) but Noto et. al. also showed the existence of T_g below < 200° C[41, 42] by a very precise modulated DSC study. Further, investigation on the PyPBI derivatives for determining the T_g (< 200° C) may be undertaken for understanding the PyPBI chains relaxation behaviour.

Table 4.2. Extracted thermo-mechanical data from Figure 4.13

Derivatives of PyPBI membranes	E' (MP_a) at 100 °C	E' (MP_a) at 350°C	T_g (°C) from E''	T_g (°C) from tan δ
PyPBI-COOH-OBA	5369	2550	311	336
PyPBI-CF_3-OBA	3603	2374	292	311
PyPBI-OH-OBA	2681	2109	270	285
PyPBI-COOH-HFIPA	4104	1948	328	345

4.3.6. Oxidative stability

Oxidative stability is an important physical property which need to be studied for long term use of PEM in oxidative environment and generally it was carried out by using Fenton's reagent (Fe^{+2} and H_2O_2) test. In this test, hydroxyl radical ($OH^{\cdot}$) and hydroperoxyl radicals ($OOH^{\cdot}$**)** were generated from the degradation of H_2O_2 and these radical react with the polymer hydrogen-carbon bonds and thus the polymer chain degradation occur.[40-44] Oxidative stability of PyPBI derivatives assessed from the remaining weight (%) vs function of time (h) plot (Figure 4.14). Derivatives of PyPBI polymer membranes have shown greater oxidative stability when compared with the convention-

al PBI. Earlier results on OBA based PBI display above 40 % oxidative degradation after 100 h[35, 36, 45] whereas in the current study OBA based PyPBI display less than 30% degradation. In this study, PyPBI derivatives PyPBI-COOH-OBA and PyPBI-COOH-HFIPA (Figure 4.14) membranes obtained from DMSO solution show the oxidative degradation ~ 18 and 27 %, respectively. The stable membrane obtained from formic acid (FA) solution in two cases: PyPBI-COOH-OBA and PyPBI-COOH-HFIPA (Table 4.1) display comparable oxidative degradation in comparison with DMSO membranes (Fig. 4.14). Other two example of OBA based (PyPBI-OH-OBA, PYPBI-CF_3-OBA) PyPBI derivatives display comparable stability with the conventional PBI. The explanation to this observation is that in case of PyPBI-COOH polymer, –COOH functional group makes strong crosslinking with other polymer chain of imidazole group or carboxylic group; thereby preventing the attack of hydroxyl radical on the PyPBI polymer chain. The most important points to be noted that, the stability is dependent on the type of functional groups (-COOH, -OH and –CF_3) in the PyTAB monomer. The data (Figure 4.14) clearly demonstrate that –COOH derivatives are much higher stable than both –OH and –CF_3 derivatives which may be due to the possible cross-linking as explained above.

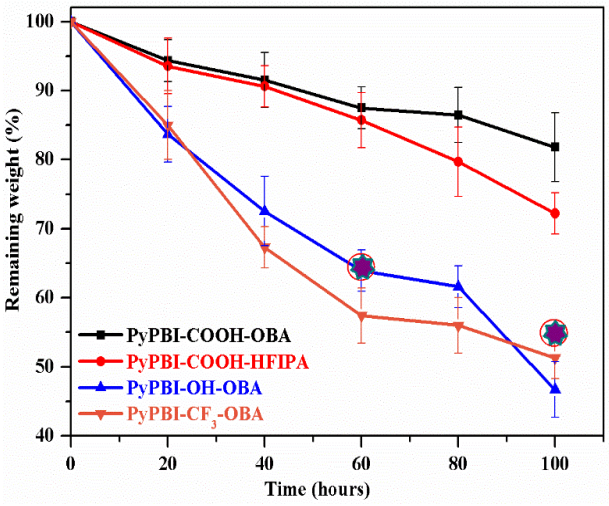

Figure 4.14. Oxidative stability (weight vs time) of PyPBI derivative polymer membranes. ⬣ indicates the data of OBA based conventional PBI (OPBI) obtained from the literature.[35]

4.3.7. Phosphoric loading, water uptake and swelling ratio studies

Phosphoric acid (PA) loading all of three types of PyPBI derivative membranes are tabulated in the Table 4.3. PA loaded membranes were obtained by immersing the dry membrane in H_3PO_4 for 3 days at room temperature. Carboxylic acid based PyPBI polymer derivatives were immersed in 85% phosphoric acid while both hydroxyl and trifluoromethyl group polymer derivatives were immersed in 70% PA since these two sets of polymers get dissolved in 85% PA and therefore we had to do the loading in PA process by using 70% PA only. It is to be noted that unfunctionalized PyPBI can withstand only up to 60% PA, the polymers get dissolved in PA when PA concentration is higher than 60 %.[20] However, in the current study functionalised PyPBI (derivatives) are showing stability up to 85% PA. The enhanced stability of these polymer derivatives towards PA might be due to the functional groups that influence the hydrogen bonding interaction between the polymer chains. In the case of PyPBI-COOH polymer derivative, there is a possibility that some of the carboxylic acid groups may involve in imidization with tetraamine monomer and results in developing another branched polymer chain along with the main chain polymer. This might be helping in the enhancing the stability up to 85% PA in case of –COOH based PyPBI. The PEM performance highly depends on the PA loading of the sample and hence high PA loaded membranes are desirable to obtain higher proton conductivity PEM. The PA doping level of the PyPBI derivative membranes are in the range of 11-13 moles phosphoric acid per repeat unit (shown in Table 4.3) and do not show any significant variation on the attached functional groups in PyTAB monomer.

However, we have observed an important dependency of PA loading on the solvent from which the membranes were made. We could get stable (free standing film) using formic acid (FA) solution in two cases: PyPBI-COOH-OBA and PyPBI-COOH-HFIPA as shown in the Table 4.1. We measured the PA loading of these two FA membranes and results are included in Table 4.3. Very surprisingly, we observed that the membranes made from FA solvent have significantly higher acid loading capacity than

their corresponding membranes made from DMSO solvent. The PA loading of FA membranes is 25 moles per PBI repeat unit which is almost double than that of the DMSO membranes. We do not know the exact reasons for this but our preliminary circumstantial evidences attributes that the polymer behaviour changes in the acidic polar solvents which may help in yielding a favourable morphology for loading high PA and thereby FA membranes shows higher PA loading. In later section we have discuss about the morphological features of these polymers in both DMSO and FA which may have some influence in PA loading.

Table 4.3. PA loading, water uptake and swelling ratio values of PyPBI derivative membranes. Numbers in the bracket are the standard deviations in the measurements.

PyPBI derivative membranes	PA doping (moles/RU)	Water uptake Wt (%)	Swelling ratio (%)
PyPBI-COOH-OBA	12.33 (0.23)	10.82 (1.84)	1.52 (0.4)
PyPBI-COOH-HFIPA	13.07 (2.32)	9.54 (3.88)	2.36 (0.30)
PyPBI-OH-OBA	11.20 (1.09)	--	--
PyPBI-CF_3-OBA	11.48 (1.67)	--	--
PyPBI-COOH-OBA #	23.35 (3.43)	9.48 (0.54)	0.96 (0.3)
PyPBI-COOH-HFIPA #	24.57 (1.11)	8.54 (1.64)	2.77 (0.46)

These two membranes were obtained from 2% (w/v) formic acid solution.

Polybenzimidazoles are very hygroscopic in nature, absorbing moisture up to 5-10% from its weight, due to the formation of hydrogen bonding interaction between water molecules and –NH- of the imidazole groups. In this study, we observed that water uptake varies from ~ 8 to 11 wt (%) (Table 4.3) depending on the DCA structure and solvent used to get the membrane. Both the formic acid membranes display lower water uptake than their corresponding DMSO membranes. Always HFIPA membranes are absorbing comparatively less amount of water uptake than the OBA membranes. This is due to hydrophobic nature of hexafluoroisopropyledene group present in the HFIPA

polymer backbone and hydrophilic nature of oxygen atom present in the OBA polymer. Swelling ratio of the membrane is also another important parameter to be considered for the PEM use. Higher swelling of the membranes yields to the lower mechanical and dimensional stability which in turn increases the problem of durability of the membrane. Earlier, we have observed that PyPBI shows about 3% swelling, however in the current study PyPBI derivative membranes are displaying swelling ratio values below 3 (%) as seen from Table 4.3. This is a very significant as we can expect better dimensional stability of the membrane prepared from these derivatives. In addition, the all values (PA loading, water uptake, swelling ratio) of current membranes are much favourable for use as PEM in comparison to conventional PBI membrane.

4.3.8. Proton conductivity

The proton conductivities at various temperature of PA loaded PyPBI derivative membranes were measured and results are shown in the Figure 4.16. Measurements were carried out from 30 to 160 °C temperature range in a home-made cell and the resistance value obtained from Nyquist plot. Nyquist plots of representative samples are shown in the Figure 4.15. As expected in all the membranes proton conductivities increases with the increasing temperature.[43-48] The results clearly show that the influence of functional groups (-COOH, -OH and -CF_3) in the polymer backbone. A careful look indicates the order of conductivity for OBA based PyPBI is PyPBI-COOH > PyPBI-OH > PyPBI-CF_3. Also, it is to be noted that among -COOH based polymers, HFIPA polymers has higher conductivity than OBA based which may be due to the presence of hexafluoro group.[20, 49, 50] In the current study conductivity value at 160 °C for all the samples (PyPBI polymers) is more than 0.01 S/cm and in fact in case of –COOH derivative, it is ≥ 0.02 S/cm: ~ 0.02 S/cm in case of OBA and greater than 0.02 S/cm for HFIPA. However, it must be noted that the proton conductivity at 160°C of non-functionalised PyPBIs, as reported by us earlier,[20, 21] is approximately equal to 0.01 S/cm as shown in the Figure by star mark despite the fact that in both the case PA loading are almost similar (close to 10-12 moles/r.u. of PBI).

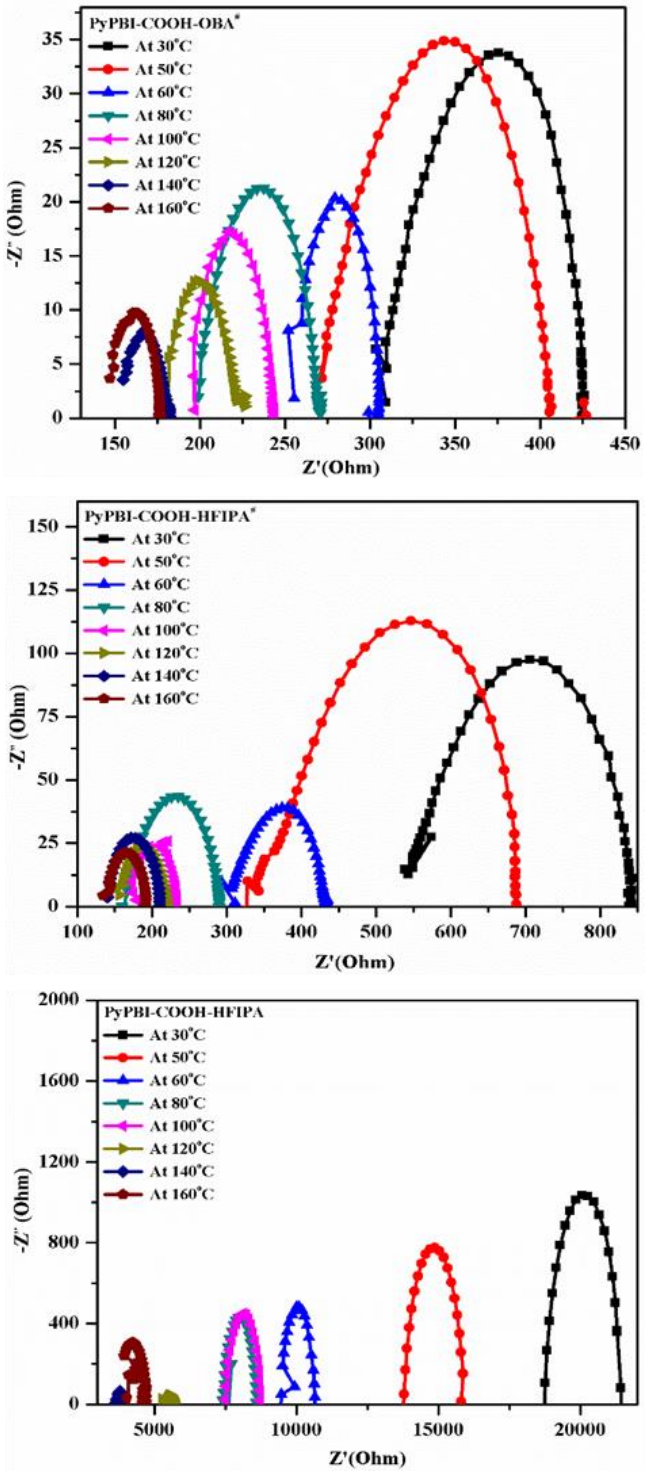

Figure 4.15. Nyquist plots of the representative PyPBI derivative membranes at various temperatures.

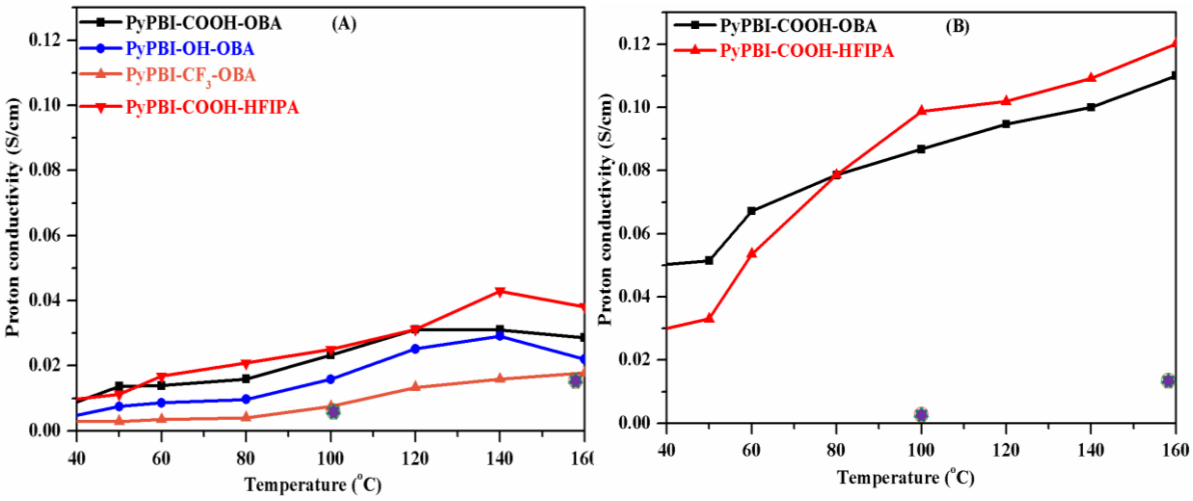

Figure 4.16. Variation of proton conductivity of the PA loaded membrane with temperature. Membrane obtained from (A) DMSO solution and (B) formic acid solution. indicates our previous result of PA doped PyPBI.[20, 21]

Since in the previous section, we noticed a huge increase in PA loading when membranes are made from formic acid instead of DMSO. So we measured their conductivity as a function of temperature for these membranes as well and data are plotted in Figure 4.16 (B). The FA membranes show significantly higher proton conductivities than their corresponding DMSO membranes. The proton conductivity at 160 °C for OBA and HFIPA membranes are 0.110 S/cm and 0.120 S/cm, respectively and these values are very high (at least one order) in comparison to PyPBI and other conventional PBI. We generally observed these kinds of high values for PBI nanocomposites.[35, 43, 44] The higher value of conductivity for FA membrane in comparison to DMSO membrane is primary due to higher PA loading which is the manifestation of very significantly different morphology of the FA based membrane compared to DMSO based membrane as show in Figure 4.17. The porous nature of the FA membrane allows more acid to be impregnated in the cross-linked structure and thereby allows higher PA loading and hence conductivity. On the other hand, DMSO membrane has no specific morphological features. So in summary, we may conclude that the conductivity of PyPBI depends on various factors and they are mainly (1) type of functionality in the backbone (2) solvent

used in the membrane fabrication (3) DCA structure and (4) the morphology of the membrane.

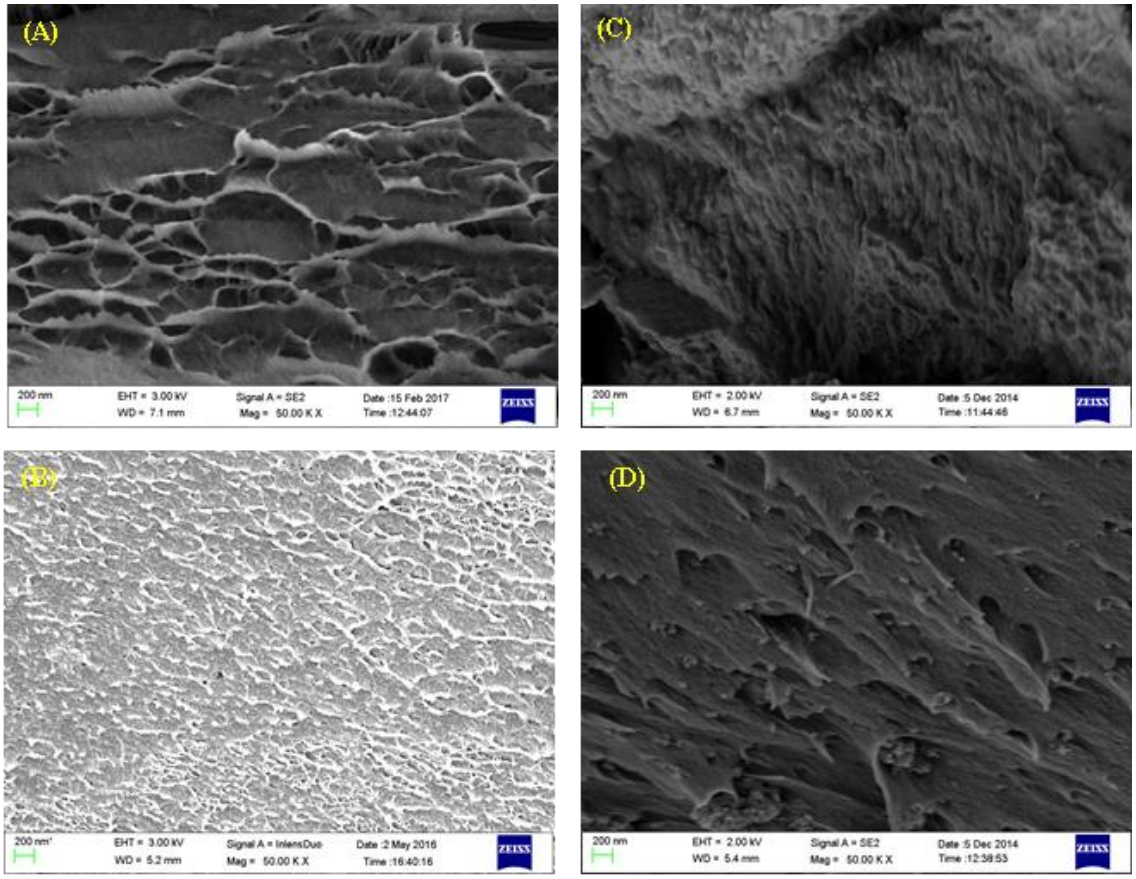

Figure 4.17. Cross sectional morphology of the PyPBI derivative membranes obtained from FA (A and B) and DMSO (C and D); A-PyPBI-COOH-OBA, B-PyPBI-COOH-HFIPA, C-PyPBI-COOH-OBA and D- PyPBI-COOH-HFIPA membranes.

4.4. CONCLUSION

Three series of novel pyridine bridged polybenzimidazoles derivatives have been synthesized and each series having different functionality in the tetraamine monomer. All these polymers are synthesized from efficient, economically less expensive PyTAB monomer derivatives and are reliable alternatives to conventional PBIs. The polymeri-zations conditions are optimized by changing the monomer concentrations to achieve

high molecular weight of PyPBI derivatives. Spectroscopic studies confirmed the newly synthesized PyTAB monomer derivatives as well as molecular structures of the resulting PyPBI polymer derivatives. PyPBI polymer derivatives display higher oxidative stability and mechanical stability than the conventional PBI. These functionalised PyPBI displayed higher stability towards phosphoric acid compared to already report non-functionalised PyPBI. This validates the fact that these membranes are more stable in PA than the normal PyPBI polymers which were earlier reported. The significantly low (mostly ~ 1%) swelling ratio clearly attributed higher dimensional stability than PyPBI or conventional PBI. PA loading and proton conductivities were achieved higher than the conventional PBI and normal PyPBIs. The HFIPA-COOH-FA and OBA-COOH-FA membranes proton conductivities are 12 × 10^{-2} S/cm and 11 × 10^{-2} S/cm, respectively which are comparable with the PBI based nanocomposite. These conductivity values are more than 10 times higher than the normal PyPBIs and conventional PBIs. In this comprehensive investigation, we observed that the functional group alterations on PyPBI backbones and varying the solvent used for membrane fabrication have a profound effect in achieving desired potential PEM properties.

REFERENCES

[1] Li, Q.; He, R.; Jensen, J. O.; Bjerrum, N. J. *Fuel Cells* **2004**, *4*, 147.

[2] Shabanikia, A.; Javanbakht, M.; Amoli, H. S.; Hooshyari, Kh.; Enhessari, M. *Electrochim. Acta* **2015**, *154*, 370.

[3] Shabanikia, A.; Javanbakht, M.; Amoli, H. S.; Hooshyari, Kh.; Enhessari, M. *Ionics* **2015**, *21*, 2227.

[4] Sana, B.; Jana, T. *Eur. Polym. J.* **2016**, *84*, 421.

[5] Sannigrahi, A.; Arunbabu, D.; Sankar, R. M.; Jana, T. *Macromolecules* **2007**, *40*, 2844.

[6] Ahn, T. K.; Kim, M.; Choe, S. *Macromolecules* **1997**, *30*, 3369.

[7] Musto, P.; Karasz, F. E.; MacKnight, W. J. *Macromolecules* **1991**, *24*, 4762.

[8] Pu, H.; Liu, Q.; Liu, G. *J. Membr. Sci.* **2004**, *241*, 169.

[9] Sannigrahi, A.; Ghosh, S.; Lalnuntluanga, J.; Jana T. *J. Appl. Polym. Sci.* **2009**, *111*, 2194.

[10] Klaehn, J. R.; Luther, T. A.; Orme, C. J.; Jones, M. G.; Wertsching, A. K.; Peterson, E. S. *Macromolecules* **2007**, *40*, 7487.

[11] Asensio, J. N.; Borros, S.; Gomez-Romero, P. *J. Electrochem. Soc.* **2004**, *151*, A304.

[12] Qing, S.; Huang, W.; Yan, D. *Eur. Polym. J.* **2005**, *41*, 1589.

[13] Qing, S.; Deyue Yan, W.-H. *J. Polym. Sci., Part A: Polym. Chem.* **2005**, *43*, 4363.

[14] Xiao, L.; Zhang, H.; Jana, T.; Scanlon, E.; Chen, R.; Choe, E.-W.; Ramanathan, L. S.; Yu, S.; Benicewicz, B. C. *Fuel Cells* **2005**, *5*, 287.

[15] Carollo, A.; Quartarone, E.; Tomasi, C.; Mustarelli, P.; Belotti, F.; Magistris, A.; Maestroni, F.; Parachini, M.; Garlaschelli, L.; Righetti, P. P. *J. Power Sources* **2006**, *160*, 175.

[16] Li, Z. X.; Liu, J. H.; Yang, S. Y.; Huang, S. H.; Lu, J. D.; Pu, J. L. *J. Polym. Sci., Part A: Polym. Chem.* **2006**, *44*, 5729.

[17] Maity, S.; Sannigrahi, A.; Ghosh, S.; Jana, T. *Euro. Polym. J.* **2013**, *49*, 2280.

[18] Kumbharkar, S. C.; Kharul, U. K. *J. Membr. Sci.* **2010**, *360*, 418.

[19] Potrekar, R. A.; Kulkarni, M. P.; Kulkarni, R. A.; Vernekar, S. P. *J. Polym. Sci., Part A: Polym. Chem.* **2009**, *47*, 2289.

[20] Maity, S.; Jana, T. *Macromolecules* **2013**, *46*, 6814.

[21] Maity, S.; Jana, T. *Polym. Int.* **2015**, *64*, 530.

[22] Liu, J. G.; Wang, L. F.; Yang, H. X.; Li, Y. F.; Yang, S. Y. *J. Polym. Sci., Part A: Polym. Chem.* **2004**, *42*, 1845.

[23] Mader, J.; Xiao, L.; Schmidt, T. J.; Benicewicz, B. C. *Adv. Polym. Sci.* **2008**, *216*, 63.

[24] Mader, J. A.; Benicewicz, B. C. *Macromolecules* **2010**, *43*, 6706-6715.

[25] Neuse, E. W. *Adv. Polym. Sci.* **1982,** *47*, 1.

[26] Dang, T. D.; Narayanan V.; Mark, J. E. *Polyimides and Other High Temperature Polymers*, **2009**, *5*, 145.

[27] Qian, G. Q.; Smith, D. W.; Benicewicz, B. C. *Polymer* **2009**, *50*, 3911.

[28] Sannigrahi, A.; Arunbabu, D.; Sankar, R. M.; Jana, T. *J. Phys. Chem. B* **2007**, *111*, 12124.

[29] Sannigrahi, A.; Ghosh, S.; Maity, S.; Jana, T. *Polymer* **2010**, *51*, 5929.

[30] Kumbharkar, S. C.; Islam, M. N.; Potrekar, R. A.; Kharul, U. K. *Polmer* **2009**, *50*, 1403.

[31] Wang, G.; Xiao, G.; Yan, D. *J. Membr. Sci.* **2011**, *369*, 388.

[32] Deimede, V.; Voyiatzis, G. A.; Kallitsis, J. K.; Qingfeng, L.; Bjerrum, J. N. *Macromolecules* **2000**, *33*, 7609.

[33] Mecerreyes, D.; Grande, H.; Miguel, O.; Ochoteco, E.; Marcilla, R.; Cantero, I. *Chem. Mater.* **2004**, *16*, 604.

[34] Kannan, R.; Kagaiwale, H. N.; Chaudhari, H. D.; Kharul, U. K.; Kurungot, S.; Pillai, V. K. *J. Mater. Chem.* **2011**, *21*, 7223.

[35] Ghosh, S.; Sannigrahi, A.; Maity, S.; Jana, T. *J. Phys. Chem. C* **2011**, *115*, 11474.

[36] Hazarika, M.; Jana, T. *ACS Appl. Mater. Interfaces* **2012**, *4*, 5256.

[37] Chuang, S. W.; Hsu, S. L. C. *J. Polym. Sci., Part A: Polym. Chem.* **2006**, *44*, 4508.

[38] Jouanneau, J.; Mercier, R.; Gonon, L.; Gebel, G. *Macromolecules* **2007**, *40*, 983.

[39] Sannigrahi, A.; Ghosh, S.; Maity, S.; Jana, T. *Polymer* **2010**, *51*, 5929.

[40] Han, M.; Zhang, G.; Liu, Z.; Wang, S.; Li, M.; Zhu, J.; Li, H.; Zhang, Y.; Lew, C. M.; Na, H. *J. Mater. Chem.***2011**, *21*, 2187.

[41] Nawn, G.; Pace, G.; Lavina, S.; Vezzu, K.; Negro, E.; Bertasi, F.;` Polizzi, S.; Di Noto, V. *Macromolecules* **2015**, *48*, 15.

[42] Nawn, G.; Pace, G.; Lavina, S.; Vezzu, K.; Negro, E.; Bertasi, F.;` Polizzi, S.; Di Noto, V. *Chem. Sus. Chem.* **2015**, *8*, 1381.

[43] Liu, C.; Wang, X.; Li, Y.; Zhang, S.; Wang, J.; Jian, X. *Journal of Polymer Rsearch* **2017**, *24*, 23.

[44] Sun, G., Han, K., Yu, J., Zhu, H., & Wang, Z. *RSC Advances*, **2016**, *6*, 91068.

[45] Singha, S.; Jana, T. *ACS Appl. Mater. Interfaces* **2014**, *6*, 21286.

[46] Singha, S.; Jana, T. *Polymer* **2016**, *98*, 20.

[47] Hazarika, M.; Jana, T. *Eur. Polym. J.* **2013**, *49*, 1564.

[48] Liu, S.; Zhou, L.; Wang, P.; Zhang, F.; Yu, S.; Shao, Z.; Yi, B. *ACS Appl. Mater. Interfaces* **2014**, *6*, 3195.

[49] Seo, K.; Seo, J.; Nam, K.-H.; Han, H. *Polymer Composites* **2017**, *38*, 87.

[50] Mikami, T.; Miyatake, K.; Watanabe, M. *ACS Appl. Mater.Intefaes* **2010**, *2*, 1714.

[51] Devrim, Y.; Devrim, H.; Eroglu, I. *International Journal of Hydrogen Energy* **2016**, *41*, 10044.

[52] Eguizábal, A.; Lemus, J.; Pina, M. *J. Power Sources* **2013**, *222*, 483.

Chapter 5

Alkali stable polymeric membrane with dual hydroxide ion conducting sites

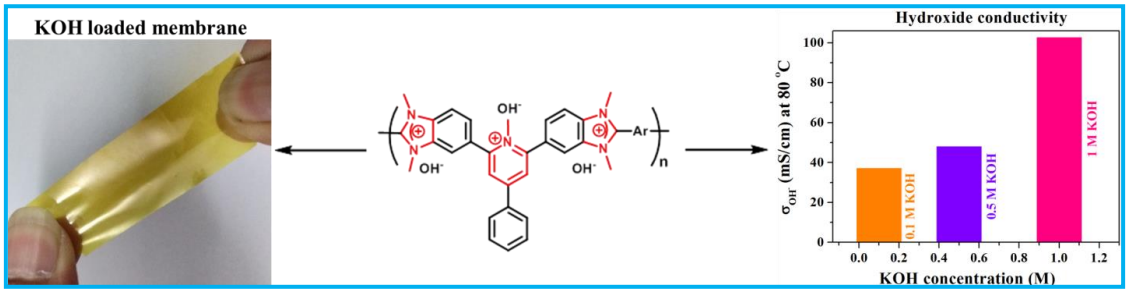

In this chapter, dual cationic sites containing alkaline anion exchange membranes (AEMs) have been developed from the pyridine bridged polybenzimidazoles. The simultaneous presence of dual OH^- ion conducting sites namely pyridinium and imidazolium in the polymer chain has been credited for achieving better AEM properties.

Sana, B.; Jana, T. communicated to ACS Macro Letters

5.1. INTRODUCTION

Huge benefits, particularly use of non-precise metal catalyst and faster electrode kinetics, of alkaline anion exchange membrane fuel cell (AAEMFC) have generated great deal of attention in developing various kinds of AAEMs.[1] Variety of polymers e.g. poly (phenylene),[2] poly(phenylene oxides),[3-5] fluorinated ethylene propylene,[6] poly(ether-imide),[7] poly(arylene ether sulfone),[8-13] polystyrene,[14, 15] polyolefin[16,17] have been investigated as AAEMs. One of the cationic functionality among the following six: pyridinium,[18] ammonium,[19] phosphonium,[17] sulphonium,[20] guanidinium,[14] imidazolium[21] is often introduced in the polymer chain to create an anion conducting site.

Though, quaternary ammonium (QA) has better stability than all other quaternary cations but vulnerability of QA to undergo β-hydrogen (Hofmann) elimination and also possibility of direct nucleophilic substitution under alkaline condition are the major cause of concerns.[22] Preparation of QA based AAEMs by chloromethylation followed by quaternization suffers a set of severe drawbacks like potential carcinogenicity of methoxy methyl chloride reactant, lack of control in the degree of chloromethylation and generation of undesired byproducts.[23] Alternative efforts were made to make AAEMs consisting of pyridinium group[18] but this membrane resulted poor ionic conductivity owing to the weak stability of the pyridinium group which is readily converted into neutral pyridone in alkaline condition. Sterically crowded imidazolium site has been found to be displaying higher alkaline stability and OH^- ion conductivity.[24] Despite all these progress, poor stability in alkaline medium and low OH^- conductivity of the polymer membranes remain as prime challenges to be resolved.

To address the aforesaid issues, we hypothesized that inclusion of two (dual) anion conducting sites like pyridinium and imidazolium together in a polymer chain will certainly increase the OH^- ion conductivity and appropriate steric crowding around pyridinium and imidazolium can definitely improve the alkaline stability. Keeping this plan, we synthesized poly(methylated pyridinium benzimidazolium) iodide (PMPBI)

(Scheme 5.2) which possesses both pyridinium and imidazolium functionality. Both of these can act as OH^- conducting sites in the process of OH^- ion mobility and hence will be resulting higher total net OH^- conductivity than the other reported OH^- conductivity where only one site is present. Also, PMPBI structure is such that pyridone formation from the pyridinium is not possible since both the α-positions of pyridinium functionality of PMPBI is blocked by benzimidazole moieties and hence higher alkaline stability is expected from the PMPBI.

5.2 EXPERIMENTAL SECTION

Details of the materials and characterization methods used in this study are included in the Chapter 2. Polymer synthesis, membrane preparation and anion exchange reaction are described below.

5.2.1. Synthesis of polymers

Pyridine bridge polybenzimidazoles (PyPBI) were synthesized following our previously reported work[1]. Briefly, the method was as follows: equimolar ratio of Py-TAB and dicarboxylic acid monomers were taken along with PPA in a three necked round bottom flask equipped with mercury sealed overhead mechanical stirrer. The reaction was continued for 26 h at 210 °C temperature under N_2 atmosphere. The obtained viscous solution was poured into the cold deionized water. The obtained fibrous polymer was neutralized with sodium bicarbonate solution and washed thoroughly with deionized water for the removal of excess base. Finally, the fibrous polymer was dried in vacuum oven at 100 °C for 24 h and stored in desiccator for further characterization. The reaction scheme for the synthesis of Py-PBI is shown in supporting information Scheme 5.1. The Py-PBI obtained by using IPA, TPA, OBA, HFIPA and BPDA dicarboxylic acids are abbreviated as Py-PBI-IPA, Py-PBI-TPA, Py-PBI-OBA, Py-PBI-HFPA and Py-PBI-BPDA, respectively.

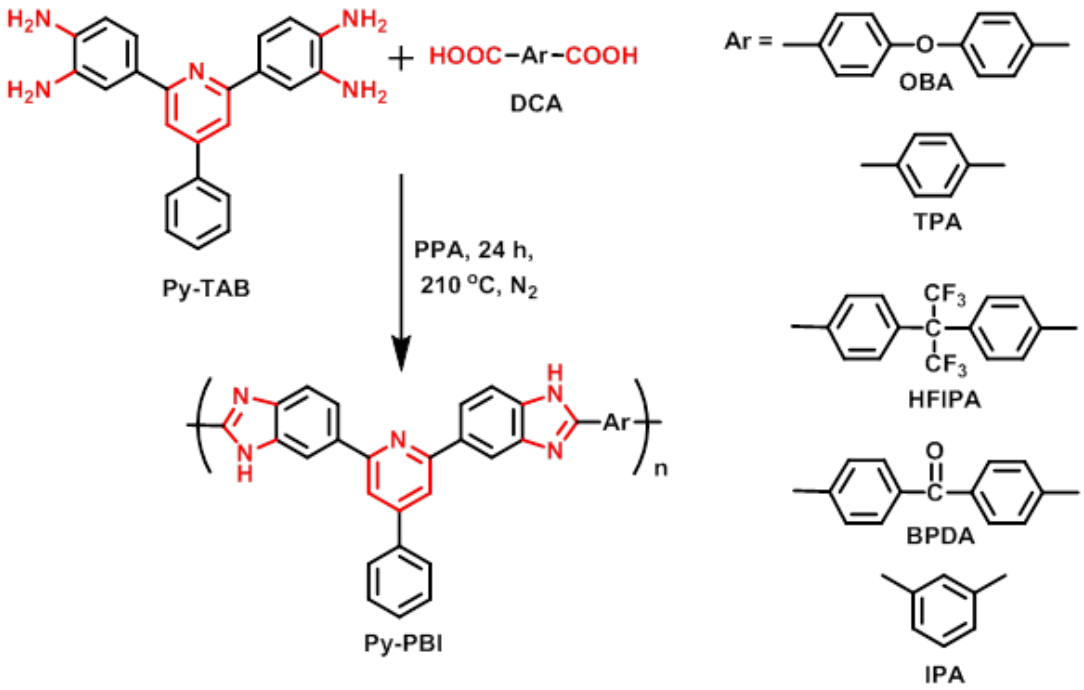

Scheme 5.1. *Synthesis of pyridine bridge polybenzimidazoles (Py-PBI) polymers from Py-TAB monomer using various types of dicarboxylic acids.*

5.2.2. Synthesis of poly (methylated pyridinium benzimidazolium) iodide (Abbreviated as PMPBI)

1.0 g of Py-PBI polymer was dissolved in 60 mL of dry DMSO solvent at 80 °C in a 100 mL round bottom flask fitted with a reflux condenser and connected with nitrogen inlet and out let for maintaining inert atmosphere. The polymer solution was cooled to ambient temperature after complete dissolution of polymer in DMSO. Then sodium hydride (3.6 mmol, 0.0867g) was added to this polymer solution and the temperature was raised to 80 °C. The solution was stirred for 14 h, and was cooled to the ambient temperature. Methyl iodide (9.05 mmol, 0.563 mL) was added to this reaction mixture and continued the stirring for another 4 h at 80 °C. After 4 h of stirring, the same amount (9.05 mmol) of CH_3I was added for the second time and continued the stirring for another 16 h. After completion of this period, the reaction mixture was poured into water and a precipitate formation was observed. The

precipitate was filtered off and washed thoroughly with deionized water for the removal of excess methyl iodide. The polymer was dried under vacuum oven at 75 °C for 24 h. The reddish brown coloured product was obtained and used for further characterizations to confirm the structure.

The PMPBI obtained from five Py-PBI polymers of various dicarboxylic acids using above protocol were denoted as PMPBI-OBA, PMPBI-IPA, PMPBI-TPA, PMPBI-HFIPA and PMPBI-BPDA as shown in Scheme 5.2 of the main article.

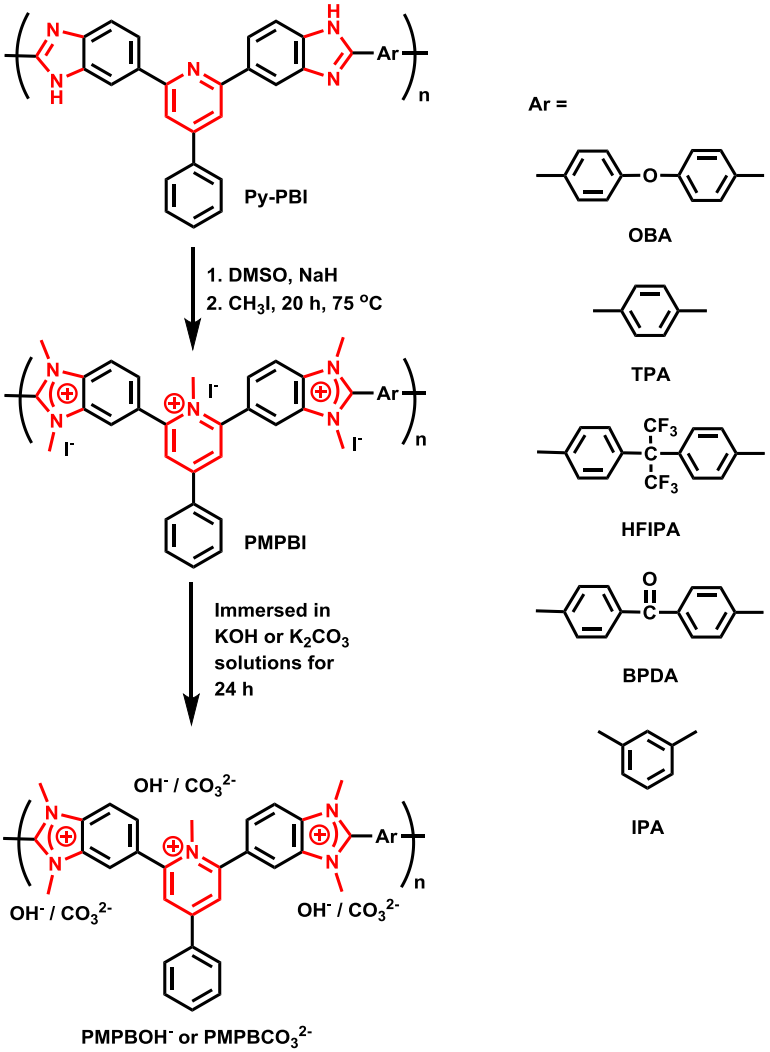

Scheme 5.2. *Synthesis of hydroxide and carbonates ion loaded poly(methylated pyridinium imidazolium) membranes.*

5.2.3. PMPBI membrane casting

A 1% (w/v) PMPBI polymer solution was prepared by dissolving the polymer in DMSO solvent over a period of 24 h stirring at room temperature. The obtained clear solution was then poured into a clean flat glass Petridis, followed by the solvent evaporation in a hot air oven at 85 ^{o}C for 10-12 h. After this period, the dried membrane was peeled off from the glass Petridis and was soaked in boiled water to remove the trace amount of residual solvent. The membranes were dried in a vacuum oven at 100 °C for 24 h. The membrane thickness was maintained between 20-30 µm and was stored in desiccator for further analysis.

5.2.4. Loading of OH^- and CO_3^{2-} into PMPBI membrane

The above prepared five PMPBI membranes were immersed in aqueous KOH, and K_2CO_3 solutions of various strength (0.1, 0.5 and 1 M) at ambient temperature for 24 h to load OH^- and CO_3^{2-} into the PMPBI membrane. The OH^- and CO_3^{2-} loaded membranes are abbreviated as PMPBOH$^-$ and PMPBCO$_3^{2-}$, respectively (Scheme 5.2). Then, the hydroxide ion or carbonate ion membranes were washed thoroughly with deionized water to remove excess ions from the surface of the membranes. These membranes were then stored in deionized water for 24 h prior to analysis so as to avoid the formation of carbonate salt in contact with air.

5.3. RESULTS AND DISCUSSIONS

5.3.1. Polymer synthesis and confirmation studies

The disappearance of imidazole (-NH) proton peak at ~ 13.3 ppm and appearance of peaks between 4 to 4.3 ppm (see ^{1}H NMR spectra in Fig. 5.1) due to methylation confirm the conversion of Py-PBI to PMPBI (Scheme 5.2). The degree of methylation of PMPBI does not display any definite trend (Table 5.1) for different type of PMPBI which were synthesized from Py-PBI (Scheme 5.2) and referred as PMPBI-OBA, PMPBI-TPA, PMPBI-HFIPA, PMPBI-BPDA and PMPBI-IPA.

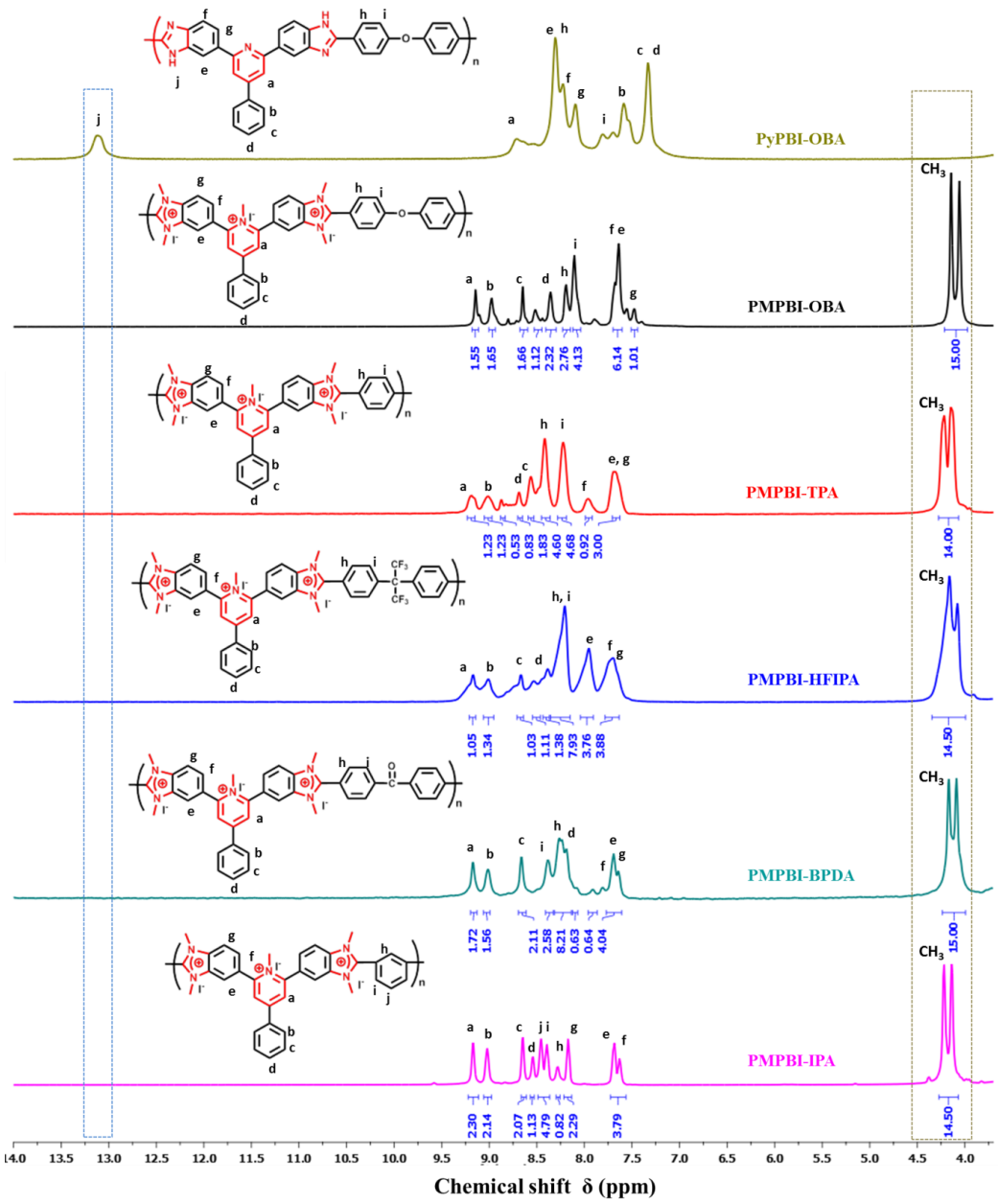

Figure 5.1. *^{1}H NMR spectra of all the poly (methylated pyridinium benzimidazolium iodide) (PMPBI) samples recorded in DMSO-d_6 solvent at room temperature. Peak assignments along with the structure are also shown in the figure ^{1}H NMR spectra of Py-PBI-OBA is also included for ease of comparison of the peak with PMPBI. Highlighted peak at 13.3 ppm disappeared in all PMPBI sample and CH_3 peak at 4 to 4.3 appeared in the all PMPBI.*

5.3.2. Ion exchange capacity (IEC)

The ion exchange capacity (IEC) of PMPBI membranes treated with various alkaline solutions displays dependency on polymer backbone structure, concentration of alkaline solution and the type of alkaline anions (Table 5.1). Higher IEC is obtained in case of membranes loaded with OH^- than CO_3^{2-} ion. The reason for this observation may be attributed to the size and nature of the anion.[25] Also, 0.5 M KOH treated samples display higher IEC values than when they were treated with 0.1 M KOH. Among all the polymers, PMPBI-OBA results the highest IEC (2.57 meq/g) when treated with 0.5 M KOH. Whereas the 0.1 M KOH doped PMPBI-IPA and 0.5 M K_2CO_3 doped PMPBI-IPA membranes result lowest IEC values 0.93 and 0.91 meq/g, respectively. It is to be noted that there is no correlation between degree of methylation and IEC values (Table 5.1). IEC values of the 0.5 M KOH treated PMPBI-BPDA and PMPBI-IPA polymer membranes could not be measured since these were found to be very unstable and were rapidly broken into very small species while doing the experiment.

Table 5.1. *Degree of methylation and IEC values of all the PMPBI polymers.*

Polymer identity	Degree of methylation (%) [a]	IEC (meq/g) [b]		
		0.1 M KOH	0.5 M KOH	0.5 M K_2CO_3
PMPBI-OBA	94	2.13	2.57	1.79
PMPBI-TPA	84.2	2.00	2.04	1.57
PMPBI-HFIPA	94.5	1.83	1.89	1.37
PMPBI-BPDA	97.6	1.78	–	1.20
PMPBI-IPA	84.8	0.93	–	0.91

[a] obtained from peak integration of ^{1}H NMR spectra as shown in Figure 5.1. [b] IEC data calculated from the samples which were treated with the respective alkaline solution for 24 h.

5.3.3. Alkaline stability

The alkaline stability results evidently display zero degradation of all the membranes when treated with 0.1 M KOH solution in the temperature range 27 °C - 60 °C. However, in strong alkaline condition like 0.5 M KOH and 0.5 M K_2CO_3, the membrane stability depends upon various factors like type of alkaline condition, temperature and the polymer backbone structure (Table 5.2 to 5.4). Among all the membranes, PMPBI-OBA shows the best stability upto 14 days in K_2CO_3 at 27 °C. This membrane is stable upto 9 days at 27 °C when kept in 0.5 M KOH. In comparison to all the literature report on AAEM published so far, the current membrane shows the best stability in high concentrated alkaline (0.5 M KOH) solution. To our knowledge, till now no reports has mentioned the stability of PBI based membrane at 0.5 M KOH except the acid-base crosslinked PBI membrane.[24] Though the current membrane consists of both imidazolium and pyridinium functionality but significantly high stability of the current membranes is due to the blocking of α-position of pyridinium site with two imidazolium groups and therefore the irreversible oxidation of pyridinium into neutral pyridone is not possible at all.[1, 26]

Table 5.2. *Alkaline stability studies of PMPBI-OBA membrane in various alkaline condition and temperature. The all other polymer alkaline stability are summarized in Table 5.3.*

Solution type [a]	Temperature of solution [b]	Duration of observation [c]
0.1 M KOH	27 °C	No change observed even after 2 yrs
0.1 M KOH	60 °C	No change observed even after 2 yrs
0.5 M KOH	27 °C	9 days
0.5 M KOH	60 °C	4 days
0.5 M K_2CO_3	27 °C	14 days
0.5 M K_2CO_3	60 °C	9 days

[a] The solution in which PMPBI-OBA membrane was treated for 24 h. [b] Solution temperature at which membranes were kept. [c] Number of days upto which membranes were stable, free standing, flexible and can be handled without any breaks.

Table 5.3. *The alkaline stability of PMPBI membranes when treated with 0.5 M KOH solution. All the membranes are completely stable in 0.1 M KOH solution in the temperature range 27 to 60 °C.*

Polymer membranes	Temperature of solution	Duration of observation	Observation
PMPBI-TPA	27 °C	6 days	Breaking started
PMPBI-TPA	60 °C	4 days	Broken when handled
PMPBI-HFIPA	27 °C	6 days	Breaking started
PMPBI-HFIPA	60 °C	4 days	Broken when handled
PMPBI-BPDA	60 °C & RT	1 h	Colour changed/ broken
PMPBI-BPDA	60 °C & RT	15 h	Breaking started
PMPBI-IPA	60 °C & RT	1 h	Breaking & Colour changes observed
PMPBI-IPA	60 °C & RT	15 h	Breaks into very small species

Table 5.4. *The alkaline stability of PMPBI membranes when treated with 0.5 M K_2CO_3 solution.*

Polymer membrane	Temperature of solution	Duration of observation	Observation
PMPBI-TPA	27 °C	7 days	Flexible
PMPBI-TPA	60 °C	6 days	Broken when handled
PMPBI-HFIPA	27 °C	6 days	Flexible
PMPBI-HFIPA	60 °C	4 days	Breaking & colour changes observed
PMPBI-BPDA	27 °C	4 days	Breaking & colour changes observed
PMPBI-BPDA	60 °C	3 days	Breaking & colour changes observed
PMPBI-IPA	27 °C	15 h	Breaking observed
PMPBI-IPA	60 °C	15 h	Breaking observed

A closer look at the degradation mechanism (Scheme 5.3) which is proposed based on FT-IR and NMR spectral evidences clearly reveals the nature of degradation and reinforces our argument (as stated above) for significantly high alkaline stability of the current membrane. The ring opening of the imidazolium moiety due to nucleophilic attack of OH^- ion on the C2 position of the imidazolium resulting in amine-amide formation.[27-32] along with the decomposition of the polymer chain.

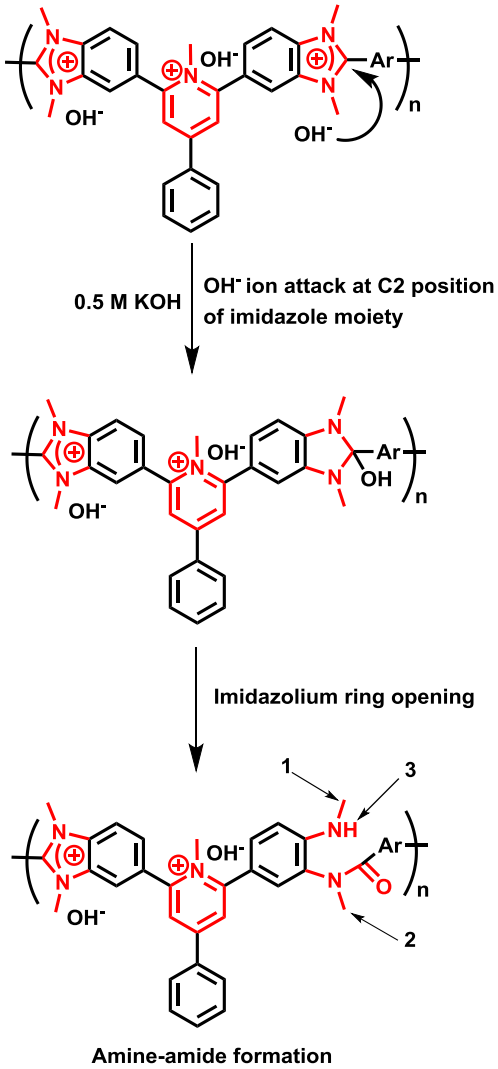

Scheme 5.3. *Imidazolium degradation mechanism in PMPBOH membranes upon alkali treatment. Newly appeared various types of protons upon degradation are labeled as 1, 2 & 3 in the scheme and corresponding peaks are assigned in Figure 5.2.*

^{1}H NMR spectra of alkali loaded membrane (Figure 5.2) when compared with PMPBI spectra evidently display appearance of new peaks at ~ 2.9 ppm corresponding to the methyl (-CH_3) protons attached to the secondary amine (labelled as '**1**'), another new peak at ~ 3.23 ppm corresponding to the methyl protons attached to the tertiary amide (labelled as '**2**') and secondary amine (-NH) peak (labelled as '**3**') at ~ 3.9 ppm. The FT-IR spectra (Figure 5.3) of PMPBOH displayed a peak at 1650 cm^{-1} corresponding to the formation of aromatic amide C=O functional group and another peak at 3630 cm^{-1} corresponding to the vibration of N-H bond. Therefore, both the spectral studies clearly prove that the degradation (ring opening of imidazole) takes place as shown in the Scheme 5.3.

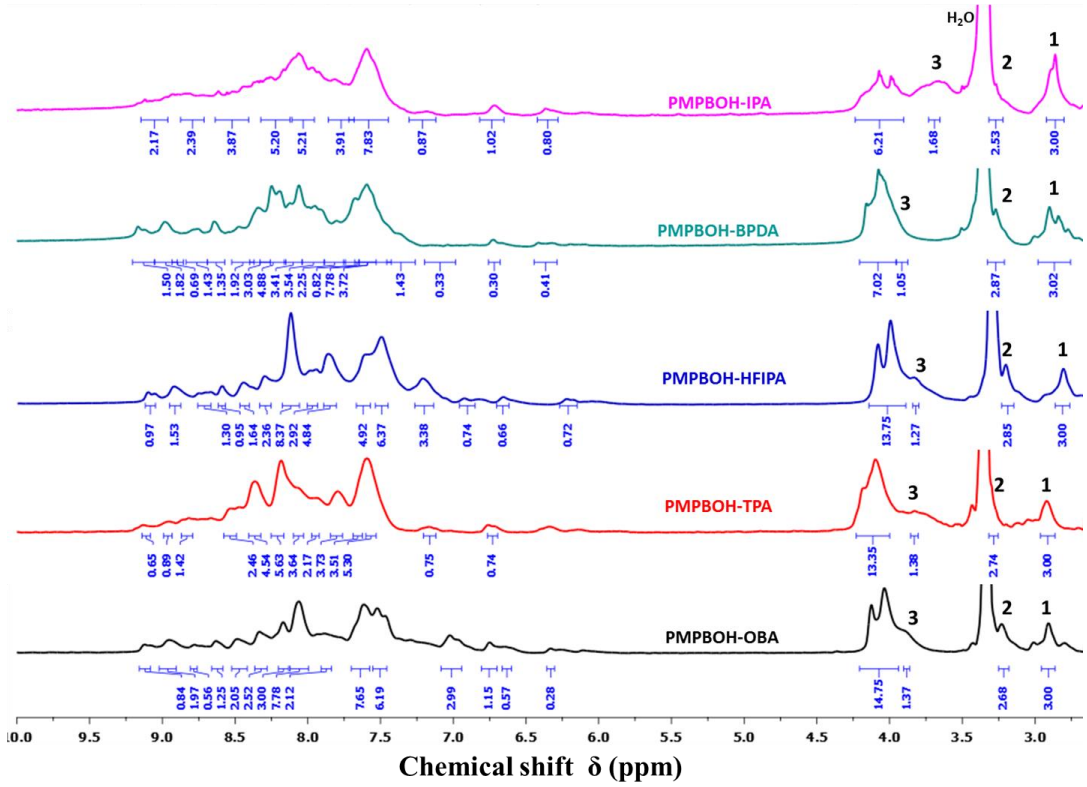

Figure 5.2 *^{1}H NMR spectra of all the PMPBOH form membranes after treatment with 0.5 M KOH for 24 h. New peaks are assigned using 1, 2, 3 numbers for the newly appeared proton as indicated in the Scheme 5.3.*

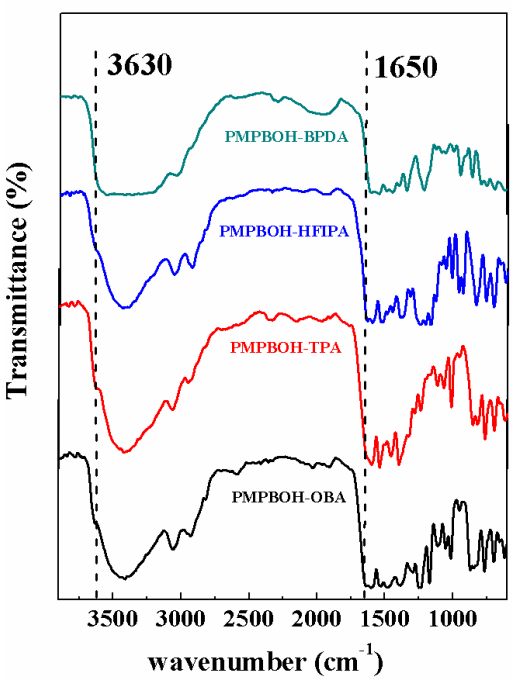

Figure 5.3. *IR spectra of PMPBOH form membranes. The appearance of new peaks are highlighted in the Figure.*

A comparison of aromatic position (Figure 5.4) chemical shift between post and after treatment with alkali clearly prove that the spectral features remain identical attributing that the OH^- only attack the imidazole moiety of the chain, remaining all part of the chain are unaffected. This again proves that the pyridine functionality remain unaffected as the α-position are blocked by crowded functionality.

The degree of degradation owing to ring opening of imidazolium was calculated using the relative integrations of the proton resonances and values (Table 5.5) are found to be highly depended on the PMPBI backbone structure. The lowest degradation is observed in case of OBA and highest in case of IPA based polymers. It is to be noted that there is no correlation between degree of methylation and degree of degradation as shown in Table 5.1 and 5.5, respectively.

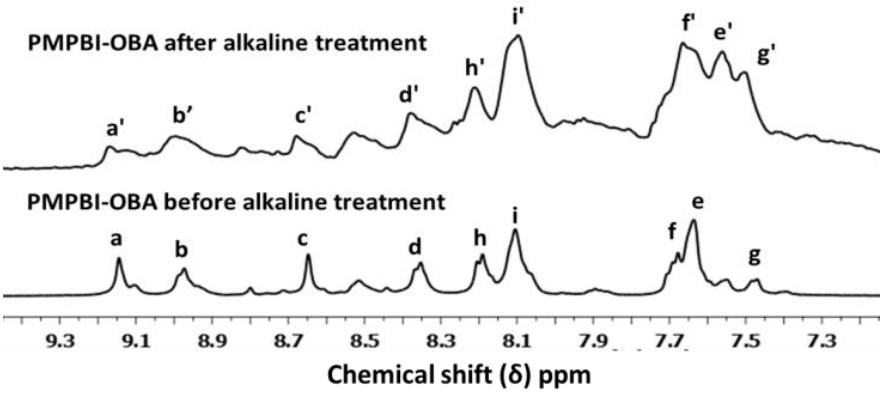

Figure 5.4. *^{1}H NMR spectra of aromatic region before and after alkali treatment. PMPBI/OH-OBA is chosen as a representative one. Similar observation were made for all other cases. Peaks are identified into assigned as a, b, c… and a', b', c'… before and after alkali treatment respectively for easy comparison. These all peaks are due to aromatic protons as assigned in the Figure 5.1.*

Table 5.5. *Degree of degradation and ionic conductivity of membranes.*

Polymer identity	Degree of degradation (%) [a]	σ_{OH^-} (mS/cm) at 80 °C		$\sigma_{CO_3^{2-}}$ (mS/cm) at 80 °C [d]
		0.1 M KOH [b]	0.5 M KOH [c]	
PMPBI-OBA	16.8	37.3±1.4	48±1.0	35.1±1.8
PMPBI-TPA	19.0	36.0±0.7	40±0.8	32.8±0.7
PMPBI-HFIPA	18.0	27.1±1.0	34±0.8	22.8±0.8
PMPBI-BPDA	30.0	10.1±0.9	–[e]	–[e]
PMPBI-IPA	33.0	–[e]	–[e]	–[e]

[a] calculated from the peak integrations of ^{1}H NMR spectra as show in Figure 5.2. [b, c, d] membranes were treated with 0.1 M KOH, 0.5 M KOH and 0.5 M K_2CO_3, respectively for 24 h. [e] could not be measured owing to instability of the membranes at 80 °C.

5.3.4. Ionic conductivity

The ionic conductivity of AAEMs loaded with aqueous alkaline solutions displays a large dependence on both the IEC value and temperature. Higher IEC value, which again depends upon the polymer chain structure and the concentration of the alkaline solution (Table 5.1), yields higher anion conductivity (Table 5.5). The hydroxide doped membranes exhibit higher ionic conductivities than the carbonate doped membranes (Table 5.5) owing to the higher mobility of OH^- ions. The concentration of doping alkaline solution and the temperature also play vital roles in conductivity (Table 5.5 and Fig. 5.5). The ionic conductivity of PMPBI-OBA membrane is the highest at all temperature and in all type of alkaline condition among all the AAEMs (Fig. 5.5 and Fig. 5.6) indicating the influence of polymer backbone structure and IEC value. A comparison with the literature data evidently shows considerably higher OH^- ion conductivity in the current study. For example, the OH^- ion conductivity of PMPBI-OBA at 30 °C and 80 °C when loaded with 1 M KOH are 28.1, 102.4 mS/cm, respectively (Figure 5.5) whereas the highest OH^- conductivity reported so far is in the range of 33.0 to 60.0 mS/cm at 60-80°C in case of PBI based membrane.[25] The reason for the significantly higher conductivity is because of the introduction of additional phenyl substituted methyl pyridinium group between the two benzimidazolium moieties. This pyridinium group also acts as anion conducting site and helps to transport hydroxide (OH^-) ions or carbonate (CO_3^{2-}) ions through the anion exchange membrane along with benzimidazolium moieties. The possibility of pyridinium groups converted into neutral pyridone resulting lower conductivity is prevented by blocking the pyridine moiety at 2, 4 and 6 positions by benzimidazolium moieties and phenyl groups.[1, 26]

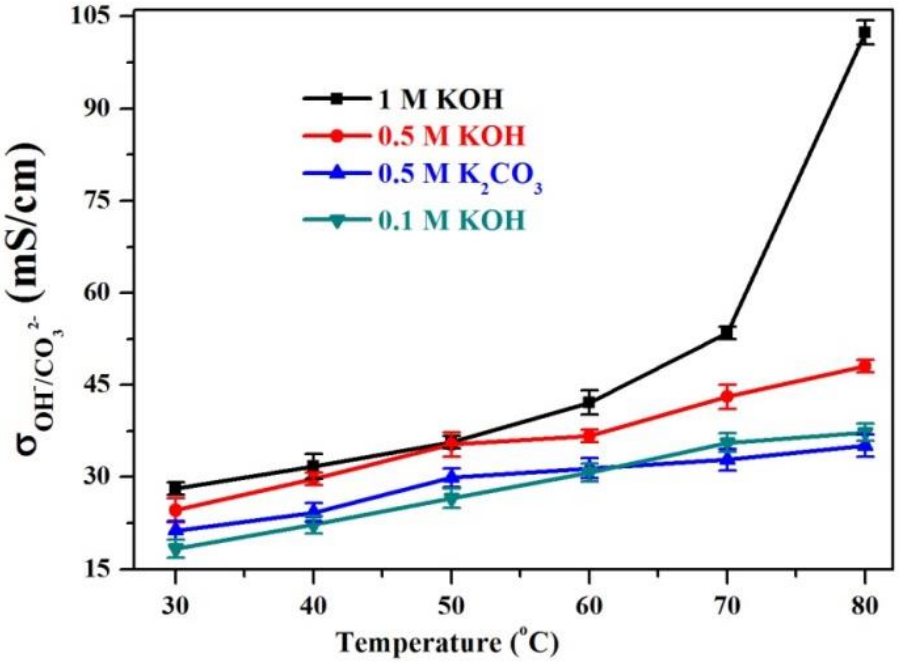

Figure 5.5. *Temperature dependent plots of OH^- and CO_3^{2-} ion conductivity of PMPBOH/ CO_3^{2-}-OBA which treated with various alkaline concentrations for 24 h.*

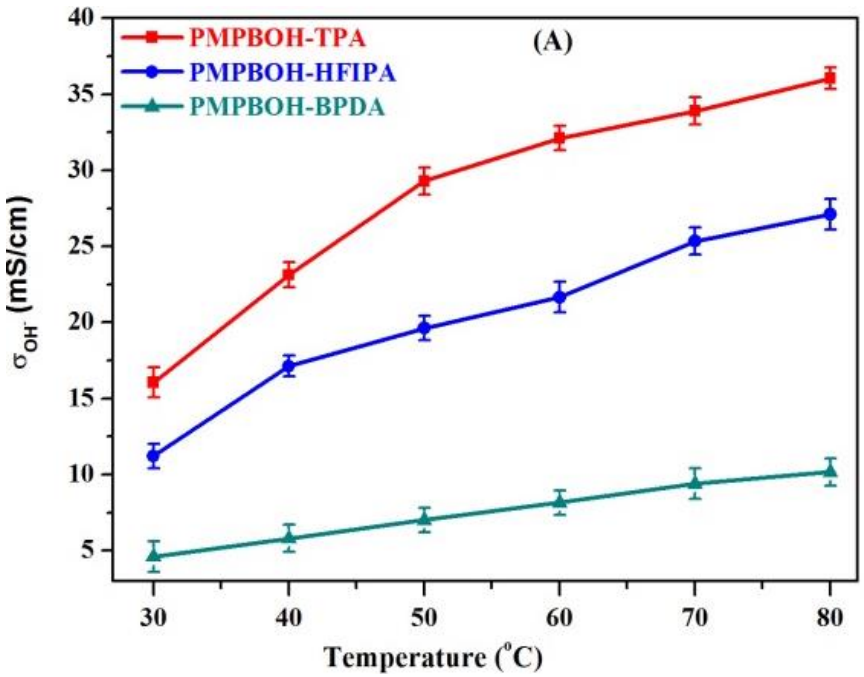

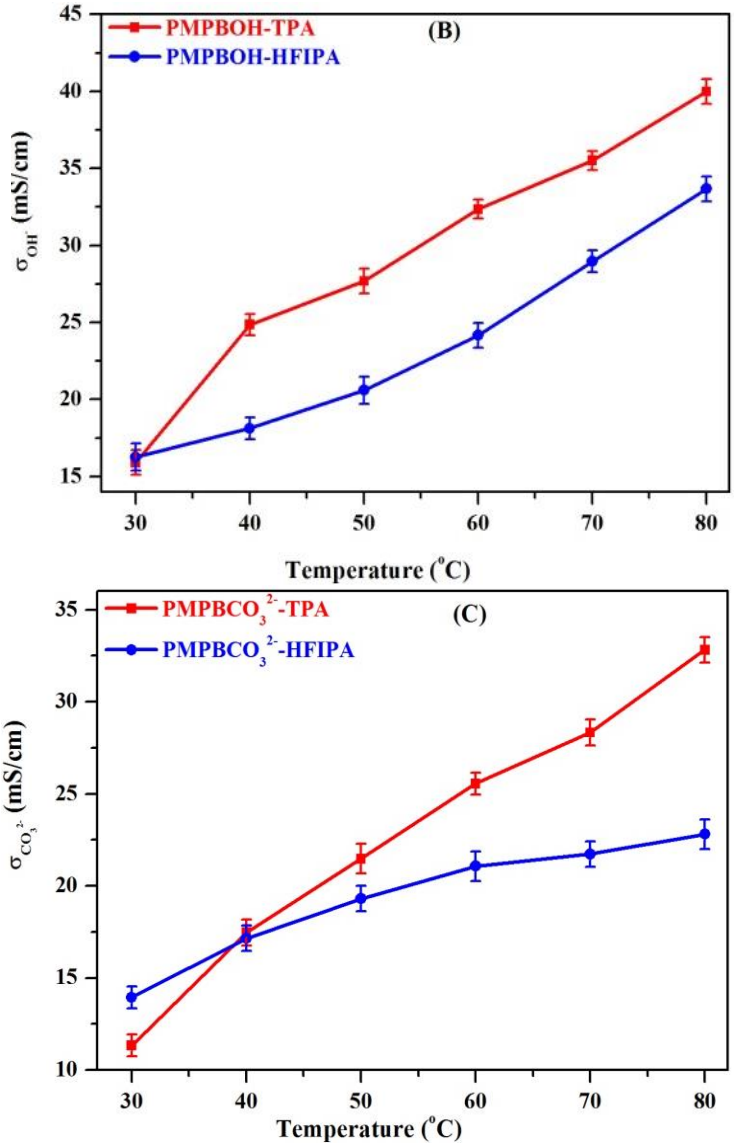

Figure 5.6 *The ionic conductivity of various PMPBI membranes doped with (A) 0.1 M KOH, (B) 0.5 M KOH and (C) 0.5 M K_2CO_3 alkaline solutions.*

5.3.5. Thermal stability

Thermal stability studies (Figure 5.7) clearly prove the significantly higher stability of OH^- and CO_3^{2-} doped membrane than I^- membrane. Except the initial weight loss due to presence of H_2O, membranes are stable up to 250-300 °C and the stability largely depends on the polymer structure.

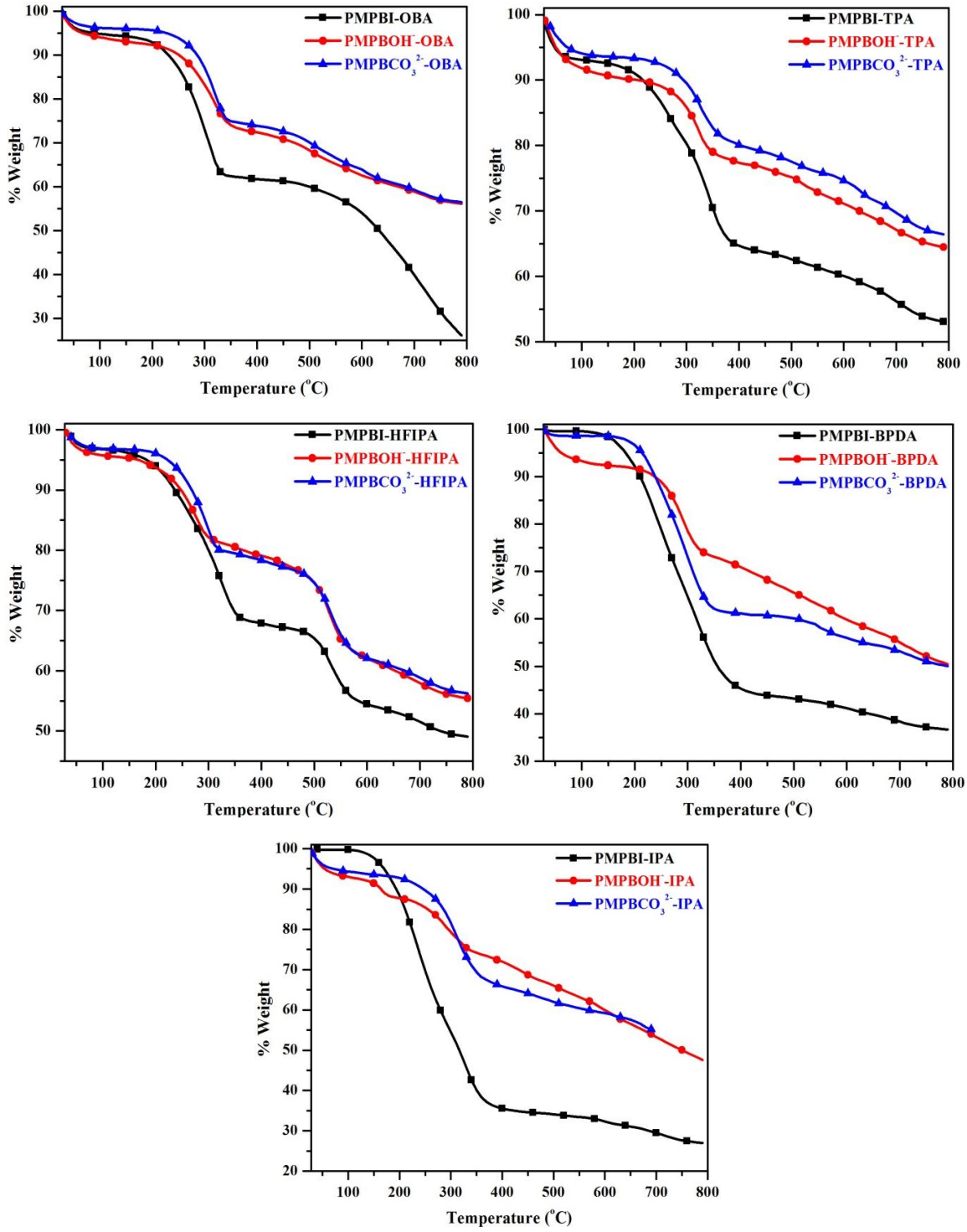

Figure 5.7. *Thermal stability of all the PMPBI, hydroxide (OH^-) ion and carbonate (CO_3^{2-}) ion containing membranes.*

5.3.5. Mechanical stability

The tensile measurements of the membranes display higher tensile strength and higher elongation at break in case of I^- ion membranes compared to that of OH^- and CO_3^{2-} ion membranes (Figure 5.8 and Table 5.6). This might be due to the presence of unreacted (unalkylated) imidazole groups having proton donor (-NH-) and proton acceptor (-N=) sites in case of iodide form membranes which might form hydrogen bonding. But in the alkali loaded membranes, hydrogen bonding interaction gets disturbed or partially cleaved leading to the decrease in the mechanical strength.[33] Both thermal and mechanical studies clearly demonstrate the good thermal and dimensional stability of the membrane which are essential properties to become efficient AAEMs.

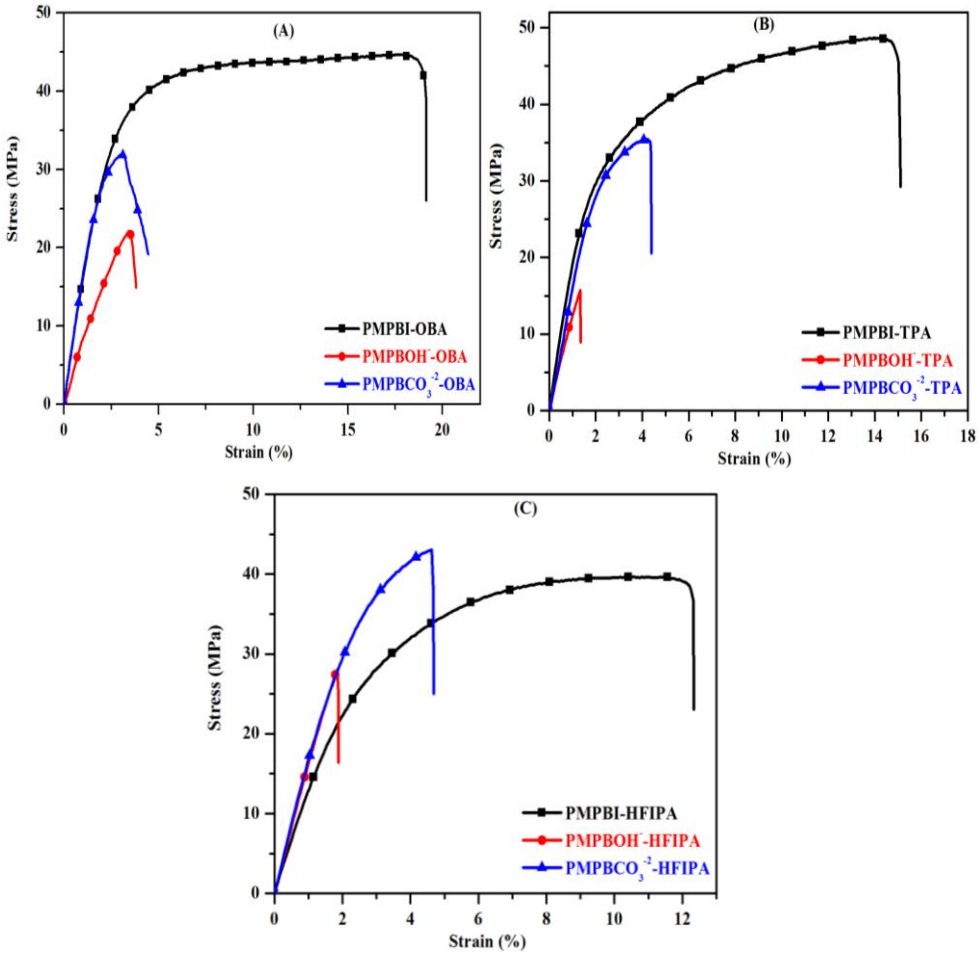

Figure 5.8. *Stress-strain plots of all the AEMs obtained from tensile study; (A) OBA, (B) TPA and (C) HFIPA based AEMs.*

Table 5.6 *Tensile strength and elongation data of all the AAEMs ($I^-/OH^-/CO_3^{2-}$ form) obtained from tensile measurement.*

Sample	Tensile strength (MPa)	Elongation at break (%)
PMPBI-OBA	44.61	19
PMPBOH$^-$-OBA	22.25	3.5
PMPBCO$_3^{2-}$-OBA	32.20	3.1
PMPBI-TPA	49.00	14
PMPBOH$^-$-TPA	15.84	1.3
PMPBCO$_3^{2-}$-TPA	35.33	4.3
PMPBI-HFIPA	39.44	12
PMPBOH$^-$-HFIPA	28.13	1.8
PMPBCO$_3^{2-}$-HFIPA	43.2	4.3

5.4. CONCLUSION

Series of pyridine bridged polybenzimidazole (Py-PBI) have been converted into AAEMs by treating hydroxide or carbonate ions. Excellent IEC, ionic conductivity, thermal, mechanical and chemical stabilities were obtained in these membranes. Remarkable alkaline stability and very high OH^- conductivity, the highest so far, are due to the structural integrity of the Py-PBI in which pyridine functionality is shielded from any possible degradation. The presence of dual anion conducting sites: pyridinium and imidazolium enhanced the ionic conductivity significantly. These membranes are promising candidates for new class of AAEMs.

REFERENCES

[1] Merle, G.; Wessling, M.; Nijmeijer, K. *J. Membr. Sci.* **2011**, *377*, 1.

[2] Hibbs, M. R.; Fujimoto, C. H.; Cornelius, C. J. *Macromolecules* **2009**, *42*, 8316.

[3] Pan, J.; Han, J.; Zhu, L.; Hickner, M. A. *Chem. Mater.* **2017**, *29*, 5321.

[4] Zhu, L.; Pan, J.; Christensen, C. M.; Hickner, M. A. *Macromolecules* **2016**, *49*, 3300.

[5] Zhu, L.; Zimudzi, T. J.; Wang, Y.; Yu, X.; Pan, J.; Han, J.; Kushner, D. O.; Zhuang, L.; Hickner, M. A. *Macromolecules* **2017**, *50*, 2329.

[6] Slade, R. C.; Varcoe, J. R. *Solid State Ionics* **2005**, *176*, 585.

[7] Wang, G. H.; Weng, Y. M.; Zhao, J.; Chu, D.; Xie, D.; Chen, R. R. *Polym. Adv. Technol.* **2010**, *21*, 554.

[8] Lee, K. H.; Cho, D. H.; Kim, Y. M.; Moon, S. J.; Seong, J. G.; Shin, D. W.; Sohn, J.-Y.; Kim, J. F.; Lee, Y. M. *Energy Environ. Sci.* **2017**, *10*, 275.

[9] Guo, D.; Lai, A. N.; Lin, C. X.; Zhang, Q.; Zhu, A.; Liu, Q. L. *ACS Appl. Mater. Interfaces* **2016**, *8*, 25279.

[10] Wang, J.; Li, S.; Zhang, S. *Macromolecules* **2010**, *43*, 3890.

[11] Gu, S.; Cai, R.; Yan, Y. *Chem. Commun.* **2011**, *47*, 2856.

[12] Lai, A. N.; Wang, L. S.; Lin, C. X.; Zhuo, Y. Z.; Zhang, Q. G.; Zhu, A. M.; Liu, Q. L. *ACS Appl. Mater. Interfaces* **2015**, *7*, 8284.

[13] Tanaka, M.; Fukasawa, K.; Nishino, E.; Yamaguchi, S.; Yamada, K.; Tanaka, H.; Bae, B.; Miyatake, K.; Watanabe, M. *J. Am. Chem. Soc.* **2011**, *133*, 10646.

[14] Varcoe, J. R.; Slade, R. C. T.; Yee, E. L. H.; Poynton, S. D.; Driscoll, D. J.; Apperley, D. C. *Chem. Mater.* **2007**, *19*, 2686.

[15] Luo, Y.; Guo, J.; Wang, C.; Chu, D. J. Power Sources 2010, 195, 3765.

[16] Robertson, N. J.; Kostalik, H. A., IV; Clark, T. J.; Mutolo, P. F.; Abruna, H. D.; Coates, G. W. *J. Am. Chem. Soc.* **2010**, *132*, 3400.

[17] Noonan, K. J.; Hugar, K. M.; Kostalik, H. A., IV; Lobkovsky, E. Abruna, H. D.; Coates, G. W. *J. Am. Chem. Soc.* **2012**, *134*, 18161.

[18] (a) Li, X.; Yu, Y.; Liu, Q.; Meng, Y. *Int. J. Hydrogen Energy* **2013**, *38*, 11067. (b)

Huang, A. B.; Xia, C. Y.; Xiao, C. B.; Zhuang, L. *J. Appl. Polym. Sci.* **2006**, *100*, 2248.

[19] (a) Zhu, L.; Pan, J.; Wang, Y.; Han, J.; Zhuang, L.; Hick-ner, M. A. *Macromolecules* **2016**, *49*, 815. (b) Pan, J.; Chen, C.; Zhuang, L.; Lu, J. *Acc. Chem. Res.* **2012**, *45*, 473. (c) Wang, Y.-J.; Qiao, J.; Baker, R.; Zhang, J. *Chem. Soc. Rev.* **2013**, *42*, 5768. (d) Li, N. W.; Leng, Y. J.; Hickner, M. A.; Wang, C. Y. *J. Am. Chem. Soc.* **2013**, *135*, 10124.

[20] Dewi, E. L.; Oyaizu, K.; Nishide, H.; Tsuchida, E. *J. Power Sources* **2003**, *115*, 149.

[21] (a) Varcoe, J. R.; Atanassov, P.; Dekel, D. R.; Herring, A. M.; Hickner, M. A.; Kohl, P. A.; Kucernak, A. R.; Mustain, W. E.; Nijmeijer, K.; Scott, K.; Xu, T.; Zhuang, L. *Energy Environ. Sci.* **2014**, *7*, 3135. (b) Hugar, K. M.; Kostalik, H. A., IV; Coates, G. W. *J. Am. Chem. Soc.* **2015**, *137*, 8730. (c) Wright, A. G.; Holdcroft, S. *ACS Macro Lett.* **2014**, *3*, 444. (d) You, W.; Hugar, K. M.; Coats, G. W. *Macromolecules* **2018**, 51, 3212.

[22] (a) Chempath, S.; Einsla, B. R.; Pratt, L. R.; Macomber, C. S.; Boncella, J. M.; Rau, J. A.; Pivovar, B. S. *J. Phys. Chem. C* **2008**, *112*, 3179. (b) Edson, J. B.; Macomber, C. S.; Pivovar, B. S.; Boncella, J. M. *J. Membr. Sci.* **2012**, *399−400*, 49. (c) Mohanty, A. D.; Bae, C. *J. Mater. Chem. A* **2014**, *2*, 17314.

[23] (a) Pan, J.; Lu, S. F.; Li, Y.; Huang, A. B.; Zhuang, L.; Lu, J. T. *Adv. Funct. Mater.* **2010**, *20*, 312. (b) Fang, J.; Shen, P.K. *J. Membr. Sci.* **2006**, *285*, 317. (c) Xiong, Y.; Liu, Q. L.; Zeng, Q. H. *J. Power Sources* **2009**, *193*, 541. (d) Wang, G. G.; Weng, Y. M.; Zhao, J.; Chen, R. R,; Xie, D. *J. Appl. Polym. Sci.* **2009**, *112*, 721. (e) Wu, L.; Xu, T. W.; Wu, D.; Zheng, X. *J. Membr. Sci.* **2008**, *310*, 577. (f) Yan, X. M.; He, G.H.; Gu, S.; Wu, X. M.; Du, L.G.; Zhang, H. Y. *J. Membr. Sci.* **2011**, *375*, 204.

[24] (a) Thomas, O.D.; Soo, K.J.W.Y.; Peckham, T.J.; Kul-karni, M.P.; Holdcroft, S. *J. Am. Chem. Soc.*, **2012**, *134*, 10753. (b) Thomas, O. D.; Soo, K. J. W. Y.; Peckham, T. J.; Kul-karni, M. P. Holdcroft, S. *Polym. Chem.* **2011**, *2*, 1641.

[25] (a) Lee, H. J.; Choi, J.; Han, J. Y.; Kim, H. J.; Sung, Y. E.; Kim, H. *Polym. Bull*. **2013**, *70*, 2619. (b) Henkensmeier, D.; Kim, H-J.; Lee, H-J.; Lee, D. H.; Oh, I-H.; Hong, S-A.; Nam, S-W.; Lim, T-H. *Macromol. Mater. Eng*. **2011**, *296*, 899.

[26] Vöge, A.; Deimede, V.; Kallitsis, J. K. *RSC Adv*. **2014**, *4*, 45040.

[27] Henkensmeier, D.; Cho, H.-R.; Kim, H.-J.; Nunes Kirch-ner, C.; Leppin, J.; Dyck, A.; Jang, J. H.; Cho, E.; Nam, S.-W.; Lim, T.-H. *Polym. Degrad. Stab*. **2012**, *97*, 264.

[28] Ye, Y.; Elabd, Y. A. *Macromolecules* **2011**, *44*, 8494.

[29] Meek, K. M.; Elabd, Y. A. *Macromolecules* **2015**, *48*, 7071.

[30] Price, S. C.; Williams, K. S.; Beyer, F. L. *ACS Macro Lett*. **2014**, *3*, 160.

[31] Jheng, S. L. c. Hsu, B. y. Lin and Y. l. Hsu, *J. Membr. Sci.*, **2014**, *460*, 160.

[32] Dong, H.; Li, Y.; Si, Z.; Gu, F.; Yan, F. *Macromolecules* **2014**, *47*, 208.

[33] Hou, H. Y.; Sun, G. Q.; He, R. H.; Sun, B. Y.; Jin, W.; Liu, H.; Xin, Q. *Int. J. Hydrogen Energy* **2008**, *33*, 7172.

Chapter 6

Effect of alkylation on polybenzimidazoles for alkaline anion exchange membranes

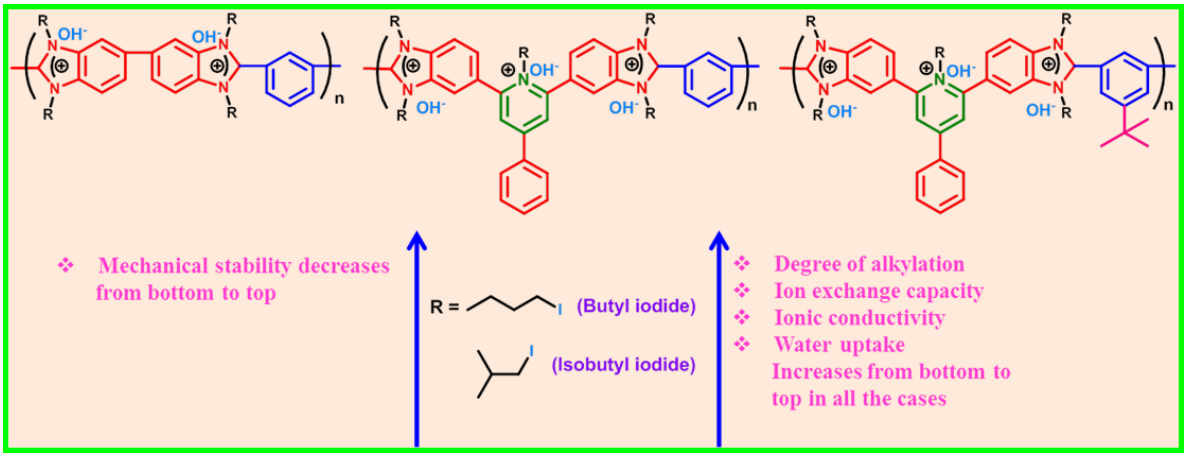

Various poly(alkylated pyridinium benzimidazolim) anion exchange membranes (AEMs) have been developed from different types of polybenzimidazoles by changing alkyl iodides and evaluated their properties for the use as AEMs.

Sana, B.; Jana, T. (Manuscript under preparation)

6.1. INTRODUCTION

Fuel cells are one of the most promising power generation technologies in recent times as they are efficient in converting chemical energy into electrical energy.[1-3] Among fuel cells, proton exchange membrane fuel cells (PEMFCs) were studied extensively in the literature. Nafion is one of the highly studied proton exchange membranes (PEM) among different available PEMs owing to its intrinsic properties. However, PEMFCs are still suffer from certain drawbacks such as high cost in the preparation of membranes, also high priced catalysts palladium or platinum used for the conversion of hydrogen into electrons and protons required to generate energy. They also suffer from high fuel permeability and slower reaction kinetics.[4] Since a decade or so, alkaline anion exchange membrane fuel cells (AAEMFCs) have gained as a low-cost alternative to the PEMFCs.[5, 6]

Recently, several research groups focused on the development of alkaline anion exchange membrane fuel cells (AAEMFCs) operated with anion exchange membranes (AEMs) because they have more attractive advantages than the PEMFCs.[7-9] The AEMFCs are operated under alkaline conditions wherein the electrode kinetics are much faster than those in acidic conditions and low cost non-noble metal (Co, Ni) catalysts are used as cathode.[10-15] Alkaline anion exchange membranes (AAEMs) play an important role in the development of AAEMFCs. The alkaline stability of the AEMs is influenced by the cationic groups and the chemical structure of the polymer backbone. To fulfil the basic required properties of AEMFCs, the ideal AAEMs could possess higher ionic conductivity, excellent alkaline stability, good thermal stability, moderate mechanical robustness and sufficient long-term durability at higher temperatures in the presence of alkaline condition.[5, 16-18] Development of such kind of AAEMs with all these properties is a major challenge. The most of the AAEMs developed so far are based on various polymer backbones such as poly(aryl ether),[19] poly(ether ether ketone),[20] poly(arylene ether sulfone),[21] polysulfone,[22] poly(ether ketones),[23] polybenzimidazole,[24] polyethylene,[25, 26] poly(vinylbenzyl chloride),[27] poly(phenylene oxide),[28-31] poly(styrene-co-vinylbenzyl chloride),[32, 33] fluorinated

polymers.[34] These polymer employ various cationic backbones groups such as quaternary ammonium (QA),[35, 36] imidazolium,[37] benzimidazolium,[38] phosphonium,[39] tertiary sulfonium,[40] guanidinium,[41] pyridinum,[42] pyrrolidinium,[43] based membranes were synthesized and investigated.

In the literature, many research groups have employed QA groups as anion exchange site among various cationic species because it is simple and very easy to introduce on the polymer backbone. However, QA groups show the degradation by the nucliophilic substitution (S_N2) under alkaline condition and it exhibit Hoffmann elimination or E2 elimination when the hydrogen is present at β position from the positive charge.[44] In the literature, few reports discussed about the pyridinium groups containing polymers as AAEMs in AEMFCs, but these AAEMs show very less ionic conductivity because of the hydroxide ions attack at electrophilic centres of the pyridinium moiety in the presence of oxygen at elevated temperature which results in the irreversible conversion of pyridinium groups into neutral pyridone. Hence, it was argued by several authors that the pyridinium groups containing AAEMs could not suitable for AEMFCs and an alternative for this method is required in order to improve the efficiency.[45] Both J. Fang's and F. Yan's groups have developed imidazolium based AAEMs and the results demonstrated good chemical and thermal stabilities compared to that of quaternary ammonium groups.[46, 47] After that many research groups worked on developing the polymers with imidazolium groups as AEMs in AEMFC applications. Recently polybenzimidazolium (PBI) based AAEMs were studied and displayed good ionic conductivity and ion exchange capacity (IECs). But these membranes were suffers from the alkaline stability. In other report, Henkensmeier *et al.*, studied alkaline stability and degradation mechanism of the PBI AAEMs and they suggested the alkaline stability of this polymer membrane should be improved further.[48] So far, no one has achieved sufficient alkaline stability of the PBI based AAEMs and it is still a challenging issue.

In Chapter 5, we have demonstrated that pyridine bridged PBI (PyPBI) can be used as a dual ion conducting sites where both pyridine and imidazole functionalities can be converted to ion conducting site which resulted higher ionic conductivity. We

also showed that the blocking of pyridine α-position helped in preventing degradation of pyridine moiety and hence over all stability of the AAEM has increased significantly. But even after this, we believe there is a scope of improvement in alkaline stability and hydroxide ion conductivity.

In this Chapter we want to achieve higher alkaline stability and hydroxide ionic conductivity of poly(alkylated pyridinium benzimidazolim) iodide membranes by resulting the alkyl structure. Therefore, in this chapter we have made a thorough investigation is the effect alkylation on the AAEM properties particular on ionic conductivity and alkaline stability.

6.2 EXPERIMENTAL SECTION

Details of the materials and characterization methods used in this study are included in the Chapter 2. Polymer synthesis, membrane formation method and anion exchange reaction are described below.

6.2.1. Synthesis of polymers

Poly [2,2'-(*m*-phenylene)-5,5'-benzimidazole] or *meta*-polybenzimidazoles (*m*-PBI), pyridine bridged polybenzimidazole (PyPBI) and 5-tertiary butyl pyridine bridged polybenzimidazoles (PyPBI-t_{But}) were synthesized by following procedure according to our previous work[49] as shown in Scheme 6.1. Equimolar ratio of tetra amine (TAB or PyTAB) and dicarboxylic acids (IPA or IPA-t_{But}) monomers were taken along with PPA in a 250 mL, three necked round bottom flask equipped with mercury sealed overhead mechanical stirrer. The reaction mixture was stirred for approximately 24 h at 210 °C temperature under inert conditions. After completion of polymerization reaction, the obtained viscous solution was slowly poured into the deionized water and the polymers were obtained in the form of fibre. The obtained fibrous polymers were neutralized with aqueous sodium bicarbonate solution and washed thoroughly with deionized water for the removal of excess base. Finally, the fibrous polymers were dried in vacuum oven at 100 °C for 24 h. The PyPBI-t_{But} polymer structure was confirmed by recording ^{1}H NMR spectrum and it is placed in the Figure 6.1. The polymer structure and important peaks

are assigned in the spectrum. The chemical shift values of the tertiary butyl group, aromatic protons and imidazole proton peaks was appeared at 1.5, 7.3-9.2 and 13.4 ppm, respectively. The structures of m-PBI and PyPBI have also been confirmed using ^{1}H NMR spectra as presented in other chapters.

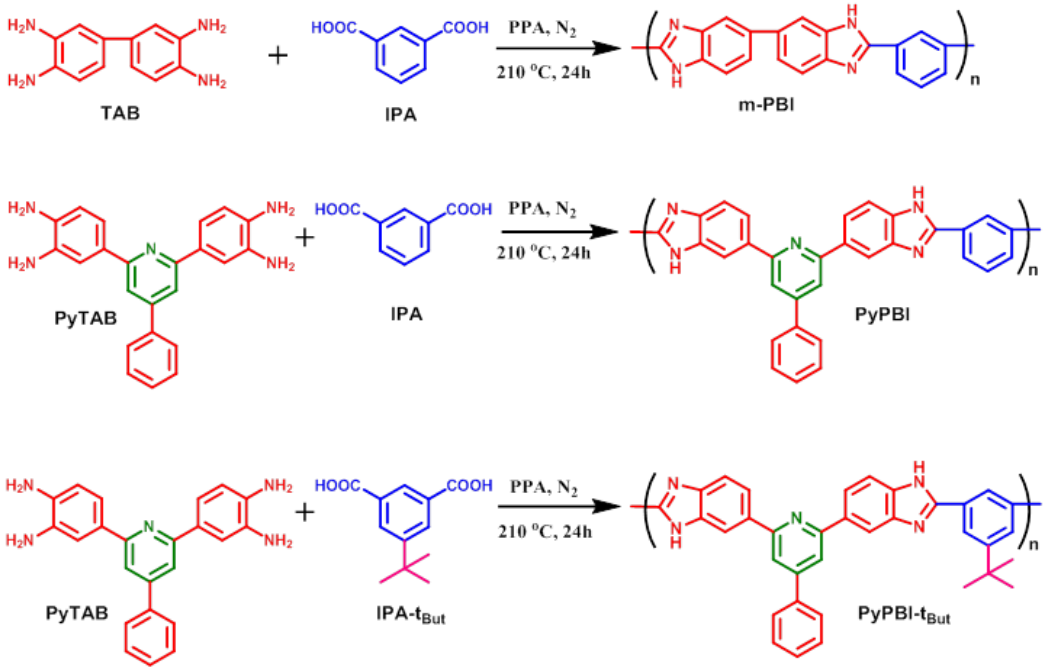

Scheme 6.1. *Synthesis of three types of polybenzimidazole polymers (PBI, PyPBI and PyPBI-t_{But}).*

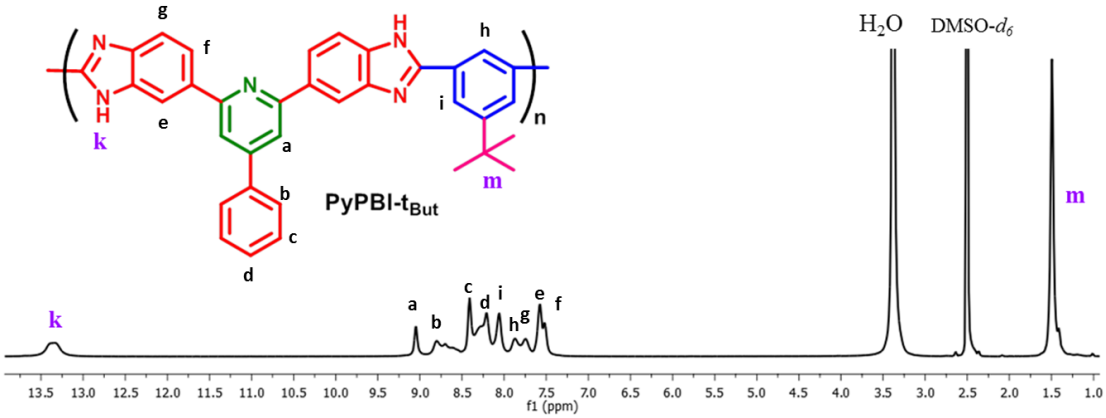

Figure 6.1. *^{1}H NMR spectrum of the tertiary butyl pyridine bridged polybenzimidazole.*

6.2.2. Synthesis of poly(alkylated pyridinium benzimidazolium) iodides

PyPBI-t_{But} polymer (1.0 g, 0.0019342 moles) was dissolved in 60 mL of dry DMSO solvent at 80 °C temperature and the dissolved polymer was transferred to a 100 mL round bottom flask fitted with a reflux condenser. Inert atmosphere was maintained throughout the reaction. After dissolution, the polymer solution was allowed to cool to room temperature and sodium hydride (0.09284 g, 0.0038684 moles) was added. The temperature of the reaction mixture was again raised to 80 °C. The reaction solution was stirred for 12 h and was allowed to cool to the room temperature and alkyl iodide (MeI=1.373 g, 0.0096711 moles), was added and continued the stirring for 4 h at 80 °C. The mole ratios of the polymer, sodium hydride and alkyl iodide was maintained as 1:2:5. After 4 h of alkylation same amount of MeI was added for the second time and continued the stirring for 16 h. After completion of this period, the reaction mixture was poured into the water and obtained a reddish brown precipitation. The precipitate was filtered off and washed thoroughly with deionized water for several times for the removal of excess alkyl iodide and sodium hydride. The obtained PyPBI-t_{But}-MeI polymer was dried in vacuum oven at 70 °C for 24 h. The dried polymer was stored in vacuum desiccator for further characterization. Similar reaction conditions were applied on PBI, PyPBI and PyPBI-t_{But} to alkylates both imidazole and pyridine functionality in the polymer chain using various alkyl iodide. And these are methyl iodide (MeI), butyl iodide (BuI) and isobutyl iodide (IbuI). Other remaining iodide form polymers (PBI-MeI, PBI-BuI, PBI-IbuI, PyPBI-MeI, PyPBI-BuI, PyPBI-IbuI, PyPBI-t_{But}-BuI and PyPBI-t_{But}-IbuI) were synthesized by applying same synthetic process as mentioned above.[50] The synthetic reactions are shown in Scheme 6.2.

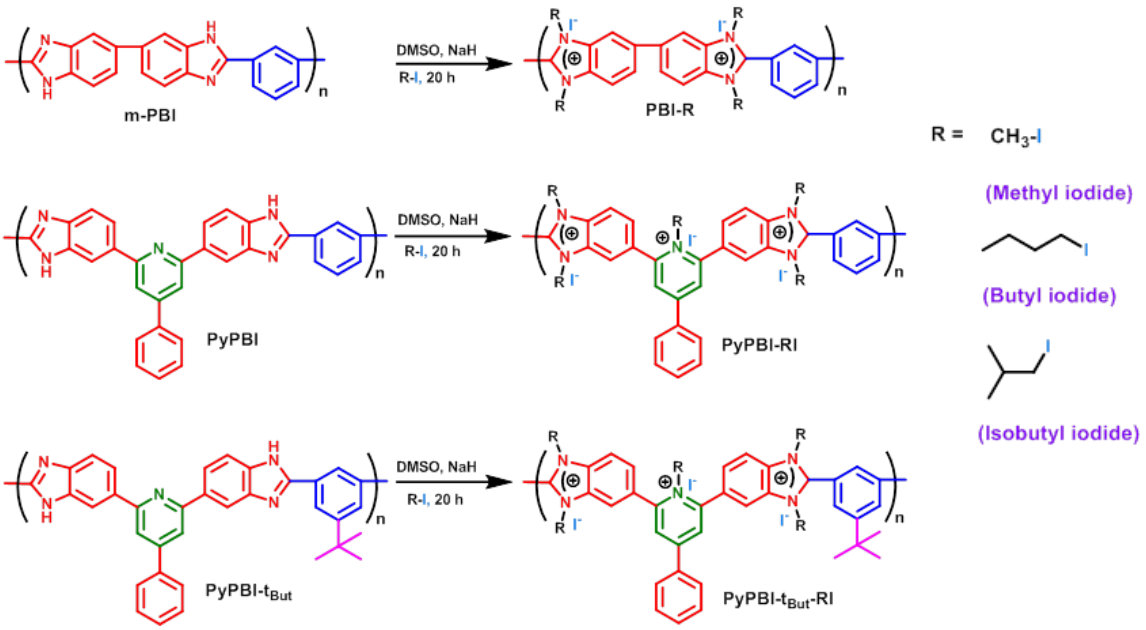

Scheme 6.2. *Synthesis of poly(alkylated pyridinium benzimidazolium) iodides by varying alkyl chains on different polybenzimidazoles.*

6.2.3. Membrane formation and anion exchange reaction

A 1% (w/v) polymer solution was prepared by dissolving the polymer in iodide form in DMSO solvent over a period of 24 h stirring at room temperature. The obtained clear solution was then poured into a clean flat glass Petri dish, followed by the solvent evaporation in a hot air oven at 80 °C for 10-12 h. After this period, the dried membrane was peeled off from the glass Petri dish. The membranes were soaked in hot boiled water to remove the trace amount of DMSO solvent. The membranes were dried in a vacuum oven at 100 °C for 24 h. This dried membrane was stored in a desiccator for further studies.

The obtained poly(alkylated pyridinium benzimidazolium) iodide membranes were immersed in 1 M KOH aqueous solutions at room temperature for 24 h to convert them from iodide (I^-) form to hydroxide (OH^-) form membranes. Then, the hydroxide ion membranes were washed thoroughly with deionized water several times to remove excess base on the surface of the membranes. These membranes were soaked in

deionized water for 24 h prior to analysis. The structures of the OH^- ion loaded membrane are shown in Scheme 6.3.

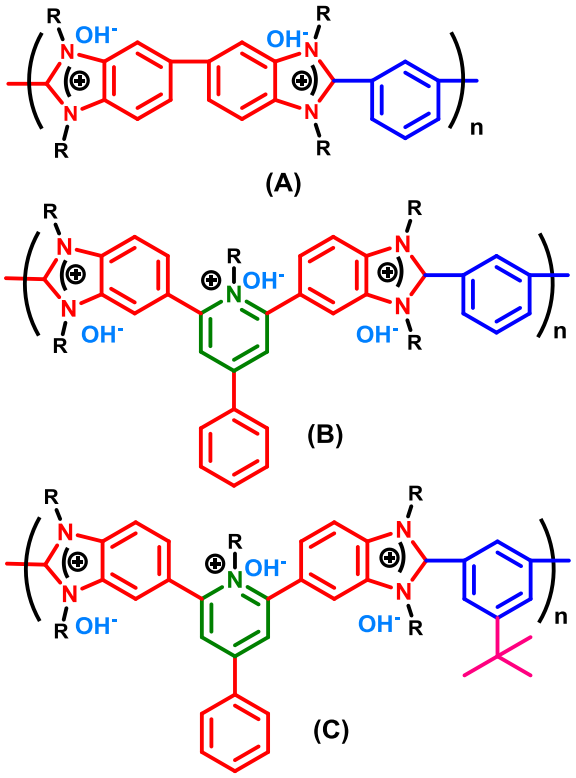

Scheme 6.3. *Chemical structure of hydroxide ion loaded poly(alkaylated pyridinium benzimidazolium) membrane: (A) PBI-ROH, (B) PyPBI-ROH, (C) PyPBI-t_{but}-ROH.*

6.3. RESULTS AND DISCUSSIONS

6.3.1. Polymer synthesis and spectroscopic characterizations

In the present work three different polybenzimidazoles: (PBI, PyPBI, and PyPBI-t_{But}) polymers were prepared (Scheme 6.1) and alkylated using various alkyl iodides: methyl iodide, butyl iodide and isobutyl iodide to obtain quaternized anion exchange polymers. PBI treated with methyl iodide yielded methylated iodide form PBI polymer (PBI-MeI). Similarly the butyl iodide and isobutyl iodide were reacted with PBI to obtain PBI-BuI and PBI-IbuI. Similarly, PyPBI and PyPBI-t_{But} polymers reacted with three alkyl iodides to produced six alkylated iodide form polymers: PyPBI-MeI, PyPBI-

BuI, PyPBI-IbuI, PyPBI-t_{But}-MeI, PyPBI-t_{But}-BuI and PyPBI-t_{But}-IbuI, respectively. Altogether three series (nine different types) of alkylated iodide form polymers were synthesised. The chemical structures of the poly(alkylated pyridinium benzimidazolium) iodide polymers were presented in Scheme 6.2 and confirmed by FT-IR and ^{1}H NMR spectroscopic studies. Proton NMR spectra of the all the three series of poly(alkylated pyridinium benzimidazolium) iodide polymers are shown in the Figure 6.2-6.4. In all the three series, degree of alkylation on the nitrogen atoms of the polymers is calculated from the peak integration of ^{1}H NMR spectra. The polymer structure and peak assignments are represented along with their spectra. The polymer main chain peaks are represented by alphabets and alkyl chain peaks are represented by numbers. In each proton, NMR spectrum the imidazole protons disappears and at the same time alkylated protons appears as result of alkylation. In three series of polymers, the aromatic proton peaks chemical shift values are observed in the range of 7.4 to 9.3 ppm in their proton NMR spectra. In three series, the methyl substituted polymers (PBI-MeI, PyPBI-MeI, and PyPBI-t_{But}-MeI) of the methyl group chemical shift values are observed between 4.0 to 4.3 ppm. In the case of butyl substituted polymers (PBI-BuI, PyPBI-BuI, and PyPBI-t_{But}-BuI), butyl group of the first methylene attached to the nitrogen atom are observed at 3.95 to 4.75 ppm. The proton resonance of the second and third methylene groups appears around at 1.8 ppm and 1.23 ppm respectively. Another peak is observed around at 0.80 ppm which is corresponding to the methyl group. In the case of isobutyl substituted polymers (PBI-IbuI, PyPBI-IbuI, and PyPBI-t_{But}-IbuI), nitrogen atom attached methylene group chemical shift value is obtained at around 4.0 to 4.5 ppm. The peak of the single proton known as the methyne appears around at 2.0 ppm and other two methyl group chemical shift values appears in the range of 0.6 to 1.25 ppm.

The degree of alkylation of poly(alkylated pyridinium benzimidazolium) iodide form polymers is calculated from ^{1}H NMR spectra (Figure 6.2 to 6.4) by comparing the integrations of alkyl protons and aromatic protons and calculated by using equation (6.1). Degree of alkylation (%) of all the polymers is summarized in the Table 6.1.

$$\text{Degree of alkylation} = \frac{\text{Integral of alkyl H} \times \text{Aromatic H per repeat unit}}{\text{Integral of Aromatic H} \times \text{alkylated H per repeat unit}} \quad (6.1)$$

Degree of alkylation with methyl iodide and butyl iodide for all the synthesized polymers are found to be higher when compared to the alkylation with isobutyl iodide. The reason might be due to the bulky nature of the isobutyl group restricts the substitution reaction. Also, PBI and PyPBI based AAEMs are displaying higher degree of alkylation than the PyPBI-t_{But} based polymer which may be once again related to the crowding nature of the later.

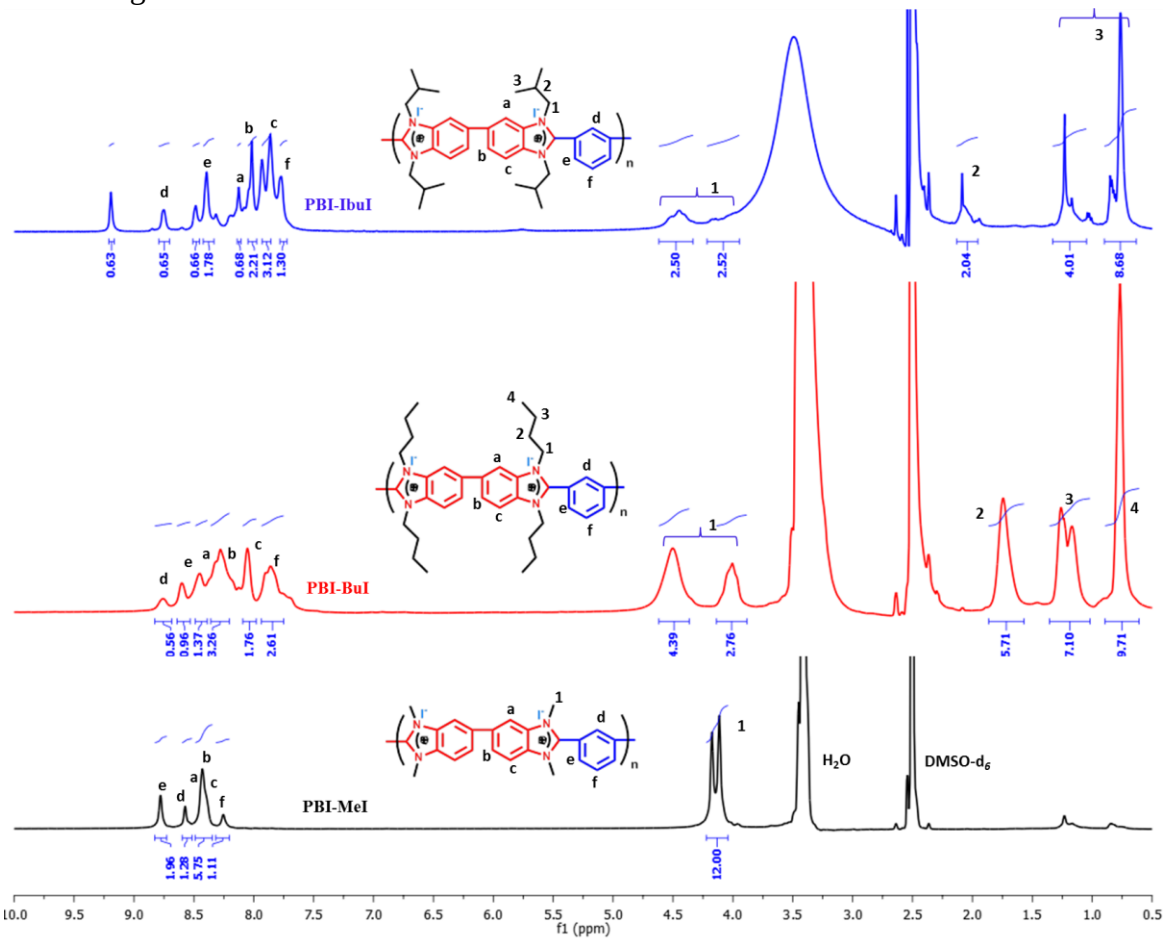

Figure 6.2: *^{1}H NMR spectra of poly(alkylated pyridinium benzimidazolium)iodide form of m-PBI.*

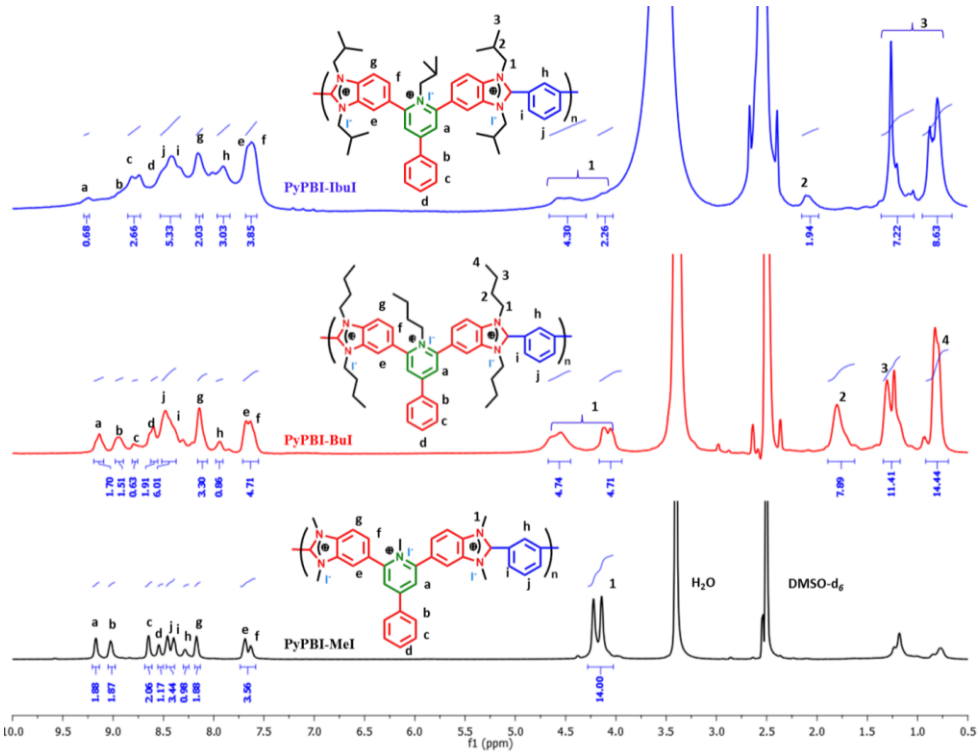

Figure 6.3: *^{1}H NMR spectra of poly(alkylated pyridinium benzimidazolium)iodide form of Py-PBI.*

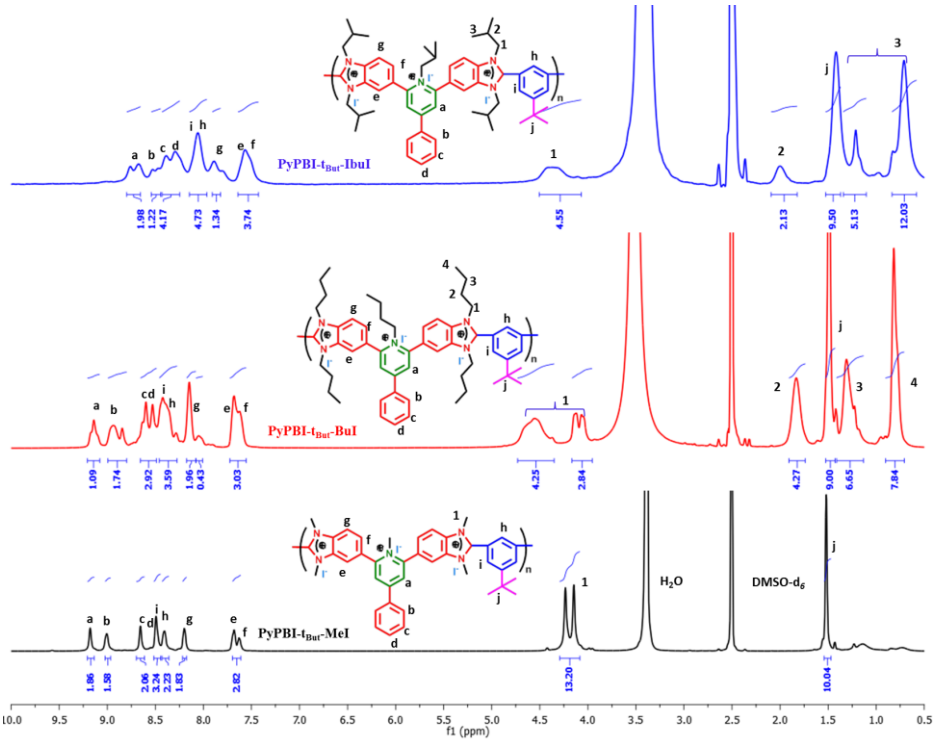

Figure 6.4: *^{1}H NMR spectra of poly(alkylated pyridinium benzimidazolium)iodide form of Py-PBI-t_{But}.*

Table 6.1. *Degree of alkylation, water uptake and ion exchange capacity of all the poly(alkylated pyridinium benzimidazolium) iodide polymers.*

S.No	Sample Identity	Degree of alkylation (%)	IEC (mequiv.g^{-1})	Water uptake (%)
1	PBI-MeI	99.0	–	–
2	PBI-BuI	86.2	2.84	11.35
3	PBI-IbuI	57.0	2.08	7.00
4	PyPBI-MeI	94.2	–	–
5	PyPBI-BuI	78.0	3.37	18.00
6	PyPBI-IbuI	64.0	2.78	9.25
7	PyPBI-t_{But}-MeI	90.2	–	–
8	PyPBI-t_{But}-BuI	76.6	2.55	8.69
9	PyPBI-t_{But}-IbuI	43.0	0.95	–

The FT-IR spectra of all the poly(alkylated pyridinium benzimidazolium) iodide form are displaced in Figure 6.5. In the IR spectra of iodide polymer, the important bands at 2845-2985 cm^{-1} are ascribed to the vibration of the aliphatic C-H frequency.[51] The peaks in the range of 3050-3060 cm^{-1} are attributed to the stretching frequency of aromatic C-H bond and another important band is observed at 820-831 cm^{-1} corresponding to the C-H stretching vibration of pyridine ring. The other two important peaks at 1602-1613 cm^{-1} and 1450-1470 cm^{-1} are ascribed to the C=C/C=N, in plane benzimidazole ring deformation and are also reported by several authors in the literature earlier.[52-56]

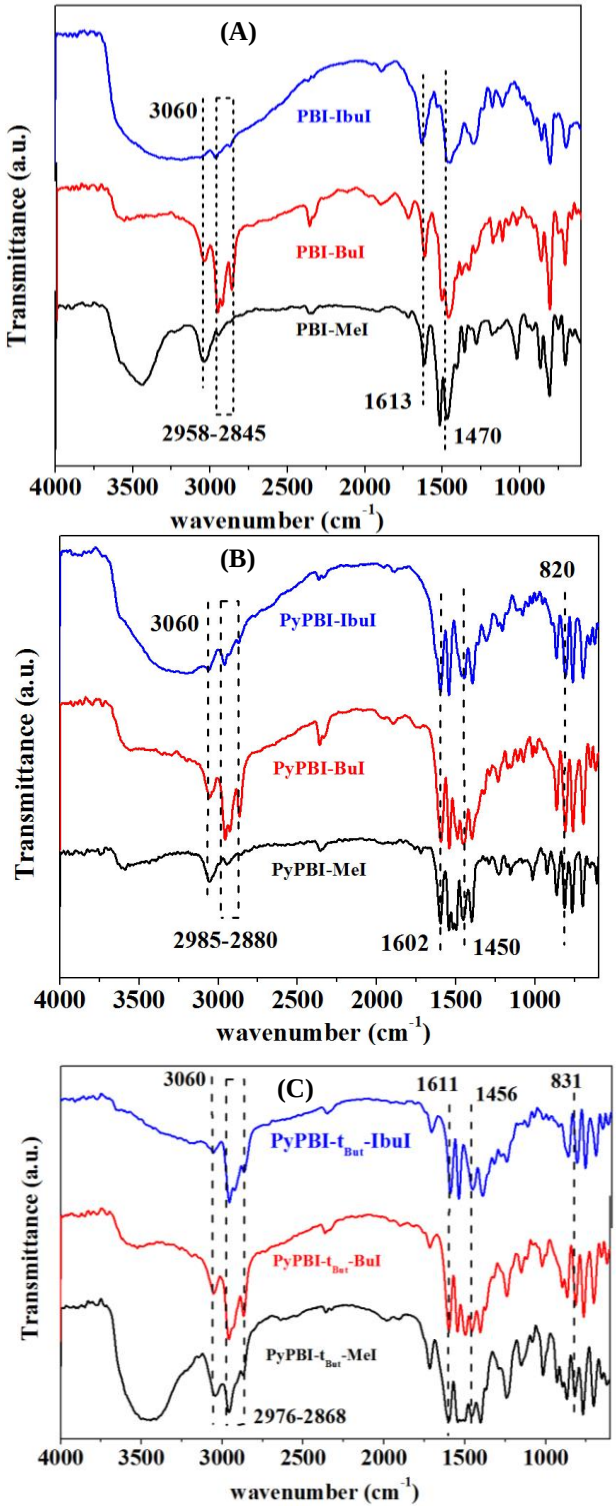

Figure 6.5. *FT-IR spectra of three series of poly(alkylated pyridinium benzimidazolium) iodide: (A) PBI, (B) PyPBI and (C) PyPBI-t_{But}.*

6.3.2. Ion exchange capacity (IEC)

The poly(alkylated pyridinium benzimidazolium) iodide membranes were treated with 1 M aqueous KOH solutions to replace iodide ions with hydroxide (OH^-) ions. The measured ion exchange capacity (mequiv.g^{-1}) values of the anion exchange membranes are presented in the Table 6.1. The ion exchange capacity provides indications of the ion exchangeable groups present in the membranes.[57] All methylated AAEMs were completely broken into very small species while doping in 1 M KOH solution. Hence, we were unable to measure the IEC of these samples (PBI-MeI, PyPBI-MeI, and PyPBI-t_{But}MeI) due to the instability in alkaline condition. The IECs of all the three butylated AAEM membranes (PBI-BuI, PyPBI-BuI, and PyPBI-t_{But}BuI) are found to be in the range of 2.55-3.37 mequiv.g^{-1} and also higher than the IECs value isobutylated AAEMs which exhibit IEC in the range of 0.95-2.78 mequiv.g^{-1}. High degree of alkylation is the reason for obtaining higher IECs with butylated polymers when compared to the polymers with isobutyl groups. The PyPBI-t_{But}-IbuI polymer is displaying less IEC than PBI and PyPBI system and this could be due to the low degree of alkylation of this polymer compared to other two. Also, it is to be noted that this polymer absorbed less water (Table 6.1) than other two. IEC values are highly dependent on the degree of alkylation and water uptake. All the butylated AAEMs display higher water uptake than the isobutylated AAEMs resulting higher IEC and this is due to the less bulky nature of butyl groups than the isobutyl group.

6.3.3. Chemical stability

Chemical stability is an important parameter to be measured for alkaline anion exchange membranes (AAEMs) since the working fuel cell operates in the complete basic environment.[58] The chemical stability of all the poly(alkylated pyridinium benzimidazolium) iodide form membranes was studied by soaking them into the 1 M and 5 M aqueous KOH solutions at room temperature (30 °C) and at 60 °C temperature and the stability was monitored as a function of time. The chemical stability data are presented in Table 6.2 clearly demonstrates the effect of polymer structure and the alkyl

iodide structure. It is to be noted that the chemical stability was monitored as function of time by checking the membrane flexibility brittleness and by observing the colour change of the alkaline solution. Earlier Henkensmeier *et al.*, also reported that the simple methylated PBI became brittle when exposed to the 0.5 M potassium hydroxide solution.[59] Holdcraft *et al.*, reported methylated *meta*-PBI membrane rapidly broken when exposed to 0.5 M KOH solutions at room temperature and breaks when touched with tweezers.[60] We also observed that both PBI-MeI and PyPBI-MeI polymer membranes are rapidly broken into smaller pieces within 1 hour of time even at room temperature. The AAEM of the PyPBI-t_{But}-MeI polymer displays better chemical stability than the former two polymers (PBI-MeI and PyPBI-MeI); it shows stability upto 15 hours (Table 6.2). The reason for this might be due to the presence of the bulky tertiary butyl group in the PyPBI-t_{But}-MeI polymer which could hinder the attacking of the hydroxide ions on the second carbon (C2) of the imidazolium group. However, this bulky tertiary butyl group could not influence much on the overall chemical stability of the membrane.

AAEMs of all the butylated and isobutylated polymers treated with 1 M KOH solution display flexibility and stability even after 21 days at room temperature as well as at 60 °C and we did not find any difference before and after alkaline treatment. Based on this observation of stability in 1 M KOH, all the butylated and isobutylated AAEM were exposed to 5 M KOH solution and this stability were treated as a function of time at RT and 60 °C. Interestingly, we did not observe any degradation of these membranes both of RT and 60 °C till 21 days. In case of butylated membrane, we noticed very little colour change of the alkaline solution otherwise there is no change. This remarkably high alkaline stability of butylated and isobutylated samples of all three types of PBI is very significant, considering the fact that both PBI and PyPBI samples found to be degrade quickly in 1 M KOH solution as observed by us (in Chapter 5) and others. Therefore, it is very clear that alkyl iodide plays a significant role in contributing the chemical (alkaline) stability of these membranes.

Table 6.2. *Chemical stability of the poly(alkylated pyridinium benzimidazolium) iodide membranes in 1 M and 5 M KOH solution at ambient and 60 °C.*

Polymer Identity	Stability test in 1 M KOH solution		Stability test in 5 M KOH solution [b]	
	Temperature at which stability checked	Observation [a]	Temperature at which stability checked	Observation [a]
PBI-MeI	RT & 60 °C	Degradation observed within 1 hr.	–	–
PBI-BuI	RT & 60 °C	No degradation observed	RT & 60 °C	No degradation observed
PBI-IbuI	RT & 60 °C	No degradation observed	RT & 60 °C	No degradation observed
PyPBI-MeI	RT & 60 °C	Degradation observed within 1 hr.	–	–
PyPBI-BuI	RT & 60 °C	No degradation observed	RT & 60 °C	No degradation observed
PyPBI-IbuI	RT & 60 °C	No degradation observed	RT & 60 °C	No degradation observed
PyPBI-t_{But}-MeI	RT & 60 °C	Degradation observed 8-15 hr.	–	–
PyPBI-t_{But}-BuI	RT & 60 °C	No degradation observed	RT & 60 °C	No degradation observed
PyPBI-t_{But}-IbuI	RT & 60 °C	No degradation observed	RT & 60 °C	No degradation observed

[a] We trested the membrane stability upto 21 days. [b] Membranes which showed degradation in 1 M KOH were not subjected to stability study in 5 M KOH.

We have discussed the possible degradation of imidazolium functionality in the chapter 5 (Scheme 5.3). In which the imidazolium cation would degrade via a ring-opening mechanism which was triggered by the nucleophilic attack of OH^- ions on the imidazolium ring at the C2 position.[61] The imidazolium ring is converted into an amine-amide after the ring-opening reaction as shown in Scheme 5.3.[48, 50, 62-66] However, pyridinium group could not be degraded as the all α-positions are of pyridinium are

blocked. In this chapter, we noticed that the methylated samples display degradation but both butylated and isobutylated samples show no degradation as shown in Table 6.2. To confirm this, we did a thorough investigation by recording ^{1}H NMR spectra of hydroxide treated samples. Since methylated samples are degrading in 1 M KOH so we treated them with 1 M KOH for 21 days, however we treated butylated and isobutylated samples with 5 M KOH for 21 days before recording NMR since they display stability even in this condition.

A portion of the alkali treated ^{1}H NMR spectra for better clarity of presentation of all the three types of polymers (PBI, PyPBI and PyPBI-t_{But}) for various alkylation are compared in Figure 6.6 to 6.8 in all the three cases methylated samples show appearance of three new peaks (denoted as a, b and c in the spectra) which are absent for both in case of butylated and isobutylated samples, and as well as unalkylated samples (see Figure 6.2 to 6.4).

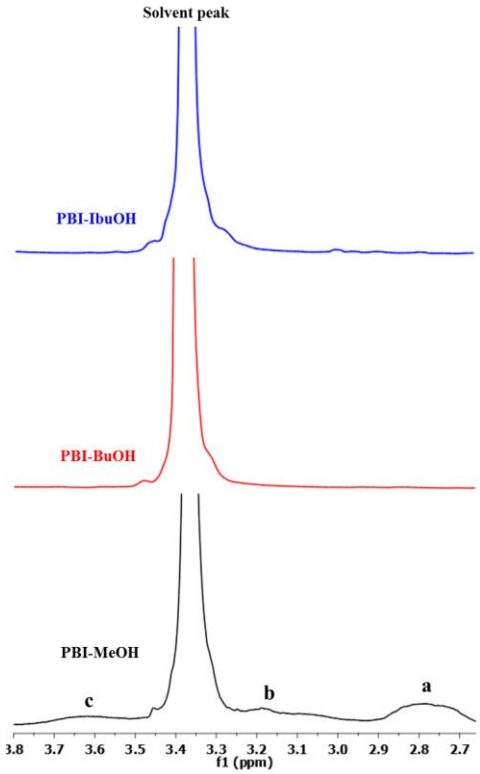

Figure 6.6. *^{1}H NMR spectra of the poly(alkylated pyridinium benzimidazolium) iodide form membranes after alkaline stability test.*

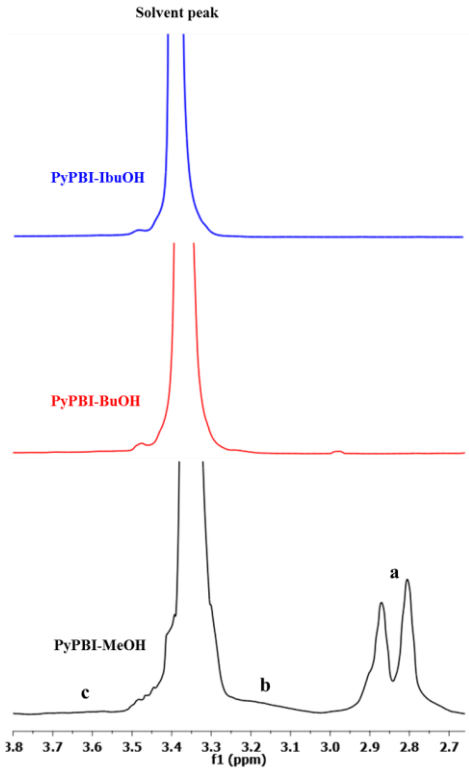

Figure 6.7. *^{1}H NMR spectra of the poly(alkylated pyridinium benzimidazolium) iodide form membranes after alkaline stability test.*

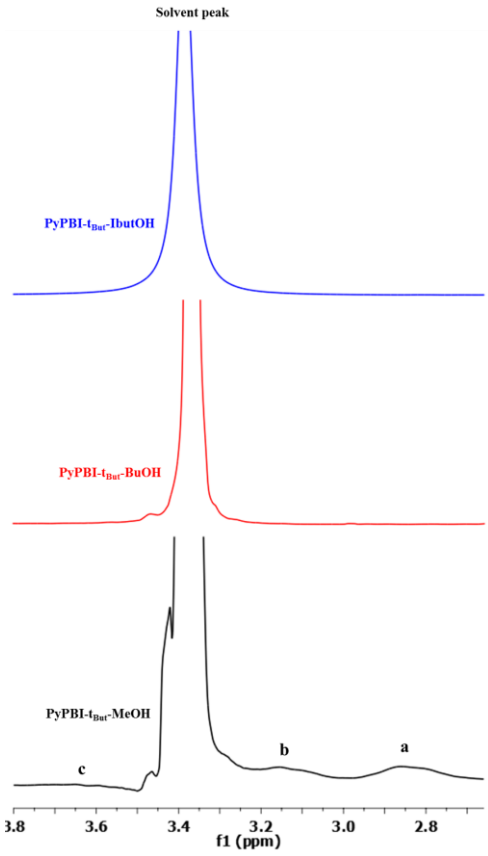

Figure 6.8. *^{1}H NMR spectra of the poly(alylated pyridinium benzimidazolium) iodide form membranes after alkaline stability test. PyPBI-t_{But} polymer used in this case.*

The new peak ‘a’ at ~ 2.9 ppm is attributed to the methyl (-CH_3) protons attached to the secondary amine. Another new proton resonance signal 'b’ observed at ~ 3.23 ppm, is attributed to the methyl protons attached to the tertiary amide and new signal appeared at ~ 3.9 ppm ‘c’ attributed to the secondary amine (-NH) proton. The aromatic signals appeared in the region of 6.0-9.0 ppm do not display any change before and after alkali treatment indicating that the degradation mechanism is as proposed in Scheme 5.3. However, degradation of butylated and isobutylated AAEMs is negligible after the treatment of KOH as evident from ^{1}H NMR spectra (Figure 6.6-6.8). The ^{1}H NMR spectra of the 5 M KOH treated butylated and isobutylated membranes are exactly identical to their untreated membranes which is given in the Figure 6.2-6.4 and no new peaks like a, b, c are observed. This clearly indicates absolutely zero degradation of butylated and isobutylated samples. The reason could be that the imidazole groups substituted by the butyl and isobutyl groups completely prevents the degradation of imidazolium because of the bulky nature of the long butyl and isobutyl chains which prevents the attack of OH^- at C2 position of the imidazole moiety after treating with KOH. Hence, these membranes demonstrate excellent alkaline stability.

6.3.4. Ionic conductivity

The ionic conductivity is an essential property of AAEMs and plays a key role in the AEMFC applications. It is significantly influenced by the IEC values and water uptake. The ionic conductivities of the AAEMs were measured after doping with 1 M KOH alkaline solutions for 24 hours. The hydroxide (OH^-) ionic conductivity of the AAEMs was measured after the membranes were fully hydrated in deionized water for 24 h at ambient temperature. The ionic conductivity of the poly(alkylated pyridinium benzimidazolium) hydroxide membranes was studied as a function of temperature and the results are show in Figure 6.9. We have not measure the methylated samples since they were unstable in alkaline condition. The hydroxide conductivity values at 80 °C and the activation energy (E_a) of all the samples are tabulated in the Table 6.3. The hydroxide ions react with the atmospheric carbon dioxide[67, 68] and which results in producing the bicarbonate (HCO_3^-) ions. Therefore some of the hydroxyl ions are

transformed into the HCO_3^- ions in the AAEM membrane. The resulted ionic conductivity of the AAEM decreases as the mobility of HCO_3^- in dilute solution is much lower than the mobility of OH^- ions.[69, 70] Hence the decrement of the hydroxide conductivity is depending upon the exposure of OH^- form membranes to CO_2. The ionic conductivity in the three series of methylated AEMs was difficult to measure due to the instability of the membranes in 1 M KOH solution during the doping process. The hydroxide ionic conductivities of the butylated and isobutylated AEMs were increasing with the temperature due to the increasing free volume for ion transport and the enhancement of the mobility of anions. All the butylated and isobutylated AEMs display good ionic conductivity, the reason might be due to the bulky nature of these alkyl chains helps to increase the distance between the polymer chains. It is to be noted that the methylated PyPBI sample which was also studied in Chapter 5 did not show any ionic conductivity. The methylated PyPBI which showed ionic conductivity in Chapter 5 had different structure. All the butylated AAEMs show high ionic conductivity than their corresponding isubutylated AAEMs due to higher degree of alkylation and high IEC values of butylated polymers. That means more number of cationic groups are available for ion exchange and to transport the hydroxide ions throughout the AAEM. Among all the membranes, AAEM of PyPBI-BuI has the highest ionic conductivity with a value of 128.6 mS/cm. The reason for this is the presence of three cationic exchange sites (one pyridinium and two benzimidazolium groups) in the polymer which displays high degree of alkylation. In the literature, it has been reported that the pyridinuim groups containing AAEMs are not useful in the AEM fuel cell because those membranes yield less ionic conductivities. The reason explained was that the pyridinium groups would be converted into neutral pyridone in the presence of oxygen at elevated temperatures.[71, 72] Pyridone formation was completely prevented in this work by blocking the electrophilic centres (2, 4 and 6 positions) of the pyridinium group with benzimidazolium and phenyl groups as discussed in the previous section, the PyPBI sample did not show any degradation what so ever indicating the stabilities of the AAEM obtained from PyPBI. Membranes having pyridinium groups additionally help to give high ionic conductivity along with benzimidazolium cationic sites.

The activation energy (E_a) was estimated from the Arrhenius slopes (Figure 6.10) and all the tested samples exhibits different values. The activation energy is the minimum energy required for ion conduction through the AAEM. The low activation energy is attributed to fast ion conduction process. The activation energy of the poly(alkylated pyridinium benzimidazolium) hydroxide membranes are obtained in the range of 13.58-20.55 kJ/mol which is comparable with reported literature data.[11, 73, 74]

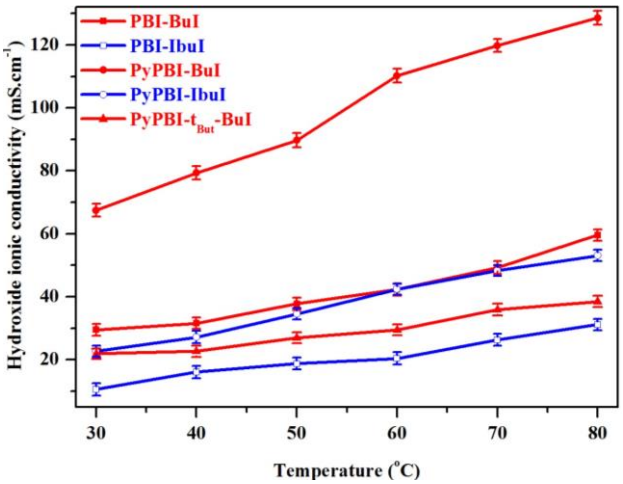

Figure 6.9. *Hydroxide ionic conductivity of the poly(alkylated pyridinium benzimidazolium) membranes as a function of temperature.*

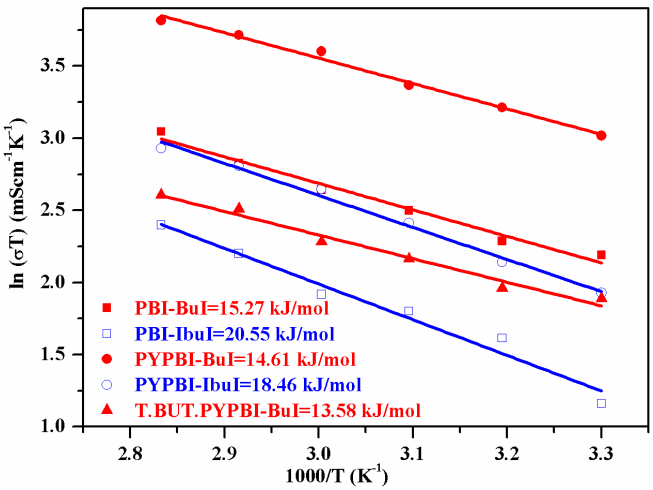

Figure 6.10. *Temperature dependence of hydroxide ionic conductivities of the poly(alkylated pyridinium benzimidazolium) membranes. Data points are fit into straight line using Arrhenius equation to obtain E_a which are listed in Table 6.3.*

Table 6.3. *Ionic conductivity values at 80 °C and activation energy (E_a) values of the poly(alkylated pyridinium benzimidazolium) membranes.*

AAEM	σ_{OH^-} (mS/cm) at 80 °C	*Ea* (kJ/mol)
PBI-BuI	59.6	15.27
PBI-IbuI	31.1	20.55
PyPBI-BuI	128.6	14.61
PyPBI-IbuI	53.0	18.46
PyPBI-t_{But}-BuI	38.4	13.58

6.3.5. Thermal properties

The thermal stability of the poly(alkylated pyridinium benzimidazolium) membranes were investigated by TGA analysis. The TGA plots of the AAEMs was recorded from 30-800 °C temperature under the nitrogen gas by 10 °C heating scan. TGA plots shows in Figure 6.11 display three degradation steps. The first degradation step was noticed below 130 °C which is attributed to the moisture or water absorption from the membranes. The second degradation step is observed between 200 °C to 300 °C temperature which is attributed to the cleavage of the imidazolium rings.[57, 75, 76] The final degradation step was found to be above 450 °C temperature which is representing to the main chain decomposition of the AAEMs. Among all the samples poly(alkylated pyridinium benzimidazolium) hydroxide membranes exhibit higher thermal stability than their corresponding iodide form membranes. Thermal stability depends on the counter ion nucleophilic strength. Because of the lower nucliophilic strength of the hydroxide ions, membranes with hydroxide counter ion showed higher thermal stability.[77] As mentioned in the literature, the more basic counter ion causes reduction in the overall nucleophilicity of benzimidazolium ring.[59] Among all the samples isobutylated AAEMs display highest thermal stability, the reason might be less degree of isobutylation.

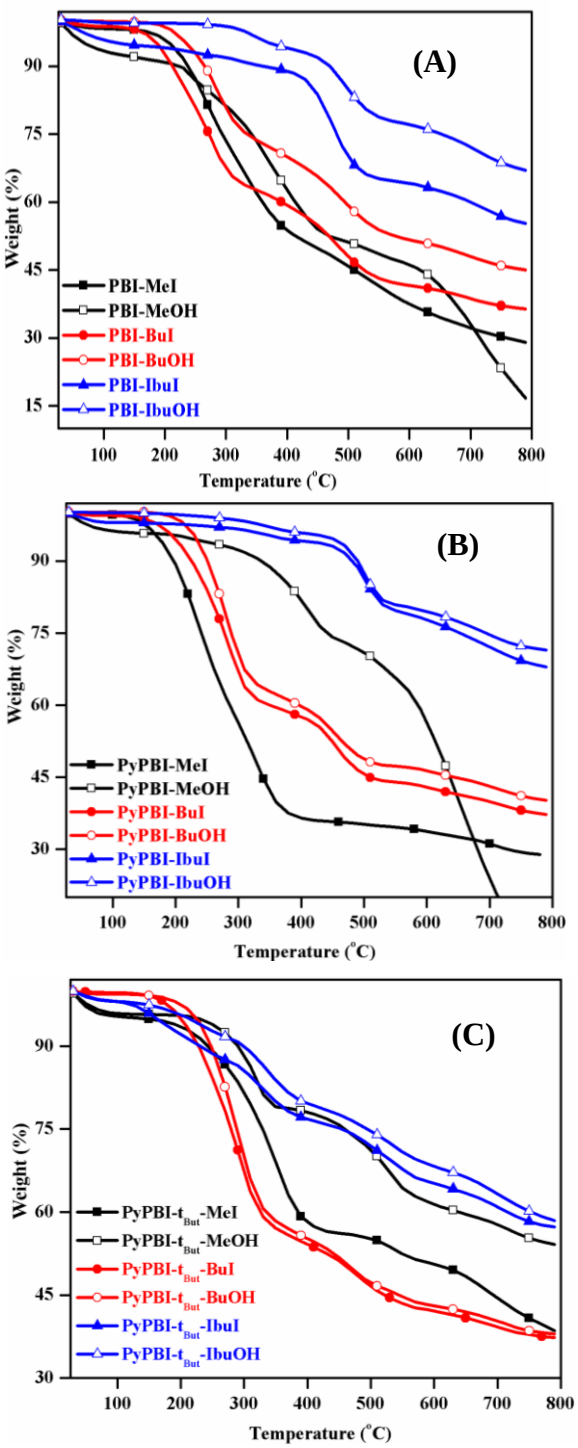

Figure 6.12. *TGA analysis of three series of poly(alkylated pyridinium benzimidazolium) membranes both in iodide (I⁻) form and hydroxide (OH⁻) form. (A) PBI, (B) PyPBI and (C) PyPBI-t$_{But}$.*

6.3.6. Tensile properties

The tensile properties of the poly(alkylated pyridinium benzimidazolium) iodide (I^-) and hydroxide (OH^-) AEMs are shown in Figure 6.13. The tensile strength and yield strain values obtained from the plots of all the polymer membranes are listed in Table 6.4. In all the AEMs, the iodide form membranes display slightly higher tensile properties than that of hydroxide (OH^-) form membranes (Table 6.4 and Figure 6.13). Also isobutylated samples (both in I^- and OH^- forms) show better tensile properties than butylated samples in all these series of polymers. The reason for this may be attributed to the structure of alkyl chain. The other reason could be due to the lower degree of alkylation in case isobutylated polymers than the butylated polymers. Since in the former case some of the unalkylated imidazole groups having proton donor (-NH-) and proton acceptor (-N=) active sites may form hydrogen bonding interaction between polymer chains which might resulted increased mechanical strength. The PyPBI-t_{But} isobutylated AEMs shows better tensile strength and strain when compared to the PBI and PyPBI isobutylated AEMs. This could be due to the additionally introduced bulky tertiary butyl group on the aromatic ring of the polymer which in turn causing intermolecular interactions. Overall, the tensile stability of these membranes could be useful in making these membranes in the development of AAEMs.

Table 6.4. Tensile strength and yield strain data of all the AAEMs (I^- and OH^- form) obtained from the tensile measurement.

Sample	Tensile strength (MPa)	Yield Strain
PBI-BuI	45.67	5.77
PBI-BuOH	27.70	4.38
PBI-IbuI	78.70	7.75
PBI-IbuOH	60.00	7.29
PyPBI-BuI	45.01	4.65
PyPBI-BuOH	39.36	4.53
PyPBI-IbuI	76.19	5.43
PyPBI-IbuOH	65.48	4.31
PyPBI-t_{But}-IbuI	34.98	2.62
PyPBI-t_{But}-IbuOH	29.95	1.98

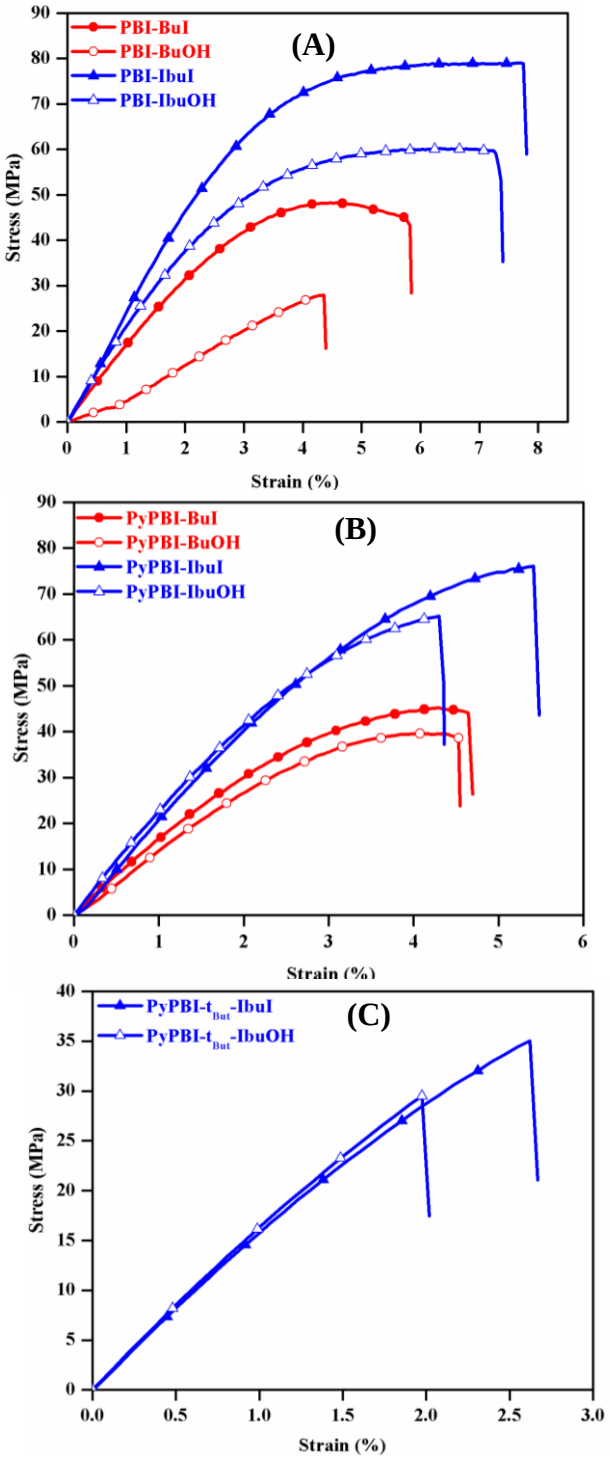

Figure 6.13. *Stress-strain plots of all the AEMs (both I⁻and OH⁻ forms) obtained from tensile study: (A) PBI, (B) PyPBI and (C) PyPBI-t_{But}*

6.3.7. Thermo mechanical studies

Temperature dependent dynamic mechanical properties of the poly(alkylated pyridinium benzimidazolium) iodide (I^-) and hydroxide (OH^-) AEMs were measured by using the dynamic mechanical analyser (DMA). Temperature dependent storage modulus (E') plots of all the AAEMs are given in Figure 6.14 which clearly suggests that mechanical strength of the membrane becomes poorer at higher temperatures. Alkylated PBI polymers show higher storage modulus when compared to alkylated PyPBI and PyPBI-t_{But} polymer membranes which may be attributed to interchain distance between the polymer chains. Storage modulus of the hydroxide form membranes is similar or comparable to their corresponding iodide form membranes in each set of the polymers. This observation could also explain the membrane stability towards alkaline condition. Isobutylated AEMs shows higher mechanical strength than the butylated polymers. The reason might be due to the isobutylated polymers have lower degree of alkylation. The similar observation identified in TGA studies and tensile properties. The KOH doped methylated AEMs having brittle nature, so we could not perform DMA study.

Loss modulus (E'') and tan δ plots of all the three series of AEMs are presented in the Figure 6.15 and 6.16, respectively. Glass transition temperature (T_g) of all the AEMs are summarised in the Table 6.5. In general, depending on the polymer structure T_g of PBI varies from 350-450 °C. In this work, we observed that the hydroxide form membrane T_g values are higher than their corresponding iodide form AEMs. This may be due to different counter ion, It is also observed that T_g values decreases increase in the bulky nature of the alkyl group. The alkylated polymers T_g values order is as follows methylated > butylated > isobutylated which is similar to degree of alkylation.

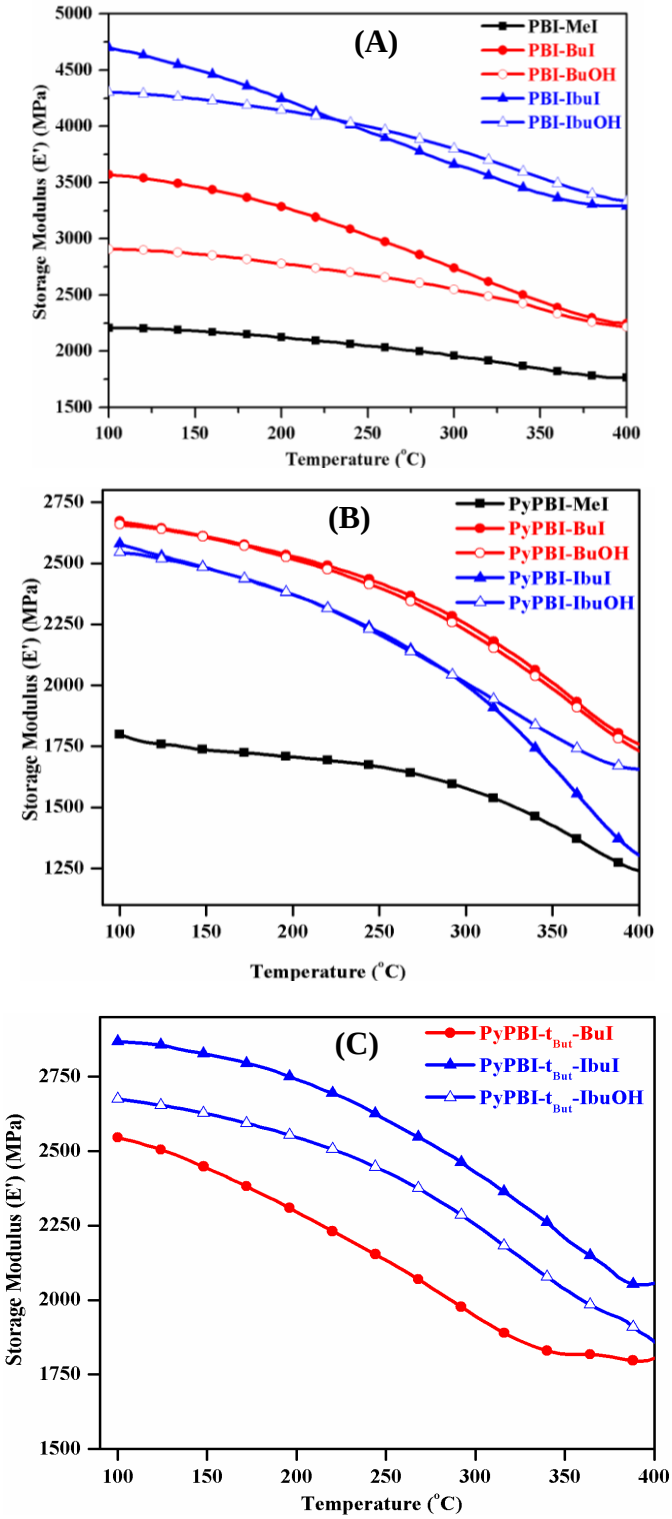

Figure 6.14. *Storage modulus (E') of all the AAEMs obtained from DMA instrument. (A) PBI, (B) PyPBI and (C) PyPBI-$t_{But.}$*

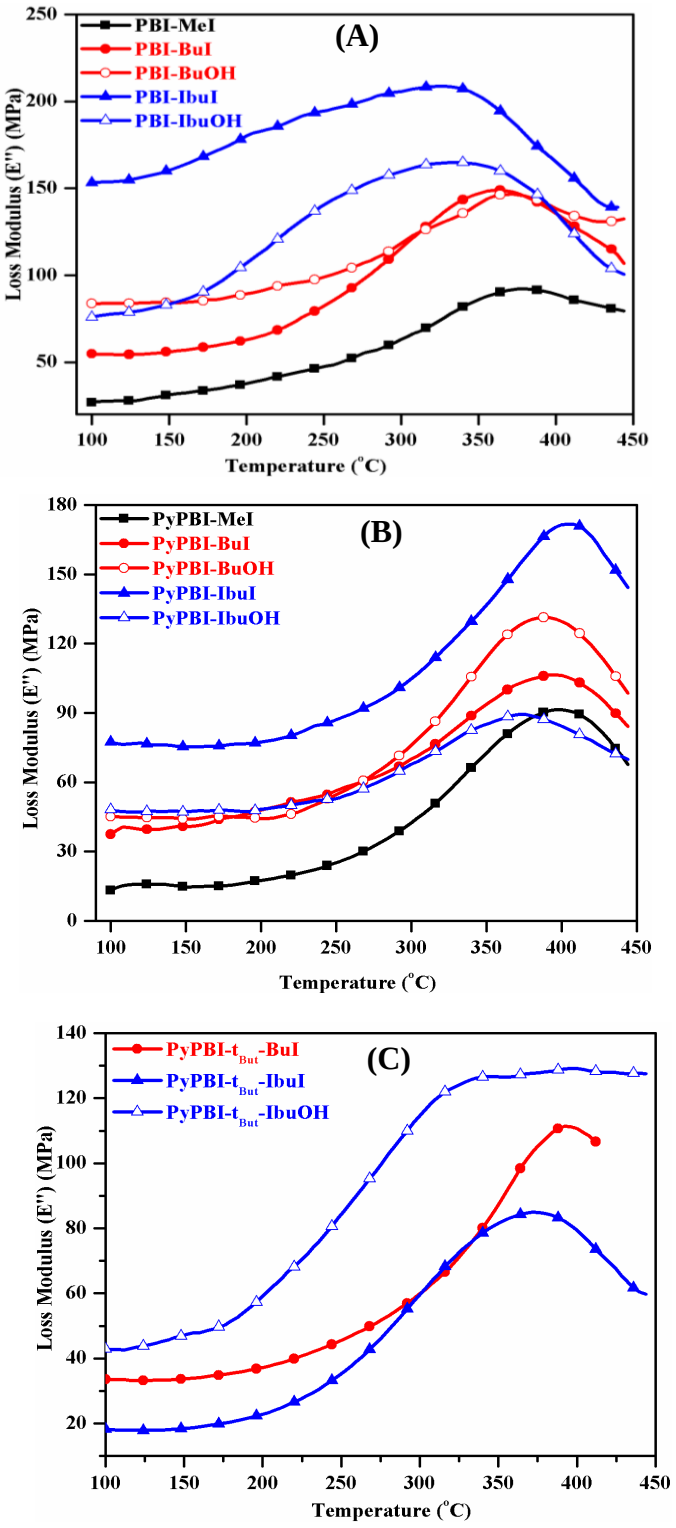

Figure 6.15. *Loss modulus (E˝) of all the three series of poly (alkylated pyridinium benzimidazolium) AEMs. (A) PBI, (B) PyPBI and (C) PyPBI-$t_{But.}$*

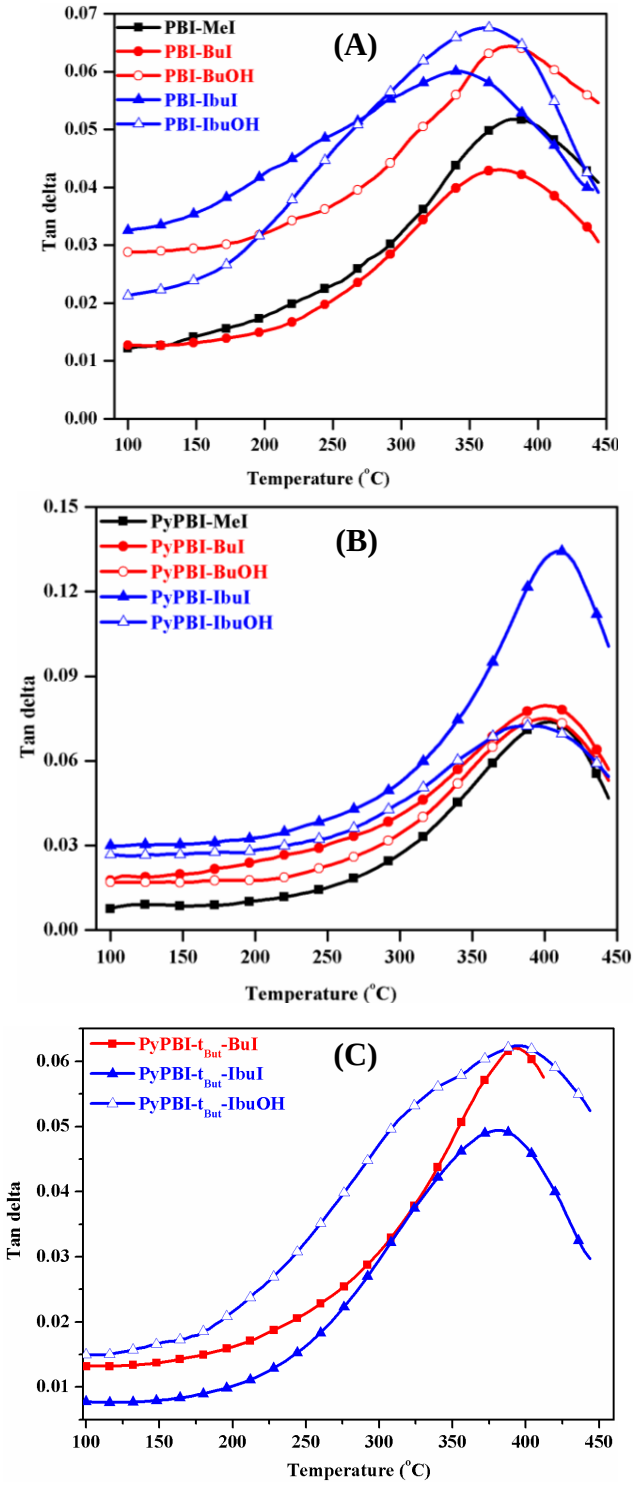

Figure 6.16. *Tan δ plots Loss modulus (E¨) of all the three series of poly (alkylated pyridinium benzimidazolium) AEMs. (A) PBI, (B) PyPBI and (C) PyPBI-t$_{But.}$*

Table 6.5. *Glass transition temperatures data of all the AEMs obtained from DMA instrument.*

Sample name	*T_g (°C) from E"*	*T_g (°C) from tan δ*
PBI-MeI	378	385
PBI-BuI	360	370
PBI-BuOH	372	380
PBI-IbuI	331	343
PBI-IbuOH	341	366
PyPBI-MeI	403	408
PyPBI-BuI	392	403
PyPBI-BuOH	390	403
PyPBI-IbuI	382	409
PyPBI-IbuOH	400	403
PyPBI-t_{But}-BuI	393	395
PyPBI-t_{But} -IbuI	373	380
PyPBI-t_{But} -IbuOH	390	398

6.4. CONCLUSION

Three types of polybenzimidazoles: PBIs, PyPBIs and Tertiary butyl PyPBIs) have been synthesized and used to prepare poly(alkylated pyridinium benzimidazolium) iodides by varying different alkyl iodides. Iodide form membranes are made by dissolving the polymers in DMSO solvent. All the iodide form membranes were converted into the hydroxide ion form by treating with 1 M KOH solution. FT-IR and ^{1}H NMR spectroscopic studies are used to confirm structure of the iodide and hydroxide form membranes. The degree of alkylation is calculated from the ^{1}HNMR spectra. All the methylated AEMs are less stable under alkaline condition but butylated and isobutylated AEMs exhibits excellent alkaline stability and display excellent IEC, ionic

conductivities. The butylated and isobutylated AEMs are found to be highly ionically conducting and hence they are promising candidate for the use as alkaline anion exchange membranes.

REFERENCES

[1] Noto, V. D.; Negro, E.; Sanchez, J.-Y.; Iojoiu, C. *J. Am. Chem. Soc.* **2010**, *132*, 2183.

[2] Gu, F.; Dong, H.; Li, Y.; Sun, Z.; Yan, F. *Macromolecules* **2014**, *47*, 6740.

[3] He, G.; Li, Z.; Zhao, J.; Wang, S.; Wu, H.; Guiver, M. D.; Jiang, Z. *Adv. Mater.* **2015**, *27*, 5280.

[4] Wu, H.; Jia, W.; Liu, Y. *J Mater Sci* **2017**, *52*, 1704.

[5] Merle, G.; Wessling, M.; Nijmeijer, K. *J. Membr. Sci.* **2011**, *377*, 1.

[6] Mohanty, A. D.; Tignor, S. E.; Krause, J. A.; Choe, Y. K.; Bae, C. *Macromolecules* **2016**, *49*, 3361.

[7] Oshiba, Y.; Hiura, J.; Suzuki, Y.; Yamaguchi, T. *J. Power Sources* **2017**, *345*, 221.

[8] Dong, X.; Xue, B.; Qian, H.; Zheng, J.; Li, S.; Zhang, S. *J. Power Sources* **2017**, *342*, 605.

[9] Mohanty, A. D.; Bae, C. *J. Mater. Chem. A* **2014**, *2*, 17314.

[10] Lin, B.; Qiu, L.; Qiu, B.; Peng, Y.; Yan, F. *Macromolecules* **2011**, *44*, 9642.

[11] Tanaka, M.; Fukasawa, K.; Nishino, E.; Yamaguchi, S.; Yamada, K.; Tanaka, H.; Bae, B.; Miyatake, K.; Watanabe, M. *J. Am. Chem. Soc.* **2011**, *133*, 10646.

[12] Lu, Z. Y.; Xu, W. W.; Ma, J.; Li, Y. J.; Sun, X. M.; Jiang, L. *Adv. Mater.* **2016**, *28*, 7155.

[13] Sa, Y. J.; Park, C.; Jeong, H. Y.; Park, S. H.; Lee, Z.; Kim, K. T.; Park, G. G.; Joo, S. H. *Angew. Chem., Int. Ed.* **2014**, *53*, 4102.

[14] Lan, R.; Tao, S. *J. Power Sources* **2011**, *196*, 5021.

[15] Z. B. Zhuang, S. A. Giles, J. Zheng, G. R. Jenness, S. Caratzoulas, D. G. Vlachos, Y. S. Yan, Nat. Commun. 7 (2016).

[16] Si, Z.; Sun, Z.; Gu, F.; Qiu, L.; Yan, F. *J. Mater. Chem. A* **2014**, *2*, 4413.

[17] Hugar, K. M.; Kostalik, H. A., IV; Coates, G. W. *J. Am. Chem. Soc.* **2015**, *137*, 8730.

[18] Han, J.; Liu, Q.; Li, X.; Pan, J.; Wei, L.; Wu, Y.; Peng, H.; Wang, Y.; Li, G.; Chen, C.; Xiao, L.; Lu, J.; Zhuang, L. *ACS Appl. Mater. Interfaces* **2015**, *7*, 2809.

[19] Liu, G. S.; Shang, Y. M.; Xie, X. F.; Wang, S. B.; Wang, J. H.; Wang, Y. W.; Mao, Z. Q. *Int. J. Hydrogen Energy* **2012**, *37*, 848.

[20] Xu, S.; Zhang, G.; Zhang, Y.; Zhao, C. J.; Ma, W. J.; Sun, H. C.;Zhang, N.; Zhang, L. Y.; Jiang, H.; Na, H. *J. Power Sources* **2012**, *209*, 228.

[21] Rao, A. H. N.; Kim, H. J.; Nam, S.; Kim, T. H. *Polymer* **2013**, *54*, 6918.

[22] Chen, C.; Pan, J.; Han, J.; Wang, Y.; Zhu, L.; Hickner, M. A.;Zhuang, L. *J. Mater. Chem. A* **2016**, *4*, 4071.

[23] Jasti, A.; Prakash, S.; Shahi, V. K. *J. Membr. Sci.* **2013**, *428*,470.

[24] Xia, Z. J.; Yuan, S.; Jiang, G. P.; Guo, X. X.; Fang, J. H.; Liu, L.L.; Qiao, J. L.; Yin, J. *J. Membr. Sci.* **2012**, *390-391*, 152.

[25] Zhang, M.; Kim, H. K.; Chalkova, E.; Mark, F.; Lvov, S. N.;Chung, T. C. M. *Macromolecules* **2011**, *44*, 5937.

[26] Li, Y. F.; Liu, Y.; Savage, A. M.; Beyer, F. L.; Seifert, S.; Herring,A. M.; Knauss, D. M. *Macromolecules* **2015**, *48*, 6523.

[27] Vengatesan, S.; Santhi, S.; Sozhan, G.; Ravichandran, S.; Davidson, D. J.; Vasudevan, S. *RSC Adv.* **2015**, *5*, 27365.

[28] Zhu, L.; Pan, J.; Christensen, C. M.; Hickner, M. A. *Macromolecules* **2016**, *49*, 3300.

[29] Zhu, L.; Zimudzi, T. J.; Li, N.; Pan, J.; Lin, B.; Hickner, M. A. *Polym. Chem.* **2016**, *7*, 2464.

[30] Pan, J.; Zhu, L.; Han, J.; Hickner, M. A. *Chem. Mater.* **2015**, *27*, 6689.

[31] Li, N.; Leng, Y.; Hickner, M. A.; Wang, C.-Y. *J. Am. Chem. Soc.* **2013**, *135*, 10124.

[32] Vengatesan, S.; Santhi, S.; Jeevanantham, S.; Sozhan, G. *J. Power Sources* **2015**, *284*, 361.

[33] Jheng, L.C.; Tai, C.K.; Hsu, S.L. C.; Lin, B. Y.; Chen, L.; Wang, B. C.; Chiang, L. K.; Ko, W.C. *Int. J. Hydrogen Energy* **2017**, *42*, 5315.

[34] Varcoe, J. R.; Slade, R. C.; Yee, E. L. H. *Chem. Commun.* **2006**, *13*, 1428.

[35] Dai, P.; Mo, Z. H.; Xu, R. W.; Zhang, S.; Wu, Y. X. *ACS Appl. Mater. Interfaces* **2016**, *8*, 20329.

[36] Zhu, L.; Zimudzi, T. J.; Wang, Y.; Yu, X.; Pan, J.; Han, J.; Kushner, D. I.; Zhuang, L.; Hickner, M. A. *Macromolecules* **2017**, *50*, 2329.

[37] Guo, D.; Lai, A. N.; Lin, C. X.; Zhang, Q. G.; Zhu, A. M.; Liu, Q. L. *ACS Appl. Mater. Interfaces* **2016**, *8*, 25279.

[38] Weissbach, T.; Wright, A. G.; Peckham, T. J.; SadeghiAlavijeh, A.; Pan, V.; Kjeang, E.; Holdcroft, S. *Chem. Mater.*, **2016**, *28*, 8060.

[39] Gu, S.; Cai, R.; Luo, T.; Chen, Z. W.; Sun, M. W.; Liu, Y.; He, G. H.; Yan, Y. *Angew. Chem., Int. Ed.* **2009**, *48*, 6499.

[40] Zhang, B.; Gu, S.; Wang, J.; Liu, Y.; Herring, A. M.; Yan, Y. *RSC Adv.* **2012**, *2*, 12683.

[41] Zhang, Q.; Li, S.; Zhang, S. *Chem. Commun.* **2010**, *46*, 7495.

[42] Choi, Y.-J.; Park, J.-M.; Yeon, K.-H.; Moon, S.-H. *J. Membr. Sci.* **2005**, *250*, 295.

[43] Dö bbelin, M.; Azcune, I.; Bedu, M.; Ruiz de Luzuriaga, A.; Genua, A.; Jovanovski, V.; Cabañ ero, G.; Odriozola, I. *Chem. Mater.* **2012**, *24*, 1583.

[44] Qu, C.; Zhang, H.; Zhang, F.; Liu, B. *J. Mater. Chem.* **2012**, *22*, 8203.

[45] Li, X.; Yu, Y.; Liu, Q.; Meng, Y. *Int. J. Hydrogen Energy* **2013,** *38*, 11067.

[46] Guo, M.; Fang, J.; Xu, H.; Li, W.; Lu, X.; Lan, C.; Li, K. *J. Membr. Sci.* **2010**, *362*, 97.

[47] Lin, B.; Dong, H.; Li, Y.; Si, Z.; Gu, F.; Yan, F. *Chem. Mater.* **2013**, *25*, 1858.

[48] Henkensmeier, D.; Cho, H.-R.; Kim, H.-J.; Nunes Kirchner, C.; Leppin, J.; Dyck, A.; Jang, J. H.; Cho, E.; Nam, S.-W.; Lim, T.-H. *Polym. Degrad. Stab.* **2012**, *97*, 264.

[49] Maity, S.; Jana, T. *Macromolecules* **2013**, *46*, 6814.

[50] Thomas, O. D.; Soo, K. J. W. Y.; Peckham, T. J.; Kulkarni, M. P.; Holdcroft, S. *J. Am. Chem. Soc.* **2012**, *134*, 10753.

[51] Chen, D.; Hickner, M. A. *ACS Appl. Mater. Interfaces* **2012**, *4*, 5775.

[52] Ghosh, S.; Sannigrahi, A.; Maity, S.; Jana, T. *J. Phys. Chem. C* **2011**, *115*, 11474.

[53] Kannan, R.; Kagaiwale, H. N.; Chaudhari, H. D.; Kharul, U. K.; Kurungot, S.; Pillai, V. K. *J. Mater. Chem.* **2011**, *21*, 7223.

[54] Ghosh, S.; Sannigrahi, A.; Maity, S.; Jana, T. *J. Mater. Chem*. **2011**, *21*, 14897.

[55] Hazarika, M.; Jana, T. *ACS Appl. Mater. Interfaces* **2012**, *4*, 5256.

[56] Chung, S.-W.; Hsu, S. L.-C.; Liu, Y.-H. *J. Membr. Sci*. **2007**, *305*, 353.

[57] Li, W.; Fang, J.; Lv, M.; Chen, C.; Chi, X.; Yang, Y.; Zhang, Y. *J. Mater. Chem.* **2011**, *21*, 11340.

[58] Chen, Y.; Tao, Y.; Wang, J.; Yang, S.; Cheng, S.; Wei, H.; Ding, Y. *J. Polym. Sci., Part A: Polym. Chem.* **2017**, *55*, 1313.

[59] Henkensmeier, D.; Kim, H.-J.; Lee, H.-J.; Lee, D. H.; Oh, I.-H.; Hong, S.-A.; Nam, S.-W.; Lim, T.-H. *Macromol. Mater. Eng.* **2011**, *296*, 899.

[60] Thomas, O. D.; Soo, K. J. W. Y.; Peckham, T. J.; Kulkarni, M. P.; Holdcroft, S. *Polym. Chem.* **2011**, *2*, 1641.

[61] Ye, Y.; Elabd, Y. A. *Macromolecules* **2011**, *44*, 8494.

[62] Meek, K. M.; Elabd, Y. A. *Macromolecules* **2015**, *48*, 7071.

[63] Price, S. C.; Williams, K. S.; Beyer, F. L. *ACS Macro Lett.* **2014**, *3*, 160.

[64] Hu, J.; Wan, D.; Zhu, W.; Huang, L.; Tan, S.; Cai, X.; Zhang, X. *ACS Appl. Mater. Interfaces* **2014**, *6*, 4720.

[65] Jheng, L. C.; Hsu, S. L. C.; Lin, B. Y.; Hsu, Y. L. *Journal of Membrane Science*, **2014**, *460*, 160.

[66] Dong, H.; Li, Y.; Si, Z.; Gu, F.; Yan, F. *Macromolecules* **2014**, *47*, 208.

[67] Ertem, S. P.; Tsai, T. H.; Donahue, M. M.; Zhang, W. X.; Sarode, H.; Liu, Y.; Seifert, S.; Herring, A. M.; Coughlin, E. B. *Macromolecules* **2016**, *49*, 153.

[68] Varcoe, J. R.; Atanassov, P.; Dekel, D. R.; Herring, A. M.; Hickner, M. A.; Kohl, P. A.; Kucernak, A. R.; Mustain, W. E.; Nijmeijer, K.; Scott, K.; Xu, T.; Zhuang, L. *Energy Environ. Sci.* **2014**, *7*, 3135.

[69] Yan, L.; Hickner, M. A. *Macromolecules* **2010**, *43*, 2349.

[70] Zha, Y.; Disabb-Miller, M. L.; Johnson, Z. D.; Hickner, M. A.; Tew, G. N. *J. Am. Chem. Soc*. **2012**, *134*, 4493.

[71] Li, X.; Yu, Y.; Liu, Q.; Meng, Y. *Int. J. Hydrogen Energy* **2013**, *38*, 11067.

[72] Huang, A. B.; Xia, C. Y.; Xiao, C. B.; Zhuang, L. *Int. J. Hydrogen Energy* **2006**, *100*, 2248.

[73] Wang, J.; Li, S.; Zhang, S. *Macromolecules* **2010**, *43*, 3890.

[74] Gu, S.; Cai., R.; Yan, Y. *Chem. Commun.* **2011**, *47*, 2856.

[75] Zarrin, H.; Jiang, G.; Lam, G. Y.-Y.; Fowler, M.; Chen, Z. *Int. J. Hydrogen Energy* **2014**, *39*, 18405.

[76] Zhang, F.; Zhang, H.; Qu, C. *J. Mater. Chem.* **2011**, *21*, 12744.

[77] Lee, H. J.; Choi, J.; Han, J. Y.; Kim, H. J.; Sung, Y. E.; Kim, H. *Polym. Bull.* **2013**, *70*, 2619.

[78] Zarrin, H.; Jiang, G.; Lam, G. Y.-Y.; Fowler, M.; Chen, Z. *Int. J. Hydrogen Energy* **2014**, *39*, 18405.

Chapter 7

Alkaline stable anion exchange membranes developed from the cross-linked polybenzimidazoles

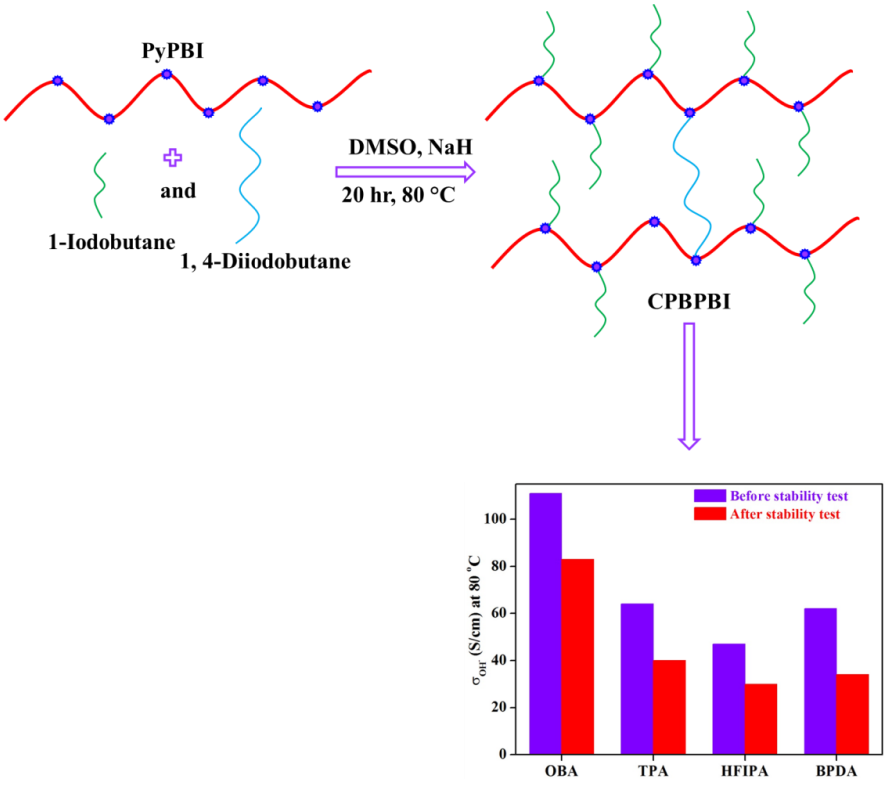

In this chapter, we have developed series of cross-linked poly(butylated pyridinium benzimidazolium) iodides (CPBPBI) polymers and then studied the required properties to find their suitability as alkaline anion exchange membranes (AAEMs).

Sana, B.; Jana, T. (Manuscript under preparation)

7.1. INTRODUCTION

Recently, many research groups have started to focus on developing the alkaline anion exchange membranes (AAEMs) for the use in fuel cell.[1-3] AAEMs are constituted to provide enough hydroxyl ions for ion exchange during electrochemical reactions in fuel cells. This kind of cells has more advantages in cost and operation reliability over the proton exchange membrane fuel cell.

As key components in alkaline anion exchange membrane fuel cells (AEMFCs), usually different kind of AAEMs with rigid backbone structures such as poly(ether ketones),[4-6] polysulfone,[7-9] poly(phenylene),[10] polystyrene,[11–13] and poly(phenylene oxide),[14–17] have been reported in the past years. However, all these AAEMs showed insufficient ionic conductivity and chemical (alkaline) stability. A typical AAEM is composed of a polymer main chain with tethered cation ionic-exchange groups such as quaternary ammonium (QA),[18] imidazolium,[19] benzimidazolium,[20] pyridinum,[21] phosphonium,[22] guanidinium,[23] and pyrrolidinium[24] to facilitate the loading of free hydroxyl ions. The AAEMs are predominantly based on QA cationic species pendant to a polymer main chain. The stability of QA cationic species is often poor under more basic conditions. Thus, the performance of those polymers are rather poor and displayed a rapid degradation with time.[25] To overcome all these drawbacks, it is essential to discover new membrane and explore positively charged polymers like poly(benzimidazolium) based analogues that may fulfill the potential performance and chemical stability. Recently, Henkensmeier *et al.*, reported the methylation of poly(benzimidazolium) polymer, but in that case the chemical stability under alkaline solution was not upto the mark.[26] Holdcroft *et al.*, reported that the mesitylene-poly(dimethyl benzimidazolium) hydroxide (Mes-PDMBI-OH^-) polymer membrane showed no degradation in 2 M KOH solution at 60 °C, because of the sterically crowded mesitytene group which protected the C2 position against hydroxide (OH^-) attack. But the problem associated with this approach was the easy solubility of the polymer in water.[27]

To address all these above problems, in this study, cross-linked poly(butylated pyridinium benzimidazolium) iodide (CPBPBI) is proposed in which the cross-linker increases the alkaline stability of the AAEM. Here, we have used a simple alkylation method and did not use the chloromethylation method in which it is very difficult to control the degree of methylation. The selected polymers in this which are having pyridinium and benzimidazolium ion exchange sites, which are useful for increasing hydroxide ionic conductivity and IEC. Apart from that we have studied the IEC, FT-IR spectra, ^{1}HNMR spectra and ionic conductivity data of the AAEMs and are compared the results before and after the alkaline treatment.

7.2. EXPERIMENTAL SECTION

Details of the materials and characterization methods used in this study are included in the Chapter 2. Synthesis of PyPBI polymers described in the Chapter 5, Synthesis of iodide polymers, membrane formation method and anion exchange reaction are described below.

7.2.1. Synthesis of cross-linked poly(butylated pyridinium benzimidazolium) iodides (CPBPBI)

1.0 g of PyPBI-OBA (for structure see the Scheme 5.1 and Scheme 7.1) polymer was dissolved in 60 mL of dry DMSO solvent at 80 °C in a 100 mL round bottom flask fitted with a reflux condenser. After dissolution, the polymer solution was cool down to room temperature. At this condition, sodium hydride (3.6 mmol, 0.0867g) was added to the reaction mixture and again increased the temperature to 80 °C. The solution was stirred for overnight. Once to this reaction mixture butyl iodide (BuI) (7.233 mmol, 0.823 mL) was added and continued the stirring for 4 h at 80 °C. After that 1, 4-diiodobutane (1,4 DIB 0.904 mmol, 0.124 mL) was added to this solution and continued the stirring for 16 h. After completion of this period, the reaction mixture was poured into the water and a reddish brown colored precipitation was observed. The precipitate was filtered off and washed thoroughly with deionized water for the removal of excess

butyl iodide and 1, 4-diiodobutane (1,4 DIB). The polymer was dried under vacuum oven at 80 °C for 24 h. The reddish brown coloured cross-linked poly(butylated pyridinium benzimidazolium) iodide (CPBPBI-OBA) polymer was obtained and stored in desiccator for further characterization. The reaction scheme is presented in scheme 7.1.

The other four polymer structures of cross-linked poly(butylated pyridinium benzimidazolium) iodides (CPBPBI-IPA, CPBPBI-TPA, CPBPBI-HFIPA and CPBPBI-BPDA) (Scheme 7.1) were synthesized following the same procedure as mentioned above.[27]

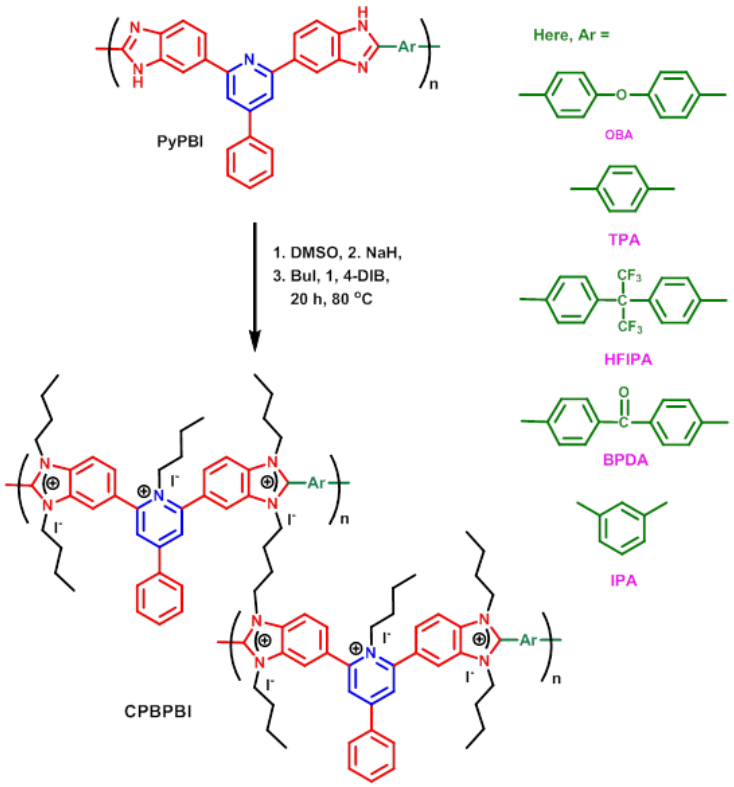

Scheme 7.1. *Synthesis of cross-linked poly(butylated pyridinium benzimidazolium) iodides (CPBPBI)*

7.2.2. Membrane fabrication and anion exchange reaction

A 1% (w/v) polymer solution was prepared by dissolving the iodide form polymer

in DMSO solvent over a period of 24 h stirring at room temperature. The obtained clear solution was then poured into a clean flat glass petridish, followed by the solvent evaporation in a hot air oven at 85 °C for 10-12 h. After this period, the dried membrane was peeled off from the glass petridish and was soaked in boiled water to remove the trace amount of residual solvent. The membranes were dried in a vacuum oven at 100 °C for 24 h. All the membranes were mechanically stronger except CPBPBI-IPA which was brittle in nature.

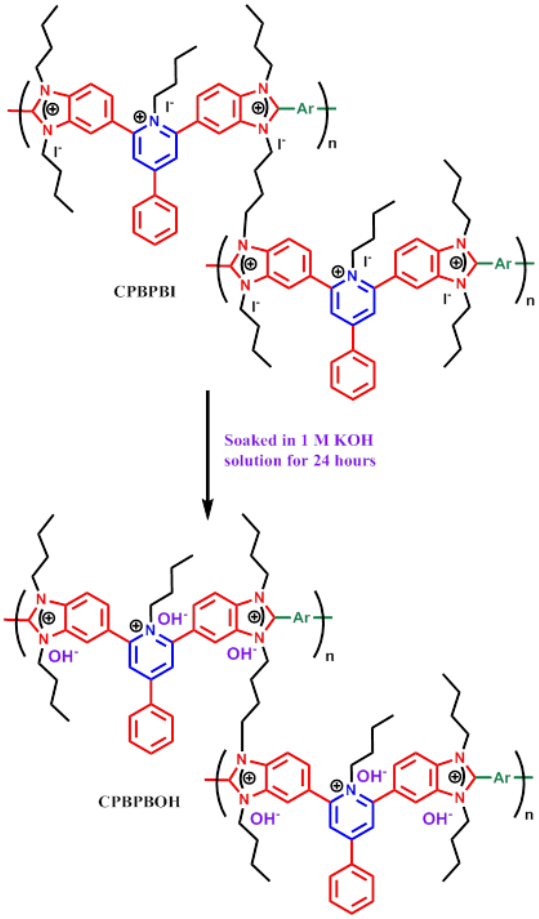

Scheme 7.2. *Anion exchange reaction of cross-linked poly(butylated pyridinium benzimidazolium) iodide (I⁻) form membrane converted into hydroxide (OH⁻) form membrane.*

The above prepared five cross-linked poly(butylated pyridinium benzimidazolium) iodide (CPBPBI) membranes were immersed in aqueous 1 M KOH,

solutions at ambient temperature for 24 h to convert them from iodide (I^-) to hydroxide (OH^-) form named as CPBPBOH. Then, the hydroxide ion membranes were washed thoroughly with deionized water to remove excess basic counter ions from the surface of the membranes. These membranes were soaked in deionized water for 24 h prior to analysis. The whole procedure of anion exchange reaction is shown in Scheme 7.2.

7.3. RESULTS AND DISCUSSIONS

7.3.1. Polymer synthesis and spectroscopy studies

Cross-linked poly(butylated pyridinium benzimidazolium) iodides (CPBPBI) were synthesized from pyridine bridged polybenzimidazoles as represented in Scheme 7.1. All the five different polymer structures names are represented as CPBPBI-OBA, CPBPBI-TPA, CPBPBI-HFIPA, CPBPBI-BPDA and CPBPBI-IPA. The obtained polymeric membranes were characterized by using different analytical techniques. The chemical structures of CPBPBI polymers are confirmed by ^{1}HNMR and FT-IR spectroscopy studies. The proton NMR spectra of the CPBPBI polymers are displayed in the Figure 7.1. The structure of iodide form polymer and peak assignments are represented along with their corresponding spectrum. The iodide form polymer backbone peaks are coming in the aromatic region and butyl group peaks are indicated with the numbering. In all the cases imidazole protons peaks is completely disappeared and at the same time butylated proton peaks appeared as result of butylation. The aromatic proton peaks chemical shift values are observed in the range of 7.5 to 9.2 ppm. The peak resonance observed from 3.95 to 4.75 ppm are assigned as methylene group of butyl directly attached to the imidazole nitrogen atom. The proton resonance of the second and third methylene groups which are away from the nitrogen atom appeared around at 1.82 ppm and 1.23 ppm, respectively. Another peak which is methyl protons, the peak is observed around 0.81 ppm. The cross-linked butyl group proton NMR signals are very difficult to distinguish from the uncross-linked butyl groups since both of them are in the same chemical environment.

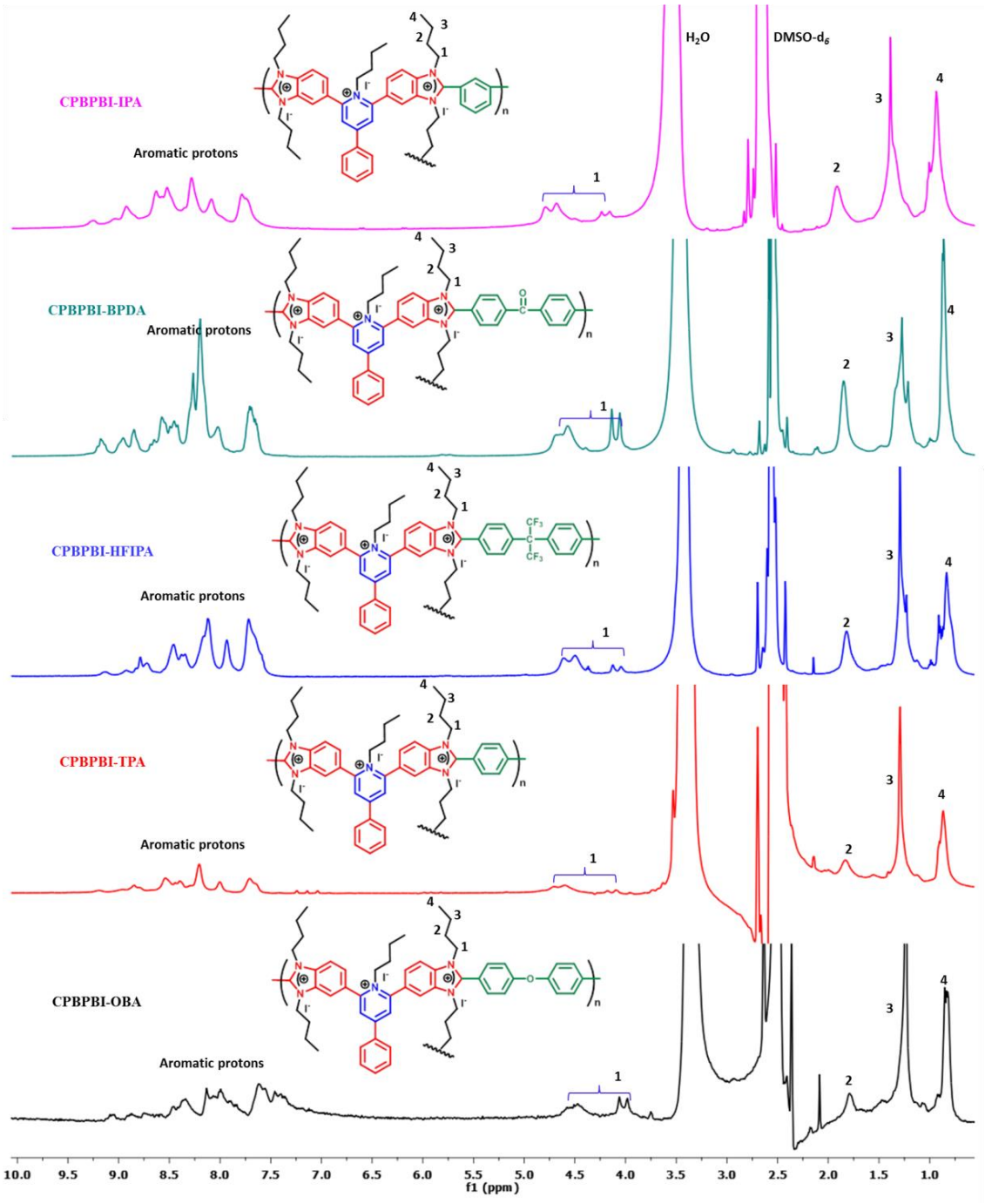

Figure 7.1. *^{1}H NMR spectra of cross-linked poly(butylated pyridinium benzimidazolium) iodide (CPBPBI) membranes.* ~~~ Implies another polymer chain with which cross-linking happened.

The FT-IR spectra of cross-linked poly(butylated pyridinium benzimidazolium) iodide polymer membranes are presented in the Figure 7.2. In the IR spectra, the peak at 3060 cm^{-1} is attributed to the stretching vibration of aromatic C-H bond and another peak observed in the range of 2982-2880 cm^{-1} is representing the vibration of the aliphatic C-H bond.[28] The aromatic pyridine ring C-H stretching frequency is observed at 830 cm^{-1}. The other desired peaks at 1600 cm^{-1} and 1477 cm^{-1} are ascribed to the stretching vibration C=C/C=N, in plane benzimidazole ring deformation, respectively.[29-32]

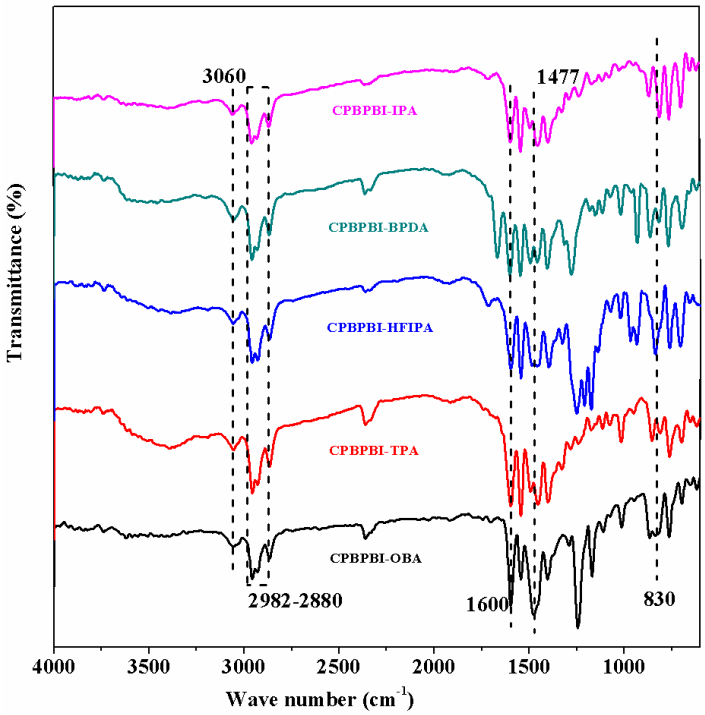

Figure 7.2. *IR spectra of all the cross-linked poly(butylated pyridinium benzimidazolium) iodide form membranes.*

7.3.2. Ion exchange capacity (IEC) and water uptake

IEC and water uptake capacity are key properties to be evaluated for checking the suitability of membrane as AAEMs. The results of ion exchange capacity (IECs) in milliequiv.g^{-1} after treatment with various concentrations (1 M and 5 M) of KOH and water uptake in percentages (%) of the CPBPBI membranes are listed in Table 7.1. The

results clearly indicate that both the IEC and water uptake highly dependent on the polymer structure. The IEC value follows the same trend as it was for uncross-linked sample as shown in Chapter 5. It must be also noted that the IEC values of the cross-linked membrane (as in this Chapter) much higher than the uncross-linked samples. The highest IEC (3.97 meq/g) is obtained in case of CPBPBI-OBA whereas the uncross-linked samples with similar structure (Chapter 5) resulted IEC value 2.57 meq/g. This may be due to the cross-linked became of the concentration of alkali by which the membranes were treated. Since the cross-linked membrane were stable so treatment was carried out using 1 M and 5 M KOH whereas in case of uncross-linked membrane with maximum 0.5 M KOH. It is worth to note that, IPA and BPDA based samples IEC could not be measured in case of uncross-linked samples (see Table 5.1 in Chapter 5). Whereas in the cross-linked samples, both IPA and BPDA polymer resulted very good IEC values (Table 7.1). This observation is kind of indirect proof of crosslinking. Unless, otherwise crosslinking happens, we could not measure IEC of many PyPBI polymeric structures. We did not find any significant variation in IEC values between 1 M and 5 M treated samples which may be due to over saturation. Again, water uptake of the sample largely alters based on the polymer structure.

Table 7.1. *The IEC and water uptake of CPBPBI anion exchange membranes.*

S.NO	Sample name	IEC (meq/g)		Water uptake (%)
		5 M KOH[#]	1 M KOH	1 M KOH
1	CPBPBI-OBA	3.28	3.97	7.77
2	CPBPBI-TPA	2.74	2.98	6.42
3	CPBPBI-HFIPA	2.18	2.30	1.43
4	CPBPBI-BPDA	2.37	2.33	2.65
5	CPBPBI-IPA	2.00	2.36	1.66

[#] this measurement was carried out after treatment of samples in 5 M KOH for 16 days.

7.3.3. Ionic conductivity

Hydroxide ionic conductivity is one of the most important properties for the AAEMs. The ionic conductivity of the AAEMs is significantly influenced by the water uptake and IEC. The ionic conductivity of the AAEMs of CPBPBI was measured after doping with 1 M KOH alkaline solutions for 24 hours. The membranes were completely hydrated in deionised water for 24 h at room temperature before measurement. The hydroxide conductivity of the AAEMs as a function of temperature is presented in Figure 7.3. The ionic conductivities of the CPBPBI are increasing with the increase in temperature as the mobility of the hydroxide ions increases with the temperature. In general, conductivity increases with increasing IEC due to an increase in the water content which enhances the local mobility of water and induced long-range ionic domain percolation.[33] Among all samples, the CPBPBOH-OBA membrane shows higher IEC (3.97 meq/g) and hence highest hydroxide conductivity is upto 111 mS/cm. In this work, all the AEMs are demonstrating excellent hydroxide conductivity which is may be due to the bulky nature of butyl and cross-linked butyl groups helped to keep the OH^- ions away from the imidazolium cations. The ionic conductivities of CPBPBI membranes have been considerably improved in contrast to the corresponding imidazolium cationic based polymeric membranes and other cationic membranes. For better understanding the results of the current study obtained values are compared with the literature data and are shown in Table 7.2. The introduction of the additional phenyl substituted pyridinium group between the two benzimidazolium moieties resulted in the enhanced conductivity. This pyridinium group can act as an anion exchange site as well, and it also helps to transport hydroxide (OH^-) ions through the AAEM along with benzimidazolium cationic sites. The AAEMs containing the pyridinium groups as cationic sites, displayed less ionic conductivity because the pyridinium groups degrades when it is in contact with oxygen at higher temperatures and part of the pyridinium groups are converted into neutral pyridone.[34, 35] In the current work, we emphasized that the pyridinium groups are employed in improving the ionic conductivity by preventing the formation of pyridone at elevated temperatures. The

pyridine moiety is blocked at 2, 4 and 6 positions by benzimidazolium moieties and phenyl groups and hence no degradation takes place.

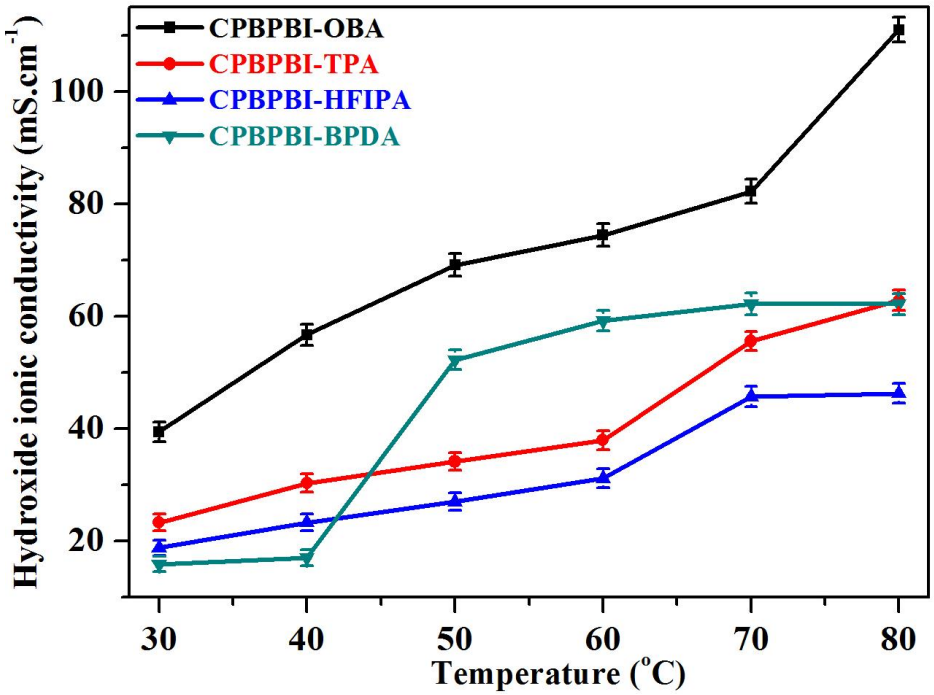

Figure 7.3. *The ionic conductivity plots of all the CPBPBI membranes doped with 1 M KOH alkaline solution.*

A comparison of OH^- conductivity of the current cross-linked membrane with uncross-linked membrane (Chapter 5) clearly indicates significant improvement in conductivity in this cross-linked case. For example the highest conductivity obtained in case of cross-linked sample at 80 °C is in case CPBPBI-OBA which shows conductivity value ~111 mS/cm. Whereas same structural polymer in uncross-linked sample resulted conductivity at 80 °C is equal to 48 mS/cm (refer Table 5.5). Similarly in all the cross-linked samples shows significant improvement. This is because of higher IEC and crosslinking.

Table 7.2. *The IEC and hydroxide ionic conductivity data of the present work and compared with reported literature data.*

Polymer backbone and reference number in the bracket	Cationic site	IEC (meq/g)	Hydroxide conductivity (mS/cm)
Present work	Im & Py	3.97	111 (80 °C)
Poly phenylene oxide based AEM with Jeffamine cross linker (3)	Am	3.21	52 (80 °C)
Cross-linked Poly phenylene oxide based AEM (14)	Am	3.59	110.2 (80 °C)
Polysulfone-based alkaline polymer electrolyte (19)	Am	2.04	108.3 (80 °C)
Quaternary ammonium polysulfone based AEM (20)	Am	1.0	100 (80 °C)
Quaternary ammonium polysulfone based polymer (21)	Am	1.18	~ 35 (65 °C)
Poly phenylene based AEM (22)	Am	1.57	50 (80 °C)
Polyphenylene oxide with long alkyl side chains (27)	Am	2.75	43 (RT)
Poly vinyl benzyl polymer with N_3 substituted imidazolium cations (54)	Im	0.97	15.8 (60 °C)

Im=Imidazolium, Py=Pyridinium and Am=Ammonium.

7.3.4. Chemical stability

The chemical stability of the AAEMs in the presence of strong basic solutions is always a crucial parameter for AAEMFC applications. In the development of AAEMs, the chemical stability under high pH alkaline solution is a major challenging issue because chemical stability effects on the ionic conductivity and cell performance.[36] We did not observe any degradation of all the CPBPBI membrane in 1 M KOH solution. In this study, we also examined the chemical stability of the CPBPBI membranes by

immersing them in 5 M aqueous KOH solutions at 80 °C for a certain period of time. All the CPBPBI membranes display excellent chemical stability with a flexible nature even after 16 days of alkaline treatment in 5 M basic (KOH) condition. There occurs a colour change from brown to light yellow during alkaline treatment in 5 M KOH solutions. We did not find any degradation except this very little color change in the current case. The very high stability of all the samples is the manifestation of crosslinking. The presence of 1, 4-diiodobutane as a cross-linker between the polymer chains makes the membrane very stable in strong alkaline condition. The bulky nature of the butyl group and cross-linker are very much helpful for prevention of attacking the hydroxide ion nucleophile on C2 position of the imidazolium moiety.

After the chemical (alkali) stability test, the CPBPBI membranes were further investigated by recording FT-IR and ^{1}H NMR spectra and measuring their IEC and OH^- conductivity. The FT-IR spectra of all the hydroxide membranes after treatment with 5 M KOH for 16 days are displayed in the Figure 7.4. For the easy of comparison, we also included the CPBPBI spectra in the figure for all the samples. The FT-IR spectra of these membranes are similar to the IR spectra of CPBPBI membranes but one very low intense new peak appeared at 3648 cm^{-1} in case of alkali treated samples. This new peak is representing the vibration of secondary amine (N-H) stretching frequency. This low intense peak for secondary amine stretching indicates that hydroxide ion (OH^-) must have attacked on C2 position of the imidazolium of moiety and the ring opening mechanism of the imidazolium moiety as shown in Scheme 5.3 may have happened to transformed into amine-amide from.[37-40] But the degree of these ring opening must be very small, therefore we are observing high stability or negligible degradation of the membranes even after 5 M KOH treatment.

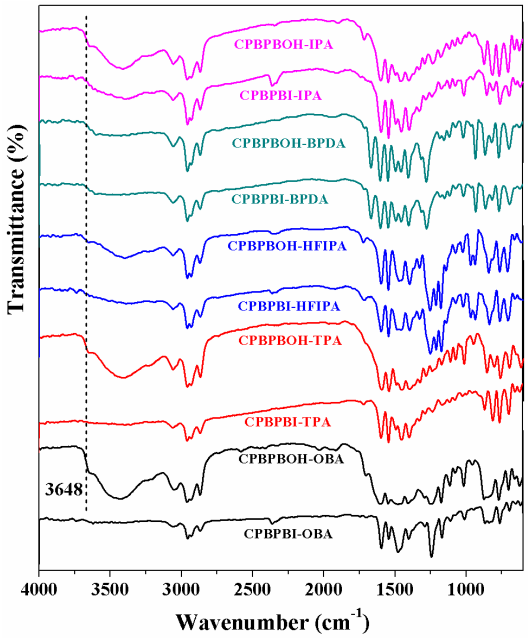

Figure 7.4. *IR spectra of all the cross-linked poly(butylated pyridinium benzimidazolium) hydroxide form membranes after alkaline stability test. i.e. after treatment with 5 M KOH for 16 days for comparison purpose CPBPBI spectra (before alkali test) are also included in the Figure for all samples.*

The alkaline stability tested samples were also investigated by the ^{1}H NMR analysis and the spectra are placed in the Figure 7.5 along with the CPBPBI sample for easy comparison. From the Figure 7.5 it is observed that both before and after treatment spectra are identical. There is no presence of any peaks which are supposed to appear if any degradation happens as shown earlier in Chapter 5 in Scheme 5.3 and Figure 5.2. This indicates almost negligible or none degradation of cross-linked membrane even after treatment with 5 M KOH for 16 days. This observation is because of the fact that the imidazolium degradation is prevented by the cross-linked butyl groups which are present between the polymer chains. The bulky nature of the long chain butyl and cross-linked butyl groups are completely insulating the imidazolium C2 carbon from the attack of OH^- ion. So both IR and NMR spectra of alkali treated samples confirmed the very negligible or none degradation of the cross-linked membranes. Finally we are suggesting that these membranes demonstrate excellent alkaline stability under high pH conditions.

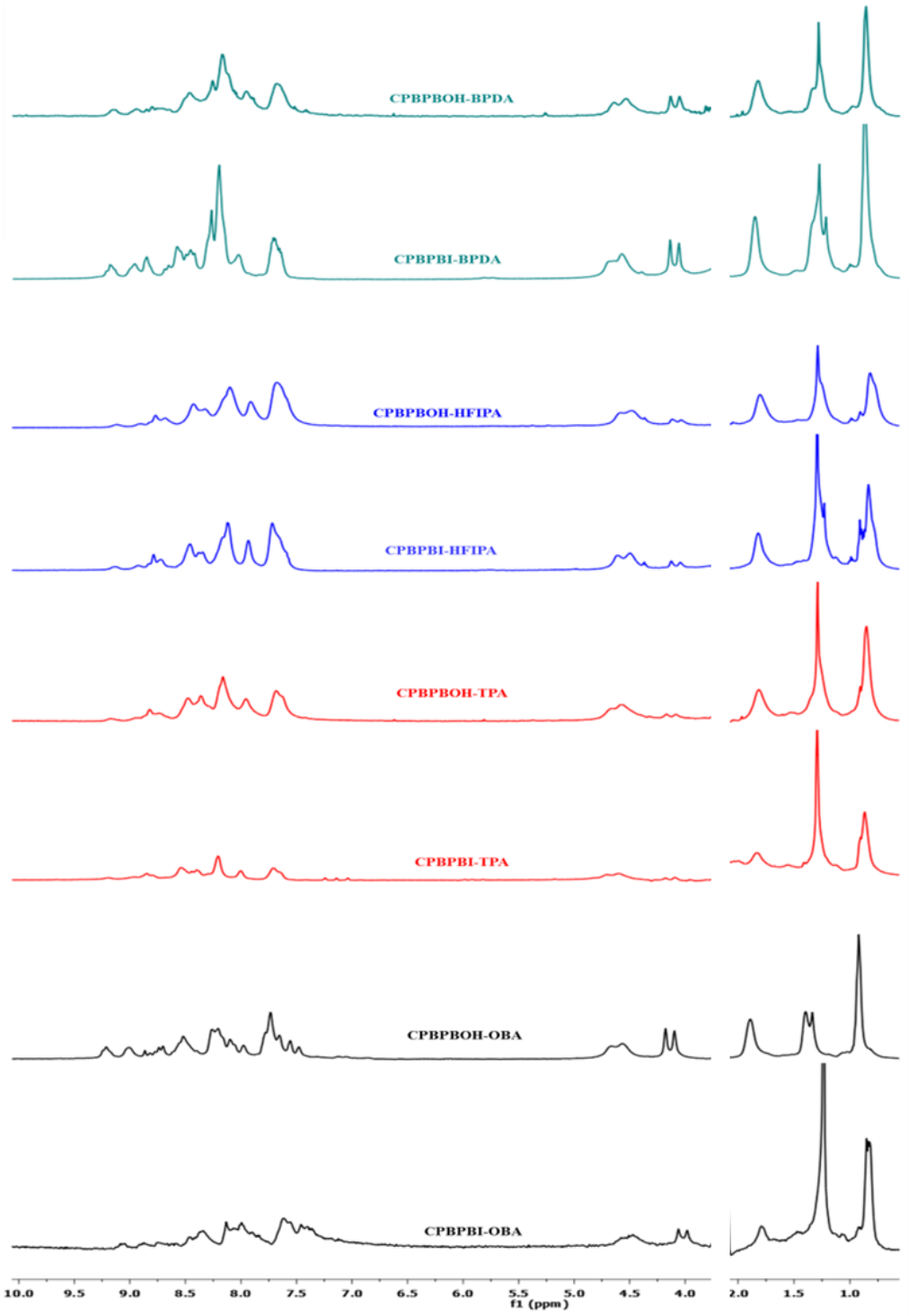

Figure 7.5. *^{1}H NMR spectra of all the hydroxide form membranes after alkaline stability test. Along with untreated CPBPBI samples for ready reference. For better clarity solvent peaks are removed.*

The IEC values were measured with chemical stability tested samples after 16 days of alkaline (5 M KOH) treatment and the results are reported in the Table 7.1. The chemical stability tested CPBPBOH membranes are showing similar IEC values with the 1 M KOH doped samples. Hence, this also confirms the stability of cross-linked membranes in 5 M KOH. To see whether the 5 M KOH treatment for 16 days alters the hydroxide conductivity or not, we measured the conductivity of all the alkali treated samples and the data are presented in Figure 7.6. As expected, the conductivity depends on the CPBPBOH structure and increases with increasing temperature. To compare the effect of alkali treatment, we have tabulated σ_{OH^-} value at 80 °C before and after alkali treatment in Table 7.3.

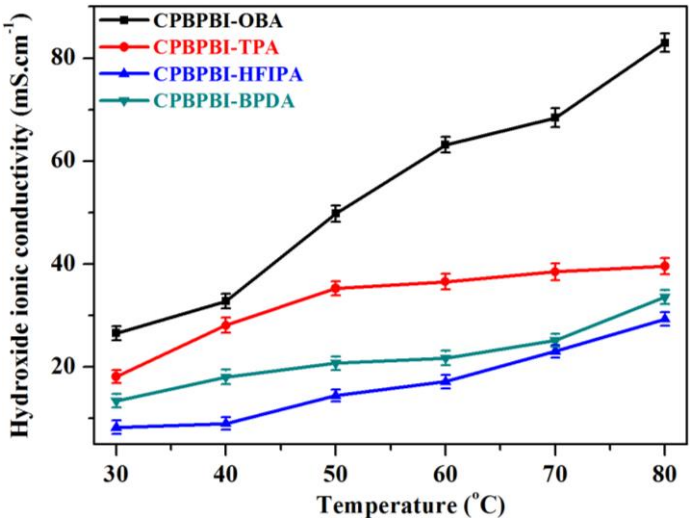

Figure 7.6. *The hydroxide conductivity as a function of temperature of all the CPBPBOH membrane after treatment with 5 M KOH for 16 days.*

The hydroxide ion (OH^-) conductivity of CPBPBOH-OBA and CPBPBOH-BPDA membranes are found to be 82.9 mS/cm and 33.6 mS/cm, respectively after alkali treatment which are to 25.3 and 45.8% less than the values measured before alkali stability test. So the σ_{OH^-} data clearly indicates a decrease in values, however, IR, NMR and IEC studies as described above could not find any degradation or negligible degradation which suggests that the reason of σ_{OH^-} decrease after alkali treatment may be some other reason which requires further investigation.

Table 7.3. *Ionic conductivities at 80 °C before and after stability test, of the CPBPBI samples.*

Sample Identity	OH^- conductivity (mS/cm) at 80 °C	OH^- conductivity (mS/cm) after stability test at 80 °C	Decrease in OH^- conductivity (%)
CPBPBOH-OBA	111	82.9	25.3
CPBPBOH-TPA	62.8	39.5	37.1
CPBPBOH-HFIPA	46.2	29.3	36.5
CPBPBOH-BPDA	62.1	33.6	45.8

7.3.5. Thermal studies

The thermal studies of the cross-linked poly(butylated pyridinium benzimidazolium) iodide and hydroxide form AEMs were investigated by the TGA analysis as shown in the Figure 7.7. All the AEMs exhibit three-steps degradation behaviour: the first step decomposition occurred below 130 °C temperature is due to the absorbed water or might be due to the DMSO as a residual solvent. The second stage decomposition occurred between 200 °C to 300 °C which is assigned to the decomposition of the imidazolium moieties.[41] The third step decomposition is obtained at 450 °C which is attributed to the degradation of the main chain polymer backbone. The decomposition temperature of the CPBPBI and CPBPBOH samples are almost similar owing to the cross-linking nature of the sample. In all the samples hydroxide form membranes demonstrating a little bit higher thermal stability due to the lower nucliophilic strength of the OH^- ions than the iodide ions since thermal stability of the AAEMs depends on the nucliophilic strength of the counter ion.[42] In the literature, it is reported that more basic counter ion causes reduction of overall nucleophilicity of benzimidazolium moiety.[43]

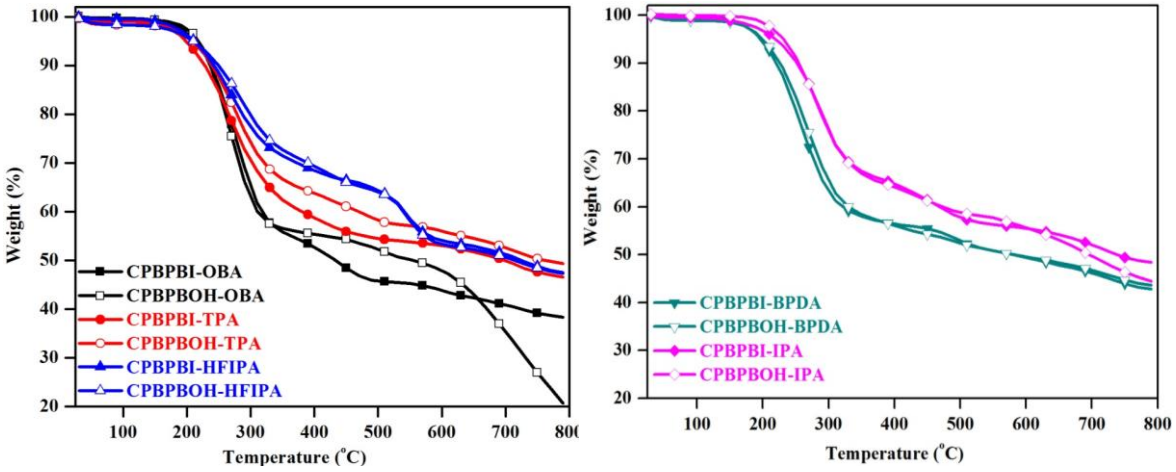

Figure 7.7. *Thermal stability of the CPBPBI and CPBPBOH AAEMs.*

7.3.6. Tensile properties

The results of stress-strain plots of the CPBPBI and CPBPBOH membranes are shown in Figure 7.8 and the data tensile strength and elongation at break are presented in Table 7.4. The CPBPBI/OH AEMs exhibits a tensile strength of maximum load in the range of 34-54 MPa and a maximum elongation at a break in the range of 13-2.5 (%). The CPBPBI-TPA AEM displays a good tensile strength and highest elongation at break which are 53 MPa and 13 %, respectively. The data presented in stress-strain plot and in Table 7.4 clearly indicates the dependence of polymer (PyPBI) structure, however we did not find much difference between I^- and OH^- form. The mechanical strength of the current membrane is much higher than the uncross linked membrane of Chapter 5. The high strength and less elongation of membranes are attributed to the presence of cross-linking in the current membrane.

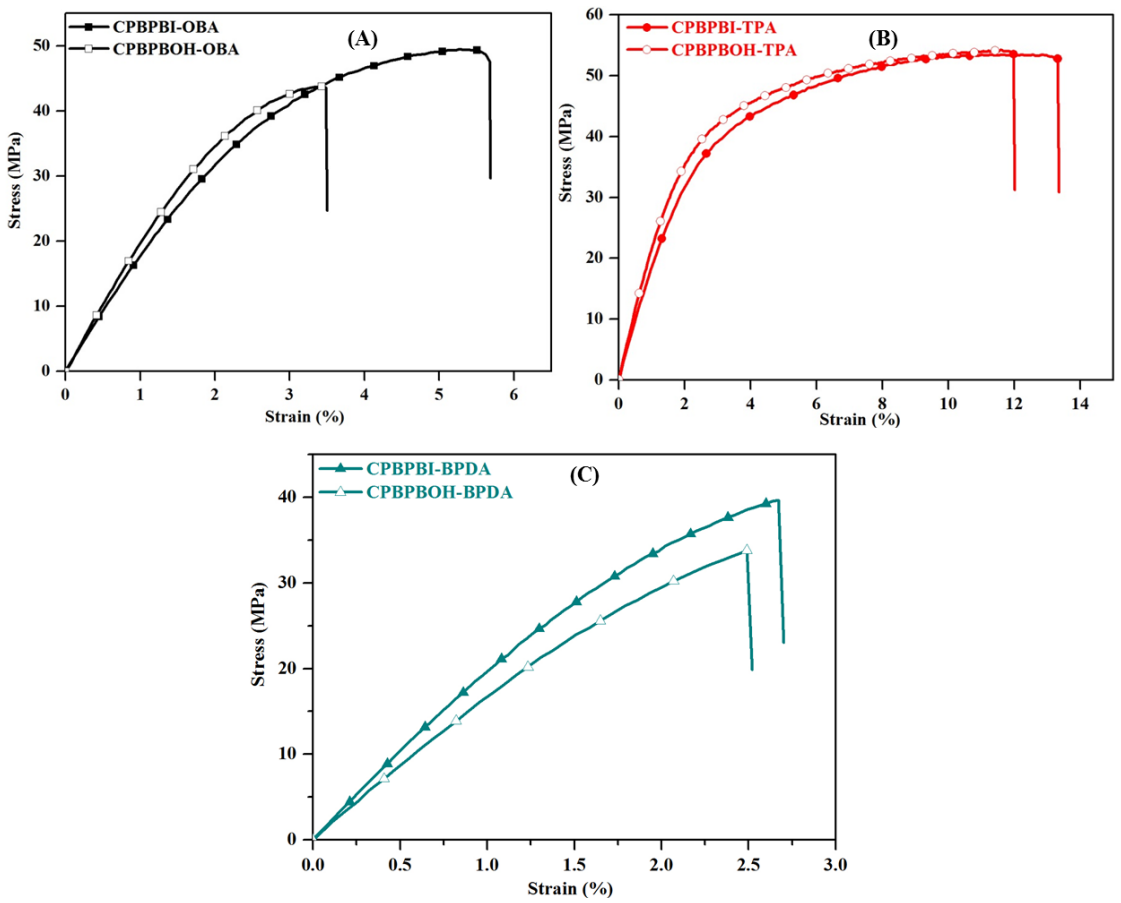

Figure 7.8. *Stress-strain plots of the CPBPBI and CPBPBOH AEMs obtained for the UTM measurement: (A) OBA (B) TPA (C) BPDA based samples.*

Table 7.4. *Tensile strength and elongation at break (%) data of CPBPB (I^- and OH^- form) AEMs obtained from tensile plots.*

Sample	Tensile strength (MPa)	Elongation at break (%)
CPBPBI-OBA	50	5.6
CPBPBOH-OBA	44	3.5
CPBPBI-TPA	53	13
CPBPBOH-TPA	54	12
CPBPBI-BPDA	40	2.7
CPBPBOH-BPDA	34	2.5

7.4. CONCLUSION

Five different type of cross-linked poly(butylated pyridinium benzimidazolium) iodides (CPBPBI) have been synthesized successfully from PyPBIs by utilizing simple alkylation method. The hydroxide form (CPBPBOH) membranes were generated from the iodide form (CPBPBI) membranes by immersing in 1 M aqueous KOH solution. The IEC values of the CPBPBI membrane were found to be much higher than the uncross-linked membrane. Among various samples the CPBPBI-OBA sample showed higher IEC and higher hydroxide conductivity compared to other samples. The CPBPBI-TPA membrane showed higher mechanical strength (storage modulus, tensile strength=53 MPa and elongation=13%) than the remaining membranes. The IEC, FT-IR spectra, ^{1}HNMR spectra and ionic conductivities of all the samples were compared before and after the chemical stability test. The studies clearly indicated almost zero or very negligible degradation in alkaline condition and all the membranes were found to be stable in 5 M KOH. After stability test, the hydroxide ion (OH^-) conductivity of membranes was decreased to a certain extent but not significantly. Overall, the crosslinking of the PyPBI chains immensely helped in improving various physical properties particularly σ_{OH^-}, alkaline stability and mechanical robustness which are important for developing useful AAEMs.

REFERENCES

[1] Varcoe, J. R.; Slade, R. T. C.; Yee, E. L. H. *Chem. Commun.* **2006**, *13*, 1428.

[2] Han, J., Zhu, L., Pan, J., Zimudzi, T. J., Wang, Y., Peng, Y., Hickner, M. A. Zhuang, L. *Macromolecules* **2017**, *50*, 3323.

[3] Mohanty, A. D.; Tignor, S. E.; Krause, J. A.; Choe, Y. K.; Bae, C. *Macromolecules* **2016**, *49*, 3361.

[4] Jasti, A.; Prakash, S.; Shahi, V. K. *J. Membr. Sci.* **2013**, *428*, 470.

[5] Han, J.; Peng, H.; Pan, J.; Wei, L.; Li, G.; Chen, C.; Xiao, L.; Lu, J.; Zhuang, L. *ACS Appl. Mater. Interfaces* **2013**, *5*, 13405.

[6] Wang, J.; Wang, J.; Zhang, S. *J. Membr. Sci.* **2012**, *415-416*, 205.

[7] Chen, C.; Pan, J.; Han, J.; Wang, Y.; Zhu, L.; Hickner, M. A.; Zhuang, L. *J. Mater. Chem. A* **2016**, *4*, 4071.

[8] Pan, J.; Chen, C.; Li, Y.; Wang, L.; Tan, L.; Li, G.; Tang, X.; Xiao, L.; Lu, J.; Zhuang, L. *Energy Environ. Sci.* **2014**, *7*, 354.

[9] Pan, J.; Lu, S.; Li, Y.; Huang, A.; Zhuang, L.; Lu, J. *Adv. Funct. Mater.* **2010**, *20*, 312.

[10] Hibbs, M. R.; Fujimoto, C. H.; Cornelius, C. J. *Macromolecules* **2009**, *42*, 8316.

[11] Zeng, Q. H.; Liu, Q. L.; Broadwell, I.; Zhu, A. M.; Xiong, Y.; Tu,X. P. *J. Membr. Sci.* **2010**, *349*, 237.

[12] Vandiver, M. A.; Caire, B. R.; Poskin, Z.; Li, Y.; Seifert, S.; Knauss, D. M.; Herring, A. M.; Liberatore, M. W. *J. Appl. Polym. Sci.* **2015**, *132*, 41596.

[13] Varcoe, J. R.; Slade, R. C. T.; Yee, E. L. H.; Poynton, S. D.; Driscoll, D. J.; Apperley, D. C. *Chem. Mater.* **2007**, *19*, 2686.

[14] Zhu, L.; Zimudzi, T. J.; Li, N.; Pan, J.; Lin, B.; Hickner, M. A. *Polym. Chem.* **2016**, *7*, 2464.

[15] Li, N.; Leng, Y.; Hickner, M. A.; Wang, C.-Y. *J. Am. Chem. Soc.* **2013**, *135*, 10124.

[16] Zhu, L.; Pan, J.; Christensen, C. M.; Hickner, M. A. *Macromolecules* **2016**, *49*, 3300.

[17] Pan, J.; Zhu, L.; Han, J.; Hickner, M. A. *Chem. Mater.* **2015**, *27*, 6689.

[18] Dai, P.; Mo, Z. H.; Xu, R. W.; Zhang, S.; Wu, Y. X. *ACS Appl. Mater. Interfaces* **2016**, *8*, 20329.

[19] Guo, D.; Lai, A. N.; Lin, C. X.; Zhang, Q. G.; Zhu, A. M.; Liu, Q. L. *ACS Appl. Mater. Interfaces* **2016**, *8*, 25279.

[20] Weissbach, T.; Wright, A. G.; Peckham, T. J.; Sadeghi Alavijeh, A.; Pan, V.; Kjeang, E.; Holdcroft, S. *Chem. Mater.* **2016**, *28*, 8060.

[21] Gu, S.; Cai, R.; Luo, T.; Chen, Z. W.; Sun, M. W.; Liu, Y.; He, G. H.; Yan, Y. *Angew. Chem., Int. Ed.* **2009**, *48*, 6499.

[22] Zhang, Q.; Li, S.; Zhang, S. *Chem. Commun.* **2010**, *46*, 7495.

[23] Choi, Y.-J.; Park, J.-M.; Yeon, K.-H.; Moon, S.-H. *J. Membr. Sci.* **2005**, *250*, 295.

[24] Dö bbelin, M.; Azcune, I.; Bedu, M.; Ruiz de Luzuriaga, A.; Genua, A.; Jovanovski, V.; Cabañ ero, G.; Odriozola, I. *Chem. Mater.* **2012**, *24*, 1583.

[25] Vega, J. A.; Chartier, C.; Mustain, W. E. *J. Power Sources* **2010**, *195*, 7176.

[26] Henkensmeier, D.; Cho, H.-R.; Kim, H.-J.; Nunes Kirchner, C.; Leppin, J.; Dyck, A.; Jang, J. H.; Cho, E.; Nam, S.-W.; Lim, T.-H. *Polym. Degrad. Stab.* **2012**, *97*, 264.

[27] Thomas, O.D.; Soo, K. J. W. Y.; Peckham, T. J.; Kulkarni, M. P.; Holdcroft, S. *J. Am. Chem. Soc.*, **2012,** *134*, 10753.

[28] Chen, D.; Hickner, M. A. *ACS Appl. Mater. Interfaces* **2012**, *4*, 5775.

[29] Kannan, R.; Kagaiwale, H. N.; Chaudhari, H. D.; Kharul, U. K.; Kurungot, S.; Pillai, V. K. *J. Mater. Chem.* **2011**, *21*, 7223.

[30] Ghosh, S.; Sannigrahi, A.; Maity, S.; Jana, T. *J. Mater. Chem.* **2011**, *21*, 14897.

[31] Hazarika, M.; Jana, T. *ACS Appl. Mater. Interfaces* **2012**, *4*, 5256.

[32] Chung, S.-W.; Hsu, S. L.-C.; Liu, Y.-H. *J. Membr. Sci*. **2007**, *305*, 353.

[33] Lin, B.; Dong, H.; Li, Y.; Si, Z.; Gu, F.; Yan, F. *Chem. Mater*. **2013**, *25*, 1858.

[34] Li, X.; Yu, Y.; Liu, Q.; Meng, Y. *Int. J. Hydrogen Energy* **2013**, *38*, 11067.

[35] Huang, A. B.; Xia, C. Y.; Xiao, C. B.; Zhuang, L. *Int. J. Hydrogen Energy* **2006**, *100*, 2248.

[36] Wang, Y. J.; Qiao, J. L.; Baker, R.; Zhang, J. J. *Chem. Soc. Rev.* **2013**, *42*, 5768.

[37] Ye, Y.; Elabd, Y. A. *Macromolecules* **2011**, *44*, 8494.

[38] Meek, K. M.; Elabd, Y. A. *Macromolecules* **2015**, *48*, 7071.

[39] Price, S. C.; Williams, K. S.; Beyer, F. L. *ACS Macro Lett.* **2014**, *3*, 160.

[40] Dong, H.; Li, Y.; Si, Z.; Gu, F.; Yan, F. *Macromolecules* **2014**, *47*, 208.

[41] Lai, A. N.; Wang, L. S.; Lin, C. X.; Zhuo, Y. Z.; Zhang, Q. G.; Zhu, A. M.; Liu, Q. L. *ACS Appl. Mater. Interfa*ces **2015**, *7*, 8284.

[42] Lee, H. J.; Choi, J.; Han, J. Y.; Kim, H. J.; Sung, Y. E.; Kim, H. *Polym. Bull.* **2013**, *70*, 2619.

[43] Henkensmeier, D.; Kim, H.-J.; Lee, H.-J.; Lee, D. H.; Oh, I.-H.; Hong, S.-A.; Nam, S.-W.; Lim, T.-H. *Macromol. Mater. Eng.* **2011**, *296*, 899.

Chapter 8

SUMMARY and CONCLUSIONS

8.1 SUMMARY

This thesis entitled "***Imidazole based Polymers as Ion Exchange Membranes***" describes the development of composite membranes of polybenzimidazole with small organic acidic molecules, synthesis and characterization of various polymer systems (pyridine bridged polybenzimidazoles and their derivatives) for the development of proton exchange membrane (PEM) and alkaline anion exchange membrane (AAEM). The thesis contains seven chapters, an introductory chapter followed by methods and experimental chapter and five working chapters. The summary of the contents of each chapter is as follows.

CHAPTER 1

This chapter deals with a brief introduction of fuel cell, various types of fuel cells, working principle of PEMFC, properties of PEM and their types, including PA doped PBI membrane and fabrication methods. In this chapter we have discussed about AEMFC principle, properties of AEM and different types of cationic groups along with the various polymer backbones. We have discussed brief introduction of polybenzimidazoles (PBIs), types and importance of PBI in terms of PEM and AEM, and their nanocomposites. Finally, this chapter describes the scope of the thesis work.

CHAPTER 2

This chapter describes the details of materials that were used for all the working chapters and details of experimental procedures, various instrumentation techniques used for characterization of samples and property evaluation of all polybenzimidazole nanocomposites and pyridine bridged polybenzimidazole derivatives and various types of anion exchange membranes.

CHAPTER 3

In the present work, proton exchange membrane (PEM) based on series of polybenzimidazoles (PBI) composites are prepared with acidic surfactant like molecules

(ASMs) with an objective to improve properties of PEM especially proton conductivity. Composites are obtained by homogenizing poly (4, 4-diphenylether-5, 5-bibenzimidazole) (OPBI) in three different ASMs namely camphorsulfonic acid (CSA), p-toluenesulfonic acid (PTSA) and mono-n-dodecyl phosphate (MDP). FT-IR and solid-state NMR studies indicate the presence of interactions between OPBI and ASMs which are necessary for obtaining homogeneous composite membranes. Mechanical reinforcement is observed in case of composite membranes and storage modulus increases with increasing ASM loading in the composite. The detailed thermal analysis shows that phosphoric acid loaded (PA) composite membranes have higher thermal stability than the PA loaded pristine OPBI, it increases with increasing loading of ASM and it largely depends upon the type of ASM in the composite. Though OPBI is an amorphous polymer but ASMs self-organizes themselves in the polymer matrix owing to the strong interaction between OPBI and ASMs. As a result composite membranes display the crystalline character which in turn significantly influences the morphological features of the composites. Fibrillar to porous morphology are observed in composites depending on the type and loading of ASM. This morphological features and the crystalline nature of the composites are found to be responsible for mechanical reinforcement and significant increase in PA loading. The PA doped pristine OPBI, OPBI/CSA-20%, OPBI/PTSA-20% and OPBI/MDP-20% composite membranes proton conductivities are 8.6×10^{-2} S/cm, 2.82×10^{-1} S/cm, 1.71×10^{-1} S/cm and $\times 10^{-1}$ S/cm, respectively at 180 °C. OPBI/ASM composite membranes also display very low acid leaching in comparison to pristine OPBI owing to the formation of strong interaction between PA and polymer chains through ASMs.

CHAPTER 4

We report successful synthesis of three types of pyridine bridged tetraamine (PyTAB) monomers namely PyTAB-COOH, PyTAB-OH and PyTAB-CF_3 where additional functional groups –COOH, -OH, and –CF_3, respectively have been tagged in the parent PyTAB for the synthesis of soluble polybenzimidazoles (PBI). These newly

designed PyTAB monomers were polymerized with varieties of dicarboxylic acids to yield series of pyridine bridged PBIs (PyPBIs). Thermal stability, mechanical strength (storage modulus) and glass transition temperature of PyPBIs were found to be influenced by the presence of additional functionalities in the PyTAB monomer and attributed to the hydrogen bonding capability and hydrophobicity of the functional groups. Newly synthesized PyPBIs displayed greater stability in phosphoric acid (PA) when compared with the non-functionalized PyPBIs, former is stable up to 85% PA whereas later is only up to 65% PA. The increased intermolecular interactions and possibility of crosslinking between the polymer chains owing to the presence of functional groups in the functionalized PyPBIs caused the increased stability in PA. The significantly low swelling (< 1%) in water of PyPBIs considered to be a new benchmark of water swelling of PBI based polymers. Proton conductivities of PA loaded PyPBI were considerably higher than the conventional PBIs and non-functionalised PyPBIs and also depends on the functionality, structure of DCA and solvent used to make membranes. Functionalized PyPBIs (current study) showed conductivity as high as 0.12 S/cm whereas non-functionalized PyPBIs usually displayed conductivity around 0.01 S/cm. Porous and well connected network morphology of formic acid treated PyPBI membrane were attributed to the high PA loading and conductivity of PyPBI membrane.

CHAPTER 5

Two important concerns namely low hydroxide ion (OH^-) conductivity and weak alkaline stability of the polymeric membrane in regard to the development of alkaline anion exchange membranes (AAEMs) have been resolved in this work by synthesizing a series of pyridine bridged polybenzimidazole (Py-PBI) polymers consisting of dual OH^- conducting sites. Both the pyridine and imidazole functionalities of Py-PBI chains were quaternized by methylation to synthesize poly(methylated pyridinium benzimidazolium) iodide (PMPBI) which was readily converted to OH^- loaded AAEMs. The OH^- ion conductivities of KOH loaded PMPBI at 30 °C and 80 °C were found to be 28.1 and 102 mS/cm, respectively which are considerably higher than the most of the

reported membranes. The simultaneous presence of dual OH^- ion conducting sites namely pyridinium and imidazolium in the polymer chain has been credited for very high ion conductivity of the AAEMs developed in this work. The current membranes showed excellent alkaline stability and mechanical robustness. The blocking of pyridinium α-positions in the PMPBI structure prevented irreversible oxidation of pyridinium into neutral pyridone which facilitated in improving alkaline stability.

CHAPTER 6

Three types of polybenzimidazoles (PBIs, PyPBIs and Tertiary butyl PyPBIs) have been synthesized successfully in this Chapter. Various kinds of iodide form polybenzimidazoliums were synthesized by varying alkyl iodides (methyl iodide, butyl iodide and isobutyl iodide) with polybenzimidazoles. The iodide form polybenzimidazolium membranes were immersed in 1 M KOH solution to generate hydroxide form anion exchange membranes (AEMs). All these membranes structures were confirmed by FT-IR and ^1H NMR spectroscopy. Iodide and hydroxide AAEMs were studied for ion exchange capacity (IEC), ionic conductivity, thermal, mechanical and alkaline stability. Polybenzimidazoliums with butyl chains showed higher IEC (PyPBI-BuI = 3.37) and maximum hydroxide conductivity (PyPBI-BuI = 12.86×10^{-2}) among the studied alkyl modified membranes. Isobutyl and butyl chains containing polybenzimidazolium polymeric AAEMs were demonstrated excellent alkaline stability even in 5 M KOH aqueous solution. This might be due to the bulky nature of the alkyl moieties which prevented the hydroxide ion attack on imidazolium groups.

CHAPTER 7

Cross-linked poly(butylated pyridinium benzimidazolium) iodides (CPBPBI) were synthesized from pyridine based polybenzimidazoles (PyPBIs) by using butyl iodide as alkylating agent and 1,4-diiodo butane as cross-linker to develop alkaline anion exchange membranes (AAEMs). The hydroxide form membranes were generated from their iodide counter parts by doping in 1 M KOH and 5 M KOH solution. The ion exchange capacity (IEC) of these AAEMs was introduced to be in range of 2.30–3.97

mequiv.g^{-1} which is significantly high compared to other AAEMs structure developed so far. The hydroxide conductivity of these crosslinked membranes largely depedent upon the polymer backbone structure and found to be much higher than the already reported values. The higher σ_{OH}^- obtained in the current study is 111 mS/cm at 80 °C which is highest reported so far in case of imidazole based polymer. Though these membranes having both pyridinium and imidazolium cationic sites but they display very high alkaline stability even in 5 M KOH solution at 80 °C which is attributed to the cross-linked structure of the polymer backbone. The IEC, FT-IR spectra, ^{1}HNMR spectra and ionic conductivity data of the AAEM were compared before and after alkali test and these investigations proved that the membranes are highly stable under concentrated basic solution owing to the cross-linking formation. Furthermore, we studied thermal and mechanical properties of these AEMs and found that these membranes were thermally stable and mechanically robust. In summary, all the data convincingly suggested the development of potential AAEMs.

8.2 CONCLUSIONS

The following conclusions are drawn from the studies carried out in this thesis work.

- Three sets of various composite membranes of polybenzimidazoles with organic fillers have been prepared and explored for their potential use as PEM.
- The TGA studies of these membrane concluded that the phosphoric acid (PA) doped composite membranes have high thermal stability than PA doped pristine PBI.
- Morphology of the composite membranes revealed the fibre like network structure which helped in accommodate more amount of PA and eventually led to higher proton conductivities and reduced acid leaching.
- Three series of functionalized pyridine bridged polybenzimidazoles (PyPBIs) derivatives have been synthesized from tetraamine called 2,6-bis(3′ ,4′ -

d

iaminophenyl)-4-phenylpyridine (PyTAB) monomer derivatives.

- These functionalised PyPBI polymers showed higher stability towards phosphoric acid compared to non-functionalised PyPBI due to the crosslinking by means of hydrogen bonding between the chains.
- PA loading and proton conductivities of the functionalised PyPBI polymer derivatives were higher than the conventional PBI and unfunctionalized PyPBIs.
- Five different types of poly (methylated pyridinium benzimidazolium) iodides (PMPBI) have been synthesized from pyridine bridged polybenzimidazole (PyPBI) polymers via simple methylation for the development alkaline anion exchange membranes (AAEMs)
- In these polymeric AAEMs both pyridinium and benzimidazolium acted as anion exchange sites or cationic groups.
- These "AAEMs showed higher ion exchange capacity (IEC), excellent ionic conductivity and good chemical" stability.
- Various kinds of poly(alkylated pyridinium benzimidazolim) iodide have been synthesized from different polybenzimidazoles (PBIs, PyPBIs and tertiary butyl PyPBIs) by changing alkyl iodides (methyl iodide, butyl iodide and isobutyl iodide).
- Butylated AAEMs showed higher IEC, ionic conductivity and water uptake compared to the isobutylated AAEMs due to the high degree of alkylation.
- Poly(alkylated pyridinium benzimidazolim) polymers demonstrated excellent chemical stability upto 5 M KOH at 60 °C which is attributed to the effect of bulky alkyl chains.
- Five different types of cross-linked poly(butylated pyridinium benzimidazolium) iodides (CPBPBI) have been synthesized successfully from Py-PBIs by

u

tilizing alkylation method.

- These cross-linked poly(butylated pyridinium benzimidazolium) membranes showed higher IEC and higher hydroxide conductivity and very high alkaline stability even in 5 M KOH at 80 °C.

8.3 Scope for Future Work

The present thesis has addressed three important aspects of *Polybenzimidazole: functionalized polybenzimidazoles, quaternized polybenzimidazoles and nanocomposites*. We believe the findings of this thesis will have great impact on the future development of polybenzimidazole (PBI) chemistry in general, especially the use of PBI as PEM and as well as AAEM. We believe the potential and scope of future work of this thesis are enormous. Few of these are listed below

- Attempts should be made for the insertion of varieties of organic nanofillers (or small amount) to make the composite of PBI polymer to enhance PEM properties.
- Efforts can be made to develop various functionalized PyPBIs by making new PyTAB monomer derivative.
- Attempts must be made to synthesize new type of PBI by developing new dicarboxylic acid monomers (DCAs).
- Synthesis of block copolymers and random copolymers can be done from functionalized PyPBI polymers.
- Further study on the stability of small molecule analogues led to greater understanding of the process involved in the benzimidazolium degradation of these polymers.
- Quaternized PyPBI block copolymers can be synthesized and can be used as AAEMs.
- Finally, the fuel cell testing of the alkali doped PBI based AAEM obtained from the PyPBI may be conducted to evaluate the performance.

PUBLICATIONS and PRESENTATIONS

PUBLICATIONS

1. **Balakondareddy Sana** and Tushar Jana, Polybenzimidazole composite with acidic surfactant like molecules: A unique approach to develop PEM for fuel cell
   European Polymer, 82, 421-434 (2016)
2. Baku Nagendra, Angel Mary Joseph, **Balakondareddy Sana**, Tushar Jana and E. Bhoje Gowd, Layered double hydroxide nanoplatelets with ultra high specific surface area for significantly enhanced crystallization rate and thermal stability of polypropylene
   ACS Applied Nano Materials, 1, 111-121 (2018)
3. **Balakondareddy Sana** and Tushar Jana, Polymer electrolyte membranes from polybenzimidazoles: Influence of tetraamine monomer structure
   Polymer, 137, 312-323 (2018)
4. Satheesh Kumar, **Balakondareddy Sana**, Dona Mathew, G. Unnikrishnan, Tushar Jana and K. Santhosh, High molecular weight PBI-nanocomposite membranes: Enhanced proton conductivity with low content of amine-functionalized nanoparticles
   Polymer, 145, 434-446 (2018)
5. **Balakondareddy Sana** and Tushar Jana, Alkali stable polymeric membrane with dual hydroxide ion conducting sites
   (Communicated to ACS Macro Letters)
6. **Balakondareddy Sana,** Rambabu Koyilapu, Sengottuvelu Dineshkumar, Athianna Muthusamy Tushar Jana, High temperature PEMs developed from the blends of polybenzimidazole and poly(azomethine-ether)
   (Communicated to Polymer Bulletin)
7. **Balakondareddy Sana** and Tushar Jana, Effect of alkylation on polybenzimidazoles for alkaline anion exchange membranes
   (Manuscript under preparation)

8. **Balakondareddy Sana** and Tushar Jana, Chemically stable anion exchange membranes developed from the cross-linked polybenzimidazoles. **(Manuscript under preparation)**
9. Satheesh Kumar, **Balakondareddy Sana**, G. Unnikrishnan, Tushar Jana and K. Santhosh, Polybenzimidazole as proton conducting filler in poly(dimethylsiloxane) matrix; Preparation and properties **(To be communicated)**
10. **Balakondareddy Sana,** Radhika, Tushar Jana and Jorphin Joseph, Porous PEM developed from the blends of polybenzimidazoles and polyamic acid **(Manuscript under preparation)**
11. Rambabu Koyilapu, **Balakondareddy Sana,** Shuvra Singha and Tushar Jana, Polyamine phosphate ester blends with oxypolybenzimidazole to improve the properties of proton exchange membrane. **(Manuscript Under preparation)**
12. Rambabu Koyilapu, S.N. Raju Kutcherlapati, **Balakondareddy Sana** and Tushar Jana, Poly quaternary vinylimidazole grafted silica nanoparticles via *grafting-from* RAFT plymerization and its nanocomposite with polybenzimidazole to improve the properties of PEM. **(Manuscript Under preparation)**

Note: Only publications 1, 3, 5, 7 and 8 are included in this thesis as chapter 3, 4, 5, 6 and 7, respectively.

CONFERENCE PRESENTATIONS

1. **Balakondareddy Sana** and Tushar Jana, Polybenzimidazole composite with acidic surfactant like molecules: A unique approach to develop PEM for the use in fuel cell.

   MACRO-2015, January, 23-26, 2015, IACS, Kolkata, India. **(Poster Presentation)**
2. **Balakondareddy Sana,** Sengottuvelu Dinesh Kumar and Tushar Jana-Polybenzimidazole/polyazomethinebisphenol blend PEM membranes for use in high temperature fuel cell applications.

   APA-2015, October, 29-31, 2015, Saurashtra University, Rajkot, India. **(Oral and Poster Presentation)**
3. **Balakondareddy Sana** and Tushar Jana, Polybenzimidaole/ Poly(azomethine-ether) blend PEMs for use in high temperature fuel cell applications

   CHEMFEST-2016 (13th annual in-house symposium) March 18-19, 2016, University of Hyderabad, Hyderabad, India. **(Poster Presentation)**
4. **Balakondareddy Sana** and Tushar Jana-Poly(methylated pyridinium benzimidazolium): A new class of anion exchange membrane **(Poster Presentation)**

   MACRO-2017, January 8-11, 2017, CSIR-NIIST & VSSC, Trivandrum, India.
5. **Balakondareddy Sana** and Tushar Jana, Poly(methylated pyridinium benzimidazolium): A new class of anion exchange membrane

   CHEMFEST-2017, (14th annual in-house symposium) March 3-4, 2017, University of Hyderabad, Hyderabad, India. **(Oral Presentation)**
6. **Balakondareddy Sana** and Tushar Jana, Effect of alkylation on polybenzimidazoles for alkaline fuel cell membranes

   NMSTC-2017, October 13-14, 2017, University of Hyderabad, Hyderabad, India. **(Poster Presentation)**

7. **Balakondareddy Sana** and Tushar Jana, Ionic conductive pyridinium and benzimidazolium containing novel polymers for use in anion exchange membrane fuel cells
   RTMST-2017, November 22-23, 2017, CSIR-CSMCRI, Bhavnagar, India **(Poster Presentation)**.